University of Southampton

Faculty of Social Sciences

Mathematical Sciences

Black Hole Microstates in the D1-D5 Orbifold CFT

by

Joan Garcia i Tormo

Thesis for the degree of Doctor of Philosophy

March 2019

University of Southampton

Abstract

Faculty of Social Sciences

Mathematical Sciences

Thesis for the Degree of Doctor of Philosophy

Black Hole Microstates in the D1-D5 Orbifold CFT

by Joan Garcia i Tormo

This thesis presents work extending the precision holography calculations for the D1-D5 CFT. The context of these calculations is the fuzzball proposal, which is the most widely accepted string theory answer for black hole microstates. According to this proposal, associated to a black hole there is an exponentially large number of microstates, called fuzzballs, which are regular, horizonless stringy solutions. These account for the whole entropy of the black hole, and solve all the paradoxes arising from the semi-classical study.

The D1-D5 system has an orbifold point in its moduli space, at which it may be described by an $\mathcal{N} = (4, 4)$ supersymmetric sigma model with target space $M^N/S(N)$, where M is $\mathbb{T}^4$ or $K3$. In this thesis correlation functions involving chiral operators constructed from twist fields are considered, as well as one and n-point functions. Explicit expressions for processes involving a twist n operator joining n twist operators of arbitrary twist are obtained. One point functions for chiral primary operators are calculated, extending the known CFT results in the literature. The suppression of the long string one point functions with respect to the short string ones is corroborated. Bounds for n-point functions of twist operators are also presented.

On a different direction, work towards the counting of the so-called superstrata subclasses of black hole microstates is presented. To do so, some integer partition results in the context of number theory are introduced. The generating functions for the partitions are obtained, as well as a novel formula to count them exactly. A computer program which implements such formula is described.

Who controls the past,
commands the future.
Who commands the future,
conquers the past.
Kane

Table of Contents

List of Figures

Declaration of Authorship

I, Joan Garcia i Tormo, declare that the thesis entitled *Black Hole Microstates in the D1-D5 Orbifold CFT* and the work presented in the thesis are both my own, and have been generated by me as the result of my own original research. I confirm that:

- this work was done wholly or mainly while in candidature for a research degree at this University;
- where any part of this thesis has previously been submitted for a degree or any other qualification at this University or any other institution, this has been clearly stated;
- where I have consulted the published work of others, this is always clearly attributed;
- where I have quoted from the work of others, the source is always given. With the exception of such quotations, this thesis is entirely my own work;
- I have acknowledged all main sources of help;
- where the thesis is based on work done by myself jointly with others, I have made clear exactly what was done by others and what I have contributed myself;
- parts of this work have been published as:
  - J. Garcia i Tormo and M. Taylor, *Correlation functions in the D1-D5 orbifold CFT*, *Journal of High Energy Physics* **2018** (Jun, 2018) 12
  - J. Garcia, Tormo and M. Taylor, *One point functions for black hole microstates*, `1904.10200`

Signed: .....

Date: .....

Acknowledgements

First of all I would like to thank my supervisor, Marika Taylor, for her help and guidance during my PhD and for her support on my personal progression during all this time. She is a great role model. I would also like to thank my cosupervisor, Kostas Skenderis, for his help and guidance in the early stages of the studies, as well as David Turton and Sami for useful discussions. I also thank George Andrews for his very helpful communication regarding integer partitions, and Rodolfo Russo and Oscar Dias for the discussion and comments. This work was funded by EPSRC and by the University of Southampton, which I thank as well.

I cannot write these acknowledgements without thanking Tomeu Fiol, for his early advice and guidance at the start of my career. I have learned many useful skills from him. I also want to thank Jaume Garriga, Roberto Emparan and the rest of the theory group from Barcelona, for the hospitality they showed during my Christmas visits and for the journal club sessions.

I would like to thank Jordi Carmona (espero que ens seguim veient com a mínim a l'Estartit!), Ramon Sala and the schools Súnion and Garbí Esplugues, as well as Jamal, Salma and the Pint of Science organisers of 2016 in Southampton, for the possibilities I have had to explain black hole science and my experience to many different audiences.

All my former and present colleagues and friends in the group deserve my gratitude as well, for making this period of time a happy one. I would like to thank in particular William, Ariana, Stanislav, Elliot, Aaron, Giorgos, Fabian, Federico, Brian, Adam, Vanessa and Alice. I also want to thank Ramon, with whom I started this journey and shared most of it. Me n'alegro molt que tinguéssim la possibilitat de venir junts aquí a Southampton. Sense la teva amistat no hauria estat el mateix.

I want to thank all the other friends I have made during this period of time in Southampton as well. Thank you Ilectra, George, Aragorn, Martina, Diksha, Marija, Roberto, Elena, Hynek, Gerardo, Felipe, Przemysław, Kate, Ollie and all the others, for making me always feel like at home. A big shout-out to the people I have met at the Jubilee, and to Clide, Jon and Chris in particular, for helping me stay sane.

A big thank you to Guillem as well, for hosting me in Kyoto, for our friendship and for all the moments we have had and we will have together. Fighto! I also want to thank Kiko for his joyfulness, climbing lessons and spiritual guidance, as well as all my other friends from Barcelona to make me feel like no time has passed when I go there. Thank you Duatis, Gerard, Kirian, Ana, Laura, Milena, Jorge, Sònia, Santa, Carlos, Dani, Néstor, Domingo, Enciso and all the others I'm forgetting! And of course, I want to thank Armajac, Sandra, Andreu, Arnau, Pau, Enric and the rest of the group as well, for our (at least) yearly meetings. Sometimes I think I keep up with the news just to rant and laugh about them with you guys. També dono gràcies al procés per compensar la falta d'episodis de GoT.

Moving to the south, I also want to thank all the lovely people I have met from Seville. Me alegro mucho de haberos podido conocer a todos. Gracias por aceptarme y hacerme sentir como otro más desde el primer momento. Sois todos gente maravillosa!

One of my biggest thanks goes to my parents and my brothers, for their unconditional help, support and guidance during this thesis, before it and in the future. I want to thank Albert for his grü$\beta\Omega$ly amazing help, and Xavier for his comments on the draft and for the discussions on black holes... and on white holes? As well, as well. Potze ze que el Doctor Nino ja no farà més de taxista.

Last, but very, very far from least I would like to thank Tania, for her constant caring, support, love and company, and for everything that will come in the next stages of our life. Venga, un empujoncito más y ya lo tienes tu también!

Part I

Context

CHAPTER 1

General introduction

In this chapter we give an overview of the background needed, and motivate the study of the field. After setting up the topic, we briefly review the main issues that led to the study of quantum black holes. Within the context of string theory we introduce the holographic principle, and one of its main answers to the quantum structure of black holes: the fuzzball proposal. At the end we give an outline of the other chapters of this thesis.

1.1 Motivation

The Standard Model of particle physics [3] describes three out of the four fundamental forces in nature: the electromagnetic, the strong nuclear and the weak nuclear. It leaves some questions unanswered though, such the nature of dark matter. It is also unable to describe the fourth fundamental force: gravity. The current theory to describe gravity is general relativity (GR) [4], but it is classical. This means that it is incomplete, and it will thus break down at some point. Black holes are of great theoretical interest because they are systems where, indeed, general relativity seems to be giving the wrong description when considering quantum effects on top of it.

As reviewed in the next section there are many mysteries regarding black holes. All these mysteries arise because a quantum theory of gravity is not being used. Therefore,

to answer and solve them there is the need to work towards constructing an extension of general relativity at the quantum level. String theory [5, 6] is a consistent theory of quantum gravity, and is the best candidate discovered so far. The work presented in this thesis uses the fuzzball proposal within string theory to learn new things about quantum black holes in this context.

Another motivation to pursue the fuzzball proposal is the recent detection of gravitational waves by the Laser Interferometer Gravitational-wave Observatory (LIGO). The LIGO team has been able to detect gravitational waves from black hole binaries [7–11] and also from neutron stars [12], along with the electromagnetic counterpart in this second case. These new detections provide the most concrete evidence there is for the existence of black holes, and they have opened a new field of research: gravitational wave astronomy.

Gravitational wave astronomy gives observations which are direct experimental data that can be used to further test general relativity. These measurements can also be used to test extensions of GR. In the forthcoming years LIGO is predicted to give more accurate observations, which may be used to eventually see the quantum corrections in the gravitational wave signals. The Laser Interferometer Space Antenna (LISA) mission [13] has also been accepted, and is predicted to launch in the 2030s. This new mission will have increased accuracy with respect to LIGO, and so more and better data will be available to compare with the theory. See [14] for a recent review.

All these facts make the study of black holes very exciting and with a promising future as, most likely, there will be many new gravitational wave detections in the upcoming years. These detections will allow people to check theoretical predictions, and thus confirm or rule out the proposed extensions of general relativity. As it will be obvious by the end of this chapter, the study of black holes in this context is also a very important building block in holography, as the D1-D5 system is one of the prime examples of the duality. In other words, a better understanding of this system may give insights in understanding string theory further. In the following sections some more details on the main issues that have been just mentioned are given, as a warm up and context for the rest of the thesis.

1.2 Black hole puzzles

According to general relativity black holes are predicted to have a singularity. Consider for instance the Schwarzschild black hole [15],

$$\mathrm{d}s^2 = -\left(1-\frac{2GM}{rc^2}\right)c^2\mathrm{d}t^2 + \frac{1}{\left(1-\frac{2GM}{rc^2}\right)}\mathrm{d}r^2 + r^2\mathrm{d}\Omega_2^2. \tag{1.2.1}$$

This is a spherically symmetric solution of the geometry of spacetime. In other words, it is a spacetime with rotational invariance, where t is time and r is the radial coordinate. At $r = 2M$ there is the event horizon, which is the boundary of the no return region. At $r = 0$ the geometry is singular, and this singularity can be reached in finite proper time by an observer. This is a problem in the theory, as these objects can be formed from gravitational collapse of a cloud of dust [16]. As mentioned above, astrophysical black holes have now been detected in the universe, so this needs to be resolved. Certainly singularities are hidden behind a horizon [17], but they are still an issue which needs to be dealt with.

The source of the main problems around black holes are horizons though. When adding quantum fields to the system, Hawking showed that black holes evaporate emitting thermal radiation, semi-classically [18] (see, for instance, [19] for a comprehensive explanation). If Bekenstein's work is added to this result [20] then the Bekenstein-Hawking relation for the black hole entropy is found. It is

$$S_{\mathrm{BH}} = \frac{Ac^3}{4G\hbar}. \tag{1.2.2}$$

This raises a new question: if entropy is an extensive quantity, why is the entropy of a black hole proportional to its area? This may be taken as a first hint towards holography: the information of black holes is encoded on their horizon.

Also, if one puts on the statistical mechanics hat, one may realise that this is a macroscopic system with an entropy associated to it. Therefore, there should be a description of this system as an ensemble of microstates. This is the next puzzle: what are these microstates? Can they be identified?

Hawking radiation also gives rise to one of the most famous problems in theoretical physics: the black hole information paradox [21]. There are several interpretations of this paradox, none of them being completely controversy free. The basic idea behind it is the following. Consider figure 1.2.1. Hawking radiation originates from particle creation close to the horizon. Imagine that one of the particles falls into the black hole, while the other radiates away. Both particles are originally entangled, however at some point the black hole evaporates completely and all that remains is a mixed state which is not entangled with anything. Therefore, unitarity is lost in the process, as the start point could have been at Σ_1 with a pure state. In other words, from the Hawking radiation resulting from the black hole evaporation the initial states that fell in cannot be recovered. This is the usual wording of the black hole information paradox [23–26].

In the next subsection we present what we think is the strongest argument to see the information paradox in black holes, due to Page [27]. The introduction of that paper is a

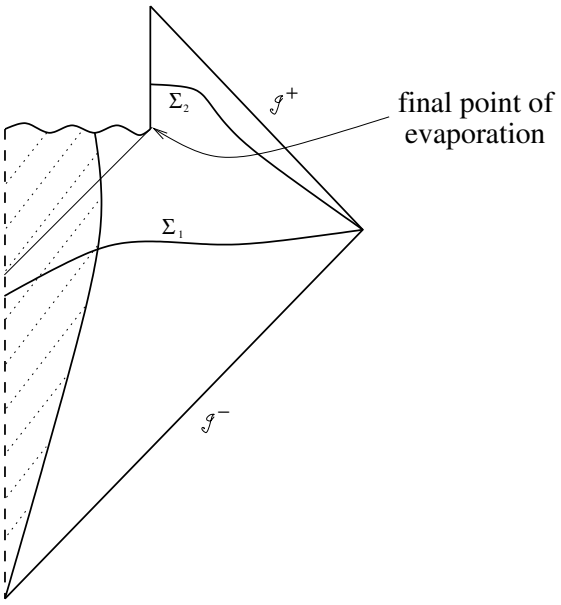

Figure 1.2.1: Penrose diagram of an evaporating black hole. At Σ_1 the observables outside and inside the black hole are entangled, and the infalling state may be pure. At Σ_2 the observables are not entangled with anything, and the state is mixed. Unitarity is lost in the evolution from Σ_1 to Σ_2. Figure taken from [22].

very good and concise reference on the information paradox and all the main discussion around it at the time, 1993. Before we review Page's argument, let us make a side comment. We consider quantum effects on black holes as we strongly believe that our world is very well described by quantum field theory. The Standard Model has given the most precise measurements that humanity has ever achieved, and physics is no more than finding the best model which fits observation. Hence, at present there is no logic route to solve these problems other than quantum gravity. Let us now understand information loss in black holes.

1.2.1 Information loss

The main point of this argument is that semiclassical physics at the horizon cannot solve the paradox. In other words, small quantum corrections localised to the neighbourhood of the black hole are not the answer, as Mathur showed [24]. Consider figure 1.2.2a. It shows the expected behaviour of the entanglement entropy for a unitary process. This curve can be understood in the following way: the first radiation that comes out of the black hole is entangled with the interior, and so the entanglement entropy that is measured increases. After some point the entanglement entropy has to start decreasing, as all the interior will be radiated and so the entanglement will all be within the emitted radiation. Similarly, information is expected to start coming out mainly after the middle point is crossed. Before that there is radiation coming out, but it is entangled with the inside still,

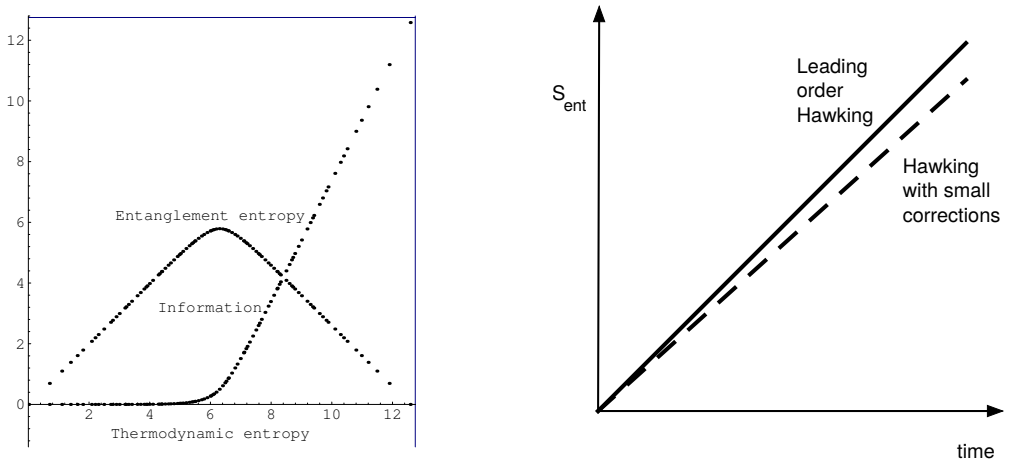

(a) (b)

Figure 1.2.2: (a) Plot of the average entanglement entropy and information against the thermodynamic entropy, for an evaporating black hole. Figure taken directly from [27]. (b) The growth of entanglement entropy for the traditional black hole in the leading order Hawking computation (solid line), and with small corrections allowed (dashed line). Figure taken directly from [28].

and so information can remain hidden. Once radiation is only entangled with itself or, in other words, when the interior can no longer hold all the information, it has to be radiated away.

Consider now figure 1.2.2b. The solid line represents the growth of entanglement entropy for a traditional black hole which emits Hawking radiation. Clearly, its behaviour is very different from 1.2.2a. One could think that small quantum corrections to Hawking's semiclassical calculation could correct the behaviour to the expected one. However, this is not the case. As mentioned above, Mathur showed [24] that the small quantum corrections are not enough. In the figure, the dotted line represents Hawking's result with small quantum corrections. Clearly, the expected behaviour cannot be recovered like this. In other words, there is a paradox: the entanglement entropy of an evaporating black hole does not match with the expected behaviour for the entanglement entropy of a unitary process.

A relevant argument within this story is the firewall discussion [29–31]. The main point of the discussion is that one of the following three statements must not hold:

1. Hawking radiation is in a pure state.

2. The information carried by the radiation is emitted from the region near the horizon, with low energy effective field theory valid beyond some microscopic distance from the horizon.

3. The infalling observer encounters nothing unusual at the horizon.

The fuzzball proposal, which is introduced in this thesis in section 1.5.1, gives an answer to this contradiction by proposing that the black hole microstates, the fuzzballs, are pure states which have no horizon. Related to it there is the fuzzball complementarity discussion [28, 32]. We refer to the given references for the discussion in depth.

After all this, it is now clear that there is the need to go beyond general relativity. A first attempt would of course be to directly quantise general relativity. However, many issues arise when trying to do so [19]; the resulting theory is not renormalisable for instance. Therefore, a new theory is required. The most promising candidate for quantum gravity that there is so far is string theory, and so it is the one considered in this work.

1.3 String theory

As its name advocates, string theory is based on the idea that the most fundamental constituents of the universe are one-dimensional bodies called strings. Here we will just very briefly mention some of the aspects that are used later. We refer to [5, 6] for a comprehensive introduction to the theory.

One of the predictions or requirements in the best understood version of this theory is that the universe has ten spacetime dimensions. Obviously people do not see ten dimensions in their everyday life, but the compactification of the extra ones on a very small scale renders them invisible to all measurements that have been performed so far.

Superstring theory assumes that the universe is supersymmetric[1], and so attempts to explain all existing particles. In the spectrum of the theory there are gravitons, which are the particles associated to the gravitational field. The low energy limit of string theory is classical supergravity [33], from which Einstein's equations can be recovered.

Now, the worldsheet theory describes the motion of strings. It is understood by worldsheet the two-dimensional surface that strings sweep with their motion. Strings can be open or closed, with the open ones having Dp-branes as their endpoints. D-branes are $p+1$ dimensional (p spatial dimensions plus time) dynamical objects, with their analogous worldvolume. The worldsheet action can be thought of as a two-dimensional field theory. Let σ^1 and σ^2 be the coordinates of the worldsheet, and consider the Euclidean

[1] Supersymmetry [6] is a proposed symmetry which relates bosons and fermions. Supersymmetric string theory is usually called superstring theory.

space complex coordinates

$$w = \sigma^1 + i\sigma^2, \qquad \bar{w} = \sigma^1 - i\sigma^2. \tag{1.3.1}$$

Holomorphic fields are such that they only depend on w, and antiholomorphic fields only depend on $\bar{w}$. In the literature the usual notation is to call left-moving the holomorphic fields and right-moving the antiholomorphic ones. Consider now the theory on a cylinder, which is achieved by compactifying the space coordinate. The world-sheet action for a flat background is then

$$S = \frac{1}{4\pi}\int \mathrm{d}^2 w \left(\frac{2}{\alpha'}\partial_w X^\mu \partial_{\bar{w}} X_\mu + \psi^\mu \partial_{\bar{w}}\psi_\mu + \tilde{\psi}^\mu \partial_w \tilde{\psi}_\mu\right), \tag{1.3.2}$$

where α' is the Regge slope, ψ^μ, $\tilde{\psi}^\mu$ (with the μ index being a spacetime index) are fermions and X_μ are the bosons. In order for the fermion action to be invariant under the periodicity of the cylinder there are two possible choices for the fermions, which separate the theory in two different sectors. When the fermions are periodic the theory is said to be in the Ramond (R) sector, and when they are antiperiodic the theory is said to be in the Neveu-Schwarz (NS) sector. In short,

$$\psi^\mu(w + 2\pi) = e^{2\pi i\nu}\psi^\mu(w), \qquad \tilde{\psi}^\mu(\bar{w} + 2\pi) = e^{-2\pi i\tilde{\nu}}\tilde{\psi}^\mu(\bar{w}), \tag{1.3.3}$$

with $\nu = \tilde{\nu} = 0$ being the R sector and $\nu = \tilde{\nu} = 1/2$ being the NS sector.

Now, black holes in string theory are solutions of the corresponding supergravity theory. If one constructs a configuration of intersecting branes wrapped in the compact dimensions, the dimensional reduction is the black hole geometry. There are simple rules to write some of the black hole geometries that are obtained from brane configurations [34]. This thesis focuses on the D1-D5 system, which means type IIB string theory compactified on $X_4 \times S^1$ with D5-branes wrapping the whole compact space and D1-branes wrapping the S^1. Here X_4 is a four-dimensional compact space, which can be $\mathbb{T}^4$ or $K3$. This system has a supergravity black hole solution that has only D1 charge Q_1 and D5 charge Q_5, with metric [35]

$$\mathrm{d}s^2 = \frac{1}{\sqrt{h_1 h_5}}\left(-\mathrm{d}t^2 + \mathrm{d}z^2\right) + \sqrt{h_1 h_5}\left(\mathrm{d}r^2 + r^2 \mathrm{d}\Omega_3^2\right) + \sqrt{\frac{h_1}{h_5}}\mathrm{d}s^2(X_4), \tag{1.3.4}$$

where r is the radius of the noncompact space, z is the string direction and

$$h_i = 1 + \frac{Q_i}{r^2}, \tag{1.3.5}$$

for the single-centered solution. When adding momentum along the circle we add a third charge, Q_p, and we obtain the three-charge black hole. The metric for this three-charge

black hole then is, using the same notation as above,

$$\begin{aligned} \mathrm{d}s^2 =& \frac{1}{\sqrt{h_1 h_5}}\left(-(\mathrm{d}t^2-\mathrm{d}z^2)+\frac{Q_p}{r^2}(\mathrm{d}z-\mathrm{d}t)^2\right)+ \\ &+\sqrt{h_1 h_5}\left(\mathrm{d}r^2+r^2(\mathrm{d}\theta^2+\cos^2\theta\mathrm{d}\psi^2+\sin^2\theta\mathrm{d}\phi^2)\right)+ \\ &+\frac{2\sqrt{Q_1Q_5Q_p}}{r^2\sqrt{h_1h_5}}(L_1-L_2)(\mathrm{d}t-\mathrm{d}z)(\cos^2\theta\mathrm{d}\psi-\sin^2\theta\mathrm{d}\phi)+\sqrt{\frac{h_1}{h_5}}\mathrm{d}s^2(X_4), \end{aligned} \tag{1.3.6}$$

where L_1 and L_2 are related to the parameters of the metric of the corresponding type IIB solution. See [35] for all the details.

The last thing that needs to be mentioned in this section are orbifolds. Let H be a group of discrete symmetries of some manifold $\mathcal{M}$. Then the coset space $\mathcal{M}/H$ is called an orbifold. In the case of a string theory, this means that the strings will be propagating on the coset space $\mathcal{M}/H$. For example, given a space $\mathcal{M}$, if the spacetime is identified under the reflection of coordinates then the space $\mathcal{M}/\mathbb{Z}_2$ is obtained. This will introduce twisted sectors in the theory, as is shown in chapter 2 with a torus and the symmetric group.

String theory has had many successes, like the derivation of the black hole entropy using a counting of microstates. This is presented in section 1.5, as the calculations of this thesis follow from these early results. However, string theory's biggest success is probably the concrete realisation of the holographic principle [36–38].

1.3.1 Holography and the AdS/CFT correspondence

As mentioned before, the Bekenstein-Hawking black hole entropy formula suggests that all the information of a black hole is somehow encoded on its horizon, that is, on the area that "limits" it. This is the main idea of the holographic principle: in a quantum theory of gravity, the information stored in a volume of spacetime is encoded in the degrees of freedom living on the boundary of that region. The first realisation of the holographic principle was the Anti-de Sitter/Conformal Field Theory (AdS/CFT) correspondence [39–41], and its prime example is $\mathcal{N}=4$ Supersymmetric Yang-Mills theory (SYM) being equivalent (dual) to type IIB superstring theory on an $\mathrm{AdS}_5\times\mathrm{S}^5$ background. A precise mapping between the elements in both theories has been well established since its discovery. This mapping is commonly called the holographic dictionary. See, for instance, [42] for a review.

A remarkable property of this conjectured duality is that it relates the theories when one is at weak coupling and the other at strong coupling. By taking appropriate limits, it can relate a classical string theory to a gauge theory in the 't Hooft limit, or it can also

relate a classical supergravity theory to a strongly coupled gauge theory. All this thesis is focused on a two-dimensional CFT, which is the dual theory of the AdS_3 region that is obtained by taking the near-horizon limit of (1.3.4). The focus in this thesis is put on the three-charge case, the so-called D1-D5-P system, where momentum charge Q_p is added. The CFT description of this system is explained in detail in chapter 2. As a warm up, a very brief introduction to CFT is given in the next section. After that section 1.5 explains how string theory resolves the black hole puzzles.

1.4 Conformal Field Theory essentials

In this section two-dimensional CFTs are introduced. For a comprehensive review see [43] (which this section mainly follows), or [5] for a shorter one. As it has been said in the previous section, the worldsheet of the string is described by a conformal field theory, and so coordinates for a two dimensional CFT have already been introduced in equation (1.3.1). Taking a step back, the conformal group is defined to be the subgroup of coordinate transformations that leave the metric invariant up to an overall scale change. In the two-dimensional case, the CFT is governed by the Virasoro algebra, which is presented in this section.

A field Φ is said to be a primary field of conformal weight $(h, \tilde{h})$ if under a change of coordinates $w \to f(w)$ it transforms as

$$\Phi(w, \bar{w}) \to \left(\frac{\partial f}{\partial w}\right)^h \left(\frac{\partial \bar{f}}{\partial \bar{w}}\right)^{\tilde{h}} \Phi(f(w), \bar{f}(\bar{w})). \tag{1.4.1}$$

Let us recall that $(w, \bar{w})$ are cylinder coordinates. In order to be able to use usual complex analysis tools for the calculations it is common to consider a conformal map to the complex plane, defined by

$$z = e^w. \tag{1.4.2}$$

Now, the standard Noether prescription is used to construct the symmetry generators. The stress-energy tensor $T_{\mu\nu}$ can be obtained considering translations in the world-sheet. In a classical theory with conformal invariance, this tensor is traceless. Also, its conservation implies

$$\bar{\partial} T_{zz} = \partial T_{\bar{z}\bar{z}} = 0 \qquad \Longrightarrow \qquad T(z) = T_{zz}(z),\ \tilde{T}(\bar{z}) = T_{\bar{z}\bar{z}}(\bar{z}). \tag{1.4.3}$$

Leaving the radial ordering implicit, it is important to understand the product of two local operators when they are close together. This is the so-called Operator Product Expansion (OPE): the product of two operators O_1, O_2 can be approximated to arbitrary accuracy

by a sum of local operators O_i,

$$O_1(\sigma_1)O_2(\sigma_2) = \sum_i c_i(\sigma_1 - \sigma_2)O_i(\sigma_2), \tag{1.4.4}$$

where the c_i are numerical coefficients. The conformal transformation properties of an operator Φ can be found by taking the OPE with the stress-energy tensor,

$$\begin{aligned} T(z)\Phi(w,\bar{w}) &= \frac{h}{(z-w)^2}\Phi(w,\bar{w}) + \frac{1}{z-w}\partial_w\Phi(w,\bar{w}) + ... \\ \tilde{T}(\bar{z})\Phi(w,\bar{w}) &= \frac{\bar{h}}{(\bar{z}-\bar{w})^2}\Phi(w,\bar{w}) + \frac{1}{\bar{z}-\bar{w}}\partial_{\bar{w}}\Phi(w,\bar{w}) + ... \,. \end{aligned} \tag{1.4.5}$$

Taking the OPE of T with itself yields

$$T(z)T(w) = \frac{\frac{c}{2}}{(z-w)^4} + \frac{2}{(z-w)^2}T(w) + \frac{1}{z-w}\partial T(w), \tag{1.4.6}$$

where c is a constant which is known as the central charge. Its value is theory dependent.

Consider now the Laurent expansion of the stress-energy tensor,

$$T(z) = \sum_{n\in\mathbb{Z}} z^{-n-2}L_n, \qquad \tilde{T}(\bar{z}) = \sum_{n\in\mathbb{Z}} \bar{z}^{-n-2}\tilde{L}_n. \tag{1.4.7}$$

The exponent $-n-2$ is chosen so that the modes have scaling dimension n, *i.e.* so that under the scale change $z \to z/\lambda$ the modes transform as $L_{-n} \to \lambda^n L_{-n}$. To compute the commutation relations of the modes first the expansions above need to be inverted,

$$L_n = \oint \frac{\mathrm{d}z}{2\pi i} z^{n+1}T(z), \qquad \tilde{L}_n = \oint \frac{\mathrm{d}\bar{z}}{2\pi i} \bar{z}^{n+1}\bar{T}(\bar{z}). \tag{1.4.8}$$

Then the OPE needs to be used, and after that the evaluation of the contour integral can be performed. Doing all this results in the following formulas

$$\begin{aligned} [L_n, L_m] &= (n-m)L_{n+m} + \frac{c}{12}(n^3-n)\delta_{n+m,0} \\ \left[\tilde{L}_n, \tilde{L}_m\right] &= (n-m)\tilde{L}_{n+m} + \frac{\tilde{c}}{12}(n^3-n)\delta_{n+m,0} \\ \left[L_n, \tilde{L}_m\right] &= 0. \end{aligned} \tag{1.4.9}$$

The generators L_n, $\tilde{L}_n$ span two copies of an infinite dimensional algebra, which is called the Virasoro algebra [44]. See appendix A for more details on this.

Now, let $O(z,\bar{z})$ be an operator of conformal dimension $(h,\tilde{h})$. Its adjoint is

$$(O(z,\bar{z}))^\dagger = O\left(\frac{1}{\bar{z}}, \frac{1}{z}\right)\frac{1}{\bar{z}^{2h}}\frac{1}{z^{2\tilde{h}}}. \tag{1.4.10}$$

In analogy with usual Euclidean field theory, since the origin of the complex plane corresponds to negative infinite time in the cylinder (which can be read from the coordinate transformation above, equation (1.4.2)), states are associated with operators as

$$|O\rangle = \lim_{z,\bar{z}\to 0} O(z,\bar{z})\,|0\rangle\,, \tag{1.4.11}$$

where $|0\rangle$ is the vacuum. Similarly,

$$\langle O| = \lim_{z,\bar{z}\to 0} \langle 0|\, O(z,\bar{z}) z^{2h}\bar{z}^{2\tilde{h}}. \tag{1.4.12}$$

For the stress-energy tensor modes, for instance, this gives the following relation

$$L_m^\dagger = L_{-m}. \tag{1.4.13}$$

Now, the vacuum $|0\rangle$ is called the $SL(2,\mathbb{C})$ invariant vacuum, for the following reason. If regularity of

$$T(z)\,|0\rangle = \sum_{n\in\mathbb{Z}} L_n z^{-n-2}\,|0\rangle \tag{1.4.14}$$

is required, as well as for $\langle 0|$ and for the right-moving modes, then the only modes which annihilate them all are subalgebra $\{L_{\pm 1,0}, \tilde{L}_{\pm 1,0}\}$.

One can use the modes of the stress-energy tensor to construct the so-called descendant fields, *i.e.* the remaining fields in the representation of each primary field. Let Φ be a primary field, and ϕ its corresponding state, of weight h. ϕ is then called a highest weight state, and is annihilated by all positive modes of the Virasoro algebra. That is, when considering the state

$$|h\rangle = \phi(0)\,|0\rangle\,, \tag{1.4.15}$$

it satisfies

$$L_0\,|h\rangle = h\,|h\rangle\,, \qquad L_n\,|h\rangle = 0,\ n\in\mathbb{Z}^+. \tag{1.4.16}$$

Descendant states are thus obtained by acting with the negative modes of the stress-energy tensor. Notice that if one wishes to compute the correlation function of L_0 with this state, the whole operator can be plugged in: the positive modes will annihilate $|0\rangle$ and the negative terms will annihilate $\langle 0|$.

Consider now the free massless fermion, described by the action

$$S = \frac{1}{8\pi}\int \left(\psi\bar{\partial}\psi + \tilde{\psi}\partial\tilde{\psi}\right), \tag{1.4.17}$$

where the normalisation is chosen so that

$$\psi(z)\psi(w) = -\frac{1}{z-w}, \qquad \tilde{\psi}(\bar{z})\tilde{\psi}(\bar{w}) = -\frac{1}{\bar{z}-\bar{w}}. \tag{1.4.18}$$

From the OPE with the stress-energy tensor it is found that ψ is a primary field of conformal weight (1/2, 0). From what was said above it can be deduced that the zero mode of the fermion does not change the eigenvalue of L_0, and thus it can be used to raise the spin on a state without modifying its dimension.

In this thesis we work with a SCFT, that is, a supersymmetric CFT. In chapter 2 we present the CFT at hand, which is an extension of what we described above. In appendix A we give its algebra, which should look more familiar now. Since we have already reviewed conformal field theory we can continue with the black hole story.

1.5 Quantum black holes

In the previous sections black holes have been very briefly reviewed, as well as the main problems that arise around them semi-classically. After seeing that their full quantum description is needed in order to resolve the problems, string theory, which nowadays is the most popular candidate for a consistent theory of quantum gravity, has been introduced. Therefore, string theory should be able to give a quantum description of black holes and resolve all the issues that have been mentioned.

Historically, the first result was obtained by Strominger and Vafa [45], preceding the first AdS/CFT results. They were able to reproduce the entropy for the D1-D5-P supersymmetric black hole using D-branes. More precisely, they computed the degeneracy in the brane description, and changing the gravitational strength understood the result in terms of the corresponding black hole. This calculation is possible because there is supersymmetry protection when considering BPS states.

Using the holographic principle this process can be generalised to non-supersymmetric solutions [35]. In the system at hand, since the D1-D5-P black hole has an AdS_3 factor in its near-horizon limit, if one manages to compute the degeneracy in the CFT description using Cardy's formula [46], then the result can be translated in the black hole regime. By doing so an exact match with the Bekenstein-Hawking entropy is found. Namely, by doing a gravity/CFT calculation the entropy of this black hole can be reproduced. This entropy is

$$S_{BH} = 2\pi\sqrt{N_1 N_5 N_p}, \tag{1.5.1}$$

where the charges N_i are related to the Q_i ones introduced in section 1.3 by [35]

$$Q_1 = \frac{N_1 g_s \alpha'^3}{V}, \qquad Q_5 = N_5 g_s \alpha', \qquad Q_p = \frac{N_p g_s^2 \alpha'^2}{R_z^2}, \tag{1.5.2}$$

with V being proportional to the volume of $\mathcal{M}_4$, R_z being the radius of the S^1, g_s the string

coupling and α' the Regge slope. This calculation however does not give any information about the microstates themselves. As it has been pointed out in section 1.2.1, the quantum structure of the microstates has to embrace all the black hole, up to the horizon radius. In general relativity there are the no-hair theorems [47–51], which greatly restrict the geometries that can be written. In string theory these theorems do not apply, as there are many extra fields.

Using the AdS/CFT correspondence the microstates can be characterised. Take the metric (1.3.4) and consider the following limit,

$$\alpha' \to 0, \qquad \frac{r}{\alpha'},\ R_z,\ \frac{V}{\alpha'^2} \text{ fixed.} \tag{1.5.3}$$

This is the decoupling limit; in this limit the black hole has an AdS_3 factor. Similarly, in the three charge case, equation (1.3.6), we obtain the decoupling limit by focusing on the region $r^2 \ll Q_1, Q_5$. Taking the near extremal limit as well, with large Q_1 and Q_5 charges, we find that in this case the metric also has an AdS_3 factor (to be more precise, in this case we find the extremal BTZ black hole; see, for instance, [35] for details). Therefore, the AdS_3/CFT_2 correspondence can be used.

Hence, one should be able to find a CFT state corresponding to each microstate of the black hole. And one should also be able to find the duals of these CFT states, which can be described by asymptotically AdS regular geometries. All the gravity duals are not necessarily classical geometries; this will be discussed in more depth later. Since the near horizon region of the original black hole also has the AdS factor and is asymptotically flat, the asymptotically flat region can also be attached to these microstate geometries. Therefore these black hole microstate geometries look like the black hole up to the horizon scale. Mathur and collaborators found this characterisation of the microstates for eternal, supersymmetric black holes, and called them fuzzballs [52–56].

1.5.1 The fuzzball proposal

Let S be the entropy of the black hole. As stated in the previous sections, associated to a black hole there must be e^S microstates describing it. The fuzzball proposal says that these microstates are regular, horizonless solutions, which give the black hole geometry after a coarse grained average over all of them. So, fuzzballs propose a change at the horizon level, as was required before. This is depicted as a cartoon in figure 1.5.1. Generically fuzzballs are string theory states but, as it will be shown in the next section, a fraction of them can be described in supergravity. The important point here is that only a small fraction of them is visible within supergravity; not all of them [35, 57]. This thesis deals exactly with this last observation: to characterise and count what fraction of the microstates is

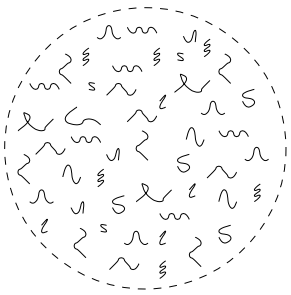

Figure 1.5.1: Cartoon representing a fuzzball. Namely, a graphical representation of a string theory state which is one of the microstates of the black hole.

well described by supergravity, in the three-charge case.

Since the AdS/CFT correspondence is believed to be exact and the dual field theory is unitary, holography implies that the black hole dynamics are unitary. Therefore, there is no information loss [24,58]. This proposal for the microstates deals with all the other initial issues about black holes as well, because the fuzzballs do not have a singularity. They do not have a horizon either, but they still radiate [59, 60], and this radiation matches the expected Hawking radiation for fuzzballs. This radiation does carry information, precisely because there is no horizon [61, 62].

Fuzzballs give a complete description of black holes in string theory and holography. They do not only describe the evaporation process, but also formation and evolution: Mathur showed that a shell of collapsing matter will tunnel to these microstates [63]. The probability of tunneling is exponentially small, but this is compensated by the exponentially large number of microstates (fuzzballs) corresponding to that classical black hole. Also, this collapse and tunneling will happen in a time much shorter than the evaporation time [64], and so the process of formation and evaporation is well described. There is also ongoing work on whether fuzzballs can be observed [65, 66], including their traces on gravitational waves as exotic objects [67]. For reviews on the proposal see [23, 35, 68–70].

This thesis is not centered around the fuzzball proposal itself, but around the study of the CFT duals of some of the microstates in the D1-D5 system. The next section reviews the major developments that have been obtained for this proposal in the last few years.

1.5.1.1 Latest results

There is a long running programme to construct putative black hole microstates as supergravity solutions. This began with the construction of two-charge D1-D5 microstates [52, 56, 71–73]. In this case the corresponding black hole does not have a macroscopic horizon, but this two-charge case is nonetheless a useful arena to construct microstates

explicitly and to make sharp identifications between geometries and the dual CFT states using precision holography [73–75].

For three-charge microstates, the original examples of supergravity solutions were highly non-generic, with, for example, atypically large angular momentum. Early discussions of (non-generic) microstates for macroscopic black holes can be found in [59, 60, 76–81]. Recent constructions of microstates illustrate more generic features, using concepts such as superstrata, see for example [82–100]. As already mentioned, one of the aims of this thesis is to further study what fraction of the black hole microstates such constructions can represent.

Most progress so far has been focused on finding the aforementioned solutions. However there are some recent results on possible traces on gravitational waves caused by the existence of fuzzballs as well [67, 101, 102].

We have just given a broad overview of the fuzzball proposal and the constructions that have been found recently; we leave the more specific context and introduction for the start of each chapter. Closing this introduction comes the outline for the thesis.

1.6 Outline

This thesis deals with the study of the CFT states which are dual to the fuzzball black hole microstates in the D1-D5 system. So far we have given context and presented the proposal, without any explicit technical details. Chapter 2 introduces in full detail the D1-D5 CFT in which the rest of the thesis is based. It reviews the known properties and structure of the theory, and introduces some new details and explicit descriptions that will be used in part II. We also give there some basic notation and results of elementary additive number theory, as it is used throughout this thesis.

Part II deals with the study of correlation and one point functions in this system. In chapter 4 we consider correlation functions involving chiral operators constructed from twist fields. We find explicit expressions for processes involving a twist n operator joining n twist operators of arbitrary twist. These expressions are universal, in that they are independent of the choice of M, the total twist, and the final results can be expressed in a compact form. This result is essential for the calculations of chapter 5. This chapter is based on the publication [1].

Chapter 5 starts by reviewing the known CFT calculations for the field theory side superstrata three charge states, mainly based on [88, 89]. Then, the chapter is divided

in two: in the first part we extend the reviewed calculation, for more generic one point functions, in the short strand case. In the second part of this chapter we calculate the same one point functions again, but now in the long strand limit. The results are general and can be used for a wide range of chiral primaries; we compute explicitly some one point functions to illustrate the process. From these we recover the expected relation between long and short strand one point functions.

Motivated by the results in the previous chapters, in chapter 6 we calculate all possible ways of joining single strands into a state of twist n. Some more results on number theory are introduced, in particular on integer partitions, as they are needed for the countings involved to accomplish this. We give bounds for the one point function for multi-particle states of twist two operators, and compare the result with the twist n one point function. These results, together with chapter 5 have been submitted to the General Relativity and Gravitation topical collection on the Fuzzball Paradigm.

In chapter 7 we gather all the results of part II and comment on them.

Part III has one main chapter, chapter 9, where we take a different approach. Rather than trying to study the microstates themselves, we count directly in the CFT the microstates that have been already constructed. To do so we use some more number theory: reviewing more results on integer partitions we reproduce the entropy of the two-charge case, and count the states that have been found in the three-charge case. We also explain an algorithm to implement this process in a computer program, and present some numerical results which we ran on IRIDIS4, the University of Southampton supercomputer.

Part IV discusses the results of this thesis and explains some of the future work that follows naturally from the results of this thesis.

Last, appendix A gives some more notation and background on the D1-D5 system.

CHAPTER 2

The D1-D5 CFT

In this chapter we introduce the D1-D5 CFT, on which the whole thesis is based. A great and exhaustive review of the D1-D5 system is given in [103,104], where the general picture and the construction and details of the gravity side can be found. This chapter focuses on the CFT side, giving insights on the spectral flow operation and also explicit details and expressions for the operators needed for the calculations.

2.1 Setup

Consider type IIB string theory compactified on $X \times S^1$, with X being $\mathbb{T}^4$ or $K3$. Let N_5 D5-branes wrap the five compact dimensions and N_1 D1-branes wrap the S^1. This is summarised in the standard way in table 2.1.1. X is taken to be string scale and the scale of the S^1 is assumed to be much larger (so that the circle can effectively be treated as non-compact). D1-D5 black hole solutions in the supergravity limit are asymptotic to $M^{4,1} \times S^1 \times X$. The geometry of the decoupled near horizon limit is $\mathrm{AdS}_3 \times S^3 \times X$, and there is supersymmetry enhancement (see [105] and references therein).

The CFT dual to the decoupling region geometry is a two-dimensional superconformal field theory (SCFT). In what follows, the focus is put on the theory for $X = \mathbb{T}^4$, although much of the later analysis of this thesis also holds for $K3$, i.e. it does not rely on features

	0	1	2	3	4	5	6	7	8	9
D1	-	·	·	·	·	-	·	·	·	·
D5	-	·	·	·	·	-	-	-	-	-

Table 2.1.1: Table showing the brane configuration for the D1-D5 system. The lines indicate that the brane is extended in that direction, dots represent perpendicular directions. Dimension 0 is time, 1-4 are the noncompact ones, 5 is the S^1 and 6-9 are X, which can be $\mathbb{T}^4$ or $K3$.

specific to $\mathbb{T}^4$. For toroidal compactifications, the SCFT is an $\mathcal{N} = (4,4)$ superconformal sigma model with central charges $c = \tilde{c} = 6N_1N_5$; this theory can be viewed as a deformation of a free orbifold CFT with target space $(\mathbb{T}^4)^{N_1N_5}/S(N_1N_5)$, where $S(n)$ is the symmetric group. Three point functions of (single trace) chiral primaries are protected in this theory (see [106–109]), and thus agree with the corresponding three point functions calculated in supergravity.

In chapter 5 we calculate one point functions involving chiral primary operators in the field theory. The states involved in such computations have a chiral primary operator O within them. Thus, in general the one point functions can be written as

$$\langle O_1 | \, O_2(y) \, | O_3 \rangle \, . \tag{2.1.1}$$

Therefore, using the relation between states and operators the one point functions calculated in chapter 5 can easily be related to three point functions of the form

$$\langle O_1(x) O_2(y) O_3(z) \rangle \, . \tag{2.1.2}$$

For some of them the dual supergravity one point functions are known, and for the others the matching is yet to be done. We work in Euclidean signature on a cylinder which is parametrised as

$$w = \tau + i\sigma \tag{2.1.3}$$

where $0 \leq \sigma < 2\pi$ and $-\infty < \tau < \infty$.

For the calculations in part II of the thesis it is crucial to understand the orbifold description of the theory, so let us review it. The Hilbert space of the orbifold theory decomposes into twisted sectors, which come from the action of the symmetry group $S(N_1N_5)$. They are thus labelled by the conjugacy classes of the group, which consist of cyclic subgroups of various lengths. See the discussion in [110] for further details. Let $N := N_1N_5$ be the total number of copies of the CFT, m_i the lengths of the different cycles and n_i their multiplicity. Then, in order to have full physical states in the theory

the conjugacy classes must satisfy the constraint

$$\sum_i n_i m_i = N, \tag{2.1.4}$$

where the sum is over all the cycles. There is a direct correspondence between the conjugacy classes and the long/short string picture of the D1-D5 system [111]. The symmetry group of the SCFT is $SU(1,1|2) \times SU(1,1|2)$, which breaks down into the following parts. The $SO(4)_E$ isometry of the S^3 in the gravity side is identified with the $SO(4)$ R-symmetry in the $\mathcal{N} = (4,4)$ superconformal algebra. The other $SO(4)$ symmetry of the field theory is identified with the $SO(4)_I$ of the torus. In subsection 2.1.2 an explicit index description with free fields is given.

At the orbifold point of the theory chiral primaries can be precisely described, as they are associated with the cohomology of X. Hence, chiral primaries in the NS sector are labelled as $\mathcal{O}_m^{(p,q)}$, where m is the twist of that chiral primary and (p,q) refers to its associated cohomology class. The conformal weights $(h, \tilde{h})$ and the R charges $(j_3, \tilde{j}_3)$ of these chiral primaries are given by

$$h^{\rm NS} = j_3^{\rm NS} = \frac{1}{2}(p+m-1), \qquad \tilde{h}^{\rm NS} = \tilde{j}_3^{\rm NS} = \frac{1}{2}(q+m-1). \tag{2.1.5}$$

Recalling the constraint for the cycles mentioned above, the complete set of chiral primaries is built from products adding up to the total twist,

$$\prod_l (\mathcal{O}_{m_l}^{(p_l,q_l)})^{n_l}, \qquad \sum_l n_l m_l = N, \tag{2.1.6}$$

with symmetrisation over N copies of the CFT implicit.

Chiral primaries in the NS sector are mapped to ground states in the R sector via spectral flow. Spectral flow is a deformation of the algebra, under which the quantum numbers of the R ground states transform as

$$h^{\rm R} = h^{\rm NS} - j_3^{\rm NS} + \frac{c}{24}, \qquad j_3^{\rm R} = j_3^{\rm NS} - \frac{c}{12}, \tag{2.1.7}$$

where c is the central charge of the CFT. More details on spectral flow are given in section 2.2. For chiral primaries of associated twist m the central charge is $c = 6m$; the central charge of the full theory is $c = 6N_1N_5$. Analogous expressions hold for the right moving sector. As we just said, NS chiral primaries are mapped by spectral flow to R ground state operators,

$$\prod_l (\mathcal{O}_{m_l}^{(p_l,q_l)})^{n_l} \to \prod_l (\mathcal{O}_{m_l}^{{\rm R}(p_l,q_l)})^{n_l} \tag{2.1.8}$$

with R charges

$$j_3^{\rm R} = \frac{1}{2}\sum_l (p_l - 1)n_l, \qquad \tilde{j}_3^{\rm R} = \frac{1}{2}\sum_l (q_l - 1)n_l. \tag{2.1.9}$$

Note that the Ramond operators obtained from primaries associated with the $(1,1)$ cohomology have zero R charge.

The microstates of the 2-charge D1-D5 black hole are Ramond ground states. The entropy associated to the microstates is

$$S = 2\pi\sqrt{\frac{C(X)N}{6}} \tag{2.1.10}$$

where $C(X)$ is determined by the cohomology. $C = 24$ for $K3$ and $C = 12$ for $\mathbb{T}^4$. However, the corresponding black holes do not have macroscopic horizons. The famous 3-charge black holes with macroscopic horizons discussed in [45] are obtained by exciting the left moving sector with momentum P, and they do have macroscopic horizons. The entropy is then

$$S = 2\pi\sqrt{\frac{C(X)NP}{6}}, \tag{2.1.11}$$

where implicitly it is assumed that $P \gg N$. The generic structure of the 3-charge microstates is thus

$$\mathcal{O}_P \prod_l (\mathcal{O}_{m_l}^{{\rm R}(p_l,q_l)})^{n_l}, \tag{2.1.12}$$

where $\mathcal{O}_P$ describes the excitation of momentum P. As discussed in early works such as [111], most of the 3-charge microstates are associated with excitations over maximal and near maximal twist ground states ("long strings") as there are more ways to fractionate the momentum over such states. This is our motivation to calculate one point functions of chiral primaries for short and long strings and compare their results in chapter 5, and also to count sub classes of microstates and see their distribution in short and long strings in chapter 9.

In chapters 5, 6 and especially in chapter 9 we will be using nomenclature and results of the theory of integer partitions. We introduce all necessary concepts as they are needed throughout the thesis. However, we include a short and introductory section on the topic, with the basic definition and references for further reading. The reader familiar with the concept can skip the next section.

2.1.1 Integer partitions

Let n be a positive integer. A partition of n is a finite non-increasing sequence of positive integers $m_1, ..., m_r$ such that they add up to n,

$$\sum_{i=1}^{r} m_i = n. \tag{2.1.13}$$

The m_i are called the parts of the partition. The total number of partitions of n is denoted by $p(n)$ and is called the partition function. Let us write the partitions for the first six natural numbers as an example.

$$\begin{aligned}
&p(0) = 1 \qquad \text{(the empty sequence)}\\
&p(1) = 1; \quad 1\\
&p(2) = 2; \quad 2,\ \ 1+1;\\
&p(3) = 3; \quad 3,\ \ 2+1,\ \ 1+1+1;\\
&p(4) = 5; \quad 4,\ \ 3+1,\ \ 2+2,\ \ 2+1+1,\ \ 1+1+1+1\\
&p(5) = 7; \quad 5,\ \ 4+1,\ \ 3+2,\ \ 3+1+1,\ \ 2+2+1,\ \ 2+1+1+1,\ \ 1+1+1+1+1.
\end{aligned} \tag{2.1.14}$$

For an exhaustive explanation and results on integer partitions see, for instance, [112]. In parts II and III we introduce more definitions and theorems that derive from this definition. Let us now go back to reviewing the orbifold CFT, by introducing the free field description.

2.1.2 Free field description

In this thesis we do not use explicitly the free field description of the theory for most calculations, but it is necessary to introduce part of it to define the chiral primary operators with which we work. Details of this description and also a complete classification of all chiral primaries for this theory can be found in [103]. Our notation follows closely that of [88] and [89].

Let us first define our notation and conventions. Recalling that $SO(4) \simeq SU(2) \times SU(2)$ we write the $SO(4)$ symmetry associated with the torus as $SU(2)_{\mathcal{C}} \times SU(2)_{\mathcal{A}}$. We label the $SU(2)_{\mathcal{C}}$ group with $\dot{A} = \dot{1}, \dot{2}$, and the $SU(2)_{\mathcal{A}}$ with $A = 1, 2$. The R-symmetry $SO(4)$ group also splits into two $SU(2)$ subgroups, corresponding to the left and right R-symmetry. We use the labels $\alpha, \dot{\alpha}$ to identify them, with $\alpha = \{+, -\}$ and $\dot{\alpha} = \{\dot{+}, \dot{-}\}$. To refer to the copies of the torus we use a subindex (r), which runs from 1 to $N_1 N_5$. Fields and operators corresponding to the right moving sector are denoted with a tilde.

At the orbifold point, the CFT has free fields

$$\left(X^{\dot{A}A}_{(r)}(w,\bar{w}),\psi^{\alpha\dot{A}}_{(r)}(w),\tilde{\psi}^{\dot{\alpha}\dot{A}}_{(r)}(\bar{w})\right), \tag{2.1.15}$$

that is, four bosons and four doublets of fermions. The mode expansion of the fermions in the Ramond sector is

$$\psi^{\alpha\dot{A}}_{(r)}(w)=\sum_{n\in\mathbb{Z}}\psi^{\alpha\dot{A}}_{n(r)}e^{-nw},\qquad \tilde{\psi}^{\dot{\alpha}\dot{A}}_{(r)}(\bar{w})=\sum_{n\in\mathbb{Z}}\tilde{\psi}^{\dot{\alpha}\dot{A}}_{n(r)}e^{-n\bar{w}}, \tag{2.1.16}$$

and they satisfy the following Hermitian properties,

$$\psi^{+\dot{1}\dagger}_{n(r)}=-\psi^{-\dot{2}}_{-n(r)},\qquad \psi^{+\dot{2}\dagger}_{n(r)}=\psi^{-\dot{1}}_{-n(r)}. \tag{2.1.17}$$

The right-moving sector is completely analogous. The Ramond vacuum state, which we denote as $|++\rangle_{(r)}$, is defined by

$$\psi^{+\dot{1}}_{0(r)}|++\rangle_{(r)}=\psi^{+\dot{2}}_{0(r)}|++\rangle_{(r)}=0,\qquad \tilde{\psi}^{+\dot{1}}_{0(r)}|++\rangle_{(r)}=\tilde{\psi}^{+\dot{2}}_{0(r)}|++\rangle_{(r)}=0. \tag{2.1.18}$$

The R-symmetry currents in terms of the free fermions read

$$J^{\alpha\beta}_{(r)}(w)=\frac{1}{2}\psi^{\alpha\dot{A}}_{(r)}(w)\epsilon_{\dot{A}\dot{B}}\psi^{\beta\dot{B}}_{(r)}(w),\qquad \tilde{J}^{\dot{\alpha}\dot{\beta}}_{(r)}(\bar{w})=\frac{1}{2}\tilde{\psi}^{\dot{\alpha}\dot{A}}_{(r)}(\bar{w})\epsilon_{\dot{A}\dot{B}}\tilde{\psi}^{\dot{\beta}\dot{B}}_{(r)}(\bar{w}), \tag{2.1.19}$$

where the operators are normal-ordered with respect to the $|++\rangle_{(r)}$ ground state. Another operator we are interested in is

$$\mathcal{O}^{\alpha\dot{\alpha}}_{(r)}:=-\frac{i}{\sqrt{2}}\psi^{\alpha\dot{A}}_{(r)}\epsilon_{\dot{A}\dot{B}}\tilde{\psi}^{\dot{\alpha}\dot{\beta}}_{(r)}. \tag{2.1.20}$$

Notice that all these operators have been defined to be unitary. Using its zero mode and the zero modes of the standard $SU(2)$ generators of the left R-symmetry current, which are defined as

$$J^3_{(r)}:=-J^{+-}_{(r)}+\frac{1}{2},\qquad J^+_{(r)}:=J^{++}_{(r)}\qquad\text{and}\qquad J^-_{(r)}:=-J^{--}_{(r)} \tag{2.1.21}$$

the other R ground states can be written as

$$|-+\rangle_{(r)}:=J^-_{0(r)}|++\rangle_{(r)},\qquad |+-\rangle_{(r)}:=\tilde{J}^-_{0(r)}|++\rangle_{(r)} \tag{2.1.22}$$

and

$$|00\rangle_{(r)}:=\lim_{z\to 0}\mathcal{O}^{-\dot{-}}_{00(r)}|++\rangle_{(r)}=\frac{1}{\sqrt{2}}\psi^{-\dot{A}}_{0(r)}\epsilon_{\dot{A}\dot{B}}\tilde{\psi}^{\dot{-}\dot{B}}_{0(r)}|++\rangle_{(r)}. \tag{2.1.23}$$

The operator modes change when moving from the NS to the R sector. This change is determined by the spectral flow operation mentioned above. In section 2.2 we give details on how this mode change arises.

Let us turn our attention now to the twisted sector of the theory. The twist (or gluing) operator, which is denoted by $\Sigma_\kappa^{\alpha\dot{\alpha}}$, is an operator which induces a cyclic permutation of $\kappa \geq 2$ copies of elementary fields. This operator is also a chiral primary, and it generates the twisted states. That is, it generates the cycles of length κ. In other words, the twist operator joins κ strings of winding one into a single string of winding κ. The strands of length κ are defined as

$$|++\rangle_\kappa := \lim_{z\to 0} |z|^{\kappa-1} \Sigma_\kappa^{-\dot{-}}(z,\bar{z}) \prod_{r=1}^{\kappa} |++\rangle_{(r)}\,, \tag{2.1.24}$$

where $\Sigma_\kappa^{-\dot{-}}$ is the lowest weight state in the Σ_κ multiplet. This operator has conformal dimensions $(\frac{\kappa-1}{2}, \frac{\kappa-1}{2})$ and, as can be read from the definition above, the state $|++\rangle_\kappa$ in the Ramond sector has spin $(\frac{1}{2}, \frac{1}{2})$ and winding κ. To write the expression of the twist operator Σ_κ in terms of free fields it is necessary to bosonise the fermions. Details on bosonisation and the expression of the twist operator in terms of free fields are left for section A.4 of the appendix. The normalisation of the twist operator is dealt with in section 2.1.7.

Now that the gluing operator has been introduced we can study the twisted sector of the theory. First of all, in order to facilitate the calculations, the fermion basis needs to be changed, in order to obtain independent fields for this sector. To do so we consider the following combinations, which diagonalise the boundary conditions [115]:

$$\psi_\rho^{+\dot{A}}(z) = \frac{1}{\sqrt{\kappa}} \sum_{r=1}^{\kappa} e^{2\pi i \frac{r\rho}{\kappa}} \psi_{(r)}^{+\dot{A}}(z), \qquad \psi_\rho^{-\dot{A}}(z) = \frac{1}{\sqrt{\kappa}} \sum_{r=1}^{\kappa} e^{-2\pi i \frac{r\rho}{\kappa}} \psi_{(r)}^{-\dot{A}}(z), \tag{2.1.25}$$

$$\tilde{\psi}_\rho^{\dot{+}\dot{A}}(\bar{z}) = \frac{1}{\sqrt{\kappa}} \sum_{r=1}^{\kappa} e^{-2\pi i \frac{r\rho}{\kappa}} \tilde{\psi}_{(r)}^{\dot{+}\dot{A}}(\bar{z}), \qquad \tilde{\psi}_\rho^{\dot{-}\dot{A}}(\bar{z}) = \frac{1}{\sqrt{\kappa}} \sum_{r=1}^{\kappa} e^{2\pi i \frac{r\rho}{\kappa}} \tilde{\psi}_{(r)}^{\dot{-}\dot{A}}(\bar{z}), \tag{2.1.26}$$

where $\rho = 0, 1, ..., \kappa - 1$. To obtain the other R ground states in the twisted sector the zero modes of the fermions are used, just as in the untwisted case,

$$|-+\rangle_\kappa = J_{0\rho=0}^{-} |++\rangle_\kappa\,, \qquad |+-\rangle_\kappa = \tilde{J}_{0\rho=0}^{-} |++\rangle_\kappa\,. \tag{2.1.27}$$

Similarly, for the spin zero R ground states we act with the zero mode of $\sum_{r=1}^{\kappa} \mathcal{O}_{(r)}^{-\dot{-}}$,

$$|00\rangle_\kappa = -\frac{i}{\sqrt{2}} \psi_{0\rho=0}^{-\dot{A}} \epsilon_{\dot{A}\dot{B}} \tilde{\psi}_{0\rho=0}^{\dot{-}\dot{B}} |++\rangle_\kappa\,. \tag{2.1.28}$$

The relation between ground states and their associated cohomologies is

$$\mathcal{O}_\kappa^{R(2,2)} \leftrightarrow |++\rangle_\kappa\,, \qquad \mathcal{O}_\kappa^{R(1,1)} \leftrightarrow |00\rangle_\kappa\,, \qquad \mathcal{O}_\kappa^{R(0,0)} \leftrightarrow |--\rangle_\kappa\,, \tag{2.1.29}$$

and

$$\mathcal{O}_\kappa^{R(2,0)} \leftrightarrow |+-\rangle_\kappa\,, \qquad \mathcal{O}_\kappa^{R(0,2)} \leftrightarrow |-+\rangle_\kappa\,. \tag{2.1.30}$$

In the R sector all these states have $h = \tilde{h} = \kappa/4$, while $(j, \tilde{j})$ for these states is $1/2(\alpha, \dot{\alpha})$. For instance, the state $|{+}{+}\rangle_\kappa$ has $(h, j) = (\tilde{h}, \tilde{j}) = (\kappa/4, 1/2)$, and the $|00\rangle_\kappa$ has $(h, j) = (\tilde{h}, \tilde{j}) = (\kappa/4, 0)$. In the NS sector all these correspond to chiral primaries, as we explore in detail in section 2.2 with the spectral flow operation.

In this thesis we only consider ground states associated with even cohomology classes, even though all classes can be straightforwardly considered in part III. In chapter 4 the cohomology notation for the chiral primaries is more convenient, and thus it is the one used. For the calculations in chapter 5, in order to see the effects of the operators more explicitly, the cohomology notation is dropped.

Now that we have twisted sectors we should also give the definitions of the Ramond sector and the Neveu-Schwarz sector in the twisted case. Analogous to the definition for the untwisted case, equation (1.3.3), we now define

$$\begin{aligned} \text{R sector:} \quad & \psi_{(r)} \to \psi_{(r+1)}, \quad \dots, \quad \psi_{(n)} \to \psi_{(1)} \\ \text{NS sector:} \quad & \psi_{(r)} \to \psi_{(r+1)}, \quad \dots, \quad \psi_{(n)} \to -\psi_{(1)}. \end{aligned} \tag{2.1.31}$$

So far we have defined the ground states for a single copy, namely, in the untwisted sector, and we have also seen how to construct the twisted sector ones. We have also defined all the operators for which we will compute one point functions explicitly, but only in the untwisted sector. Most of the explicit calculations in chapter 5 will be using these untwisted operators, but we are also interested in one point functions for twisted operators. Therefore, we define them in the next section.

2.1.3 Operators in the twisted sector

Let us now focus on the chiral primary operators defined in the twisted sector. All chiral primaries from single particle states of the SCFT are listed in [103], and we refer there for the exhaustive list. We calculate one point functions for a subset of them in this paper, but the methods can be easily extended to the rest.

Keeping in mind that the twist operator Σ_κ acts on a product of κ copies, the first twisted operator that would come to mind to extend $\mathcal{O}^{\alpha\dot{\alpha}}_{(r)}$ to κ copies would be to join κ $\mathcal{O}^{\alpha\dot{\alpha}}_{(r)}$ operators using a twist of length κ. This process creates chiral primary operators, but not coming from single particle states. We can see this explicitly by looking at the quantum numbers. Consider for instance the operator

$$\mathcal{O}_\kappa^{+\dot{+},*'} := \Sigma_\kappa \bigotimes_{r=1}^{\kappa} \mathcal{O}^{+\dot{+}}_{(r)}. \tag{2.1.32}$$

It is important to note here that the twist operator and the $\mathcal{O}$ operator act on different groups of copies It is a chiral primary, as it has

$$(h,j) = \left(\frac{\kappa-1}{2},\frac{\kappa-1}{2}\right) + \kappa\cdot\left(\frac{1}{2},\frac{1}{2}\right) = \left(\kappa-\frac{1}{2},\kappa-\frac{1}{2}\right)$$
$$(\tilde{h},\tilde{j}) = \left(\frac{\kappa-1}{2},\frac{\kappa-1}{2}\right) + \kappa\cdot\left(\frac{1}{2},\frac{1}{2}\right) = \left(\kappa-\frac{1}{2},\kappa-\frac{1}{2}\right). \tag{2.1.33}$$

Analogous definitions can be done for the rest of the $\mathcal{O}^{\alpha\dot{\alpha}}$ operators. These are not however "single particle" operators, as we have the product of many $\mathcal{O}^{\alpha\dot{\alpha}}_{(r)}$ operators. Let us be more precise on what we mean by single particle states.

Given a fixed gravity background, single particle states can be thought of as excitations over this background. Thus, if we have two such states, very localised in the gravity background, we can see this as two particles. However, if the two states are bound to each other and the particles cannot be separated out, we would view this as a bound, multi-particle state. As we increase the energy of the state, we can no longer view it in terms of excitations over a fixed gravity background though. Instead, we need to take into account the gravitational backreaction and give a description in terms of the curved geometry. Doing this renders the distinction between a single very heavy particle and multi-particles less clear.

Now, to connect with the one point functions discussed in this thesis, consider the operator $O_m \otimes \mathbb{1}_{N-m}$ with twist m. This would be a single particle state, which would correspond to a single excitation in gravity, that is, some specific fields with specific spherical harmonics of degree $\sim m$. On the other hand, consider now the operator $\prod_{i=1}^{k} O_{m_i}\otimes\mathbb{1}_Q$, where the twists m_i are such that $\sum_i m_i + Q = N$ to make the operator BPS. In this case we would think about this in gravity as being effectively k particles, of different spherical harmonic degrees, all bound together.

The black hole microstates for which we have geometric descriptions are generically the latter, *i.e.* large numbers of particles, all bound together to give a state of specific energy. The energy in this setup is sufficiently high that it cannot be thought in terms of small excitations over an AdS background; the multi-particle state is so energetic that it effectively caused the background geometry to change considerably, reflecting the nature of the bound state of particles.

Coming back to the twisted operators that we are constructing, we can also create analogous chiral primaries with the J currents. For instance, we can consider the κ-twist operator

$$J^{+,*'}_{\kappa} := \Sigma_\kappa \bigotimes_{r=1}^{\kappa} J^{+}_{(r)}, \tag{2.1.34}$$

which has $(h,j) = ((3\kappa-1)/2,(3\kappa-1)/2)$ and $(\tilde{h},\tilde{j}) = ((\kappa-1)/2,(\kappa-1)/2)$ and so is also a chiral primary. As in the previous case, it is important to note that the twist operator and the product of R-symmetry currents act on a different group of copies. We can analogously construct the rest of the J operators this way, and also without the twist operator. The methods for computing one point functions showed in this paper extending the work of [88] can be easily applied to these cases. We will comment on this further in subsection 5.2.9. Hence, it would be interesting to have a better understanding of the gravity duals of all these one point functions.

However, in this thesis, and more in particular in chapter 5, we are concerned with chiral primaries from single particle states. Before we go into details, let us define some conventions that will simplify the expressions and ease the notation. In what follows we will define operators like

$$\Sigma_\kappa \sum_{r=1}^{\kappa} \mathbb{1}_{(1)} \otimes ... \otimes \mathbb{1}_{(r-1)} \otimes \mathcal{O}^{\alpha\dot{\alpha}}_{(r)} \otimes \mathbb{1}_{(r+1)} \otimes ... \otimes \mathbb{1}_{(\kappa)}. \tag{2.1.35}$$

That means, we act trivially on all copies except one, on which we act with the $\mathcal{O}^{\alpha\dot{\alpha}}_{(r)}$ operator. In order to avoid long expressions, we will leave all the identity operators implicit, and instead write

$$\Sigma_\kappa \sum_{r=1}^{\kappa} \mathcal{O}^{\alpha\dot{\alpha}}_{(r)}. \tag{2.1.36}$$

From now on, and throughout this thesis, every time we write an expression like (2.1.36) we are leaving all the identity operators implicit. Let us now write the chiral primaries from single particle states. As we said, they are all listed in [103], and we give only the subset with which we work.

Chiral primaries from single particle states with $h-\tilde{h}=0$: The four chiral primaries with $h-\tilde{h}=0$ corresponding to the (1,1) cohomology are

$$\Sigma_\kappa^{\frac{\kappa-1}{2}} \sum_{r=1}^{\kappa} \psi^{+\dot{1}}_{(r)} \tilde{\psi}^{\dot{+}\dot{1}}_{(r)}, \qquad \Sigma_\kappa^{\frac{\kappa-1}{2}} \sum_{r=1}^{\kappa} \psi^{+\dot{1}}_{(r)} \tilde{\psi}^{\dot{+}\dot{2}}_{(r)}, \qquad \Sigma_\kappa^{\frac{\kappa-1}{2}} \sum_{r=1}^{\kappa} \psi^{+\dot{2}}_{(r)} \tilde{\psi}^{\dot{+}\dot{1}}_{(r)}, \qquad \Sigma_\kappa^{\frac{\kappa-1}{2}} \sum_{r=1}^{\kappa} \psi^{+\dot{2}}_{(r)} \tilde{\psi}^{\dot{+}\dot{2}}_{(r)}, \tag{2.1.37}$$

where the superindex in the twist operator corresponds to its conformal dimension. These chiral primaries have conformal dimension $(\kappa/2,\kappa/2)$. They have one fermion of the left sector and one of the right sector, and so they correspond to the $\mathcal{O}^{\alpha\dot{\alpha}}_n$ operators. Therefore, taking combinations[1] we see that the twisted sector generalisation of the chiral primary

[1] Note that the operators given in (2.1.37) correspond only to the case $\alpha=+$, $\dot{\alpha}=\dot{+}$ of the $\mathcal{O}^{\alpha\dot{\alpha}}_\kappa$ operator. That is because, as is usual in the literature, in [103] only the bottom component of the multiplet is given explicitly. We obtain the other $\mathcal{O}^{\alpha\dot{\alpha}}_\kappa$ operators that we have written above by taking other components of that same multiplet.

$\sum_{r=1}^{\kappa} \mathcal{O}_{(r)}^{\alpha\dot{\alpha}}$ is

$$\mathcal{O}_{\kappa}^{\alpha\dot{\alpha}} := \Sigma_{\kappa}^{\frac{\kappa-1}{2}} \sum_{r=1}^{\kappa} \mathcal{O}_{(r)}^{\alpha\dot{\alpha}}. \tag{2.1.38}$$

The other operators with $h - \tilde{h} = 0$ are obtained with other components of the short multiplet of the twist operator. There is another chiral primary associated to the (2,2) cohomology, which is

$$\Sigma^{\frac{\kappa-2}{2}} \sum_{r=1}^{\kappa} \psi_{(r)}^{+\dot{1}} \psi_{(r)}^{+\dot{2}} \tilde{\psi}_{(r)}^{+\dot{1}} \tilde{\psi}_{(r)}^{+\dot{2}}. \tag{2.1.39}$$

We do not use this operator in this thesis because we only want to raise the spin on the left, as we mentioned before. The sixth and last chiral primary with $h = \tilde{h}$ is the twist operator $\Sigma_{\kappa}^{\frac{\kappa}{2}}$, which also has conformal dimension $(\kappa/2, \kappa/2)$.

Chiral primaries from single particle states with $h - \tilde{h} = 1$: In this case we have

$$\Sigma_{\kappa}^{\frac{\kappa}{2}} \sum_{r=1}^{\kappa} \psi_{(r)}^{+\dot{1}} \psi_{(r)}^{+\dot{2}}, \tag{2.1.40}$$

of conformal dimensions $(\kappa/2 + 1, \kappa/2)$, from which we construct the J_n currents. Notice that in this case $0 \leq \kappa \leq N - 1$. Thus, we define

$$J_{\kappa}^{i} := \Sigma_{\kappa}^{\frac{\kappa}{2}} \sum_{r=1}^{\kappa} J_{(r)}^{i}. \tag{2.1.41}$$

Notice that J_{κ}^{i} and $J_{\kappa}^{i,*}$ have the same transformation under spectral flow, just like $\mathcal{O}_{\kappa}^{\alpha\dot{\alpha}}$ and $\mathcal{O}_{\kappa}^{\alpha\dot{\alpha},*}$ do. To finish this section let us connect these operators to other notation found in the literature (see, for instance, [113]).

Heavy and light operators In the context of one point functions in the D1-D5 system, and more generally in holographic CFT calculations, it is common in some literature to define heavy and light operators [113–115]. These are all primaries, with different conformal weights. Light operators are operators with low conformal dimension relative to the central charge c, and heavy operators have large conformal dimension (of order c). With the definitions that we have given above, if we consider the chiral primary operators alone it is natural to say that heavy operators are the ones we have constructed in the twisted case, using the gluing operator Σ and combinations of fermions. Light operators would then correspond to single trace operators in the untwisted sector.

When looking at the one point functions that we compute in section 5.2 we need to take into account that, in the definition of our states (which we will see in subsection 2.1.5), we have some operators inside the definition of the strands. As we will see mainly in chapter

5, the calculations that we make can be used to calculate both heavy and light one point functions. Now that we have defined all the strands and operators we will briefly review how to construct 1/8-BPS strands, that is, strands where we raise the left R symmetry charge. Further details can be found in [86–90].

2.1.4 Creating 1/8-BPS strands

So far we have only defined the two-charge strands in section 2.1.2. In this section we define three-charge strands. To construct the most general 1/8-BPS strands considered so far in the literature first we need to introduce fractional modes. In a sector of twist κ of our theory one can define [116]

$$J^+_{-\frac{n}{\kappa}} := \oint \frac{\mathrm{d}z}{2\pi i} \sum_{r=1}^{\kappa} J^+_{(r)}(z) e^{-2\pi i \frac{n}{\kappa}(r-1)} z^{-\frac{n}{\kappa}}, \tag{2.1.42}$$

where n is an integer. These modes allow us to increase the R charge of a state by one unit while only raising the conformal dimension by n/κ. Then, given the R ground states that we defined in section 2.1.2, one can add momentum excitations by acting with these fractional modes,

$$\left(J^+_{-\frac{n_\kappa}{\kappa}}\right)^{m_\kappa} |00\rangle_\kappa \,. \tag{2.1.43}$$

We will be writing strands generically like this in section 5.2, but it is important to keep in mind that the total momentum added to the state has to be integral [111]. In chapter 5 the attention is focused on the case when $n = \kappa$, even though the calculation can be easily extended to generic fractional modes. Fractional modes are considered explicitly in chapter 9. This state also shows us why we expect most of the 3-charge microstates to be associated with long strings: the greater κ is, the more possibilities we have to distribute the momentum excitations within the strand. We will see this very clearly when we consider the norm of the states in the next section. This long and short string difference is also our motivation to calculate one point functions in the long strand case.

We now have all the definitions for the strands and operators that we need to calculate all the one point functions that we consider explicitly in this thesis. However, so far we have only considered building blocks of our states. Recalling equation (2.1.4), we see that any state of the full theory must have strands adding up to N. We call states which satisfy this condition physical states, and in the next section we construct all the ones that we use in chapter 5, and give their norm.

2.1.5 Physical states

This section is very closely related to section 3 of [88], but we include it here for completeness. Before we start constructing states let us introduce some notation. We denote by N the total winding number, and $|gs\rangle_{(r)}$ denotes any of the ground states, i.e., $|\pm,\pm\rangle_{(r)}$ or $|00\rangle_{(r)}$, on the copy r of the CFT. When instead of writing a number in parenthesis in the subindex we write a number κ then it denotes a strand of length κ. We consider several copies of each strand, in order to satisfy the condition (2.1.4) and be able to have generic strand lengths. We denote the number of copies of each strand by $N_\kappa^{(gs)}$, where κ is the length of the strand $|gs\rangle_\kappa$. To get the $\frac{1}{8}$-BPS states we use the R-symmetry current, as explained in section 2.1.4. We denote by $N_\kappa^{m_\kappa(00)}$ the number of copies of the three-charge strand, where the new index stands for the number of insertions of the J^+ mode.

Now that we have this notation, let us write a full 1/4-BPS state. Keeping in mind that the total winding number is N we define

$$\psi(\{N_\kappa^{(gs)}\}) := \prod_{gs,\kappa} (|gs\rangle_\kappa)^{N_\kappa^{(gs)}}, \qquad \text{with} \qquad \sum_{gs,\kappa} \kappa N_\kappa^{(gs)} = N, \tag{2.1.44}$$

where $\{N_\kappa^{(gs)}\}$ denotes the partition that satisfies the condition of the total winding being N. We denote by $\mathcal{N}(\{N_\kappa^{(gs)}\})$ the norm of this state. This norm is taken to be the number of combinations in which one can produce $N_\kappa^{(gs)}$ strands $|gs\rangle_\kappa$ starting from the state

$$\bigotimes_{r=1}^{N} |++\rangle_{(r)} \,. \tag{2.1.45}$$

Recall that the Ramond ground states in a single copy have unit norm. Also, once we have created the different strands, there is a unique way to transform them to the desired ground state. We do this by acting with the $\mathcal{O}$ and J operators defined in 2.1.2, which are already normalised. Therefore we only need to consider the creation of the twisted sectors. Starting from the state (2.1.45) there are $\frac{N!}{(N-\kappa)!\kappa}$ possible ways in which we can choose κ of these copies up to cyclic permutations. Taking this number into account every time we construct another twisted sector, we produce the following number of terms

$$\frac{N!}{(N-\kappa_1)!\kappa_1} \frac{(N-\kappa_1)!}{(N-\kappa_1-\kappa_2)!\kappa_2} \cdot \ldots \cdot \frac{(N-\kappa_1-\kappa_2-\ldots-\kappa_{g-1})!}{0!\kappa_g} = \frac{N!}{\prod_{\kappa,S} \kappa^{N_\kappa^{(S)}}}, \tag{2.1.46}$$

where g simply denotes the last term. The normalisation of the twist operator is calculated in this way as well, as we show explicitly in the next section. If we have several strands of the same type it does not matter in what order we got them, and thus we have to divide

by an extra $N_\kappa^{(S)}!$. So, the norm of the physical state (2.1.44) is

$$\mathcal{N}(\{N_\kappa^{(gs)}\}) = \frac{N!}{\prod_{gs,\kappa} N_\kappa^{(gs)}! \kappa^{N_\kappa^{(gs)}}}. \tag{2.1.47}$$

Notice that the states are orthogonal,

$$\left(\psi_{\{N_\kappa^{(gs)}\}}, \psi_{\{N_\kappa'^{(gs)}\}}\right) = \delta_{\{N_\kappa^{(gs)}\},\{N_\kappa'^{(gs)}\}} \mathcal{N}(\{N_\kappa^{(gs)}\}). \tag{2.1.48}$$

Last, we write a dimensionless coefficient $A_\kappa^{(gs)}$ in front of each strand, so that our state describes the CFT dual of a black hole microstate geometry. These coefficients satisfy

$$\sum_{gs,\kappa} |A_\kappa^{(gs)}|^2 = N. \tag{2.1.49}$$

See section 4.2 and [88] for the formulas connecting these coefficients to the corresponding supergravity geometry. Including these $A^{(gs)_\kappa}$ Fourier parameters the physical states are written as

$$\psi_{\{A_\kappa^{(gs)}\}} := \sum_{\{N_\kappa^{(gs)}\}} \left(\prod_{gs,\kappa} A_\kappa^{(gs)}\right)^{N_\kappa^{(gs)}} \psi_{\{N_\kappa^{(gs)}\}} = \sum_{\{N_\kappa^{(gs)}\}} \prod_{gs,\kappa} (A_\kappa^{(gs)} |gs\rangle_\kappa)^{N_\kappa^{(gs)}}, \tag{2.1.50}$$

where the sum is restricted as in (2.1.44).

Now that we have described the $\frac{1}{4}$-BPS state, let us excite it to obtain the $\frac{1}{8}$-BPS one. As we mentioned in (2.1.43), to obtain a three-charge solution we raise the momentum of the states using modes of the $J^\pm$ operators. In chapter 5 we restrict to the -1 mode, as for the one point functions involving only this mode, some of the results have been explicitly matched with its gravity dual [88]. Thus the three-charge states that we consider are written as

$$\psi_{\{N_{\kappa,m_\kappa}^{(S)}\}} = \prod_{s=1}^{4} \prod_{\kappa} (|s\rangle_\kappa)^{N_\kappa^{(s)}} \prod_{\kappa,m_\kappa} \left(\frac{1}{m_\kappa!}(J_{-1}^+)^{m_\kappa} |00\rangle_\kappa\right)^{N_{\kappa,m_\kappa}^{(00)}}. \tag{2.1.51}$$

As we said before, in chapter 9 we start investigating a more general case. To do so we consider more general states with fractional modes for the R-symmetry current. Similar calculations can be performed in that case for the one point functions, as well. In the state (2.1.51) m_κ is the number of insertions of J_{-1}^+. As it is important for this thesis, let us explain carefully the notation and normalisation of the excited state. The operator is acting on a strand of length κ which, with the notation that we introduced above, is equivalent to writing a sum over the copies. That is, when we write the state above it is

shorthand notation for

$$\psi_{\{N^{(S)}_{\kappa,m_\kappa}\}} = \prod_{s=1}^{4}\prod_{\kappa}(|s\rangle_\kappa)^{N^{(s)}_\kappa}\prod_{\kappa,m_\kappa}\left(\frac{1}{m_\kappa!}\left(\sum_{r=1}^{\kappa}J^+_{-1(r)}\right)^{m_\kappa}|00\rangle_\kappa\right)^{N^{(00)}_{\kappa,m_\kappa}}, \tag{2.1.52}$$

which, as always, the sum for J^+ is over any κ copies. Notice that $m_\kappa \leq \kappa$, as otherwise we would have two insertions of the mode on a same copy in every term, and so the resulting term would vanish. Writing the copies out explicitly we have

$$\left(J^+_{-1(1)}\otimes \mathbb{1}_{(2)}\otimes ...\otimes \mathbb{1}_{(\kappa)} + ... + \mathbb{1}_{(1)}\otimes ...\otimes \mathbb{1}_{(\kappa-1)}\otimes J^+_{-1(\kappa)}\right)^{m_\kappa}. \tag{2.1.53}$$

We will thus have $\binom{\kappa}{m_\kappa}$ terms, up to cyclic permutations of the R-symmetry modes. We need to divide by $m_\kappa!$ to get rid of the permutations, as they all correspond to the same state. Also, let us recall that the sum says is over κ strands, but it does not give any information on which κ strands we act on. This will be taken into account by the normalisation of the state. Keeping all these comments in mind, the norm of this three charge state is analogous to the previous one, equation (2.1.47), except for an extra factor accounting for the different combinations in which this operator can act on the strands, as we just mentioned. Therefore, the norm of (2.1.51) is

$$\mathcal{N}(\{N^{(S)}_{\kappa,m_\kappa}\}) = \left(\frac{N!}{\prod_{s,\kappa}N^{(s)}_\kappa!\kappa^{N^{(s)}_\kappa}}\right)\left(\frac{1}{\prod_{\kappa,m_\kappa}N^{(00)}_{\kappa,m_\kappa}!\kappa^{N^{(00)}_{\kappa,m_\kappa}}}\right)\prod_{\kappa,m_\kappa}\binom{\kappa}{m_\kappa}^{N^{(00)}_{\kappa,m_\kappa}}. \tag{2.1.54}$$

As a side comment, let us recall that, as we said above equation (2.1.42), in the twisted sector we have fractional modes. Therefore, when writing the operator in terms of modes of the fermions we have the integer modes, but also all the combinations of the fractional modes that give the desired one.

Let us write now, as in the case of the $\frac{1}{4}$-BPS state, the state dual to the supergravity geometries. Analogous to the previous case, we define the supergravity dual as

$$\begin{aligned}\psi(\{A^{(s)}_\kappa, B_{\kappa,m_\kappa}\}) &:= \sum_{\{N^{(S)}_{\kappa,m_\kappa}\}}\left(\prod_{s,\kappa}A^{(s)}_\kappa\right)^{N^{(s)}_\kappa}\left(\prod_{\kappa,m_\kappa}B_{\kappa,m_\kappa}\right)^{N^{(00)}_{\kappa,m_\kappa}}\psi_{\{N^{(S)}_{\kappa,m_\kappa}\}} = \\ &= \sum_{\{N^{(S)}_{\kappa,m_\kappa}\}}\left(\prod_{s,\kappa}(A^{(s)}_\kappa|s\rangle_\kappa)^{N^{(s)}_\kappa}\prod_{\kappa,m_\kappa}\left(\frac{B_{\kappa,m_\kappa}}{m_\kappa!}(J^+_{-1})^{m_\kappa}|00\rangle_\kappa\right)^{N^{(00)}_{\kappa,m_\kappa}}\right),\end{aligned} \tag{2.1.55}$$

where the condition (2.1.49) also holds, adding now the new B_{κ,m_κ} coefficients. That is, the condition now reads

$$\sum_{gs,\kappa}|A^{(gs)}_\kappa|^2 + \sum_{\kappa,m_\kappa}|B_{\kappa,m_\kappa}|^2 = N. \tag{2.1.56}$$

The norm of the state is

$$|\psi(\{A_\kappa^{(s)}, B_{\kappa,m_\kappa}\})|^2 = \sum_{\{N^{(S)}_{\kappa,m_\kappa}\}} \mathcal{N}(\{N^{(S)}_{\kappa,m_\kappa}\}) \left(\prod_{s,\kappa} |A_\kappa^{(s)}|^{2N_\kappa^{(s)}}\right) \left(\prod_{\kappa,m_\kappa} |B_{\kappa,m_\kappa}|^{2N^{(00)}_{\kappa,m_\kappa}}\right). \tag{2.1.57}$$

We have now defined all ground states and three-charge states that we use throughout this thesis. However, in chapter 5 when calculating one point functions of twisted chiral primaries we will end up with other excited states, for which we will need the normalisation. We dedicate the next section to calculate these normalisations.

2.1.6 Normalisations

Before we calculate the normalisation for the excited states let us review the normalisations of all the operators and of the one point functions themselves. As we have seen in the previous sections, the $\mathcal{O}^{\alpha\dot{\alpha}}$ and the J^i operators are all normalised to one by definition. Also, in the previous section we have normalised the physical states by counting the number of combinations in which we can create them from the untwisted vacuum. As usual, we normalise the untwisted vacuum to one, that is,

$$\left\| |{+}{+}\rangle_{(r)} \right\|^2 = 1. \tag{2.1.58}$$

Therefore, the norm of the physical states is fully determined by the twist operators Σ_κ. This means that this norm is not trivial, and so we will need it when computing one point functions of twist operators. Let us calculate its norm. To calculate the norm of an operator we need to calculate its vacuum expectation value. To do so we need to calculate a two-point function; otherwise the result will be zero. First of all let us recall that the vacuum of the Ramond sector is

$$\bigotimes_{r=1}^{N} |{+}{+}\rangle_{(r)}\,. \tag{2.1.59}$$

Then, the norm of the twist operator is given by

$$|\Sigma_\kappa|^2 = \left(\bigotimes_{r=1}^{N} {}_{(r)}\langle {+}{+}|\right) \Sigma_\kappa^{+\dot{+}} \Sigma_\kappa^{-\dot{-}} \left(\bigotimes_{r=1}^{N} |{+}{+}\rangle_{(r)}\right). \tag{2.1.60}$$

This two-point function is easily calculated with the combinatorics presented in the previous section. Namely, the number of ways in which the $\Sigma_\kappa^{-\dot{-}}$ operator can act is given by the choices of κ objects among N up to cyclic permutations. Formally, the twist operator can act in any of this combinations because when we write the operator Σ_κ this is shorthand

notation for

$$\sum_{\{i_1,\ldots,i_\kappa\}} \Sigma_{(i_1\ldots i_\kappa)}, \tag{2.1.61}$$

where the sum runs over all possible choices of κ copies among the N total ones up to cyclic permutations. The only non-trivial action its complex conjugate can perform is to undo that joining, and so the norm of the twist operator is given by

$$|\Sigma_\kappa^{\alpha\dot{\alpha}}|^2 = \frac{N!}{(N-\kappa)!\kappa}. \tag{2.1.62}$$

This of course coincides with the norm given in equation (2.1.47) when we consider the state $\psi = |{+}{+}\rangle_\kappa \otimes (|{+}{+}\rangle_1)^{N-\kappa}$. We can also calculate the norm of the operators in the twisted sector. Consider for instance the chiral primary

$$\Sigma_\kappa \sum_{r=1}^{\kappa} \mathcal{O}_{(r)}^{\alpha\dot{\alpha}}. \tag{2.1.63}$$

As we said above, the $\mathcal{O}^{\alpha\dot{\alpha}}$ operators are normalised to 1, and so only the twist contributes. Therefore

$$|\Sigma_\kappa \sum_{r=1}^{\kappa} \mathcal{O}_{(r)}^{\alpha\dot{\alpha}}|^2 = \frac{N!}{(N-\kappa)!\kappa}. \tag{2.1.64}$$

Let us finish this section with a general comment regarding the normalisation that we use for the one point functions. We will always normalise them by the norm of the in state[2]. More concretely, if $\mathcal{O}$ is an operator for which we want to calculate the one point function and $|O\rangle$ is the state we are interested in, the results that we will give will be

$$\frac{\langle O|\,\mathcal{O}(y)\,|O\rangle}{\langle O|O\rangle}. \tag{2.1.65}$$

Now that we have the normalisations of all the operators we can find the norm of other excited states in which we will be interested on.

2.1.7 Other excited states

As we have said in section 2.1.3, in chapter 5 paper we will be interested in calculating one point functions for chiral primaries. The untwisted chiral primaries and twist operators will generate other ground states or three-charge states, and so the same states that we have described before will give a non-zero answer for the one point functions. However, the state resulting from acting with a twisted operator on a ground state is not any strand we have discussed before, and so we need to introduce these other excited strands. Consider for instance the operator $\mathcal{O}_\kappa^{+\dot{+}}$ defined by (2.1.38) acting on a ground state $|{+}{+}\rangle_\kappa$. It will

[2]By in state we mean the state for which we calculate the one point function. We will call out state to the state after we act on it with the operator for which we are calculating the one point function

generate an excited state, which we define as

$$|++\rangle^*_\kappa := \lim_{z\to 0} |z|^{\kappa-1}\Sigma^{-\dot{-}}_\kappa \sum_{r=1}^{\kappa} \mathcal{O}^{+\dot{+}}_{00(r)} |++\rangle_\kappa . \tag{2.1.66}$$

In the R sector this is a state with $h = \tilde{h} = \frac{\kappa}{4} + \frac{1}{2}$, $j = \tilde{j} = 1$. We do not use its norm in this thesis though, or the state itself. As we will see in section 5.2.8, we can show how the calculation would be done for these cases. But we will not give the final result, as there is more work to be done in the supergravity side necessary to finish the calculation. We give more details in that section.

Now that we have given a description of the free field theory we focus on the spectral flow operation in the next section. We leave for appendix A further details on this CFT, including OPEs, commutators and the bosonisation formulas.

2.2 Spectral flow

Spectral Flow (SF) [104, 117, 118] is an R-symmetry transformation, where a phase is added to local operators. Namely, it is a continuous deformation of the algebra generators such that after the deformation the operators still satisfy the algebra. Such deformation is possible when we consider a transformation by the angle

$$\eta(z) = is \log z. \tag{2.2.1}$$

We call a transformation by this angle spectral flow by s units. Under this operation, fermions transform as

$$\psi^{\pm\dot{A}}(z) \mapsto z^{\mp\frac{s}{2}}\psi^{\pm\dot{A}}(z), \tag{2.2.2}$$

As we can see, this transformation relates the NS and the R sectors, since odd numbers change the periodicity of the fermions.

Let $\mathcal{U}_s$ be the spectral flow operator. States transform as

$$|\psi'\rangle = \mathcal{U}_s |\psi\rangle \tag{2.2.3}$$

and operators as

$$O'(z) = \mathcal{U}_s O(z) \mathcal{U}_s^{-1}. \tag{2.2.4}$$

As shown in [104], the best way to find how operators transform under SF is by using the bosonised fermions, and writing everything out explicitly. See section A.4 for the details on how to bosonise the fermions. By doing so the following transformations for the

currents are obtained

$$\begin{aligned} J_n^{\pm} &\mapsto J_{n\mp s}^{\pm}, \\ J_n^3 &\mapsto J_n^3 - \frac{cs}{12}\delta_{n,0}, \\ G_n^{\pm A} &\mapsto G_{n\mp\frac{s}{2}}^{\pm A}, \\ T(z) &\mapsto T(z) - \frac{s}{z}J^3(z) + \frac{cs^2}{24z^2}, \\ L_n &\mapsto L_n - sJ_n^3 + \frac{cs^2}{24}\delta_{n,0}. \end{aligned} \tag{2.2.5}$$

Using these transformations the changes in the modes of the operators after the spectral flow operation are also obtained. In order to see how the quantum numbers of the states are transformed we use the modes of L_0 and J_0^3. Given a state with quantum numbers $(L_0, J_3) = (h, j)$, spectral flow generates a new state with

$$L_0 = h + js + \frac{cs^2}{24}, \qquad J_3 = j + \frac{cs}{12}, \qquad s \in \mathbb{Z}. \tag{2.2.6}$$

As we mentioned earlier, with the convention we have chosen spectral flow by an odd amount moves an R state to an NS state. In particular, R ground states map to NS chiral primaries, as we show in the next section. Now, as explained in [84,89] this transformation can also be used to find excited states in the same sector within the theory. Or it can also be used to obtain three-charge states from two-charge ones, when we consider it in a twist sector. This last case is called Fractional Spectral Flow (FSF) [84, 89, 119, 120].

2.2.1 Fractional spectral flow

We will use fractional spectral flow acting on states only, to obtain three-charge ones. The FSF transformation is the same as the SF one, but now we transform by s/κ units, where κ is the length of the strand and s is still an integer. Then, the quantum numbers transform as

$$L_0 = h + \frac{js}{\kappa} + \frac{cs^2}{24\kappa^2}, \qquad J_3 = j + \frac{cs}{12\kappa}. \tag{2.2.7}$$

Now that we have all these definitions, let us use the transformations to relate the states of this system.

2.2.2 R ground states and NS chiral primaries

In this section we show explicitly how spectral flow connects R ground states to NS chiral primaries, as a warm up for the fractional spectral flow case. We focus on two ground

states in particular: the highest weight state $|{+}{+}\rangle$ of the spin $\frac{1}{2}$ multiplet and the "singlet" combination of the $SU(2)_{\mathcal{A}}$ bispinor, $|00\rangle$. We gave their expressions in terms of free fields in section 2.1.2. We can spectral flow these states to the NS sector, which means spectral flow by $s = 1$ units. Any odd integer, positive or negative, would give an NS sector state, but we are looking for chiral primaries. Higher values of $|s|$ would give us an excited state. This applies to both untwisted and twisted sector states, with the only difference that for twisted sector ones the central charge is taken to be $c = 6\kappa$, where κ is the cycle length. Thus, the central charge is dependent of the length of the cycle.

So, let us translate the ground states, that is, the 1/4-BPS states. First,

$$|00\rangle_\kappa : \;\; h = \frac{\kappa}{4}, j = 0 \;\; (\mathrm{R}) \qquad \Longrightarrow \qquad L_0 = \frac{\kappa}{2}, \; J_3 = \frac{\kappa}{2} \;\; (\mathrm{NS}), \tag{2.2.8}$$

which comes from applying equation (2.2.6) with $s = 1$. This state is related to the (1,1) cohomology of $\mathbb{T}^4$. Thus, in the notation of [75] this state, which is a NS chiral primary, is written as $\mathcal{O}_\kappa^{(1,1)4}$, where the superindex 4 stands for the dimension of the (1,1) cohomology[3]. Note also that the spectral flow formula is the same for the left and right sectors, with tildes on h and j for the right sector, of course. Similarly,

$$|{+}{+}\rangle_\kappa : \;\; h = \frac{\kappa}{4}, j = \frac{1}{2} \;\; (\mathrm{R}) \qquad \Longrightarrow \qquad L_0 = \frac{\kappa+1}{2}, \; J_3 = \frac{\kappa+1}{2} \;\; (\mathrm{NS}). \tag{2.2.9}$$

This one is related to the (2,2) cohomology, and thus it can also be written as $\mathcal{O}_\kappa^{(2,2)}$. Last,

$$|{-}{-}\rangle_\kappa : \;\; h = \frac{\kappa}{4}, j = -\frac{1}{2} \;\; (\mathrm{R}) \qquad \Longrightarrow \qquad L_0 = \frac{\kappa-1}{2}, \; J_3 = \frac{\kappa-1}{2} \;\; (\mathrm{NS}), \tag{2.2.10}$$

which is related to the (0,0) cohomology and thus is written as $\mathcal{O}_\kappa^{(0,0)}$. All the relations are summarised in equations (2.1.29) and (2.1.30).

Now, we want to obtain the R sector excited states described in [89], as we will be using them in parts II and III. In order to do so, we spectral flow the R ground states by an amount s/κ, $s \in \mathbb{Z}$, where κ is the length of the cycle (and again, $c = 6\kappa$). This is the fractional spectral flow operation that we have first introduced in section 2.2.1, and the resulting states are $\frac{1}{8}-$BPS states. Before we go into the details though, let us do some checks on FSF.

[3]This dimension is not relevant for this thesis, as it does not play any explicit in the calculations presented.

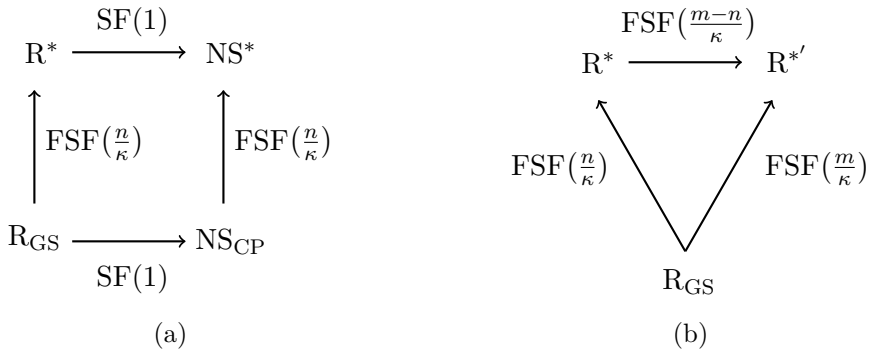

Figure 2.2.1: (Fractional) spectral flow sketch diagrams. R_{GS} stands for Ramond ground state, NS_{CP} for Neveu-Schwarz chiral primary, (F)SF for (fractional) spectral flow, the number in parenthesis right after is the amount by which we (fractional) spectral flow, R^* and NS^* denote excited states (excited with FSF by an amount n/κ, where $n \in \mathbb{Z}$ and κ is the strand length) coming from R ground states and NS chiral primaries respectively, and $^{*'}$ means that we have excited the state by a different amount (m/κ, with $m \in \mathbb{Z}$, $m \neq n$).

2.2.3 Comments on fractional spectral flow

As we just said, fractional spectral flow consists in spectral flowing states by fractional amounts, written as *(integer)/(strand length)*. By doing this we may not change sectors, but instead get an excited state in the same sector. This is more clearly understood in the covering space [116, 121], as there we are spectral flowing by integer amounts and thus we do not change sector. In figure 2.2.1 we make some checks on FSF, to see that everything works as expected. As we can see in the figure and easily prove, FSF is additive, just as the regular SF is. This means that we need to be careful when considering FSF on a state though, as there are cases where we do change sectors after this operation. Let us make more checks to see this explicitly.

Consider figure 2.2.2. As we can see in the subfigure 2.2.2b, starting from an excited Ramond state we can obtain an excited NS state, if the integer number on the numerator is taken appropriately. Similarly, starting from a Ramond ground state we can perform a fractional spectral flow which leads us directly to an excited NS state. For this to happen, however, we need the numerator s to be greater than κ. That is, we are simply adding the two operations, SF(1) and FSF(n/κ), and doing them in a simple step. If we separate the fraction in two we recover the two different steps. Notice also that to go from R^* to $NS^{*'}$, the FSF amount needed may be smaller than κ. So, by writing the integer s in the numerator of FSF in a convenient way, we can effectively do a spectral flow operation which changes the sector of our state, and then a FSF to excite the state. It is also interesting to see the (fractional) spectral flow transformations that we need to do to obtain other states of the same multiplet. For instance, to obtain a state like $NS^{*'}$ but with opposite

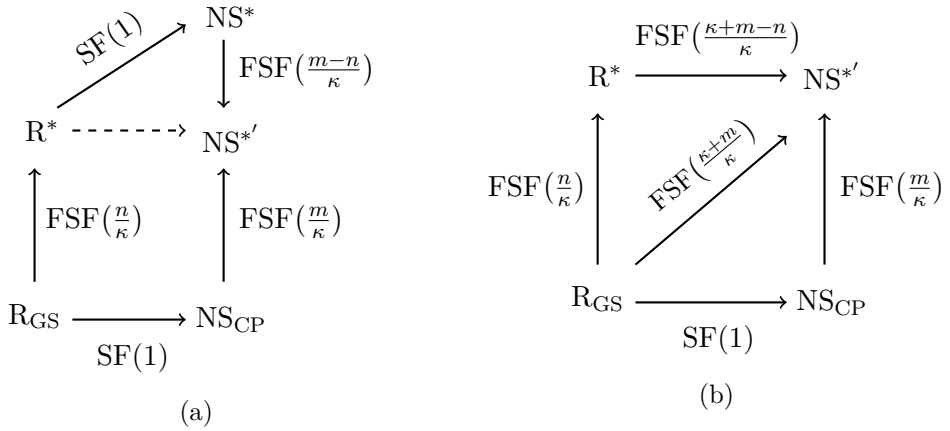

Figure 2.2.2: Same notation as in figure 2.2.1. The diagram on the left holds in general, except for the dotted line, which only holds for κ even. In this case, the diagram on the right also holds and we can FSF from a R ground state to an excited NS state.

J^3 charge we have to apply the following transformations,

$$\mathrm{R}_{\mathrm{GS}} \xrightarrow{\mathrm{FSF}(-\frac{\kappa+m}{\kappa})} \mathrm{NS}^{*',-}. \tag{2.2.11}$$

Notice that, again, this is a combination of a regular spectral flow by -1 units followed by a fractional spectral flow by $-m/\kappa$ units, or the other way around.

Now that we have a more clear idea of how SF and FSF act, we are ready to explicitly construct in the CFT three-charge states like the ones we described in equations (2.1.12) and (2.1.43).

2.2.4 Obtaining the superstrata 1/8-BPS states from FSF

As we mentioned before, in order to obtain three-charge states we have to raise the momentum of a state on the left or right, in order to create a difference in momentum. As we have said, in this thesis we only work explicitly with the case where we raise the R-symmetry current on the left. To do so we act with modes of the R-symmetry current J and, as we have mentioned, this is equivalent in some cases as doing a FSF transformation on a state. The states which can be obtained from FSF are called superstrata, and the relation between both notations is [89].

$$|gs\rangle_{\kappa,s} = \left(J^+_{-\frac{s+2j}{\kappa}}\right)^s |gs\rangle_\kappa \,, \tag{2.2.12}$$

where j denotes the R-symmetry quantum number before FSF. In what follows we use the same notation as in [89], in order to make the connection more transparent. Thus, we write the strand length as $k^2\hat{p}$ for the strands $|00\rangle$, as $k(k\hat{n}+1)$ for the $|{+}{+}\rangle$ and as

	R SECTOR			
	ground states		after FSF	
	h	j	h^*	j^*
$\|00\rangle_{k^2\hat{p}}$	$\frac{k^2\hat{p}}{4}$	0	$h+\hat{p}$	$j+k\hat{p}$
$\|{+}{+}\rangle_{k(k\hat{n}+1)}$	$\frac{k(k\hat{n}+1)}{4}$	$\frac{1}{2}$	$h+\hat{n}$	$j+k\hat{n}$
$\|{-}{-}\rangle_{k(k\hat{m}-1)}$	$\frac{k(k\hat{m}-1)}{4}$	$-\frac{1}{2}$	$h+\hat{m}$	$j+k\hat{m}$

Table 2.2.3: Overview of the R ground states and their quantum numbers. We write the quantum numbers after FSF in terms of their values before FSF to emphasize how the fractional modes of the R-symmetry current act. The FSF amounts considered for each state are, following [89], $s = 2k\hat{p}$ for the $|00\rangle_{k^2\hat{p}}$ strand, $s = 2k\hat{n}$ for $|{+}{+}\rangle_{k(k\hat{n}+1)}$ and $s = 2k\hat{m}$ for $|{-}{-}\rangle_{k(k\hat{m}-1)}$.

$k(k\hat{m}-1)$ for $|{-}{-}\rangle$, where $\hat{p}, \hat{m}, \hat{n}$ are integers. There is another difference in the notation used in this thesis, and that is the spectral flow convention. As we have said, in this thesis the s in the numerator is an integer, and spectral flow by an odd amount changes sectors. With the convention taken in [89] $s \in \frac{1}{2}\mathbb{Z}$, and to move from the R sector to the NS sector the spectral flow amount needed is 1/2. Therefore, the amounts of (fractional) spectral flow we write here need an extra factor of two to generate the same result. We summarise all the superstrata strands considered in [89] in the R sector with this notation before and after FSF in table 2.2.3.

Let us now check which fractional modes of the R-symmetry current can be obtained from FSF. In what follows we do the discussion with the $|{+}{+}\rangle$ states; the result for the other ground states is completely analogous. First we show that $J^+_{-\frac{1}{k}}$ cannot be related to any spectral flow amount. Recall that $|{+}{+}\rangle_{k(k\hat{n}+1)}$ has $(h,j) = \left(\frac{k(k\hat{n}+1)}{4}, \frac{1}{2}\right)$. Then,

$$J^+_{-\frac{1}{k}}\,|{+}{+}\rangle_{k(k\hat{n}+1)} \qquad \text{has} \qquad (h,j) = \left(\frac{k(k\hat{n}+1)}{4} + \frac{1}{k}, \frac{1}{2}+1\right), \tag{2.2.13}$$

but no FSF amount can account for this, because after FSF by an amount $2\hat{r}$, where $\hat{r} := rk(k\hat{n}+1)$ we have

$$h = \frac{k(k\hat{n}+1)}{4} + r + k(k\hat{n}+1)r^2, \qquad j = \frac{1}{2} + k(k\hat{n}+1)r, \tag{2.2.14}$$

and these equations are not consistent with (2.2.13).

We can check which modes do correspond to a FSF. From the calculation above we can see that, if we have only one insertion of the R-symmetry mode, then there is a single mode which can be accounted for with FSF, and that is $\frac{2}{k(k\hat{n}+1)}$. Let us do now the general case, i.e. for s insertions of the mode. Applying the s insertions of the fractional mode we

get

$$\begin{cases} h = \frac{k(k\hat{n}+1)}{4} \\ j = \frac{1}{2} \end{cases} \xrightarrow{(J^+_{-p})^s} \begin{cases} h = \frac{k(k\hat{n}+1)}{4} + ps \\ j = \frac{1}{2} + s \end{cases}, \tag{2.2.15}$$

where $s \in \mathbb{Z}$ (it will correspond to the integer s in the numerator of the FSF amounts in the previous sections) and $p \in \mathbb{Q}$. From FSF, the quantum numbers change like

$$\begin{cases} h = \frac{k(k\hat{n}+1)}{4} \\ j = \frac{1}{2} \end{cases} \xrightarrow{FSF(2\hat{r})} \begin{cases} h = \frac{k(k\hat{n}+1)}{4} + r(1 + k(k\hat{n}+1)r) \\ j = \frac{1}{2} + k(k\hat{n}+1)r \end{cases}, \tag{2.2.16}$$

where $\hat{r}$ has been defined above. Solving for r with the j we get that we need the following amount of FSF:

$$r = \frac{s}{k(k\hat{n}+1)}. \tag{2.2.17}$$

Imposing that both conformal dimensions are the same after the transformation, and assuming $s \neq 0$ (otherwise the transformation is trivial), we obtain

$$p = \frac{1+s}{k(k\hat{n}+1)} \qquad \left(\text{for } |{+}{+}\rangle_{k(k\hat{n}+1)}\right). \tag{2.2.18}$$

This means the following: we can have a FSF corresponding to a mode, for many modes (in short we will see which ones). However, in order to have a FSF that changes the quantum numbers in the same way the fractional mode does, we need multiple insertions of that mode. The relation between the mode and the number of insertions needed in order to have a related FSF is given by (2.2.18). Now, let us recall the result we checked and that is mentioned in [88]: if the number of insertions is greater than the strand length, then the state is annihilated. Therefore, we have a related FSF to the p mode (given by (2.2.18)) for s insertions of the operator, for $1 \leq s \leq k(k\hat{n}+1)$. Thus, the highest mode that has a related FSF is

$$p_{\max} = \frac{1+s_{\max}}{k(k\hat{n}+1)} = \frac{1+k(k\hat{n}+1)}{k(k\hat{n}+1)} = 1 + \frac{1}{k(k\hat{n}+1)}. \tag{2.2.19}$$

We have analogous results for the other two R ground states we considered. The relations analogous to (2.2.18) for the other two cases are

$$p = \frac{s}{k^2\hat{p}}, \qquad \text{for } |00\rangle_{k^2\hat{p}}, \tag{2.2.20}$$

and

$$p = \frac{s-1}{k(k\hat{m}-1)}, \qquad \text{for } |{-}{-}\rangle_{k(k\hat{m}-1)}. \tag{2.2.21}$$

Hence, with FSF we can only obtain certain modes of the R-symmetry current and with a specific number of insertions. All other states obtained by applying other modes, or those modes with with a different number of insertions cannot be expressed in terms of FSF.

	NS SECTOR			
	chiral primaries		after FSF	
	h	j	h^*	j^*
$\mathcal{O}^{(1,1)4}_{k^2\hat{p}}$	$\frac{k^2\hat{p}}{2}$	$\frac{k^2\hat{p}}{2}$	$h+\hat{p}+k\hat{p}$	$j+k\hat{p}$
$\mathcal{O}^{(2,2)}_{k(k\hat{n}+1)}$	$\frac{k(k\hat{n}+1)+1}{2}$	$\frac{k(k\hat{n}+1)+1}{2}$	$h+\hat{n}+k\hat{n}$	$j+k\hat{n}$
$\mathcal{O}^{(0,0)}_{k(k\hat{m}-1)}$	$\frac{k(k\hat{m}-1)-1}{2}$	$\frac{k(k\hat{m}-1)-1}{2}$	$h+\hat{m}+k\hat{m}$	$j+k\hat{m}$

Table 2.2.4: Overview of the NS ground states and their quantum numbers. We write the quantum numbers after FSF in terms of their values before FSF to emphasize how the fractional modes of the R-symmetry current act. The FSF amounts are the same as the ones in table 2.2.3, that is, $s=2k\hat{p}$ for the $|00\rangle_{k^2\hat{p}}$ strand, $s=2k\hat{n}$ for $|{+}{+}\rangle_{k(k\hat{n}+1)}$ and $s=2k\hat{m}$ for $|{-}{-}\rangle_{k(k\hat{m}-1)}$.

We briefly discuss some precision countings of these states in section 9.4.1.

The superstrata states are obtained in the CFT using FSF [89]. Their expression is

$$(|{+}{+}\rangle_k)^{n_1}\prod_{\hat{m},\hat{n},\hat{p}}\left((J^+_{-1/k})^{k\hat{p}}\,|00\rangle_{k^2\hat{p}}\right)^{n_{2,\hat{p}}}\left((J^+_{-1/k})^{k\hat{n}}\,|{+}{+}\rangle_{k(k\hat{n}+1)}\right)^{n_{3,\hat{n}}}\otimes \\ \otimes\left((J^+_{-1/k})^{k\hat{m}}\,|{-}{-}\rangle_{k(k\hat{m}-1)}\right)^{n_{4,\hat{m}}}, \tag{2.2.22}$$

This is the expression we will use in section 9.4.1 to count them. To finish this section we write these states in the NS sector, taking into account the mode transformations for the R-symmetry currents (2.2.5). After SF by 1 unit the modes change by the following amount,

$$\begin{aligned}
\left(J^+_{-\frac{1}{k}}\right)^{k\hat{p}}|00\rangle_{k^2\hat{p}}\quad(\mathrm{R})\qquad&\longleftrightarrow\qquad\left(J^+_{-\frac{1}{k}(1+k)}\right)^{k\hat{p}}\mathcal{O}^{(1,1)4}_{k^2\hat{p}}\quad(\mathrm{NS}),\\
\left(J^+_{-\frac{1}{k}}\right)^{k\hat{n}}|{+}{+}\rangle_{k(k\hat{n}+1)}\quad(\mathrm{R})\qquad&\longleftrightarrow\qquad\left(J^+_{-\frac{1}{k}(1+k)}\right)^{k\hat{n}}\mathcal{O}^{(2,2)}_{k(k\hat{n}+1)}\quad(\mathrm{NS}),\\
\left(J^+_{-\frac{1}{k}}\right)^{k\hat{m}}|{-}{-}\rangle_{k(k\hat{m}-1)}\quad(\mathrm{R})\qquad&\longleftrightarrow\qquad\left(J^+_{-\frac{1}{k}(1+k)}\right)^{k\hat{m}}\mathcal{O}^{(0,0)}_{k(k\hat{m}-1)}\quad(\mathrm{NS}).
\end{aligned}\tag{2.2.23}$$

We give in table 2.2.4 a summary of all the NS chiral primaries used and of their conformal dimension and J^3 charge before and after FSF. and so the superstrata states (2.2.22) in the NS sector read

$$\left(\mathcal{O}^{(2,2)}_k\right)^{n_1}\prod_{\hat{m},\hat{n},\hat{p}}\left(\left(J^+_{-\frac{1}{k}(1+k)}\right)^{k\hat{p}}\mathcal{O}^{(1,1)q}_{k^2\hat{p}}\right)^{n_{2,\hat{p}}}\left(\left(J^+_{-\frac{1}{k}(1+k)}\right)^{k\hat{n}}\mathcal{O}^{(2,2)}_{k(k\hat{n}+1)}\right)^{n_{3,\hat{n}}}\otimes \\ \otimes\left(\left(J^+_{-\frac{1}{k}(1+k)}\right)^{k\hat{m}}\mathcal{O}^{(0,0)}_{k(k\hat{m}-1)}\right)^{n_{4,\hat{m}}}. \tag{2.2.24}$$

Part II

Correlation functions

CHAPTER 3

Introduction

As explained in section 1.5.1.1, precision holography calculations in the D1-D5 system started in [73–75]. Even though the two-charge black hole does not have a macroscopic horizon, several generic lessons from the two-charge system apply to three-charge black holes with macroscopic horizons. Firstly, for the supergravity description to be valid, one needs coherent superpositions of microstates in which (single particle) chiral primaries acquire expectation values. The reason is that single particle chiral primaries are dual to supergravity fields; one needs the former to acquire expectation values for the interior supergravity geometry of the asymptotically AdS region to carry information about the microstate.

Secondly, suppose that a given geometry is postulated to be dual to a particular superposition of microstates $|F)$. The expectation values of single particle chiral primaries $\mathcal{O}_\Delta$, of dimension Δ,

$$(F|\mathcal{O}_\Delta|F) \tag{3.0.1}$$

can then be read off from the asymptotics of the AdS_3 region using Kaluza-Klein holography [122]. The matching of not just conserved charges but of whole towers of operators provides very strong evidence for the conjectured duality. This matching was carried out for low dimension operators in the two charge geometries in [73–75] and in three charge geometries in [88]. Holographic four point functions were discussed in [114, 115]. See also [122, 123] for an example of matching involving the whole tower of Kaluza-Klein op-

erators – the detailed matching between distributed D3-brane supergravity solutions and the Coulomb branch of $\mathcal{N} = 4$ SYM.

The matching of (3.0.1) between the bulk and field theory descriptions relies on being able to compute these expectation values from the dual field theory side and hence, implicitly, uses either non-renormalisation theorems or integrability/bootstrap methods. In the case of the D1-D5 system, one can explicitly compute correlation functions in the orbifold limit of the dual CFT. Correlation functions involving chiral primaries are believed to be non-renormalised as one deforms away from the orbifold point [106–109] although the matching between CFT and supergravity is subtle. This non-renormalisation implies that (3.0.1) is non-renormalised away from the orbifold point for two-charge microstates and it also has implications for expectation values of supergravity operators in three-charge microstates.

Correlation functions in the orbifold CFT have been analysed for a variety of applications previously. In what follows here, we will use heavily the pioneering work of Lunin and Mathur on computing three point functions in (super)conformal orbifold theories [116, 121]. An important part of understanding the D1-D5 system is deforming the CFT away from the orbifold limit, and the deformation process has been considered in a number of works [87, 124–140]. The methodology used here is closely related to that of [88, 131, 132], although our motivations are somewhat different. Efficient methods for computing certain extremal correlation functions in the orbifold theory and relations with spin chains were studied in [141–143].

In this part of the thesis we present work which develops the precision holography programme for black hole microstates in the D1-D5 system further. More precisely, in chapter 5 we calculate one point functions of the form (3.0.1), from the CFT side. In order to carry out such calculations, we first need to fill in certain gaps in the previous literature on correlation functions in the orbifold CFT; to be able to access expectation values for generic dimension operators, we need as a building block amplitudes involving twist n operators joining together n other twist operators.

To that end, in chapter 4 we compute them, that is, we compute amplitudes for processes in the orbifold CFT involving a twist n operator joining n operators, each of twist m_i. We solve this problem for general n and m_i. The general result is summarised in equation (4.3.102). Last, in chapter 6 we calculate one and n-point functions of twist operators, similar to the calculations performed in chapter 5, in order to start investigating the relation between them and check the preferred way of creating long strands. Notice that all these calculations can also be used as building blocks for correlation and one point functions involving less supersymmetric operators. We finish this part of the thesis with a summary of all the main results and a discussion, in chapter 7.

CHAPTER 4

Correlation function for a twist n operator

This chapter deals with correlation functions involving chiral operators constructed from twist fields. We find explicit expressions for processes involving a twist n operator joining n twist operators of arbitrary twist. These expressions are universal, in that they are independent of the choice of M, and the final results can be expressed in a compact form.

4.1 Layout

The plan of this chapter is as follows. In section 4.2 we explain why processes involving a twist n operator joining n other operators are essential to calculating expectation values of the form (3.0.1) from the field theory side. Section 4.3 contains the technical computation of the amplitude for such processes.

4.2 Twist operator amplitudes

In this chapter we focus on processes in which a twist operator of twist n joins n operators of twists $(m_1, m_2, ..., m_n)$, to form a single operator of twist $M := (m_1 + ... + m_n)$. Following the usual correspondence between twist operators and strings, we illustrate these operators

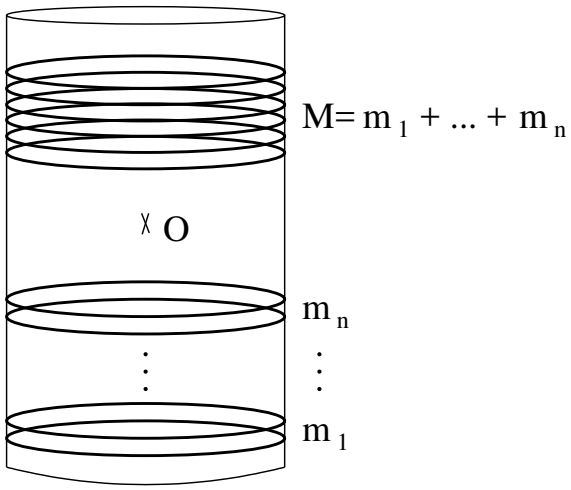

Figure 4.2.1: Joining of n component strings to form one single string.

via strings with winding equivalent to the twist. The process of interest is illustrated in figure 4.2.1.

Let us consider the following example of such a process, expressed first in NS sector language. Let each component string be generated by a chiral primary i.e.

$$\mathcal{O}_{m_i}^{(p_i,q_i)}|0\rangle_{m_i}. \tag{4.2.1}$$

Let the operator of twist n joining these component strings be a chiral primary as well, which we denote as

$$\mathcal{O}_n^{(p,q)}. \tag{4.2.2}$$

The joining process then acts as

$$\mathcal{O}_n^{(p,q)}|\prod_{i=1}^{n}\mathcal{O}_{m_i}^{(p_i,q_i)}\rangle \to |\chi\rangle. \tag{4.2.3}$$

Notice that all operators have maximum J^3 eigenvalue, *i.e.* they are the highest weight state of the spin multiplet. Here the state $|\chi\rangle$ by construction has R charges

$$j_3^{NS} = \frac{1}{2}\left(p + \sum_{i=1}^{n} p_i\right) + \frac{1}{2}M - \frac{1}{2} \qquad \tilde{j}_3^{NS} = \frac{1}{2}\left(q + \sum_{i=1}^{n} q_i\right) + \frac{1}{2}M - \frac{1}{2}. \tag{4.2.4}$$

We begin by considering processes in which

$$\left(p + \sum_{i=1}^{n} p_i\right) = P \leq 2 \qquad \left(q + \sum_{i=1}^{n} q_i\right) = Q \leq 2 \tag{4.2.5}$$

for which

$$|\chi\rangle = e^{\mathcal{O}_c}|\mathcal{O}_M^{(P,Q)}\rangle \tag{4.2.6}$$

where $e^{\mathcal{O}_c}$ describes coherent excitations of zero R charge over the NS chiral primary.

By construction the one point function

$$\langle \mathcal{O}_M^{(P,Q)} | \mathcal{O}_n^{(p,q)} (\mathbb{1})^{M-n} | \prod_{i=1}^{n} \mathcal{O}_{m_i}^{(p_i,q_i)} \rangle \tag{4.2.7}$$

is thus (generically) non-zero. In this expression we include explicitly the factor of $(M-n)$ copies of the identity operator, to emphasise that this correlation function is computed in M copies of the CFT.

The one point function (4.2.7) is not a "physical" one point function in the orbifold CFT as we have imposed neither $M = N$ nor symmetrisation over copies of the CFT, and we have not specified the full state. However, (4.2.7) is an important building block for physical one point functions of interest in the context of D1-D5 holography. For example, the one point function contribution (4.2.7) is relevant to the computation of one point functions of single trace chiral primary operators in Ramond ground states. Spectral flow of (4.2.7) gives

$$\langle \mathcal{O}_M^{R(P,Q)} | \mathcal{O}_n^{NS(p,q)} | \prod_{i=1}^{n} \mathcal{O}_{m_i}^{R(p_i,q_i)} \rangle. \tag{4.2.8}$$

The basis of Ramond ground states in the orbifold CFT was described in chapter 2. Since each Ramond ground state is an eigenstate of J^3 and $\tilde{J}^3$, the expectation of a single trace chiral primary (with non zero R charge) is necessarily zero. However, R ground states that admit holographic supergravity duals can be expressed in terms of projections of coherent superpositions [73, 75], i.e. as

$$|\mathcal{O}_c^R\rangle = \sum_A c_A |\mathcal{O}_A^R\rangle \tag{4.2.9}$$

where A labels the complete set of Ramond ground states and the coefficients c_A are inherited from projections of coherent superpositions.

More precisely, there is a direct correspondence between the curves describing the holographic supergravity solutions and these coherent superpositions, described in detail in [73,75]. In brief, the curves $\mathcal{F}(v)$ describing the supergravity solutions can be decomposed into Fourier modes

$$\mathcal{F}(v) = \sum_{n>0} \frac{1}{\sqrt{n}} \left(\alpha_n e^{-inv} + \alpha_n^* e^{inv} \right). \tag{4.2.10}$$

Now introduce auxiliary harmonic oscillators as operators, $\hat{a}_n$, and define coherent states associated with these operators as

$$\hat{a}_n \, |\alpha_n) = \alpha_n \, |\alpha_n) \,. \tag{4.2.11}$$

There is thus a coherent state associated with the curve

$$|\mathcal{F}) = \prod_n |\alpha_n) \tag{4.2.12}$$

The coherent states can be expressed in terms of Fock states in the standard way as

$$|\alpha_n) = \exp\left(-\frac{|\alpha_n|^2}{2}\right) \sum_k \frac{\alpha_n^k}{k!} (\hat{a}_n^\dagger)^k \, |0\rangle \,, \tag{4.2.13}$$

and we can then project from $|\mathcal{F})$ the Fock states that satisfy the constraint

$$\prod (\hat{a}_{n_l}^\dagger)^{m_l} |0\rangle \qquad \sum_l n_l m_l = N_1 N_5. \tag{4.2.14}$$

The final step is to retain only these terms from $|\mathcal{F})$ and map the auxiliary harmonic oscillators to CFT R operators. The Ramond ground state operators are in one-to-one correspondence with the cohomology of the target space for the orbifold CFT; thus the number of independent curves defining the supergravity geometries is given by the sum of the Hodge numbers of this target space. The result indeed gives a linear superposition of Ramond ground states (4.2.9) with superposition coefficients c_A inherited from the defining curves.

An important feature of the superposition (4.2.9) is that it is not in general an eigenstate of R symmetry. This implies that charged operators can acquire expectation values in this state. One can extract these expectation values from the supergravity solutions via holographic renormalisation. For the D1-D5 ground states, non-renormalisation theorems are believed to exist, implying that these expectation values match between supergravity and the CFT in the orbifold limit (although the required matching between supergravity and CFT operators is subtle [109]).

Hence in a generic superposition the expectation of a single trace operator is

$$\langle \mathcal{O}_c | \mathcal{O}_n^{p,q} | \mathcal{O}_c \rangle = \sum_{A,B} c_A^* c_B \langle \mathcal{O}_A^R | \mathcal{O}_n^{p,q} | \mathcal{O}_B^R \rangle. \tag{4.2.15}$$

It is now apparent that (4.2.8) is a building block for computing such one point functions: non-vanishing terms in this one point function are associated with the twist n operator joining component strings.

Computation of (4.2.15) for general twist n operators would allow precision holography for two charge microstates to be tested further, using the methods of [73–75]. A good understanding of (4.2.15) is also needed to calculate one point functions of supergravity operators (single particle chiral primaries) in three charge microstates, as shown in chapter 5. A typical 3-charge microstate is built out of superpositions of Ramond ground states

excited by left moving momenta as in (2.1.43). The one point functions will then reduce to sums of amplitudes of the type

$$\langle \mathcal{O}_{P_A} \mathcal{O}_A^R | \mathcal{O}_n^{p,q} | \mathcal{O}_{P_B} \mathcal{O}_B^R \rangle, \tag{4.2.16}$$

where $\mathcal{O}_{P_A}$ and $\mathcal{O}_{P_B}$ denote the operators exciting left moving momenta over the ground states. For excitations such as (2.1.43) one can then use commutation relations to reduce this calculation to (4.2.15); this will be discussed in future work. Note that it is the one point functions of single particle chiral primaries (single strings) that are of most interest in matching holographically with microstate geometries, as it is these values that are captured by the asymptotics of the interior AdS_3 regions.

4.3 Computation of twist operator expectation values

In this section we focus on the computation of

$$\langle \mathcal{O}_M^{R(P,Q)} | \mathcal{O}_n^{NS(p,q)} | \prod_{i=1}^{n} \mathcal{O}_{m_i}^{R(p_i,q_i)} \rangle. \tag{4.3.1}$$

Our methods follow the approach pioneered by [116, 121] and used in the case of a twist two operator in [131, 132].

The one point function is computed on the cylinder, with the operator inserted at the location w_0, i.e. the explicit computation that is required is

$$\langle \mathcal{O}_M^{R(P,Q)} | \mathcal{O}_n^{NS(p,q)}(w_0) | \prod_{i=1}^{n} \mathcal{O}_{m_i}^{R(p_i,q_i)} \rangle. \tag{4.3.2}$$

Note that the dependence on w and w_0 is fixed by conformal invariance. The Ramond ground states are eigenstates of L_0 and $\tilde{L}_0$ and thus one can freely use translations to move the insertion point around the cylinder. In practice we calculate this one point function by lifting to a covering space, and computing the appropriate $(n+2)$ point function. We begin by discussing the required maps to covering spaces.

4.3.1 Maps to covering space

We begin by working on a cylinder with coordinate w. The cylinder is mapped to the complex plane using the standard exponential map $z = \exp(w)$. The CFT fields are however multi-valued on the z plane due to the presence of the twist fields. We thus map to a covering space with coordinate t where the fields are single valued. The twist

operators are punctures on the t plane.

We can regulate the single component string insertions using the following map from the z plane to the t plane, in analogy to the map used in [131, 132]:

$$z = t^{m_1}(t-a_2)^{m_2}(t-a_3)^{m_3}\cdot ...\cdot (t-a_n)^{m_n}. \tag{4.3.3}$$

On the cylinder the initial component strings are at $w \to -\infty$, which corresponds to $z = 0$ on the z plane. On the t plane a string of winding m_i is mapped to position a_i; we set $a_1 = 0$ for simplicity, without loss of generality in what follows. The final component string is at $w \to \infty$ on the cylinder, which maps to $t \to \infty$ on the plane. The twist n operator is inserted at w_0 on the cylinder which corresponds to $\exp(w_0)$ on the z plane.

A priori the parameters a_i are not fixed in terms of the original parameter w_0 on the cylinder. However, the ramification map should be such that dz/dt has a zero of order $(n-1)$ at the location of the twist n operator. Let t_0 be the location of the twist n operator; then

$$\frac{dz}{dt} = (t-t_0)^{n-1}P_{M-n}(t) \tag{4.3.4}$$

with $P_{M-n}(t)$ a polynomial of order $(M-n)$ with no zero at t_0. We can understand this as follows. The map (4.3.3) is a polynomial of order M with M non-distinct zeros: it has a zero of order m_a at $t = 0$ and so on. Thus its first derivative is a polynomial of order $(M-1)$. Now dz/dt has a total of $(M-n)$ zeros at locations a_i: it has a zero of order (m_1-1) at $t = 0$, a zero of order (m_2-1) at $t = a_2$ etc. By the fundamental theory of algebra, dz/dt has an additional $(n-1)$ zeros, and these are located at the position of the twist n operator.

The original map (4.3.3) has $(n-1)$ parameters $(a_2, ..., a_n)$. These parameters are determined by the condition that dz/dt has a zero of order $(n-1)$ at the location t_0. Note that t_0 is related to the original insertion point on the cylinder via the map

$$\exp(w_0) = t_0^{m_1}(t_0 - a_2(t_0))^{m_2}(t_0 - a_3(t_0))^{m_3}\cdot ...\cdot (t_0 - a_n(t_0))^{m_n} \tag{4.3.5}$$

where here we indicate that the positions a_i can be expressed as functions of t_0.

Let us first illustrate these general discussions in the context of $n = 3$; the case of $n = 2$ is discussed in detail in [131, 132]. For $n = 3$ the ramification map is

$$z = t^{m_1}(t-a_2)^{m_2}(t-a_3)^{m_3} \tag{4.3.6}$$

and thus

$$\frac{dz}{dt} = t^{m_1-1}(t-a_2)^{m_2-1}(t-a_3)^{m_3-1}\left(m_1(t-a_2)(t-a_3)+m_2t(t-a_3)+m_3t(t-a_2)\right). \tag{4.3.7}$$

The requirement that this takes the form (4.3.4) imposes

$$a_2 = \bar{a}_2 t_0 \qquad a_3 = \bar{a}_3 t_0 \tag{4.3.8}$$

where $(\bar{a}_2, \bar{a}_3)$ satisfy

$$\bar{a}_2\bar{a}_3 = \frac{M}{m_1}; \qquad \bar{a}_2\left(1-\frac{m_2}{M}\right)+\bar{a}_3\left(1-\frac{m_3}{M}\right) = 2. \tag{4.3.9}$$

These equations can be solved to give

$$\bar{a}_2\left(1-\frac{m_2}{M}\right) = 1 \pm i\sqrt{\frac{m_2m_3}{m_1M}} \qquad \bar{a}_3\left(1-\frac{m_3}{M}\right) = 1 \mp i\sqrt{\frac{m_2m_3}{m_1M}}. \tag{4.3.10}$$

With these solutions we can relate w_0 and t_0 as

$$\exp(w_0) = t_0^M(1-\bar{a}_2)^{m_2}(1-\bar{a}_3)^{m_3}. \tag{4.3.11}$$

Clearly the relation between t_0 and w_0 is not unique; we will clarify this issue below in the case of general n.

We can now immediately generalise to arbitrary $n \geq 2$. The ramification map is

$$z = t^{m_1}\prod_{i=2}^{n}(t-a_i)^{m_i} \tag{4.3.12}$$

and the requirement that $t = t_0$ is a zero of dz/dt of order $(n-1)$ (4.3.4) imposes $(n-1)$ relations on the a_i: $a_i = \bar{a}_i t_0$ with

$$\prod_{i=2}^{n}\bar{a}_i = \frac{M}{m_1} \qquad n \geq 2, \tag{4.3.13}$$

together with $(n-2)$ further conditions

$$\begin{aligned}
&\sum_{i=2}^{n}\bar{a}_i\left(1-\frac{m_i}{M}\right) = (n-1) \qquad n \geq 3 \\
&\sum_{i=1}^{n}m_i\sum_{l\neq n\neq i}\bar{a}_n\bar{a}_l = M\frac{(n-1)(n-2)}{2} \qquad n \geq 4
\end{aligned} \tag{4.3.14}$$

and so on. For example, for $n \geq 5$ we would in addition need the cubic relation between the $\bar{a}_i$. Note that for $n = 2$ we can immediately read off $\bar{a}_2 = M/m_1$ from the expression above, which is in agreement with the ramification map used in [131, 132].

In analogy to the $n = 3$ case, it is natural to write the solutions of these equations as

$$\left(1 - \frac{m_i}{M}\right) \bar{a}_i = (1 + \bar{a} \exp(i\phi_i)) \tag{4.3.15}$$

where the phases ϕ_i satisfy

$$\prod_{i=2}^{n} \exp(i\phi_i) = 1 \qquad n \geq 3 \tag{4.3.16}$$

and

$$\begin{aligned} \sum_{i=2}^{n} \exp(i\phi_i) &= 0 \qquad n \geq 3 \\ \sum_{i \neq j} \exp(i(\phi_i + \phi_j)) &= 0 \qquad n \geq 4 \\ \sum_{i \neq j \neq k} \exp(i(\phi_i + \phi_j + \phi_k)) &= 0 \qquad n \geq 5, \end{aligned} \tag{4.3.17}$$

and so on. Solutions for these phases are:

$$\begin{aligned} (n-1) \in 2Z: \quad & \phi_i = \frac{(i-1)\pi}{n-1}, \quad \phi_{i+1} = -\frac{(i-1)\pi}{n-1}, \quad i \in 2Z, \quad i \geq 2 \\ n \in 2Z: \quad & \phi_2 = 0, \quad \phi_i = \frac{(i-1)\pi}{n-1}, \quad \phi_{i+1} = -\frac{(i-1)\pi}{n-1}, \quad (i-1) \in 2Z, \quad i \geq 3. \end{aligned} \tag{4.3.18}$$

Note that these solutions are not unique, i.e. any permutation of the phases will also solve the equations. One can also shift all of the phases by an equal amount, that is, $\phi_i \to \tilde{\phi}_i = \phi_i + \lambda$, satisfying (4.3.17), but now instead of (4.3.16) one has

$$\prod_{i=2}^{n} \exp(i\phi_i) = \exp(i(n-1)\lambda). \tag{4.3.19}$$

This shift can trivially be absorbed into the parameter $\bar{a}$ in (4.3.15) and thus we can always set $\lambda = 0$ without loss of generality.

The parameter $\bar{a}$ in (4.3.15) satisfies

$$1 + \bar{a}^{n-1} = \frac{M}{m_1} \prod_{i=2}^{n} \left(1 - \frac{m_i}{M}\right). \tag{4.3.20}$$

We can solve this equation as follows. First note that

$$m_1 = M - \sum_{i=2}^{n} m_i \tag{4.3.21}$$

and introduce the notation $\nu_i := m_i/M$, where clearly $0 < \nu_i < 1$. Then

$$\bar{a}^{n-1} = \frac{\prod_{i=2}^{n}(1-\nu_i)}{(1-\sum_{i=2}^{n}\nu_i)} - 1. \tag{4.3.22}$$

Now for $n > 2$

$$\prod_{i=2}^{n}(1-\nu_i) > \left(1 - \sum_{i=2}^{n}\nu_i\right). \tag{4.3.23}$$

This follows from induction: if one assumes that the identity holds for n then for $(n+1)$

$$\begin{aligned}\prod_{i=2}^{n+1}(1-\nu_i) &= (1-\nu_{n+1})\prod_{i=2}^{n}(1-\nu_i) \\ &> (1-\nu_{n+1})\left(1-\sum_{i=2}^{n}\nu_i\right) > \left(1-\sum_{i=2}^{n+1}\nu_i\right).\end{aligned} \tag{4.3.24}$$

The identity is true for $n = 3$ as

$$(1-\nu_2)(1-\nu_3) > (1-\nu_2\nu_3) \tag{4.3.25}$$

and therefore by induction (4.3.23) holds for all $n \geq 3$.

Hence we may write

$$\bar{a}^{n-1} =: Q = \frac{1}{\nu_1}\prod_{i=2}^{n}(1-\nu_i) - 1 \tag{4.3.26}$$

where $Q \in \mathbb{Q}^+$. The $(n-1)$ roots of this equation are

$$\bar{a} = Q^{\frac{1}{n-1}} \exp\left(\frac{2\pi i k}{n-1}\right), \tag{4.3.27}$$

with $k = 0, 1, ..., (n-2)$. We can however fix $k = 0$ so that $\bar{a}$ is real: other choices of k are equivalent to rotations of the phases ϕ_i.

Thus for general n we have concluded that the map between w_0 and t_0 (4.3.5) takes the form

$$\exp(w_0) = t_0^M \prod_{i=2}^{n}(1-\bar{a}_i)^{m_i} \tag{4.3.28}$$

where

$$\bar{a}_i = \frac{(1+\bar{a}\exp(i\phi_i))}{(1-\nu_i)} \tag{4.3.29}$$

with $\bar{a}$ given by (4.3.27) and the phases ϕ_i given by (4.3.18). It is useful to illustrate the structure of this ramification map as follows. If we consider the combinations

$$A_i = \bar{a}_i(1-\nu_i) \tag{4.3.30}$$

then the A_i are located at the vertices of a regular n-sided polygon, with centre one, as

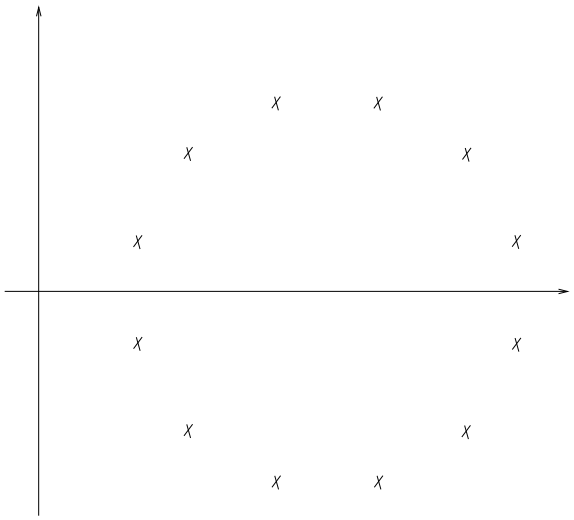

Figure 4.3.1: Illustration of structure of ramification map; the crosses denote A_i.

shown in Figure 4.3.1.

4.3.2 Computation of the one point function

In this section we explain how the required one point function (4.3.2) can be computed in terms of a correlation function in the t plane. The methodology follows closely [131, 132], which in turn exploited the techniques for computing orbifold CFT correlation functions developed in [116, 121].

The one point function (4.3.2) is calculated by first lifting to the z plane to give

$$\langle \mathcal{O}_M^{R(P,Q)} | \mathcal{O}_n^{NS(p,q)}(z_0) | \prod_{i=1}^{n} \mathcal{O}_{m_i}^{R(p_i,q_i)} \rangle = \langle \mathcal{O}_M^{R(P,Q)}(\infty) \mathcal{O}_n^{NS(p,q)}(z_0) \prod_{i=1}^{n} \mathcal{O}_{m_i}^{R(p_i,q_i)}(0) \rangle. \quad (4.3.31)$$

The conformal weight of the twist n operator gives a Jacobian factor under this conformal map. Let us recall that the weights of the insertion operator are

$$h = \frac{1}{2}(p + n - 1) \qquad \bar{h} = \frac{1}{2}(q + n - 1) \quad (4.3.32)$$

and thus the Jacobian factor induced is

$$\left(\frac{dz}{dw}\right)^{h}_{|w_0} \left(\frac{d\bar{z}}{d\bar{w}}\right)^{\bar{h}}_{|\bar{w}_0}, \quad (4.3.33)$$

which can immediately be written as

$$\exp(h w_0) \exp(\bar{h} \bar{w}_0). \quad (4.3.34)$$

To rewrite this expression in terms of t_0, we need to use (4.3.28). Here we will be primarily interested in calculating correlation functions for which $p = q = 0$ and thus the Jacobian factor gives

$$|t_0|^{M(n-1)} \left(\prod_{i=2}^{n} (1 - \bar{a}_i)^{m_i} \right)^{n-1}, \tag{4.3.35}$$

where the $\bar{a}_i$ are defined in (4.3.29).

Next we can express (4.3.31) in terms of a normalised correlation function,

$$\begin{aligned} \langle \mathcal{O}_M^{R(P,Q)}(\infty) \mathcal{O}_n^{NS(p,q)}(z_0) \prod_{i=1}^{n} \mathcal{O}_{m_i}^{R(p_i,q_i)}(0) \rangle = \\ = \lim_{|z|\to\infty} \frac{\langle \mathcal{O}_M^{R(P,Q)}(z) \mathcal{O}_n^{NS(p,q)}(z_0) \prod_{i=1}^{n} \mathcal{O}_{m_i}^{R(p_i,q_i)}(0) \rangle}{\langle \mathcal{O}_M^{R(P,Q)}(z) \mathcal{O}_M^{R(P,Q)\dagger}(0) \rangle}. \end{aligned} \tag{4.3.36}$$

Here we use the notation

$$\mathcal{O}_M^{R(P,Q)\dagger} \tag{4.3.37}$$

to denote the conjugate operator (with conjugate R charges).

Following [116, 121], the key point is then that this normalised correlation function factorises into a bare twist part (associated with a Liouville action) and a spin field part, i.e.

$$\lim_{|z|\to\infty} \frac{\langle \mathcal{O}_M^{R(P,Q)}(z) \mathcal{O}_n^{NS(p,q)}(z_0) \prod_{i=1}^{n} \mathcal{O}_{m_i}^{R(p_i,q_i)}(0) \rangle}{\langle \mathcal{O}_M^{R(P,Q)}(z) \mathcal{O}_M^{R(P,Q)\dagger}(0) \rangle} = \lim_{|z|\to\infty} \frac{\langle \Sigma_{n+2}(z, z_0) \rangle}{\langle \Sigma_2(z) \rangle} \frac{\langle S_{n+2}(t, t_0) \rangle}{\langle S_2(t) \rangle}. \tag{4.3.38}$$

Here the bare twist part is

$$\langle \Sigma_{n+2}(z, z_0) \rangle := \langle \sigma_M(z) \sigma_n(z_0) \prod_{i=1}^{n} \sigma_{m_i}(0) \rangle \tag{4.3.39}$$

with

$$\langle \Sigma_2(z) \rangle := \langle \sigma_M(z) \sigma_M(0) \rangle. \tag{4.3.40}$$

The spin field correlators are calculated on the t plane as

$$\langle S_{n+2}(t, t_0) \rangle := \langle S_M^{(P,Q)}(t(z)) S_n^{(p,q)}(t_0(z_0)) \prod_{i=1}^{n} S_{m_i}^{(p_i,q_i)}(a_i) \rangle \tag{4.3.41}$$

and

$$\langle S_2(t) \rangle := \langle S_M^{(P,Q)}(t(z)) S_M^{(P,Q)\dagger}(0) \rangle. \tag{4.3.42}$$

We discuss in section 4.3.4 how the operator/state R charges (indicated in the labelling of these spin fields) relate to the spins of the spin fields. In the rest of this section we collect all the contributions required to compute the correlation function.

4.3.3 Twist operator correlator

In this section we calculate the bare twist operator contribution, namely

$$\lim_{|z|\to\infty} \frac{\langle \Sigma_{n+2}(z, z_0)\rangle}{\langle \Sigma_2(z)\rangle} \tag{4.3.43}$$

where the twist operator correlators are defined in (4.3.39) and (4.3.40).

Following [116, 121] we work in a path integral formulation and regularise each twist operator inserted at a finite value of z by cutting out a hole of radius $\epsilon \ll 1$. The regularised twist operator σ_m^ϵ is related to the original twist operator as

$$\sigma_m = \frac{1}{\sqrt{\sigma_m^\epsilon(0)\sigma_m^\epsilon(1)}}\sigma_m^\epsilon, \tag{4.3.44}$$

and thus when working with such regularised operators we need to take into account the appropriate normalisation factors. If a twist operator is inserted at infinity, we need to cut out a hole at infinity with radius $1/\delta \gg 1$; we denote the corresponding regularised operator as σ_M^δ.

Thus we need to calculate

$$\lim_{|z|\to\infty} \frac{\langle \Sigma_{n+2}(z, z_0)\rangle}{\langle \Sigma_2(z)\rangle} = \mathcal{N}_\epsilon \frac{\langle \sigma_M^\delta(\infty)\sigma_n^\epsilon(z_0)\prod_{i=1}^n \sigma_{m_i}^\epsilon(0)\rangle}{\langle \sigma_M^\delta(\infty)\sigma_M^\epsilon(0)\rangle}, \tag{4.3.45}$$

where the normalisation factor is

$$\mathcal{N}_\epsilon = \sqrt{\frac{\langle \sigma_M^\epsilon(0)\sigma_M^\epsilon(1)\rangle}{\langle \sigma_n^\epsilon(0)\sigma_n^\epsilon(1)\rangle \prod_{i=1}^n \langle \sigma_{m_i}^\epsilon(0)\sigma_{m_i}^\epsilon(1)\rangle}}. \tag{4.3.46}$$

Note that normalisation terms cancel for the operator inserted at infinity.

The two point functions of regularised twist operators at finite separation are given by [116, 121]

$$\langle \sigma_m^\epsilon(0)\sigma_m^\epsilon(y)\rangle = y^{-(m-\frac{1}{m})}\left(m^2\epsilon^{-\frac{(m-1)^2}{m}}\right)Q^{1-m} \tag{4.3.47}$$

where Q depends on the regularization. Factors of Q cancel in the normalisation factor (4.3.46). Thus the overall normalisation factor is

$$\mathcal{N}_\epsilon = \frac{M}{n\prod_i m_i}\epsilon^{-\frac{(M-1)^2}{2M}+\frac{(n-1)^2}{2n}+\sum_i \frac{(m_i-1)^2}{2m_i}}. \tag{4.3.48}$$

The correlation functions of the regularised twist operators are calculated using the Liouville action associated with the conformal map from the z plane to the t plane. This

conformal map changes the metric by a factor of $\exp(\phi)$, where

$$\phi = \log \left| \frac{dz}{dt} \right|^2 . \tag{4.3.49}$$

Under this map the Liouville contribution to the path integral reduces to boundary contributions

$$S_L = \frac{c}{96\pi} \left(i \int_{\partial \Sigma_t} \phi \partial_t \phi + \text{c.c.} \right), \tag{4.3.50}$$

where the boundaries are the images in the t plane of the circular holes cut out in the z plane to regularise the operators. Here the central charge is $c = 6$.

Let us now calculate the Liouville contribution associated with the twist m_i operator, for which the insertion point in the t plane is $t = a_i$. In the neighbourhood of $t = a_i$ the ramification map is

$$z \approx (t - a_i)^{m_i} \prod_{i \neq j} (a_i - a_j)^{m_j} \tag{4.3.51}$$

and thus

$$(t - a_i) \approx \left(\frac{z}{\prod_{i \neq j} (a_i - a_j)^{m_j}} \right)^{\frac{1}{m_i}} . \tag{4.3.52}$$

Therefore, the Liouville field in the vicinity of $t = a_i$ is given by

$$\phi \approx 2 \log \left(m_i |t - a_i|^{m_i - 1} \prod_{i \neq j} |a_i - a_j|^{m_j} \right) \tag{4.3.53}$$

with

$$\partial_t \phi \approx \frac{m_i - 1}{(t - a_i)}. \tag{4.3.54}$$

The contribution to the Liouville action from this point is given by (4.3.50), with the integral evaluated using

$$z \approx \epsilon e^{i\theta}, \qquad (t - a_i) \approx \left(\frac{\epsilon}{\prod_{i \neq j} (a_i - a_j)^{m_j}} \right)^{\frac{1}{m_i}} e^{i\theta'}, \qquad \theta' = \frac{\theta}{m_i}, \tag{4.3.55}$$

where the range of θ' is 2π. Thus the contribution from $t = a_i$ is

$$S_L^{a_i} = -\frac{1}{2}(m_i - 1) \log \left(m_i \epsilon^{\frac{m_i - 1}{m_i}} \prod_{i \neq j} |a_i - a_j|^{\frac{m_j}{m_i}} \right). \tag{4.3.56}$$

We now consider the contribution from the point associated with the twist n operator. In the neighbourhood of the insertion point

$$z - z_0 \approx b_n (t - t_0)^n, \tag{4.3.57}$$

where the coefficient b_n will be calculated in the next section. Following the same logic as above, we can immediately write down the associated contribution to the Liouville action

$$S_L^{t_0} = -\frac{1}{2n}(n-1)\log\left(n^n|b_n|\epsilon^{n-1}\right). \tag{4.3.58}$$

For the insertion at infinity

$$z \approx t^M \tag{4.3.59}$$

and the Liouville action contribution is

$$S_L^{\infty} = \frac{1}{2}(M-1)\log\left(M\delta^{-\frac{M-1}{M}}\right). \tag{4.3.60}$$

Note that the opposite sign relative to the previous contributions follows from the direction of the boundary normal.

Collecting together all of these contributions we obtain

$$\begin{aligned} S_L^{(4)} = &-\sum_i \frac{1}{2}(m_i-1)\log\left(m_i\epsilon^{\frac{m_i-1}{m_i}}\prod_{i\neq j}|a_i-a_j|^{\frac{m_j}{m_i}}\right) - \\ &-\frac{1}{2n}(n-1)\log\left(n^n|b_n|\epsilon^{n-1}\right) + \frac{1}{2}(M-1)\log\left(M\delta^{-\frac{M-1}{M}}\right). \end{aligned} \tag{4.3.61}$$

The regularised four point function is now calculated as

$$\langle\sigma_M^{\delta}(\infty)\sigma_n^{\epsilon}(z_0)\prod_{i=1}^{n}\sigma_{m_i}^{\epsilon}(0)\rangle = e^{S_L^{(4)}}. \tag{4.3.62}$$

The calculation of the regularised two point function

$$\langle\sigma_M^{\delta}(\infty)\sigma_M^{\delta}(0)\rangle = e^{S_L^{(2)}} \tag{4.3.63}$$

is very similar. The Liouville contribution from the insertion at infinity is given by (4.3.60) and the contribution at zero is

$$S_L^{\infty} = -\frac{1}{2}(M-1)\log\left(M\epsilon^{-\frac{M-1}{M}}\right). \tag{4.3.64}$$

Thus the total Liouville action contribution to the two point function is

$$S_L^{(2)} = \frac{1}{2}(M-1)\log\left(M\delta^{-\frac{M-1}{M}}\right) - \frac{1}{2}(M-1)\log\left(M\epsilon^{-\frac{M-1}{M}}\right). \tag{4.3.65}$$

Collecting all of the holomorphic and anti-holomorphic contributions together we ultimately obtain

$$M^{\frac{1}{2}(M+1)}n^{-\frac{1}{2}(n+1)}|b_n|^{-\frac{(n-1)}{2n}}\prod_{i=1}^{n}m_i^{-\frac{1}{2}(m_i+1)}\prod_{i\neq j}|a_i-a_j|^{-\frac{m_j(m_i-1)}{2m_i}}, \tag{4.3.66}$$

where implicitly we set $a_1 = 0$. Note that all contributions depending on the regulators ϵ and δ cancel, as required.

4.3.4 Spin field correlator

In this section we calculate

$$\lim_{|z|\to\infty} \frac{\langle S_{n+2}(t(z), t_0(z_0))\rangle}{\langle S_2(t(z))\rangle}, \tag{4.3.67}$$

where the correlators are defined in (4.3.41) and (4.3.42).

The relationship between the R charge assignments of the original operator/states and the spin field labels is as follows. The operator creating a component string of twist m is mapped to

$$\mathcal{O}_m^{NS(p,q)} \to S_m^{(p,q)}\sigma_m \tag{4.3.68}$$

where σ_m is the bare twist m operator, and $S_m^{(p,q)}$ has $SU(2)_L$ and $SU(2)_R$ charges

$$\frac{1}{2}(p-1) \qquad \frac{1}{2}(q-1). \tag{4.3.69}$$

For the twist n operator, the mapping is

$$\mathcal{O}_n^{NS(p,q)} \to S_n^{(p,q)}\sigma_n \tag{4.3.70}$$

with the $SU(2)_L$ and $SU(2)_R$ charges of $S_n^{(p,q)}$ being

$$\frac{1}{2}(p+n-1) \qquad \frac{1}{2}(q+n-1). \tag{4.3.71}$$

Note that the correlation function calculations in [116] are applicable to universal operators common to both the T^4 and K3 CFTs, i.e. operators associated with the $(0,0)$ and $(2,2)$ cohomology.

As a warm up we will consider an example of twist three operator joining three components; the case of a twist two operator joining two components can be found in [132]. We consider R charge assignments such that we need to calculate

$$\langle S_5(t,t_0)\rangle := \langle S_M^{(\frac{1}{2},\frac{1}{2})}(t(z))S_3^{(1,1)}(t_0(z_0))\prod_{i=1}^{3} S_{m_i}^{(-\frac{1}{2},-\frac{1}{2})}(a_i)\rangle \tag{4.3.72}$$

and

$$\langle S_2(t)\rangle := \langle S_M^{(\frac{1}{2},\frac{1}{2})}(t(z))S_M^{(-\frac{1}{2},-\frac{1}{2})}(0)\rangle. \tag{4.3.73}$$

Thus, the original one point function involves only operators associated with the $(0,0)$

cohomology.

We begin by collecting the normalisation factors for the spin fields. For a spin field associated with a twist m operator, the ramification map by construction takes the form

$$(z - z_m) = b_m (t - t_m)^m \tag{4.3.74}$$

near the insertion point z_m (mapped to t_m). The corresponding (holomorphic) normalisation factor for the spin field insertion is then

$$b_m^{-\frac{j_3^2}{m}}, \tag{4.3.75}$$

where j_3 is the $SU(2)_L$ charge of the spin field. Here and throughout this section we explain in detail the holomorphic contributions; we then combine the holomorphic and anti-holomorphic factors to obtain the full result.

For the component strings this results in normalisation factors

$$\begin{aligned}
b_{m_1} &= (-a_2)^{m_2}(-a_3)^{m_3} \qquad & b_{m_1}^{-\frac{1}{4m_1}} &= (-a_2)^{-\frac{m_2}{4m_1}}(-a_3)^{-\frac{m_3}{4m_1}} \\
b_{m_2} &= a_2^{m_1}(a_2 - a_3)^{m_3} \qquad & b_{m_2}^{-\frac{1}{4m_2}} &= a_2^{-\frac{m_1}{4m_2}}(a_2 - a_3)^{-\frac{m_3}{4m_2}} \\
b_{m_3} &= a_3^{m_1}(a_3 - a_2)^{m_2} \qquad & b_{m_3}^{-\frac{1}{4m_3}} &= a_3^{-\frac{m_1}{4m_3}}(a_3 - a_2)^{-\frac{m_2}{4m_3}}.
\end{aligned} \tag{4.3.76}$$

Taking the product of these factors we obtain

$$t_0^{\frac{3}{4} - \frac{M}{4}\left(\frac{1}{m_1}+\frac{1}{m_2}+\frac{1}{m_3}\right)} (-\bar{a}_2)^{-\frac{m_2}{4m_1}}(-\bar{a}_3)^{-\frac{m_3}{4m_1}} \bar{a}_2^{-\frac{m_1}{4m_2}}(\bar{a}_2 - \bar{a}_3)^{-\frac{m_3}{4m_2}} \bar{a}_3^{-\frac{m_1}{4m_3}}(\bar{a}_3 - \bar{a}_2)^{-\frac{m_2}{4m_3}}. \tag{4.3.77}$$

For the twist three operator joining these component strings we find that

$$b_3 = \frac{M}{3} t_0^{M-3}(1 - \bar{a}_2)^{m_2 - 1}(1 - \bar{a}_3)^{m_3 - 1} \tag{4.3.78}$$

and thus this spin operator normalisation is

$$t_0^{1-\frac{M}{3}} \left(\frac{M}{3}(1 - \bar{a}_2)^{m_2-1}(1 - \bar{a}_3)^{m_3-1}\right)^{\frac{1}{3}}. \tag{4.3.79}$$

The normalisation factors from the twist M operator are trivial in both the five point function and the two point function since $b_M = 1$. The combination of (4.3.77) and (4.3.79) results in a term proportional to

$$t_0^{\frac{7}{4} - M\left(\frac{1}{3} + \frac{1}{4}\sum_i \frac{1}{m_i}\right)}. \tag{4.3.80}$$

The complete normalisation factor is obtained by combining both the holomorphic and anti-holomorphic parts, leading to a term proportional to

$$|t_0|^{\frac{7}{2}-M\left(\frac{2}{3}+\frac{1}{2}\sum_i \frac{1}{m_i}\right)}. \tag{4.3.81}$$

Having studied the case of three strings being joined, it is straightforward to generalise to the joining of n strings. The normalisation factors give a contribution of

$$b_n^{-\frac{(n-1)^2}{4n}} \prod_{i=1}^{n} b_{m_i}^{-\frac{1}{4m_i}}, \tag{4.3.82}$$

where

$$b_{m_i} = \prod_{j\neq i}(a_i - a_j)^{m_j}. \tag{4.3.83}$$

In (4.3.82) we have used the fact that the R charge of the twist n operator is $(n-1)/2$. Thus the complete normalisation factor from holomorphic and anti-holomorphic parts gives

$$|b_n|^{-\frac{(n-1)^2}{2n}} \prod_{i=1}^{n}\prod_{j\neq i} |a_i - a_j|^{-\frac{m_j}{2m_i}}. \tag{4.3.84}$$

We can calculate b_n explicitly as follows. From the definition of b_n in (4.3.57) it is clear that close to t_0

$$\left(\frac{dz}{dt}\right) \approx n b_n (t-t_0)^{n-1}. \tag{4.3.85}$$

Differentiating the ramification map directly gives

$$\left(\frac{dz}{dt}\right) \approx \prod_i (t_0 - a_i)^{m_i - 1}\left(Mt^{n-1} + \cdots\right). \tag{4.3.86}$$

Comparing (4.3.85) and (4.3.86) gives

$$b_n = \frac{M}{n} t_0^{M-n} \prod_i (1-\bar{a}_i)^{m_i-1}, \tag{4.3.87}$$

where we use the dimensionless quantities $\bar{a}_i$ to make the t_0 dependence of b_n manifest.

Let us now move to the spin field correlators. Each of the spin fields factorises into holomorphic and antiholomorphic fields i.e. we can write

$$S_m^{(p,q)} = S^{(j_3)}(t)\bar{S}^{(\bar{j}_3)}(\bar{t}) \tag{4.3.88}$$

where the $SU(2)_{L/R}$ charges are given in (4.3.69) and (4.3.71).

As above, let us consider first the case in which three component strings are joined,

before moving on to the general case. For operators associated with the $(0,0)$ cohomology in the holomorphic sector we therefore need to calculate

$$\frac{\langle S^{(\frac{1}{2})}(t)S^{(1)}(t_0)S^{(-\frac{1}{2})}(0)S^{(-\frac{1}{2})}(a_2)S^{(-\frac{1}{2})}(a_3)\rangle}{\langle S^{(\frac{1}{2})}(t)S^{(-\frac{1}{2})}(0)\rangle} \tag{4.3.89}$$

in the limit that $t \to \infty$. This correlation function can be computed following the methods of [116].

Using bosonisation (for simplicity we write this formula with the notation given by [131]) we can write the spin fields as

$$S^{\frac{k}{2}}(t) = \exp\left(\frac{ik}{2}(\phi_1(t) - \phi_2(t))\right). \tag{4.3.90}$$

The OPE for these fields is

$$\exp\left(ik_1\phi(t)\right)\exp\left(ik_2\phi(t')\right) \sim \exp\left(ik_1\phi(t) + ik_2\phi(t')\right)(t-t')^{k_1k_2}. \tag{4.3.91}$$

Using this OPE to complete the two point function and five point function (with appropriate ordering) we then obtain

$$\langle S^{(\frac{1}{2})}(t)S^{(-\frac{1}{2})}(0)\rangle = \frac{1}{t^{\frac{1}{2}}} \tag{4.3.92}$$

$$\langle S^{(\frac{1}{2})}(t)S^{(1)}(t_0)S^{(-\frac{1}{2})}(0)S^{(-\frac{1}{2})}(a_2)S^{(-\frac{1}{2})}(a_3)\rangle = \frac{(t-t_0)(-a_2)^{\frac{1}{2}}(-a_3)^{\frac{1}{2}}(a_2-a_3)^{\frac{1}{2}}}{t^{\frac{1}{2}}(t-a_2)^{\frac{1}{2}}(t-a_3)^{\frac{1}{2}}t_0(t_0-a_2)(t_0-a_3)}.$$

Thus as $t \to \infty$

$$\frac{\langle S^{(\frac{1}{2})}(t)S^{(1)}(t_0)S^{(-\frac{1}{2})}(0)S^{(-\frac{1}{2})}(a_2)S^{(-\frac{1}{2})}(a_3)\rangle}{\langle S^{(\frac{1}{2})}(t)S^{(-\frac{1}{2})}(0)\rangle} \to \frac{(-\bar{a}_2)^{\frac{1}{2}}(-\bar{a}_3)^{\frac{1}{2}}(\bar{a}_2-\bar{a}_3)^{\frac{1}{2}}}{t_0^{\frac{3}{2}}(1-\bar{a}_2)(1-\bar{a}_3)}. \tag{4.3.93}$$

Combining holomorphic and anti-holomorphic contributions we obtain

$$\lim_{|z|\to\infty} \frac{\langle S_5(t(z),t_0(z_0))\rangle}{\langle S_2(t(z))\rangle}\frac{\langle \bar{S}_5(\bar{t}(\bar{z}),\bar{t}_0(\bar{z}_0))\rangle}{\langle \bar{S}_2(\bar{t}(\bar{z}))\rangle} = \frac{|\bar{a}_2||\bar{a}_3||\bar{a}_2-\bar{a}_3|}{|t_0|^3|1-\bar{a}_2|^2|1-\bar{a}_3|^2} \tag{4.3.94}$$

as the final result for the spin field correlator contribution.

The generalisation to twist n operators joining n component strings is now immediate. Following (4.3.72) we choose R charge assignments such that

$$\langle S_{n+2}(t,t_0)\rangle := \langle S_M^{(\frac{1}{2},\frac{1}{2})}(t(z))S_n^{(\frac{1}{2}(n-1),\frac{1}{2}(n-1))}(t_0(z_0))\prod_{i=1}^{n} S_{m_i}^{(-\frac{1}{2},-\frac{1}{2})}(a_i)\rangle \tag{4.3.95}$$

(with $a_1 = 0$). Then

$$\langle S_{n+2}(t,t_0)\rangle = \frac{(t-t_0)^{\frac{1}{2}(n-1)}\prod_{i=1}^{n}\prod_{i<j}(a_i-a_j)^{\frac{1}{2}}}{\prod_{i=1}^{n}(t-a_i)^{\frac{1}{2}}(t_0-a_i)^{\frac{1}{2}(n-1)}}, \tag{4.3.96}$$

and thus the normalised correlator is

$$\frac{\langle S_{n+2}(t,t_0)\rangle}{\langle S^{(\frac{1}{2})}(t)S^{(-\frac{1}{2})}(0)\rangle} = \frac{\prod_{i=1}^{n}\prod_{i<j}(a_i-a_j)^{\frac{1}{2}}}{\prod_{i=1}^{n}(t_0-a_i)^{\frac{1}{2}(n-1)}}. \tag{4.3.97}$$

Combining holomorphic and anti-holomorphic contributions we obtain

$$\lim_{|z|\to\infty}\frac{\langle S_{n+2}(t(z),t_0(z_0))\rangle}{\langle S_2(t(z))\rangle}\frac{\langle \bar{S}_{n+2}(\bar{t}(\bar{z}),\bar{t}_0(\bar{z}_0))\rangle}{\langle \bar{S}_2(\bar{t}(\bar{z}))\rangle} = \frac{\prod_{i=1}^{n}\prod_{i<j}|\bar{a}_i-\bar{a}_j|}{|t_0|^{\frac{1}{2}n(n-1)}\prod_{i=2}^{n}|1-\bar{a}_i|^{(n-1)}} \tag{4.3.98}$$

for the spin field correlator associated with the given R charge assignments.

4.3.5 Final answer for the one point function

The final answer for the one point function is obtained by combining (4.3.35), (4.3.66), (4.3.84) and (4.3.98). First note that combining (4.3.66) and (4.3.84) gives

$$M^{\frac{1}{2}(M+1)}n^{-\frac{1}{2}(n+1)}|b_n|^{-\frac{1}{2}(n-1)}\prod_{i=1}^{n}m_i^{-\frac{1}{2}(m_i+1)}\prod_{i\neq j}|a_i-a_j|^{-\frac{m_j}{2}} \tag{4.3.99}$$

which can be rewritten as

$$M^{\frac{1}{2}(M+1)}n^{-\frac{1}{2}(n+1)}|b_n|^{-\frac{1}{2}(n-1)}|t_0|^{-\frac{1}{2}M(n-1)}\prod_{i=1}^{n}m_i^{-\frac{1}{2}(m_i+1)}\prod_{i\neq j}|\bar{a}_i-\bar{a}_j|^{-\frac{m_j}{2}}. \tag{4.3.100}$$

Substituting the expression for b_n from (4.3.87), the t_0 dependence is

$$|t_0|^{\frac{1}{2}n(n-1)-M(n-1)}. \tag{4.3.101}$$

Since the t_0 dependence of (4.3.35) is $|t_0|^{M(n-1)}$ and the t_0 dependence of (4.3.98) is $|t_0|^{-\frac{n(n-1)}{2}}$, all factors of t_0 cancel from the final result, as expected.

Combining the remaining terms in (4.3.35), (4.3.66), (4.3.84) and (4.3.98) gives

$$\begin{aligned}&\langle \mathcal{O}_M^{R(0,0))}|\mathcal{O}_n^{(0,0)}|\prod_{i=1}^{n}\mathcal{O}_{m_i}^{R(0,0)}\rangle = \\ &= \frac{M^{\frac{1}{2}(M+2-n)}}{n}\prod_i|1-\bar{a}_i|^{\frac{1}{2}(m_i-1)(n-1)}\prod_j m_j^{-\frac{1}{2}(m_j+1)}\prod_{j\neq k}|\bar{a}_j-\bar{a}_k|^{\frac{1}{2}(1-m_k)},\end{aligned} \tag{4.3.102}$$

where

$$\bar{a}_i = \frac{1+\bar{a}e^{i\phi_i}}{1-\frac{m_i}{M}}, \qquad \bar{a} = \left(\frac{M}{m_1}\prod_{i=2}^{n}\left(1-\frac{m_i}{M}\right)-1\right)^{\frac{1}{n-1}} \tag{4.3.103}$$

and the phases are

$$\begin{aligned}(n-1)\in 2Z: \quad & \phi_i = \frac{(i-1)\pi}{n-1}, \quad \phi_{i+1} = -\frac{(i-1)\pi}{n-1}, \quad i\in 2Z, \quad i\geq 2 \\ n\in 2Z: \quad & \phi_2 = 0, \quad \phi_i = \frac{(i-1)\pi}{n-1}, \quad \phi_{i+1} = -\frac{(i-1)\pi}{n-1}, \quad (i-1)\in 2Z, \quad i\geq 3.\end{aligned} \tag{4.3.104}$$

4.3.6 Special cases: $n = 2$ and $n = 3$

In this section we consider the limit of this correlation function in special cases. We begin with the case of $n = 2$, which was already studied in [132]. In this case the correlation function reduces to the simple expression

$$\langle \mathcal{O}_M^{R(0,0))}|\mathcal{O}_2^{(0,0)}(w_0)|\mathcal{O}_{m_1}^{R(0,0)}\mathcal{O}_{m_2}^{R(0,0)}\rangle = \frac{M}{2m_1m_2}, \tag{4.3.105}$$

in agreement with [132].

Now let us turn to the case of $n = 3$. The correlator (4.3.102) can in this case be written as

$$\begin{aligned}\frac{1}{3}M^{\frac{1}{2}(M-1)}(1-\bar{a}_2)^{m_2-1}(1-\bar{a}_3)^{m_3-1}m_1^{-\frac{1}{2}(m_1+1)}m_2^{-\frac{1}{2}(m_2+1)}m_3^{-\frac{1}{2}(m_3+1)} \\ |\bar{a}_2|^{1-\frac{1}{2}(m_1+m_2)}|\bar{a}_3|^{1-\frac{1}{2}(m_1+m_3)}|\bar{a}_2-\bar{a}_3|^{1-\frac{1}{2}(m_2+m_3)}.\end{aligned} \tag{4.3.106}$$

Note that this expression appears asymmetric between the twist m_i operators only because we have set $\bar{a}_1 = 0$; the expression could trivially be symmetrised by reinstating the $\bar{a}_1$ terms.

This expression looks extremely complicated but in fact it simplifies to give a very concise result. Using

$$\begin{aligned}|\bar{a}_2| &= \frac{M^{\frac{1}{2}}}{m_1^{\frac{1}{2}}(m_1+m_3)}\sqrt{m_1M+m_2m_3} \\ |\bar{a}_3| &= \frac{M^{\frac{1}{2}}}{m_1^{\frac{1}{2}}(m_1+m_2)}\sqrt{m_1M+m_2m_3}\end{aligned} \tag{4.3.107}$$

as well as

$$|1-\bar{a}_2| = \frac{m_2^{\frac{1}{2}}}{m_1^{\frac{1}{2}}(m_1+m_3)}\sqrt{m_3M+m_1m_2}$$
$$|1-\bar{a}_3| = \frac{m_3^{\frac{1}{2}}}{m_1^{\frac{1}{2}}(m_1+m_2)}\sqrt{m_2M+m_1m_3} \tag{4.3.108}$$

and

$$|\bar{a}_2-\bar{a}_3| = \frac{M^{\frac{1}{2}}}{m_1^{\frac{1}{2}}(m_1+m_2)(m_1+m_3)}\sqrt{m_3M+m_1m_2}\sqrt{m_2M+m_1m_3} \tag{4.3.109}$$

together with relations such as

$$(m_1M+m_2m_3) = (m_1+m_2)(m_1+m_3) \tag{4.3.110}$$

we can show that the correlator simplifies to

$$\langle \mathcal{O}_M^{R(0,0))}|\mathcal{O}_3^{(0,0)}(w_0)|\mathcal{O}_{m_1}^{R(0,0)}\mathcal{O}_{m_2}^{R(0,0)}\mathcal{O}_{m_3}^{R(0,0)}\rangle = \frac{M}{3m_1m_2m_3}. \tag{4.3.111}$$

This expression is manifestly symmetric over the m_i; furthermore, all dependence on factors of the type (m_i+m_j) cancels out.

Given the special cases considered in this section, it would be natural to conjecture that the result for the general case is

$$\langle \mathcal{O}_M^{R(0,0))}|\mathcal{O}_n^{(0,0)}(w_0)|\prod_i \mathcal{O}_{m_i}^{R(0,0)}\rangle = \frac{M}{n\prod_i m_i}, \tag{4.3.112}$$

but this is not supported by the results below.

4.3.7 Case of equal m_i

In this section we consider the case in which the n strings are of equal length i.e. $m_i = M/n$. In this case the general expression (4.3.102) simplifies considerably to

$$M^{1-n}n^{\frac{1}{2}M+\frac{1}{2}n-1}\prod_{i=2}^{n}|1-\bar{a}_i|^{\frac{1}{2}(\frac{M}{n}-1)(n-1)}\prod_{j=1}^{n}\prod_{j\neq k}|\bar{a}_j-\bar{a}_k|^{\frac{1}{2}\left(1-\frac{M}{n}\right)}. \tag{4.3.113}$$

The zeroes of the ramification map are located at:

$$\bar{a}_i = \frac{n}{(n-1)}\left(1+\bar{a}\exp(i\phi_i)\right), \qquad i\geq 2 \tag{4.3.114}$$

where

$$\bar{a}^{n-1} = n\left(1 - \frac{1}{n}\right)^{n-1} - 1 \tag{4.3.115}$$

and the phases are given as before by (4.3.18). Using the properties of the phases we can then immediately show that

$$\prod_{j=2}^{n} |\bar{a}_j|^{\frac{1}{2}(1-\frac{M}{n})} = n^{\frac{1}{2}(1-\frac{M}{n})}, \tag{4.3.116}$$

and hence we can write (4.3.113) as

$$M^{1-n} n^{\frac{1}{2}M+\frac{1}{2}n-\frac{M}{n}} \prod_{i=2}^{n} |1-\bar{a}_i|^{\frac{1}{2}(\frac{M}{n}-1)(n-1)} \prod_{j=2}^{n} \prod_{j\neq k} |\bar{a}_j - \bar{a}_k|^{\frac{1}{2}\left(1-\frac{M}{n}\right)}, \tag{4.3.117}$$

i.e. we can immediately evaluate the products involving $a_1 = 0$ (note that this evaluation gives (4.3.116) squared).

To evaluate (4.3.117) we make use of

$$(1-\bar{a}_i) = -\frac{1}{(n-1)}\left(1 + n\bar{a}\exp(i\phi_i)\right) \tag{4.3.118}$$

and

$$\bar{a}_i - \bar{a}_j = \frac{n\bar{a}}{(n-1)}\left(\exp(i\phi_i) - \exp(i\phi_j)\right). \tag{4.3.119}$$

Note that the latter expression has a geometric interpretation: the $(n-1)$ ramification zeroes $\{a_i\}$ are located at the vertices of a regular $(n-1)$ polygon in the complex plane. The expression

$$v_{ij} := \left(\exp(i\phi_i) - \exp(i\phi_j)\right) \tag{4.3.120}$$

can thus be interpreted vectorially in terms of vectors connecting the vertices of such a regular $(n-1)$ polygon, in which the vertices are unit distance from the origin of the complex plane. We represent this in figure 4.3.2.

The first product of (4.3.117) can be written as

$$\prod_{i=2}^{n}(1-\bar{a}_i) = \frac{(-1)^{n-1}}{(n-1)^{(n-1)}}\left(1 + n\bar{a}\sum_{i=2}^{n}\exp(i\phi_i) + \cdots + (n\bar{a})^{n-1}\prod_{i=2}^{n}\exp(i\phi_i)\right). \tag{4.3.121}$$

Using the properties of the phases (4.3.18) we can then show that this reduces to

$$\prod_{i=2}^{n}(1-\bar{a}_i) = \frac{(-1)^{n-1}}{(n-1)^{(n-1)}}\left(1 + n^{n-1}\bar{a}^{n-1}\right) \tag{4.3.122}$$

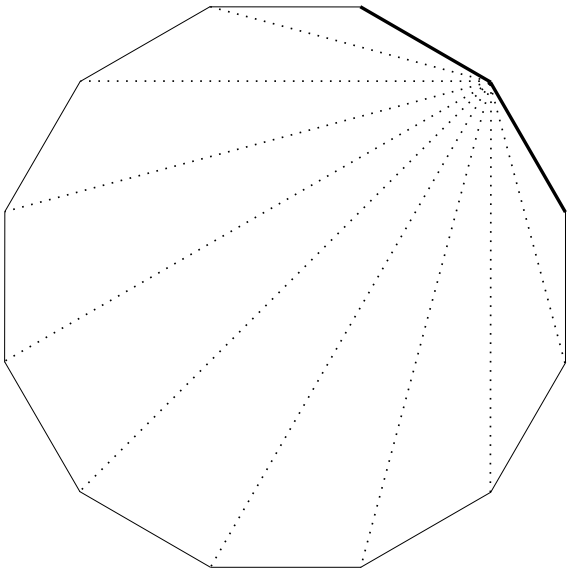

Figure 4.3.2: Polygon representing the location of the ramification zeroes. We represent with dotted lines all the diagonals of one vertex, and with thicker lines its two adjacent sides.

and thus

$$\prod_{i=2}^{n} |1-\bar{a}_i| = \frac{1}{(n-1)^{(n-1)}} \left(1 + n(n-1)^{(n-1)} - n^{(n-1)}\right). \tag{4.3.123}$$

Hence we can evaluate the following contribution to the one point function,

$$\prod_{i=2}^{n} |1-\bar{a}_i|^{\frac{1}{2}(\frac{M}{n}-1)(n-1)} = (n-1)^{-\frac{1}{2}(\frac{M}{n}-1)(n-1)^2} \left(1 + n(n-1)^{(n-1)} - n^{(n-1)}\right)^{\frac{1}{2}(\frac{M}{n}-1)(n-1)}. \tag{4.3.124}$$

It is more subtle to find a closed form expression for

$$\prod_{j=2}^{n} \prod_{j\neq k} |\bar{a}_j - \bar{a}_k| = \left(\frac{n\bar{a}}{(n-1)}\right)^{(n-1)(n-2)} \prod_{j=2}^{n} \prod_{j\neq k} |\exp(i\phi_j) - \exp(i\phi_k)| \tag{4.3.125}$$

as this requires

$$\prod_{j=2}^{n} \prod_{j\neq k} |\exp(i\phi_j) - \exp(i\phi_k)|, \tag{4.3.126}$$

i.e. the square of the product of the side lengths and all the diagonals of the regular polygon. The polygon side length is given by

$$2\sin\left(\frac{\pi}{(n-1)}\right) \tag{4.3.127}$$

while the lengths of the diagonals are given by

$$2\sin\left(\frac{j\pi}{(n-1)}\right) \qquad 2 \leq j \leq (n-2). \tag{4.3.128}$$

Now consider a specific vertex of the regular polygon. For this vertex the total product of side lengths and diagonals is, using the two previous results

$$2^{(n-2)}\prod_{j=1}^{(n-2)}\sin\left(\frac{j\pi}{(n-1)}\right) = (n-1), \tag{4.3.129}$$

where in evaluating this expression we use standard trigonometry identities.

The polygon has in total $(n-1)$ vertices and thus we obtain

$$\prod_{j=2}^{n}\prod_{j\neq k}|\exp(i\phi_j)-\exp(i\phi_k)| = (n-1)^{(n-1)}. \tag{4.3.130}$$

Collecting together all the contributions yields

$$\begin{aligned}\langle\mathcal{O}_M^{R(0,0))}|\mathcal{O}_n^{(0,0)}|\left(\mathcal{O}_{M/n}^{R(0,0)}\right)^n\rangle = \\ M^{1-n}n^{\frac{M}{2}+\frac{n}{2}-\frac{M}{n}}\left((n-1)^2(n\bar{a})^{(n-2)}\Lambda^{-1}\right)^{\frac{1}{2}(n-1)\left(1-\frac{M}{n}\right)}\end{aligned} \tag{4.3.131}$$

where we introduced the notation

$$\Lambda = \left(1+n(n-1)^{(n-1)}-n^{n-1}\right). \tag{4.3.132}$$

Note that this does not take the simple form conjectured above (4.3.112), except for $n=2$ and $n=3$.

It is useful to work out the expressions explicitly for low values of n. For $n=3$,

$$|1-\bar{a}_2| = |1-\bar{a}_3| = 1 \tag{4.3.133}$$

and

$$|\bar{a}_2-\bar{a}_3| = \sqrt{3}. \tag{4.3.134}$$

Combining the factors, the correlation function thus reduces to

$$\langle\mathcal{O}_M^{R(0,0))}|\mathcal{O}_3^{(0,0)}(w_0)|\mathcal{O}_{\frac{M}{3}}^{R(0,0)}\mathcal{O}_{\frac{M}{3}}^{R(0,0)}\mathcal{O}_{\frac{M}{3}}^{R(0,0)}\rangle = \left(\frac{M}{3}\right)^{-2}, \tag{4.3.135}$$

in agreement with the direct limit of the expression (4.3.102).

Now let us consider $n=4$. The regular polygon used to calculate (4.3.126) is an

equilateral triangle with circumradii equal to one. Elementary geometry gives the length of the triangle side as $\sqrt{3}$ and thus (4.3.126) reduces to 3^3, in agreement with (4.3.130). In this case

$$\bar{a}^3 = \frac{11}{16} \tag{4.3.136}$$

and thus

$$\langle \mathcal{O}_M^{R(0,0))} | \mathcal{O}_4^{(0,0)}(w_0)| \left(\mathcal{O}_{\frac{M}{4}}^{R(0,0)} \right)^4 \rangle = \left(\frac{4}{M} \right)^3 5^{\frac{3M}{8}-\frac{3}{2}} 11^{1-\frac{M}{4}}. \tag{4.3.137}$$

The conjecture (4.3.112) would instead give

$$\langle \mathcal{O}_M^{R(0,0))} | \mathcal{O}_4^{(0,0)}(w_0)| \left(\mathcal{O}_{\frac{M}{4}}^{R(0,0)} \right)^4 \rangle = \left(\frac{4}{M} \right)^3 \tag{4.3.138}$$

and therefore this simple form for the one point function cannot be correct for $n > 3$.

We can also take the large n limit of (4.3.131). In the limit of $n \gg 1$

$$\Lambda \approx n^n \tag{4.3.139}$$

while

$$\bar{a}^{n-1} \approx \frac{n}{e}. \tag{4.3.140}$$

The latter follows from the limit

$$\left(1 - \frac{1}{n} \right)^{n-1} \to \frac{1}{e} \tag{4.3.141}$$

for large n. Then

$$\langle \mathcal{O}_M^{R(0,0))} | \mathcal{O}_n^{(0,0)}(w_0)| \left(\mathcal{O}_{\frac{M}{n}}^{R(0,0)} \right)^n \rangle \approx \left(\frac{n}{M} \right)^n n^{-\frac{M}{2n}} e^{\frac{1}{2}(M-n)}. \tag{4.3.142}$$

In this expression we do not make any assumptions about the twist of the component strings, i.e. about the ratio M/n, beyond the fact that it is a positive integer.

CHAPTER 5

One point functions

In this chapter we calculate one point functions for chiral primary operators. Both long and short strands are considered for the case of single trace operators. Where relevant, we indicate how to generalise the results to multi trace operators.

5.1 Layout

In section 5.2 we calculate one point functions for model single trace chiral primary operators in the short strand limit. Namely, in the limit where the strand lengths are of order one and the number of strands is of order N. We first give an overview of the procedure and then we calculate some examples explicitly for untwisted and twisted operators. Section 5.3 contains the same one point functions as the previous section but in the long strand case (strand length of order N). We separate that section into two-charge states and three-charge states, as for the two-charge case we can give exact results whereas in the three-charge one we need to approximate it in some cases. In section 5.4 we briefly discuss the results obtained.

5.2 One point functions: short strand case

In this section we compute one point functions for all the chiral primaries described in sections 2.1.2 and 2.1.3, for the two and three-charge cases. Some one point functions have been calculated in [88], where strands of length one and two were considered, and also strands of arbitrary length for the operator $\Sigma_2^{\dot{-}\dot{-}}$. This section extends the CFT calculation performed in that paper, by considering arbitrary strand length for all one point functions. In what follows, first we describe the approximation used in the short strand case, and then we go case by case calculating the one point functions for all different chiral primaries.

5.2.1 Approximation used

In this section we are concerned about the case where the strands are short and we have a large number of them. That is, we consider the case where κ is of order one and $N_\kappa^{(gs)} \lesssim N$. This is the case considered in [88]. We take the same approximation, which consists in finding the saddle point on which the sum over the partitions is peaked. This saddle point is determined by the numerical coefficients $A_\kappa^{(gs)}$ and B_{κ,m_κ} accompanying each strand. In the two-charge case the norm of the state is

$$|\psi(\{A_\kappa^{(S)}\})|^2 = \sum_{\{N_\kappa^{(S)}\}} \mathcal{N}(\{N_\kappa^{(S)}\}) \prod_{S,\kappa} |A_\kappa^{(S)}|^{2N_\kappa^{(S)}}. \tag{5.2.1}$$

Let $\overline{N}_\kappa^{(S)}$ be the saddle point on which the sum is peaked. To obtain it we use Stirling's approximation in its weakest form,

$$\log n! \approx n \log n - n, \qquad n \in \mathbb{N},\ n \gg 1. \tag{5.2.2}$$

Taking the logarithm of each term of (5.2.1) and using (5.2.2) we obtain

$$N \log N + \sum_{S,\kappa} \left(N_\kappa^{(S)} \log |A_\kappa^{(S)}|^2 - N_\kappa^{(S)} \log N_\kappa^{(S)} + N_\kappa^{(S)} - N_\kappa^{(S)} \log \kappa \right). \tag{5.2.3}$$

The stationary point $\overline{N}_\kappa^{(S)}$ is then

$$\overline{N}_\kappa^{(S)} = \frac{|A_\kappa^{(S)}|^2}{\kappa}. \tag{5.2.4}$$

For the three-charge case we can use an analogous approximation, which results into

$$\overline{N}_\kappa^{(s)} = \frac{|A_\kappa^{(s)}|^2}{\kappa}, \qquad \overline{N}_{\kappa,m_\kappa}^{(00)} = \binom{\kappa}{m_\kappa} \frac{|B_{\kappa,m_\kappa}|^2}{\kappa}. \tag{5.2.5}$$

We use these relations to approximate the resulting sums after we act on the states with the chiral primaries.

Now that we have all the ingredients needed we can start calculating the one point functions in this limit. Notice that for each chiral primary we can use a state which only has the strands that will come into play. With the approximation taken in this section the norm of the state will always cancel, and so having extra strands which do not play a role in the process does not affect the result. To see this clearly and to introduce the calculation and some simplified notation we start with a review example. Afterwards we will calculate one point functions in more general cases.

5.2.2 Review example: $\Sigma_2^{+\dot{-}}$ operator

In this section we calculate the one point function of $\Sigma_2^{+\dot{-}}$, a chiral primary which joins two strands into a single one and increases the left R symmetry charge by 1/2 and lowers the right one by the same amount. This example will be used as an explanation of how to calculate the one point functions, following closely [88]. In subsequent sections we will use the notation and methods introduced here directly. Let us start calculating the one point function. In order to have a non-trivial answer for this operator we consider the following state,

$$\psi(\{A_{n_l}^{(++)}, B_i^{k(00)}\}) = \sum_{N_{m_l}^{1(00)}=0}^{N/m_l} \sum_{N_{p_l}^{0(00)}=0}^{\frac{N-N_{m_l}^{1(00)} m_l}{p_l}} \left(A_{n_l}^{(++)} |++\rangle_{n_l}\right)^{N_{n_l}^{(++)}} \left(B_{p_l}^{0(00)} |00\rangle_{p_l}\right)^{N_{p_l}^{0(00)}} \otimes \\ \otimes \left(B_{m_l}^{1(00)} J_{-1}^{+} |00\rangle_{m_l}\right)^{N_{m_l}^{1(00)}}, \tag{5.2.6}$$

where we take $m_l = n_l + p_l$. Using equation (2.1.44) we obtain the constraint

$$N_{n_l}^{(++)} n_l + N_{p_l}^{0(00)} p_l + N_{m_l}^{1(00)} m_l = N. \tag{5.2.7}$$

One of the $N^{(gs)}$ can be related to the others due to equation (2.1.6), but we will not substitute it during calculations to simplify the notation. From equation (5.2.5) we learn that the sum is peaked at

$$n_l \overline{N_{n_l}^{(++)}} = \left|A_{n_l}^{(++)}\right|^2, \qquad p_l \overline{N_{p_l}^{0(00)}} = \left|B_{p_l}^{0(00)}\right|^2, \qquad \overline{N_{m_l}^{1(00)}} = \left|B_{m_l}^{1(00)}\right|^2. \tag{5.2.8}$$

Also, using (2.1.54) we find the normalisation factor for the state ψ to be

$$\mathcal{N}\left(N_{n_l}^{(++)}, N_{p_l}^{0(00)}\right) = \frac{N!}{N_{n_l}^{(++)}! N_{p_l}^{0(00)}! N_{m_l}^{1(00)}! n_l^{N_{n_l}^{(++)}} p_l^{N_{p_l}^{0(00)}}}. \tag{5.2.9}$$

Recall that using equation (5.2.7) we can write one of the $N^{(\mathrm{gs})}$ in terms of the others, and so $\mathcal{N}$ only depends on two of them. The action of the $\Sigma_2^{+\dot{-}}$ operator on these strands is

$$\Sigma_2^{+\dot{-}}\left(|{+}{+}\rangle_{n_l}\otimes|00\rangle_{p_l}\right)\to J_{-1}^{+}\,|00\rangle_{m_l=n_l+p_l}\,. \tag{5.2.10}$$

To write the state resulting from the action of the operator exactly we need to calculate two coefficients in general. The first one, which we will always denote by α, is to ensure that we have the same number of terms before and after applying the operator, that is, in the l.h.s. and in the r.h.s. of (5.2.10). The second coefficient will only be needed when we calculate one point functions of gluing operators. We will call this second coefficient c_n, where the subindex n stands for the number of strands joined together. We give its expression later, but its general form is the main result of chapter 4.

Let us start by calculating the α coefficient for this case. The twist operator $\Sigma_2^{+\dot{-}}$ can act on any of the $N_{n_l}^{(++)}$ strands $|{+}{+}\rangle_{n_l}$ and on any of the $N_{p_l}^{0(00)}$ strands $|00\rangle_{p_l}$. So, we need to multiply the l.h.s. by this two numbers. Also, once the strands are picked, the operator can act on any of the copies within each strand. Therefore, we also need to multiply by their lengths, $n_l p_l$. Last, we also need to divide by two, for the following reason: the twist operator acts up to cyclic permutations, and so we need to take the symmetrisation of the strands over which it acts. More precisely, the one point function that we consider is

$${}_{m_l}\langle 00|\,J_{+1}^{-}\Sigma_2^{+\dot{-}}\left(|{+}{+}\rangle_{n_l}\otimes|00\rangle_{p_l}\right)_{\text{Symm.}}\,, \tag{5.2.11}$$

where

$$\begin{aligned}\left(|{+}{+}\rangle_{n_l}\otimes|00\rangle_{p_l}\right)_{\text{Symm.}} :=& \,|{+}{+}\rangle_{(1)}\otimes\ldots\otimes|{+}{+}\rangle_{(n_l)}\otimes|00\rangle_{(n_l+1)}\otimes\ldots\otimes|00\rangle_{(m_l)}+\ldots+\\ &+|00\rangle_{(1)}\otimes\ldots\otimes|00\rangle_{(p_l)}\otimes|{+}{+}\rangle_{(p_l+1)}\otimes\ldots\otimes|{+}{+}\rangle_{(m_l)}\end{aligned} \tag{5.2.12}$$

is a symmetrisation over all the copies. Notice that if we pick strands of the same kind we do not include this factor, as the symmetrisation in that case is already taken into account by the norm of the whole state. Hence, the α combinatorial factor is obtained by solving

$$\frac{N_{n_l}^{(++)}n_l N_{p_l}^{0(00)}p_l}{2}\mathcal{N}(N_{n_l}^{(++)},N_{p_l}^{0(00)},N_{m_l}^{1(00)})=\alpha\mathcal{N}(N_{n_l}^{(++)}-1,N_{p_l}^{0(00)}-1,N_{m_l}^{1(00)}+1), \tag{5.2.13}$$

which gives

$$\alpha=\frac{N_{m_l}^{1(00)}+1}{2}. \tag{5.2.14}$$

If we had included other ground state strands in our state ψ this coefficient would remain the same, as they would be unaltered after the application of the operator and thus they would cancel. Now, the c_2 coefficient was first computed in [131], and we rederived it in

chapter 4 from the general formula in equation (4.3.105). It reads

$$c_{n_l,p_l} = \frac{n_l + p_l}{2n_l\, p_l}. \tag{5.2.15}$$

Last, the commutator of the R-symmetry current with the twist operator is

$$\left[\left(J_n^i\right)^{\alpha\beta}, \Sigma_2^{\beta\dot{\alpha}}(v,u)\right] = \frac{1}{2} e^{in\frac{\sqrt{2}v}{R}} \left(\sigma^i\right)^{\alpha\beta} \Sigma_2^{\beta\dot{\alpha}}(v,u), \tag{5.2.16}$$

and so

$$\begin{aligned} {}_{m_l}\langle 00|\, J_{+1}^- \Sigma_2^{+\dot{-}} \left(|{+}{+}\rangle_{n_l} \otimes |00\rangle_{p_l}\right)_{\text{Symm.}} = \\ = e^{i\frac{\sqrt{2}v}{R}}\, {}_{m_l}\langle 00|\, \Sigma_2^{-\dot{-}} \left(|{+}{+}\rangle_{n_l} \otimes |00\rangle_{p_l}\right)_{\text{Symm.}} = {}_{m_l}\langle 00|00\rangle_{m_l}\, e^{i\frac{\sqrt{2}v}{R}}. \end{aligned} \tag{5.2.17}$$

Notice that here we are also implicitly using that, when acting on a ground state $|{+}{+}\rangle_n$, the operators $\Sigma_2^{-\dot{-}}$ and $\mathcal{O}_{(r)}^{-\dot{-}}$ commute. Plugging all the expressions together we see that the action of the twist operator yields

$$\begin{aligned} \Sigma_2^{+\dot{-}} \left[\left(|{+}{+}\rangle_{n_l}\right)^{N_{n_l}^{(++)}} \left(|00\rangle_{n_l}\right)^{N_{n_l}^{0(00)}} \left(J_{-1}^+ |00\rangle_{m_l}\right)^{N_{m_l}^{1(00)}}\right] = \\ = e^{i\frac{\sqrt{2}v}{R}} c_{n_l,p_l} \frac{N_{m_l}^{1(00)}+1}{2} \left[\left(|{+}{+}\rangle_{n_l}\right)^{N_{n_l}^{(++)}-1} \left(|00\rangle_{n_l}\right)^{N_{n_l}^{0(00)}-1} \left(J_{-1}^+ |00\rangle_{m_l}\right)^{N_{m_l}^{1(00)}+1}\right]. \end{aligned} \tag{5.2.18}$$

We are now ready to calculate the one point function. Writing it out explicitly, we get

$$\begin{aligned} \langle \Sigma_2^{+\dot{-}} \rangle = |\psi|^{-2} |\Sigma_2^{+\dot{-}}|^{-1} \langle \psi|\, \Sigma_2^{+\dot{-}}\, |\psi\rangle = \\ = |\psi|^{-2} |\Sigma_2^{+\dot{-}}|^{-1} \psi^\dagger \sum_{N_{m_l}^{1(00)}=0}^{N/m_l} \sum_{N_{p_l}^{0(00)}=0}^{\frac{N-N_{m_l}^{1(00)} m_l}{p_l}} c_{n_l,p_l} \frac{N_{m_l}^{1(00)}+1}{2} \left(A_{n_l}^{(++)} |{+}{+}\rangle_{n_l}\right)^{N_{n_l}^{(++)-1}} \otimes \\ \otimes \left(B_{p_l}^{0(00)} |00\rangle_{p_l}\right)^{N_{p_l}^{0(00)}-1} \left(B_{m_l}^{1(00)} J_{-1}^+ |00\rangle_{m_l}\right)^{N_{m_l}^{1(00)}+1} = \\ = \frac{e^{i\frac{\sqrt{2}v}{R}}}{4} \frac{(n_l+p_l)}{n_l\, p_l} A_{n_l}^{(++)} B_{p_l}^{0(00)} \overline{B_{n_l+p_l}^{1(00)}} \left(\frac{2}{N(N-1)}\right)^{\frac{1}{2}}, \end{aligned} \tag{5.2.19}$$

where in the last equality we have used the approximation (5.2.5), cancelled the norm of the out state with the norm of the in state and used equation (2.1.62) for the normalisation of the twist operator. Notice that our result differs from the one in [88] by a factor proportional to N^{-1}, the last square root factor in the equation above, which comes from the normalisation of the twist operator. That normalisation was not considered there, but for the results in this thesis will play a crucial role. Now that we have reviewed the calculation and some of its key elements we will calculate more general one point functions. We will simplify the notation used where possible, to make the equations less cumbersome.

5.2.3 $\mathcal{O}^{-\dot{-}}_{(r)}$ operator

In this section we calculate the one point function for $\sum_r \mathcal{O}^{-\dot{-}}_{(r)}$, which transforms a single strand by lowering the R-symmetry charge by 1/2 on the left and on the right. Consider the two-charge state

$$\psi(A,B) = \sum_{p=0}^{\frac{N}{n}} \left(A\left|++\right\rangle_n\right)^p \left(B\left|00\right\rangle_n\right)^{\frac{N}{n}-p}, \tag{5.2.20}$$

which has norm

$$\mathcal{N}(p) = \frac{N!}{p!\left(\frac{N}{n}-p\right)!n^{\frac{N}{n}}}. \tag{5.2.21}$$

We are assuming that n is an integer, multiple of N. With this simplified notation we already took into account the constraint (2.1.4) for the lengths and number of strands. The sum over all the possible strand combinations is peaked in this case at, from equation (5.2.5),

$$n\bar{p} = |A|^2, \qquad N - n\bar{p} = |B|^2. \tag{5.2.22}$$

As this is the first one point function that we calculate where our operator is defined as a sum over copies let us discuss the combinatorics carefully. The α coefficient goes as follows. We choose one of the p strands to act with the operator. For each strand, we are acting with n terms, corresponding to the sum over copies. However, only the action on one copy is non-trivial and so there is no extra combinatorial factor. Another way to think about this is that once we have picked up the copy, the operator can act on any of the copies within the strand. Again, though, in this case this action is only non-trivial in one copy and so there is no extra factor. This will not be the case for more complicated operators. Therefore, the action of the operator on a ground state is straightforward, as the resulting combination is just the definition of a $\left|00\right\rangle_n$ ground state,

$$\begin{aligned}&\sum_{r=1}^{n} \mathcal{O}^{-\dot{-}}_{(r)} \left|++\right\rangle_n = \\ =&\sum_{r=1}^{n} \left(\left|++\right\rangle_{(1)} \otimes ... \otimes \left|++\right\rangle_{(r-1)} \otimes \left|00\right\rangle_{(r)} \otimes \left|++\right\rangle_{(r+1)} \otimes ... \left|++\right\rangle_{(n)}\right) = \left|00\right\rangle_n .\end{aligned} \tag{5.2.23}$$

Therefore, the α factor is obtained by solving

$$p\mathcal{N}(p) = \alpha\mathcal{N}(p-1), \tag{5.2.24}$$

which gives

$$\alpha = \frac{N}{n} - p + 1. \tag{5.2.25}$$

In this case there is no c coefficient, as we are not gluing strands. The action of the operator on the strands is thus

$$\begin{aligned}\mathcal{O}^{-\dot{-}}\left[\left(|++\rangle_{n_l}\right)^p\left(|00\rangle_{n_l}\right)^{\frac{N}{n}-p}\right] &= \\ = \left(\frac{N}{n}-p+1\right)&\left[\left(|++\rangle_{n_l}\right)^{p-1}\left(|00\rangle_{n_l}\right)^{\frac{N}{n}-p+1}\right].\end{aligned} \tag{5.2.26}$$

The calculation of the one point function is now completely analogous to the one in section 5.2.2. The result is

$$\left\langle\sum_{r=1}^{n}\mathcal{O}^{-\dot{-}}_{(r)}\right\rangle = \frac{A\bar{B}}{n}, \tag{5.2.27}$$

where we understand this as a building block for more general calculations (notice that the state is not $S(N)$ invariant).

5.2.4 $\mathcal{O}^{+\dot{-}}_{(r)}$ operator

Consider now the operator $\sum_r \mathcal{O}^{+\dot{-}}_{(r)}$, which takes a strand and raises its left R charge by 1/2 and it lowers it by the same amount on the right, creating a three-charge strand from a two-charge one. This one point function is analogous to the previous one but for a 1/8-BPS state. To calculate its vacuum expectation value, consider the state

$$\psi(A,B^1) = \sum_{p=0}^{\frac{N}{n}}\left(A\,|++\rangle_n\right)^p\left(J^+_{-1}B^1\,|00\rangle_n\right)^{\frac{N}{n}-p}, \tag{5.2.28}$$

which has norm

$$\mathcal{N}(p) = \frac{N!}{p!\left(\frac{N}{n}-p\right)!n^p}. \tag{5.2.29}$$

The process is now

$$\left(\sum_{r=1}^{n_l}\mathcal{O}^{+\dot{-}}_{(r)}\right)|++\rangle_{n_l} \to \left(J^+_{-1(r)}\right)|00\rangle_{n_l}. \tag{5.2.30}$$

To find this one point function we need the commutation relation between the R-symmetry current and the $\mathcal{O}^{\alpha\dot{\alpha}}$ operator, which is given by

$$\left[\left(J^i_n\right)^{\alpha\beta},\mathcal{O}^{\beta\dot{\alpha}}(v,u)\right] = \frac{1}{2}e^{in\frac{\sqrt{2}v}{R}}\left(\sigma^i\right)^{\alpha\beta}\mathcal{O}^{\beta\dot{\alpha}}(v,u). \tag{5.2.31}$$

Then,

$$\begin{aligned}{}_n\langle 00|\left(\sum_{r=1}^{n}J^-_{+1(r)}\right)\left(\sum_{r=1}^{n}\mathcal{O}^{+\dot{-}}_{(r)}\right)|++\rangle_n &= e^{i\frac{\sqrt{2}v}{R}}\,{}_n\langle 00|\left(\sum_{r=1}^{n}\mathcal{O}^{-\dot{-}}_{(r)}\right)|++\rangle_n = \\ &= e^{i\frac{\sqrt{2}v}{R}}\,{}_n\langle 00|00\rangle_n.\end{aligned} \tag{5.2.32}$$

The combinatorial factor α is analogous to the previous case, as we now have

$$p\mathcal{N}(p) = \alpha\mathcal{N}(p-1) \tag{5.2.33}$$

which gives

$$\alpha = \frac{1}{n}\left(\frac{N}{n} - p + 1\right). \tag{5.2.34}$$

Recalling that the sum in the definition of the state is peaked at

$$n\bar{p} = |A^2|, \qquad \frac{N}{n} - \bar{p} = |B^1|^2 \tag{5.2.35}$$

we find the answer of the one point function to be

$$\left\langle \sum_{r=1}^{n} \mathcal{O}^{+\dot{-}}_{(r)} \right\rangle = \frac{1}{n} A\overline{B^1} e^{i\frac{\sqrt{2}v}{R}}. \tag{5.2.36}$$

Now that we have computed the one point functions for these untwisted chiral primaries let us go to the one point functions for twist operators.

5.2.5 $\Sigma_n^{--\dot{-}}$ operator

For this first twisted sector one point function consider the operator $\Sigma_n^{--\dot{-}}$, which joins n strands into a single one. We consider the case where we join strands of the same length, as then the formula for the result is much simpler. The generalisation to different strand lengths does not involve any extra subtleties. So, consider the state

$$\psi = \sum_{p=0}^{\frac{nN}{M}} \left(A\,|{+}{+}\rangle_{\frac{M}{n}}\right)^p \left(A_2\,|{+}{+}\rangle_M\right)^{\frac{N}{M}-\frac{p}{n}}, \tag{5.2.37}$$

where M (and thus also n) are small integers. The norm of this state is

$$|\psi|^2 = \sum_{p=0}^{\frac{nN}{M}} |A|^{2p} |A_2|^{\frac{N}{M}-\frac{p}{n}} \mathcal{N}(p), \tag{5.2.38}$$

where

$$\mathcal{N}(p) = \frac{N!}{p!\left(\frac{N}{M}-\frac{p}{n}\right)!\left(\frac{M}{n}\right)^p M^{\frac{N}{M}-\frac{p}{n}}}. \tag{5.2.39}$$

The sum over strands of the norm peaks at

$$\bar{p} = \frac{n|A|^2}{M} = \frac{n}{M}(N - |A_2|^2), \tag{5.2.40}$$

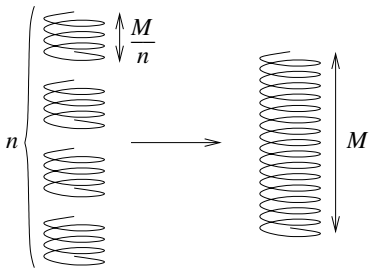

Figure 5.2.1: Initial and final states of the twist operator action. We start with n strands of length M/n and we join them all together in one step, *i.e.* we act on them with a twist n operator to join them in a single strand of length M.

like in the previous cases. Now, the action of the operator Σ_n^{--} on the strands of the state ψ is

$$\Sigma_n^{--}\left[\left(|{+}{+}\rangle_{\frac{M}{n}}\right)^p\left(|{+}{+}\rangle_M\right)^{p_2}\right]=c_n\alpha\left[\left(|{+}{+}\rangle_{\frac{M}{n}}\right)^{p-n}\left(|{+}{+}\rangle_M\right)^{p_2+1}\right], \tag{5.2.41}$$

where the c_n coefficient is the generalisation of the c_2 used in section 5.2.2. So, we start with n strands of length M/n, and at the end we have a single strand of length M. The coefficient c_n is the one obtained in chapter 4, and in the case of joining strands of the same length its expression is

$$c_n=M^{1-n}n^{\frac{M}{2}+\frac{n}{2}-\frac{M}{n}}\left((n-1)^2(n\bar{a})^{(n-2)}\Lambda^{-1}\right)^{\frac{1}{2}(n-1)\left(1-\frac{M}{n}\right)} \tag{5.2.42}$$

where

$$\Lambda=\left(1+n(n-1)^{(n-1)}-n^{n-1}\right) \tag{5.2.43}$$

and

$$\bar{a}^{n-1}=n\left(1-\frac{1}{n}\right)^{n-1}-1. \tag{5.2.44}$$

Let us now compute the α coefficient. As in the previous cases, it is a combinatorial factor obtained by matching the number of terms (the normalisation of the state) before and after the application of the gluing operator. Since we join all the strands in a single step, the only freedom we have is where within each strand we insert the operator. Thus, clearly the gluing operator can act in $\left(\frac{M}{n}\right)^n$ ways. In figure 5.2.1 we present a picture depicting this process. Therefore,

$$\binom{p}{n}\left(\frac{M}{n}\right)^n\mathcal{N}(p)=\alpha\mathcal{N}(p-n). \tag{5.2.45}$$

Solving for α we obtain

$$\alpha=\frac{M\left(\frac{N}{M}-\frac{p}{n}+1\right)}{n!}. \tag{5.2.46}$$

Assuming, as we said before, that the sum is peaked at $\bar{p}$ we obtain

$$\langle\Sigma_n^{--}\rangle=|\psi|^{-2}|\Sigma_n^{--}|^{-1}\langle\psi|\,\Sigma_n^{--}\,|\psi\rangle=$$

$$= |\psi|^{-2}|\Sigma_n^{-\dot{-}}|^{-1}\psi^\dagger \sum_{p=0}^{\frac{nN}{M}} A^p A_2^{p_2} c_n \frac{M\left(\frac{N}{M}-\frac{p}{n}+1\right)}{n!}\left(|{+}{+}\rangle_{\frac{M}{n}}\right)^{p-n}(|{+}{+}\rangle_M)^{p_2+1} =$$
$$= |\Sigma_n^{-\dot{-}}|^{-1} c_n \frac{N-\frac{\bar{p}M}{n}}{n!} A^n A_2^{-1} = A^n \bar{A}_2 \frac{c_n}{n!}\left(\frac{n}{N(N-1)\cdot\ldots\cdot(N-n+1)}\right)^{\frac{1}{2}}, \tag{5.2.47}$$

where c_n is given by equation (5.2.42). Let us now go to the analogous 1/8-BPS one point function.

5.2.6 $\Sigma_n^{+\dot{-}}$ operator

In this section we present some combinatorics needed for the calculation of the $\Sigma^{+\dot{-}}$ one point function. We do not give the final result of this one point function as it involves the calculation of a new commutator between operators, which is left as future work. Consider the state

$$\psi = \sum_{\{\mathcal{N}\}}\left(A\,|{+}{+}\rangle_{\frac{M}{n}}\right)^{N^+}\left(B\,|00\rangle_{\frac{M}{n}}\right)^{N^0}\left(C\left(J_{-1}^+\right)^{n-1}|00\rangle_M\right)^{N^1} \tag{5.2.48}$$

which has norm

$$\mathcal{N}(N^+,N^0) = \frac{N!}{N^+!N^0!N^1!\left(\frac{M}{n}\right)^{N^+ +N^0}M^{N^1}}\binom{M}{n-1}^{N^1}. \tag{5.2.49}$$

Let us recall that if we add other strands to consider a more general state the result is exactly the same using the short strand approximation, and so we only include the ones involved in the correlation at hand to ease the notation. Thus, in this section we are interested in the one point function of the twist operator $\Sigma_n^{+\dot{-}}$. Namely, we consider the following process

$$\Sigma_n^{+\dot{-}}\left(\left(|{+}{+}\rangle_{\frac{M}{n}}\right)^{n-1}\otimes|00\rangle_{\frac{M}{n}}\right)\to\left(J_{-1}^+\right)^{n-1}|00\rangle_M\,. \tag{5.2.50}$$

As in the previous section we need the c_n coefficient, which is given in equation (5.2.42). Let us now compute the combinatorial α factor. The twist operator acts on $n-1$ $|{+}{+}\rangle_{\frac{M}{n}}$ states, and on one $|00\rangle_{\frac{M}{n}}$ state. Within each strand, it can act on any of the M/n copies. However, there is a further subtlety in this case, as we explained in section 5.2.2. Recalling that the twist operator acts up to cyclic permutations, we need to take the symmetrisation of the states over which it acts, as we did in that case. Notice that in the previous section we did not need to take this into account as all the strands were the same, but now we have two different kinds of strands and need to take that into account. So, the gluing

process is

$$\Sigma_n^{+\dot{-}}\left(\left(|{+}{+}\rangle_{\frac{M}{n}}\right)^{n-1}\otimes|00\rangle_{\frac{M}{n}}\right)_{\text{Symm}}=\left(J_{-1}^{+}\right)^{n-1}|00\rangle_M\,. \tag{5.2.51}$$

Now, when we take the strands on the left hand side we have already picked the copies on which the gluing operator acts, but they have all possible orderings within all the strands. Therefore, we need to divide by the right amount to have only the distinct cycles. The number of ways in which we can order the M copies in the strands is

$$\frac{M!}{\left(\frac{M}{n}\right)!\left((n-1)\frac{M}{n}\right)!}, \tag{5.2.52}$$

which corresponds just to how many ways we can order the two distinct ground states. Now, we will need to divide by this number, and multiply by the distinct ways in which they can be arranged up to cyclic permutations, since we have the twist Σ_n acting. This second counting is less direct than the one above, and to obtain the result we need Burnside's lemma or, more generally, the Pólya enumeration theorem. Using the theorem, we find that there are

$$\frac{1}{M}\sum_{d|\gcd(\frac{M}{n},(n-1)\frac{M}{n})}\phi(d)\binom{\frac{M}{nd}+(n-1)\frac{M}{nd}}{\frac{M}{nd}} \tag{5.2.53}$$

different combinations up to cyclic permutations. There are special cases (when the number of strands we join are prime numbers for example) where this formula reduces to a compact expression, however these special cases are not relevant for the calculation at hand. Therefore, we leave the coefficient as is, defining

$$S:=\frac{\frac{1}{M}\sum_{d|\gcd(\frac{M}{n},(n-1)\frac{M}{n})}\phi(d)\binom{\frac{M}{nd}+(n-1)\frac{M}{nd}}{\frac{M}{nd}}}{\frac{M!}{(\frac{M}{n})!(n-1)\frac{M}{n})!}}, \tag{5.2.54}$$

as a parameter. Thus, the counting of terms before and after the action of the twist is

$$S\binom{N^+}{n-1}N^0\left(\frac{M}{n}\right)^n\mathcal{N}(\psi)=\alpha\mathcal{N}(\psi(N^1+1)), \tag{5.2.55}$$

where $\mathcal{N}(\psi)$ is the combinatorial factor we wrote above, and the one on the right hand side is the one after the action of the twist. Plugging in the expressions for $\mathcal{N}$ and simplifying yields

$$\alpha=S\left(N^1+1\right)\frac{(M-n+1)!}{M!}M. \tag{5.2.56}$$

With all this, the only remaining thing is to put everything together to obtain the one point function. However, to do so we need the commutator between $\Sigma_n^{+\dot{-}}$ and $\otimes_r J_{(r)}$, which in general will have a more complex expression than (5.2.16). This commutator can be obtained by bosonising the fermions for example, but this is beyond the scope of this chapter and is left as future work.

5.2.7 $(J^+_{-1})^m$ operator

In this section we consider the m-point function

$$\left\langle \left(J^+_{-1}\right)^m \right\rangle . \tag{5.2.57}$$

To do so we should a priori consider a state with all possible combinations of powers of the J operator, which is

$$\psi = \sum_{\{\mathcal{N}\}} (B\,|00\rangle_n)^p \bigotimes_m \left(B_m \left(J^+_{-1}\right)^m |00\rangle_n\right)^{p_m}, \tag{5.2.58}$$

This is a complicated state, and the equations involved cannot be written easily. We will consider such a state in section 5.3.2.5 for the long strand case. However, as we have seen in the previous sections with the short strand approximation the norm of the state cancels, and thus the result is the same as in an easier case where we only take the strands involved in the process. Therefore, for this section we consider instead the state

$$\psi = \sum_{p=0}^{\frac{N}{n}} (B\,|00\rangle_n)^p \left(B_m \left(J^+_{-1}\right)^m |00\rangle_n\right)^{\frac{N}{n}-p}, \tag{5.2.59}$$

which has norm

$$|\psi|^2 = \sum_{p=0}^{\frac{N}{n}} |B|^{2p} |B_m|^{2\left(\frac{N}{n}-p\right)} \mathcal{N}(p) \tag{5.2.60}$$

with

$$\mathcal{N}(p) = \frac{N!}{n^{\frac{N}{n}}} \frac{1}{p!} \frac{1}{\left(\frac{N}{n}-p\right)!} \binom{n}{m}^{\frac{N}{n}-p}. \tag{5.2.61}$$

This is the basic piece needed to calculate this one point function for more complex states, where we have products of modes. The α coefficient for this process is

$$p\binom{n}{m}\mathcal{N}(p) = \alpha \mathcal{N}(p-1) \qquad \Longrightarrow \qquad \alpha = \frac{N}{n} - p + 1, \tag{5.2.62}$$

and the condition for the average number of strands reads

$$\binom{n}{m} |B_m|^2 = n\left(\frac{N}{n} - \bar{p}\right). \tag{5.2.63}$$

Thus, the result for this m-point function in the short strand case is

$$\left\langle \left(J^+_{-1}\right)^m \right\rangle = B\bar{B}_m \frac{1}{n} \binom{n}{m}. \tag{5.2.64}$$

Let us now comment on some other twisted operators.

5.2.8 Twist sector $\mathcal{O}_n^{\alpha\dot{\alpha}}$ operators

Similar to section 5.2.6, we do not give results for the operators considered in this section. Rather, we explain how the calculation is analogous to the previous ones except for a few details, which we do not work out in this thesis.

Consider the following twisted sector operator,

$$\Sigma_n^{-\dot{-}}\left(\sum_{r=1}^{n}\mathcal{O}_{(r)}^{+\dot{+}}\right). \tag{5.2.65}$$

The conformal dimensions of this operator are, as we saw in equation (2.1.37), $(n/2, n/2)$. Therefore, we are raising the left and right R-symmetry charges by the same amount in both sides using this operator. The calculation of this one point function is completely analogous to the previous sections, taking into account that we now have a product of two operators and so in general we need to combine different results from previous sections.

However, the state resulting from the action of this operator is an excited one, which has not been studied in the supergravity side so far. Thus, the mapping of the supergravity coefficients of the corresponding geometry has not been given, and it is beyond the scope of this thesis. More precisely, in order to do this calculation we would need an analogous equation to the equation (5.2.63) we just used above, but for the states created with the twisted $\mathcal{O}$ operator. With that knowledge, since the combinatorics are analogous to previous sections the result would be easily obtainable. Let us move on to other cases now.

5.2.9 Other chiral primaries

Even if the matching with the supergravity side is not clear, in this section we want to point out that the CFT calculations for other operators are completely analogous. Consider for instance the chiral primary

$$\bigotimes_{r=1}^{n}\mathcal{O}_{(r)}^{\alpha\dot{\alpha}}. \tag{5.2.66}$$

Notice that this operator is not symmetric under $S(N)$; in order to get a symmetric state we should consider all possible combinations, by adding them. The calculations in this section can be understood as an essential building block towards that goal.

The operator (5.2.66) acting on a $|{+}{+}\rangle_n$ strand creates again an excited strand, just as in the previous case. However, we can also consider it acting on n copies of a unit length

strand. That is, we can now easily calculate the process

$$\bigotimes_{r=1}^{n} \mathcal{O}_{(r)}^{\alpha\dot{\alpha}} \left(|{+}{+}\rangle_1\right)^n \qquad \to \qquad \left(|00\rangle_1\right)^n . \tag{5.2.67}$$

Thus, consider the state

$$\psi = \sum_{p=0}^{N} \left(A\,|{+}{+}\rangle_1\right)^p \left(B\,|00\rangle_1\right)^{N-p} \tag{5.2.68}$$

which has norm

$$|\psi|^2 = \sum_{p=0}^{N} |A|^{2p} |B|^{2(N-p)} \frac{N!}{p!(N-p)!}. \tag{5.2.69}$$

The α coefficient in this case is

$$\binom{p}{n} \mathcal{N}(p) = \alpha \mathcal{N}(p-n) \qquad \Longrightarrow \qquad \alpha = \frac{(N-p+n)!}{n!(N-p)!}. \tag{5.2.70}$$

Using the approximation for the short strands we obtain

$$\left\langle \bigotimes_{r=1}^{n} \mathcal{O}_{(r)}^{-\dot{-}} \right\rangle = \frac{A^n}{B^n} \frac{(N-|A|^2)!}{n!(N-|A|^2-n)!}. \tag{5.2.71}$$

Notice that for $n = 1$ we recover the result found in [88].

We can also obtain the exact result using the same method as we will use in section 5.3. We refer to that section for the procedure, and we give the result directly in this case. Setting $|A|^2 = \alpha N$, $|B|^2 = (1-\alpha)N$, $0 < \alpha < 1$, where this α is unrelated to the coefficient matching the number of terms calculated above, we find that

$$\left\langle \bigotimes_{r=1}^{n} \mathcal{O}_{(r)}^{-\dot{-}} \right\rangle = A^n \bar{B}^n \frac{1}{n!} \frac{\sum_{p=0}^{N-n} \alpha^p (1-\alpha)^{-p} \frac{1}{p!(N-p-n)!}}{\sum_{p=0}^{N} \left(\frac{\alpha}{1-\alpha}\right)^p \frac{1}{p!(N-p)!}} = A^n \bar{B}^n \frac{N!}{n!} \frac{(1-\alpha)^n}{(N-n)!}. \tag{5.2.72}$$

We present the behaviour of the result in figure 5.2.2a. As we can see, the values it takes are very big for small n. As we increase n, this answer becomes bigger close to $\alpha = 0$, and very close to zero as α approaches one. We present this second case in figure 5.2.2b.

So far, apart from this last example, we have illustrated with some examples how to obtain the CFT one point functions of chiral primary operators in the short strand case. The tools that we have shown can be used to calculate more general one point functions as well, for example for the $\mathcal{O}_{\kappa}^{\alpha\dot{\alpha},*}$ operators defined in equation (2.1.32). We can also obtain one point functions for heavy and/or twisted J operators. Similarly, we can calculate one point functions for products of twist operators. The method is exactly the same, but the combinatorics will be more involved. In chapter 6 we are interested in n-point functions

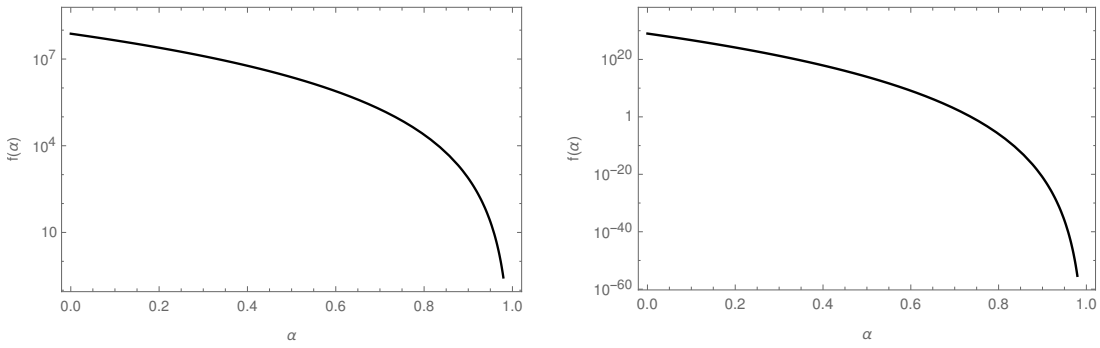

(a) n of order one

(b) n comparable to N

Figure 5.2.2: Behaviour of the n-point function in equation (5.2.72). We see that it takes very big values. In figure 5.2.2a we give the case where n is of order one, by setting $n = 5$ and $N = 100$. In figure 5.2.2b we give the case where n is of order N, by setting $n = 50$ and $N = 100$. As we can see, in this second case the n-point function is bigger for small values of α, but very close to zero for α close to one.

for products of twist operators. There we explain the combinatorics involved, reviewing some integer partition theory, and use the results to give an upper bound and a lower bound for the $\langle(\Sigma_2^{--})^n\rangle$ n-point function.

In the next section we focus on the same one point functions as the ones we have explicitly calculated in this section, but in the opposite limit; in the long strand case. Notice that some of the one point functions that we have calculated in this section, like the one above, are explicitly only possible in the short strand case. Generalisations of these can be considered also in the long strand case. We will not calculate all of them, as the examples provided should be enough to obtain these other cases.

5.3 One point functions: long strand case

In section 5.2 we have calculated one point functions for chiral primaries in the short strand length case. That is, in the case where we have a large amount of copies of each strand, with the lengths being of order one. In this section we focus on the opposite limit, that is, in the limit where the strand length is large and the number of strands is small. As in the short strand section first we will explain the approximation that we use, and then we will go case by case calculating the results. As we will see, in this limit the one point functions give much smaller results than in the opposite one in general.

We consider now the case where the strand lengths are of order N, and the number of strands is of order one. In this section we separate the results for the two and three-charge cases, as the method used differs slightly in both. In the two-charge case we will be able

to obtain exact results, whereas in the three-charge case we will strongly use the large N limit. We start with the 1/4-BPS states.

5.3.1 Two-charge states

As we just said, in this case we will be able to obtain exact results for the one point functions. As we introduced in section 2.1.5 and used in section 5.2, we work with the state given in equation (2.1.50),

$$\psi_{\{A_\kappa^{(gs)}\}} = \sum_{\{N_\kappa^{(gs)}\}} \left(\prod_{gs,\kappa} A_\kappa^{(gs)} \right)^{N_\kappa^{(gs)}} \psi_{\{N_\kappa^{(gs)}\}} = \sum_{\{N_\kappa^{(gs)}\}} \prod_{gs,\kappa} (A_\kappa^{(gs)} \, |S\rangle_\kappa)^{N_\kappa^{(gs)}}, \tag{5.3.1}$$

which has norm

$$|\psi|^2 = \sum_{\{N_\kappa^{(gs)}\}} \frac{N!}{\prod_{gs,\kappa} N_\kappa^{(gs)} \kappa^{N_\kappa^{(gs)}}} \prod_{gs,\kappa} |A_\kappa^{(gs)}|^{2N_\kappa^{(gs)}}. \tag{5.3.2}$$

Recall also that the sum is constrained by

$$\sum_{gs,k} k N_k^{(gs)} = N, \tag{5.3.3}$$

and the coefficients $A_k^{(gs)}$ satisfy

$$\sum_{k,gs} \left| A_k^{(gs)} \right|^2 = N. \tag{5.3.4}$$

In what follows, we first give an idea of how we do the calculation in this limit, and then we work case by case the answers for the one point functions.

5.3.1.1 Method

The final answer of each one point function is determined by the $A_i^{(gs)}$ coefficients, and so it is natural to set, given the condition that we have written in equation (5.3.4),

$$|A_i^{(gs)}| = N\alpha_i^{(gs)}, \qquad \text{with} \qquad \alpha_1^{(gs)} \in (0,1), \;\; \alpha_2^{(gs)} \in \left(0, 1-\alpha_1^{(gs)}\right), \;\; \ldots \tag{5.3.5}$$

where the last $\alpha_i^{(gs)}$ coefficient is given in terms of the previous ones. Since we are in the long strand case we consider the lengths κ of all the strands to be N/m_κ, where m_κ is small compared to N. Likewise, the number of strands $N_\kappa^{(gs)}$ will also be a number of order one. Now, the important thing to notice is that the only N-dependence of the norm of (5.3.1) is an $N!$ factor which comes out of the sum. To see this, we substitute in the

norm the parametrisation (5.3.5), which gives

$$|\psi|^2 = N! \sum_{\{N_\kappa^{(gs)}\}} \prod_{gs,\kappa} \frac{m_\kappa^{N_\kappa^{(gs)}}}{N_\kappa^{(gs)}!} \alpha_\kappa^{N_\kappa^{(gs)}}. \tag{5.3.6}$$

As we have seen from the previous section, this will be the denominator of all the one point functions. If the numerator has at most an $(N-1)!$ dependence in N then this will mean that, up to numbers of order one, the long strand one point functions will be suppressed by a factor of N with respect to the short strand length ones. The expression of this numerator depends on the chiral primary we use, and so we will go one by one in the following sections. As we will see the N dependence will also factor out in all the numerators, and so we will be able to obtain the exact result up to a polynomial which depends only on the $\alpha_i^{(gs)}$. We will give the polynomials for some cases as well, to see what is their behaviour for all values of the $\alpha_i^{(gs)}$. Let us start by calculating the numerator for the $\Sigma_n^{\dot{-}\dot{-}}$ operator with the most general 1/4-BPS state.

5.3.1.2 $\Sigma_n^{\dot{-}\dot{-}}$ operator

We can do the first part of this calculation in the most general case. Also, we drop the (gs) superscript, as it is redundant in this case and will only complicate the notation. We start with the strands

$$\bigotimes_{i=1}^{n} \left(A_i \left|++\right\rangle_{\frac{N}{m_i}} \right)^{p_i} \otimes \left(A \left|++\right\rangle_{\frac{N}{m}} \right)^{p}, \qquad \sum_{i=1}^{n} \frac{1}{m_i} = \frac{1}{m}. \tag{5.3.7}$$

After the action of the $\Sigma_n^{\dot{-}\dot{-}}$ operator we have

$$\left(\prod_{i=1}^{n} A_i^{p_i} \right) A^p \bigotimes_{i=1}^{n} \left(\left|++\right\rangle_{\frac{N}{m_1}} \right)^{p_i-1} \otimes \left(\left|++\right\rangle_{\frac{N}{m}} \right)^{p+1}. \tag{5.3.8}$$

As we said, we are in the limit where m_i, p_i, m, p are small numbers. These strands contribute with the corresponding term in the in state $\langle\psi|$ which has the same strands. Thus, the contraction gives

$$\left(\prod_{i=1}^{n} A_i \right) \overline{A} \left(\prod_{i=1}^{n} |A_i|^{2(p_i-1)} \right) |A|^{2p} \left\| \bigotimes_{i=1}^{n} \left(\left|++\right\rangle_{\frac{N}{m_1}} \right)^{p_i-1} \otimes \left(\left|++\right\rangle_{\frac{N}{m}} \right)^{p+1} \right\|^2. \tag{5.3.9}$$

The norm is given by

$$\frac{N!}{\prod_{i=1}^{n} \left[\left(\frac{N}{m_i}\right)^{p_i-1} (p_i-1)! \right] \left(\frac{N}{m}\right)^{p+1} (p+1)!} \sim \frac{N!}{N^{p+\sum_{i=1}^{n} p_i - n + 1}}. \tag{5.3.10}$$

The product of the moduli of the A_i yields

$$\alpha_1\alpha_2\cdot ...\cdot \alpha_{n-1}(1-\alpha_1-\alpha_2-...-\alpha_{n-1})N^{p+\sum_{i=1}^n p_i-n}, \tag{5.3.11}$$

and thus the N-dependence of the product of the two is $(N-1)!$. Now, this is not the only part of the one point function that can give N dependence. We also have the c_n and α coefficients, so we need to see what their product is. Let us start by calculating α, as it is straightforward to obtain. Analogous to the previous section, we need to match the number of terms before and after, taking into account in how many ways can the gluing operator act. Therefore,

$$\prod_{i=1}^n p_i\frac{N}{m_i}\mathcal{N}_{\text{initial}}=\alpha\mathcal{N}_{\text{final}}. \tag{5.3.12}$$

Certainly if we consider a process where we take more than one strand of the same kind the product of p_i factor will be different, and we will have instead some combinatorial number. However, as we said these are small numbers which do not affect the N behaviour, and so we give the result only for this case. The combinatorials needed for the exact result are explained in the previous section. Solving for α we obtain

$$\alpha=(p+1)\frac{N}{m}\sim N, \tag{5.3.13}$$

i.e. it scales like N. Let us now consider the c_n coefficient. We have written its expression in equation (5.2.42) for strands of the same length, but let us recall its expression here in the most general case. It is

$$c=\frac{\left(\frac{N}{m}\right)^{\frac{1}{2}(\frac{N}{m}+2-n)}}{n}\prod_{i=1}^n|1-\bar{a}_i|^{\frac{1}{2}(\frac{N}{m_i}-1)(n-1)}\prod_{j=1}^n\left(\frac{N}{m_j}\right)^{-\frac{1}{2}\left(\frac{N}{m_j}+1\right)}\prod_{j\neq k}|\bar{a}_j-\bar{a}_k|^{\frac{1}{2}\left(1-\frac{N}{m_k}\right)}, \tag{5.3.14}$$

where

$$\bar{a}_i=\frac{1+\bar{a}e^{i\phi_i}}{1-\frac{m}{m_i}},\qquad \bar{a}=\left(\frac{m_1}{m}\prod_{i=2}^n\left(1-\frac{m}{m_i}\right)-1\right)^{\frac{1}{n-1}} \tag{5.3.15}$$

and the phases are

$$\begin{aligned}(n-1)\in 2Z:\quad \phi_i &= \frac{(i-1)\pi}{n-1},\quad \phi_{i+1}=-\frac{(i-1)\pi}{n-1},\quad i\in 2Z,\quad i\geq 2 \\ n\in 2Z:\quad \phi_2 &= 0,\quad \phi_i=\frac{(i-1)\pi}{n-1},\quad \phi_{i+1}=-\frac{(i-1)\pi}{n-1},\quad (i-1)\in 2Z,\quad i\geq 3.\end{aligned} \tag{5.3.16}$$

Notice that the coefficients $\bar{a}$, $\bar{a}_i$ are independent of N. Keeping only the factors with N we see that

$$c \sim N^{1-n} \left(\frac{1}{m}\right)^{\frac{1}{2}\left(\frac{N}{m}+2-n\right)} |1-\bar{a}_i|^{n\frac{1}{2}\frac{N}{m}-\frac{1}{2}\frac{N}{m}-\frac{n}{2}+\frac{1}{2}} \frac{1}{\prod_j m_j^{-\frac{1}{2}\left(\frac{N}{m_j}+1\right)}} \prod_{j\neq k} |\bar{a}_j-\bar{a}_k|^{\frac{1}{2}\left(1-\frac{N}{m_k}\right)}. \tag{5.3.17}$$

We need to see that the product of all the factors that have an exponent dependent of N go to zero in the large N limit. Let us check some simple cases first. As noted in [1] for $n = 2, 3$ we have simple expressions for the coefficient c_n, and we also have a compact formula when all the m_i are equal. For $n = 2$ the coefficient reads

$$c_2 = \frac{1}{N}\frac{m_1+m_2}{2}. \tag{5.3.18}$$

For $n = 3$ we have

$$c_3 = \frac{1}{N^2}\frac{m_1m_2+m_2m_3+m_1m_3}{3}. \tag{5.3.19}$$

The case of equal m_i requires some more work. Let $m_i = m$ for all $i \leq n$, so that we join n strands of length N/m into a single one of length Nn/m. Then the general expression (5.3.14) reduces in this case to equation (5.2.42), which with the current notation is

$$c_n = \left(\frac{nN}{m}\right)^{1-n} n^{\frac{Nn}{2m}+\frac{n}{2}-\frac{N}{m}} \left((n-1)^2(n\bar{a})^{(n-2)}\Lambda^{-1}\right)^{\frac{1}{2}(n-1)\left(1-\frac{N}{m}\right)} \tag{5.3.20}$$

where

$$\Lambda = \left(1+n(n-1)^{(n-1)}-n^{n-1}\right) \tag{5.3.21}$$

and

$$\bar{a} = \left(n\left(1-\frac{1}{n}\right)^{n-1}-1\right)^{\frac{1}{n-1}}. \tag{5.3.22}$$

As we can see the N factor can be read straight away and agrees with (5.3.17). We need to see what happens with the other factors. Let

$$Q := (n-1)^2(n\bar{a})^{(n-2)}\Lambda^{-1}. \tag{5.3.23}$$

Using the large N approximation we can drop some terms in the exponents and rewrite the coefficient as

$$c_n \approx N^{1-n}\left(\left(\frac{n}{Q}\right)^{\frac{N}{2}(n-1)}\left(\frac{1}{n}\right)^{\frac{N}{2}}\right)^{\frac{1}{m}} \tag{5.3.24}$$

Now, the function n/Q is a monotonically decreasing function, which satisfies

$$\left[\frac{n}{Q}\right]_{n=4} = \frac{5}{11} < 1, \qquad \lim_{n\to+\infty}\frac{n}{Q} = 0. \tag{5.3.25}$$

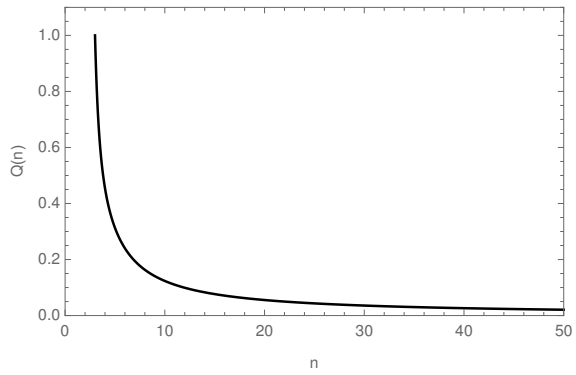

Figure 5.3.1: Behaviour of n/Q, where Q is defined in equation (5.3.23). As we can see, this function decreases exponentially in n. The c_n coefficient will thus vanish exponentially fast for $n \geq 4$, as this function appears to the power of N.

More precisely, it is a exponentially decreasing function in n. We show its behaviour in figure 5.3.1. Therefore,

$$\lim_{N\to\infty} c_n = 0, \qquad n \geq 4. \tag{5.3.26}$$

If we add the α coefficient we obtain

$$c\alpha_{\text{between } n \text{ strands of equal length}} \sim N^{2-n}\left(\left(\frac{n}{Q}\right)^{\frac{N}{2}(n-1)}\left(\frac{1}{n}\right)^{\frac{N}{2}}\right)^{\frac{1}{m}}, \tag{5.3.27}$$

and so the answer for the one point function is, adding the normalisation of the twist,

$$\begin{aligned}&\langle\Sigma_n^{\dot{--}}\rangle_{\text{long}} = \\ &= \left(\prod_{i=1}^{n} A_i\right)\bar{A}N^{1-n}\left(\left(\frac{n}{Q}\right)^{\frac{N}{2}(n-1)}\left(\frac{1}{n}\right)^{\frac{N}{2}}\right)^{\frac{1}{m}}\left(\frac{n}{N(N-1)...(N-n+1)}\right)^{\frac{1}{2}} f(\alpha_1,...,\alpha_n),\end{aligned} \tag{5.3.28}$$

where $f(\alpha_1,...,\alpha_n)$ is an N-independent polynomial which numerator is given by equations (5.3.9), (5.3.10) and (5.3.11) and with the denominator given by (5.3.6). Notice that the one point function decreases exponentially with N for $n \geq 4$, as for $n = 3$ we have $n/Q = 1$. If we compare this result to the short strand case, equation (5.2.47), we see that the only N dependence in the short strand case comes from the normalisation of the twist. Therefore, we have the following relations for the one point functions,

$$\begin{aligned}\langle\Sigma_2^{\dot{--}}\rangle_{\text{long}} &\sim \frac{1}{N}\langle\Sigma_2^{\dot{--}}\rangle_{\text{short}} \\ \langle\Sigma_3^{\dot{--}}\rangle_{\text{long}} &\sim \frac{1}{N^2}\langle\Sigma_3^{\dot{--}}\rangle_{\text{short}} \\ \langle\Sigma_n^{\dot{--}}\rangle_{\text{long}} &\sim N^{1-n}e^{-N\log n}\langle\Sigma_n^{\dot{--}}\rangle_{\text{short}} \qquad \text{(same strand length)}.\end{aligned} \tag{5.3.29}$$

We will now do this calculation for the single copy $\mathcal{O}^{--\dot{-}}_{(r)}$ operator, and afterwards we will show examples of the $f(\alpha_1, ..., \alpha_n)$ polynomials in both cases.

5.3.1.3 $\mathcal{O}^{--\dot{-}}_{(r)}$ operator

In this case we start with the strands

$$\left(A_1 \left|++\right\rangle_{\frac{N}{m}}\right)^{p_1} \left(A_2 \left|00\right\rangle_{\frac{N}{m}}\right)^{p_2}. \tag{5.3.30}$$

After the action of the $\mathcal{O}^{--\dot{-}}_{(r)}$ operator we have

$$A_1^{p_1} A_2^{p_2} \left(\left|++\right\rangle_{\frac{N}{m}}\right)^{p_1-1} \left(\left|00\right\rangle_{\frac{N}{m}}\right)^{p_2+1}. \tag{5.3.31}$$

The contraction gives

$$A_1 \bar{A}_2 |A_1|^{2p_1} |A_2|^{2(p_2-1)} \frac{N!}{(p_1-1)!(p_2+1)! \left(\frac{N}{m}\right)^{p_1-1} \left(\frac{N}{m}\right)^{p_2+1}}. \tag{5.3.32}$$

The α coefficient in this case is

$$\alpha = p_2 + 1, \tag{5.3.33}$$

and so the one point function is

$$\langle \mathcal{O}^{--\dot{-}} \rangle_{\text{long}} = A_1 \bar{A}_2 \frac{1}{N} f(\alpha), \tag{5.3.34}$$

where, again, $f(\alpha)$ is a polynomial which is independent of N. Comparing to the result of the short strand case we see that

$$\langle \mathcal{O}^{--\dot{-}} \rangle_{\text{long}} \sim \frac{1}{N} \langle \mathcal{O}^{--\dot{-}} \rangle_{\text{short}}. \tag{5.3.35}$$

Let us now write and plot some polynomials for both operators, to see how they behave.

5.3.1.4 Exact answers for the one point functions (examples)

We start with a couple of easy examples, and build up to more general ones. Let us start with the $\Sigma_2^{--\dot{-}}$ operator in the easiest case possible.

Simplest non-trivial case Consider the state

$$\psi = \left(A_1 \left|++\right\rangle_{\frac{N}{4}}\right)^4 + \left(A_1 \left|++\right\rangle_{\frac{N}{4}}\right)^2 A_2 \left|++\right\rangle_{\frac{N}{2}} + \left(A_2 \left|++\right\rangle_{\frac{N}{2}}\right)^2. \tag{5.3.36}$$

We have a non-zero one point function, which corresponds to

$$\langle \Sigma_2^{\dot{-}\dot{-}} \rangle = |\psi|^{-2} \, |\Sigma_2^{\dot{-}\dot{-}}|^{-1} \, \langle \psi | \, \Sigma_2^{\dot{-}\dot{-}} \, | \psi \rangle \, . \tag{5.3.37}$$

Since we have just a few terms, we write them all out explicitly to see exactly how the calculation works. Using the formulas of the previous sections, we see that the norm of this state is

$$|\psi|^2 = \frac{32(N-1)!}{3N^3} |A_1|^8 + \frac{16(N-1)!}{N^2} \, |A_1|^4 \, |A_2|^2 + \frac{2(N-1)!}{N} \, |A_2|^4 \, . \tag{5.3.38}$$

It is useful to write the generic expression for each term, $\mathcal{N}(p)$, to make some combinatorials easier afterwards. They read

$$\begin{aligned} \mathcal{N}(p) &= \frac{N!}{\left(\frac{N-p\frac{N}{2}}{\frac{N}{4}}\right)! \left(\frac{N}{4}\right)^{\left(\frac{N-p\frac{N}{2}}{\frac{N}{4}}\right)} p! \left(\frac{N}{2}\right)^p} = \\ &= \frac{N!}{(4-2p)! \left(\frac{N}{4}\right)^{(4-2p)} p! \left(\frac{N}{2}\right)^p}, \qquad p = 0, 1, 2. \end{aligned} \tag{5.3.39}$$

It is also more convenient to write the state (5.3.36) as a sum. We have

$$\psi = \sum_{p=0}^{2} \left(A_1 \, |{+}{+}\rangle_{\frac{N}{4}} \right)^{4-2p} \left(A_2 \, |{+}{+}\rangle_{\frac{N}{2}} \right)^p . \tag{5.3.40}$$

Now, the action of the gluing operator is

$$\Sigma_2^{\dot{-}\dot{-}} \left[\left(|{+}{+}\rangle_{\frac{N}{4}} \right)^{4-2p} \left(|{+}{+}\rangle_{\frac{N}{2}} \right)^p \right] = c_{\frac{N}{4},\frac{N}{4}} \alpha \left[\left(|{+}{+}\rangle_{\frac{N}{4}} \right)^{2-2p} \left(|{+}{+}\rangle_{\frac{N}{2}} \right)^{p+1} \right] . \tag{5.3.41}$$

The c_2 coefficient is

$$c_{\frac{N}{4},\frac{N}{4}} = \frac{4}{N}. \tag{5.3.42}$$

Now, for the combinatorial factor α, we need to choose two strands of length $N/4$, and they each have $N/4$ positions on which we can insert the gluing operator. Thus,

$$\binom{4-2p}{2} \left(\frac{N}{4} \right)^2 \mathcal{N}(p) = \alpha \mathcal{N}(p+1). \tag{5.3.43}$$

Solving for α we obtain

$$\alpha = (p+1)\frac{N}{4}. \tag{5.3.44}$$

The one point function then gives

$$\begin{aligned} \langle \Sigma_2^{\dot{-}\dot{-}} \rangle &= |\psi|^{-2} |\Sigma_2^{\dot{-}\dot{-}}|^{-1} \, \langle \psi | \, \Sigma_2^{\dot{-}\dot{-}} \, | \psi \rangle = \\ &= |\psi|^{-2} \Big[A_1^4 (\bar{A}_1)^2 \bar{A}_2 \, {}_{\frac{N}{2}}\langle {+}{+}| \left({}_{\frac{N}{4}}\langle {+}{+}| \right)^2 \left(|{+}{+}\rangle_{\frac{N}{4}} \right)^2 |{+}{+}\rangle_{\frac{N}{2}} + \end{aligned}$$

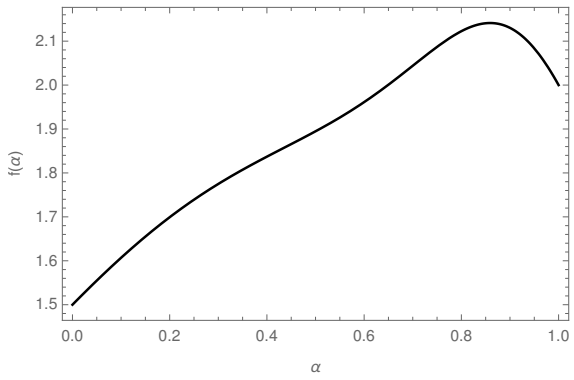

Figure 5.3.2: Behaviour of the coefficient $f(\alpha)$ which controls the relation between the one point functions for short and long strings.

$$+ A_1^2 A_2 (\bar{A}_2)^2 2 \left({}_{\frac{N}{2}}\langle ++| \right)^2 \left(|++\rangle_{\frac{N}{2}} \right)^2 \Big] =$$
$$= \frac{A_1^2 \bar{A}_2 \left(|A_1|^4 \frac{16N!}{N^3} + 2|A_2|^2 \frac{2N!}{N^2} \right)}{\frac{32}{3}\frac{N!}{N^4}|A_1|^8 + \frac{16N!}{N^3}|A_1|^4|A_2|^2 + \frac{2N!}{N^2}|A_2|^4} \left(\frac{2}{N(N-1)} \right)^{\frac{1}{2}}. \tag{5.3.45}$$

We want to relate this result to its analogous in the short strand length, large number of copies calculated in [88]. Let us recall that the expression we use for the one point function differs from the one in the paper, as we are including the normalisation for the twist operator. In this section this normalisation does not play any crucial role, and so for the rest of the section we will leave it as N_{Σ_κ}. The result for the analogous short strand one point function is

$$\langle \Sigma_2^{\dot{--}} \rangle_{\text{short}} = \frac{A_1^2 \bar{A}_2}{2} N_{\Sigma_2}, \tag{5.3.46}$$

which we obtained in equation (5.2.47) for general n. Using the substitutions $|A_1|^2 = N - |A_1|^2$ in (5.3.45), and letting $|A_2|^2 = \alpha N$, where $\alpha \in \mathbb{R}$, $0 \leq \alpha \leq 1$, as in equation (5.3.5), then (5.3.45) simplifies to

$$\langle \Sigma_2^{\dot{--}} \rangle_{\text{long}} = N_{\Sigma_2} A_1^2 \bar{A}_2 \frac{6}{N} \frac{4\alpha^2 - 7\alpha + 4}{16\alpha^4 - 40\alpha^3 + 51\alpha^2 - 40\alpha + 16}. \tag{5.3.47}$$

If we define $f(\alpha)$ to be the division of the two polynomials in α, we see that f is bounded by 2.15 for $0 \leq \alpha \leq 1$, as we can see in figure 5.3.2. Therefore, since $f(0) = 3/2$, we find that

$$A_1^2 \bar{A}_2 \frac{3}{2N} < \frac{\langle \Sigma_2^{\dot{--}} \rangle_{\text{long}}}{N_{\Sigma_2}} < A_1^2 \bar{A}_2 \frac{2.15}{N} \tag{5.3.48}$$

for all possible values of $|A_1|^2$ and $|A_2|^2$. Hence,

$$\langle \Sigma_2^{\dot{--}} \rangle_{\text{long}} \sim \frac{\langle \Sigma_2^{\dot{--}} \rangle_{\text{short}}}{N}. \tag{5.3.49}$$

Joining strands of different length Let us now do a similar calculation, but joining two strands of different lengths. The new feature in this example is that in this case we have two variables in the polynomial f. Consider the state

$$\psi = \left(A_1 \left|++\right\rangle_{\frac{N}{2}}\right)^2 + A_1 \left|++\right\rangle_{\frac{N}{2}} \left(A_2 \left|++\right\rangle_{\frac{N}{4}}\right)^2 + \left(A_2 \left|++\right\rangle_{\frac{N}{4}}\right)^4 + A_2 \left|++\right\rangle_{\frac{N}{4}} A_3 \left|++\right\rangle_{\frac{3N}{4}}. \tag{5.3.50}$$

We do this calculation explicitly term by term as well, to see exactly all terms and how it works. The norm of this state is

$$|\psi|^2 = \frac{N!}{N^2}\left(2|A_1|^4 + |A_1|^2|A_2|^4\frac{16}{N} + |A_2|^8\frac{32}{3N^2} + |A_2|^2|A_3|^2\frac{16}{3}\right). \tag{5.3.51}$$

Notice that we have two different terms now that are created with the $\Sigma_2^{-\dot{-}}$ operator,

$$\Sigma_2^{-\dot{-}}\psi \to A_1A_2^2 \left|++\right\rangle_{\frac{N}{4}} \left|++\right\rangle_{\frac{3N}{4}} + A_2^4 \left|++\right\rangle_{\frac{N}{2}} \left(\left|++\right\rangle_{\frac{N}{4}}\right)^2. \tag{5.3.52}$$

The first term is the one we are actually interested in, but as we will see the result is almost the same for both. For the first term we have

$$c_{\frac{N}{4},\frac{N}{2}} = \frac{3}{N}, \qquad \alpha_1 = \frac{3N}{4}, \tag{5.3.53}$$

and for the second one we have

$$c_{\frac{N}{4},\frac{N}{4}} = \frac{1}{N}, \qquad \alpha_2 = \frac{N}{4}. \tag{5.3.54}$$

Thus, the one point function is given by, analogous to the previous case,

$$\begin{aligned}\langle\Sigma_2^{-\dot{-}}\rangle &= |\psi|^{-2}|\Sigma_2^{-\dot{-}}|^{-1}\left\langle\psi\right| \left(A_1A_2^2\frac{9}{4}\left|++\right\rangle_{\frac{N}{4}} \left|++\right\rangle_{\frac{3N}{4}} + A_2^4\frac{1}{4}\left|++\right\rangle_{\frac{N}{2}} \left(\left|++\right\rangle_{\frac{N}{4}}\right)^2\right) = \\ &= N_{\Sigma_2}\frac{A_1A_2\overline{A}_312|A_2|^2 + \overline{A}_1A_2^2\frac{4}{N}|A_2|^4}{2|A_1|^4 + \frac{16}{N}|A_1|^2|A_2|^4 + \frac{32}{3N^2}|A_2|^8 + \frac{16}{3}|A_2|^2|A_3|^2}.\end{aligned} \tag{5.3.55}$$

Now, we set the modulus of the coefficients A_i to be

$$|A_1|^2 = N\alpha, \qquad |A_2|^2 = N\beta, \qquad |A_3|^2 = N(1-\alpha-\beta), \tag{5.3.56}$$

with

$$0 < \alpha < 1 \qquad \text{and} \qquad 0 < \beta < 1-\alpha. \tag{5.3.57}$$

Plugging these expressions in the one point function yields

$$\frac{1}{N}\frac{A_1A_2\overline{A}_312\beta + \overline{A}_1A_2^24\beta^2}{2\alpha^2 + 16\alpha\beta^2 + \frac{32}{3}\beta^4 + \frac{16}{3}\beta(1-\alpha-\beta)}. \tag{5.3.58}$$

Let $f(\alpha,\beta)$ be the coefficient without the A_i's and the N for both terms, just as in the previous case. As we can see, the polynomials that we obtain agree with the general

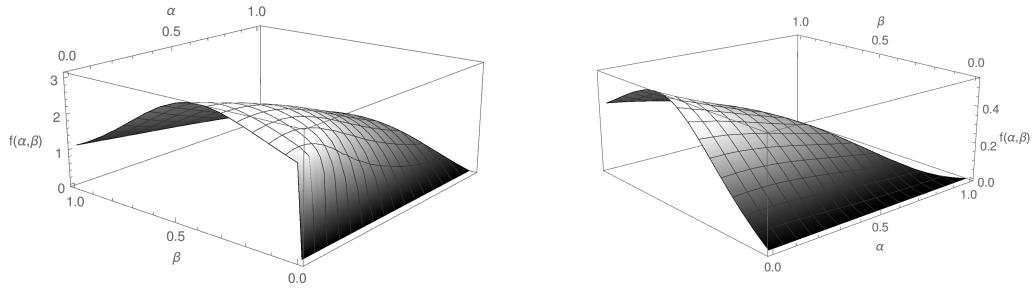

(a) First term (b) Second term

Figure 5.3.3: f coefficient comparing the long and short strand length one point functions for the $\Sigma_2^{\dot{-}\dot{-}}$ operator, in the case where it joins two strands of lengths $N/4$ and $N/2$, as shown in equation (5.3.52). The state that needs to be considered for such one point function to not vanish also enables the action of the twist on two strands of length $N/4$. Subfigure 5.3.3a corresponds to the first term that contributes, the joining of two strands of different length, which is the process we are interested in. Subfigure 5.3.3b is the second term, where two strands of the same length are joined. As we can see, the second contribution does not change the behaviour of the result.

equations (5.3.9) and (5.3.6). Then, as we show in figure 5.3.3 both terms are small in the range of interest. The point $(\alpha, \beta) = (0, 0)$ is singular, but let us recall that point is not a physical state and thus is not under consideration. Let us now study the polynomial that results from the action of the $\Sigma_2^{\dot{-}\dot{-}}$ operator in the case where it joins any two strands of equal length.

Joining two strands of the same length Consider the state

$$\psi = \sum_{p=0}^{\frac{m}{2}} \left(A_1 \left| ++ \right\rangle_{\frac{N}{m}} \right)^{m-2p} \left(A_2 \left| ++ \right\rangle_{\frac{2N}{m}} \right)^{p}. \tag{5.3.59}$$

The polynomial is, in this case,

$$f(\alpha) = \frac{1}{\alpha} \frac{\sum_{p=1}^{\frac{m}{2}} \left(\alpha^p (1-\alpha)^{-2p} \left(\frac{1}{2m} \right)^p \frac{1}{p!(m-2p)!} \right)}{\sum_{p=0}^{\frac{m}{2}} \left(\alpha^p (1-\alpha)^{-2p} \left(\frac{1}{2m} \right)^p \frac{1}{p!(m-2p)!} \right)}. \tag{5.3.60}$$

If we plug this expression in Mathematica we get

$$f(\alpha) = \frac{1 - \frac{2^{-\frac{m}{2}} \left(-\frac{(\alpha-1)^2 m}{\alpha} \right)^{m/2}}{U\left(-\frac{m}{2}, \frac{1}{2}, -\frac{(\alpha-1)^2 m}{2\alpha} \right)}}{\alpha}, \tag{5.3.61}$$

where U is a hypergeometric function. This function is of order one for most values of α. We present in figure 5.3.4 the plot of $f(\alpha)$ for $m = 17$. We see that we have an asymptote

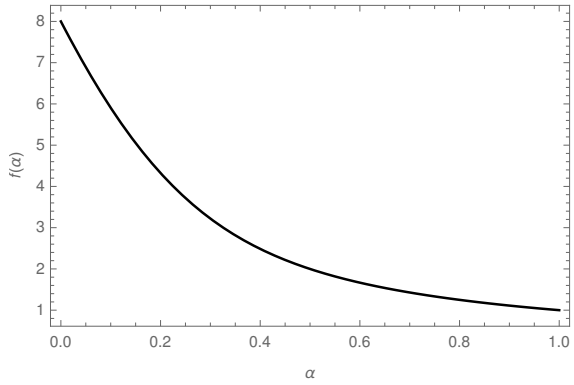

Figure 5.3.4: Behaviour of N times the coefficient (5.3.61) relating the one point function for Σ_2 in the long and short strand case. At zero the function is ill-defined. In the plot $m = 17$.

at $\alpha = 0$, as it happens in the other cases. Also, setting $m = 4$ in (5.3.61) we recover (5.3.47), as expected. Let us recall, from equation (5.3.28), that this one point functions also has a $1/N$ suppression with respect to the analogous short strand one.

Joining any two strands Consider the state

$$\psi = \sum_{p_1=0}^{m_1} \sum_{p_2=0}^{m_2\left(1-\frac{p_1}{m_1}\right)} \left(A_1 \left|++\right\rangle_{\frac{N}{m_1}}\right)^{p_1} \left(A_2 \left|++\right\rangle_{\frac{N}{m_2}}\right)^{p_2} \left(A_3 \left|++\right\rangle_{\frac{N}{m_3}}\right)^{p_3}, \tag{5.3.62}$$

where

$$p_3 = \frac{N - \frac{N}{m_1}p_1 - \frac{N}{m_2}p_2}{\frac{N}{m_3}} = m_3\left(1 - \frac{p_1}{m_1} - \frac{p_2}{m_2}\right) \tag{5.3.63}$$

and

$$\frac{N}{m_3} = \frac{N}{m_1} + \frac{N}{m_2}. \tag{5.3.64}$$

The norm of the state is

$$|\psi|^2 = \sum_{p_1=0}^{m_1} \sum_{p_2=0}^{m_2(1-\frac{p_1}{m_1})} |A_1|^{2p_1}|A_2|^{2p_2}|A_3|^{2p_3}\mathcal{N}(p_1,p_2), \tag{5.3.65}$$

where

$$\mathcal{N}(p_1,p_2) = \frac{N!}{p_1!p_2!p_3!\left(\frac{N}{m_1}\right)^{p_1}\left(\frac{N}{m_2}\right)^{p_2}\left(\frac{N}{m_3}\right)^{p_3}}. \tag{5.3.66}$$

The c_2 coefficient in this case is

$$c_{\frac{N}{m_1},\frac{N}{m_2}} = \frac{m_1+m_2}{2N}. \tag{5.3.67}$$

The action of the gluing operator is

$$\Sigma_2^{-\dot{-}}\left[\left(|{+}{+}\rangle_{\frac{N}{m_1}}\right)^{p_1}\left(|{+}{+}\rangle_{\frac{N}{m_2}}\right)^{p_2}\left(|{+}{+}\rangle_{\frac{N}{m_3}}\right)^{p_3}\right]= \\ = c_{\frac{N}{m_1},\frac{N}{m_2}}\alpha\left[\left(|{+}{+}\rangle_{\frac{N}{m_1}}\right)^{p_1-1}\left(|{+}{+}\rangle_{\frac{N}{m_2}}\right)^{p_2-1}\left(|{+}{+}\rangle_{\frac{N}{m_3}}\right)^{p_3+1}\right]. \tag{5.3.68}$$

In this case the α coefficient is

$$\alpha = \frac{N}{p_3 m_3}. \tag{5.3.69}$$

Mathematica is not able to perform the exact sums with all the coefficients for $f(\alpha_1, \alpha_2)$ in this case, and so we need to take approximations. We are in the case where the lengths of the strands are big, that is, in the limit where p_i, m_i are small integers. Thus, since

$$p_3 = m_3\left(1 - \frac{p_1}{m_1} - \frac{p_2}{m_2}\right), \tag{5.3.70}$$

and recalling as well that $0 \leq p_i \leq m_i$, we see that the factor inside the parenthesis will be of order 1, and so

$$p_3 \lesssim m_3 = \frac{m_1 m_2}{m_1 + m_2}. \tag{5.3.71}$$

Then, the total coefficient is approximated by

$$\frac{m_1 + m_2}{2p_3 m_3} \gtrsim \frac{(m_1 + m_2)^3}{2(m_1 m_2)^2}. \tag{5.3.72}$$

The polynomials are too long to write out explicitly in this case, and the formulas do not give any deeper insights. Also, we need to get rid of the factorials in the denominator so that Mathematica can perform the sums. Notice that in this case it is not straightforward to recover the results from the previous sections, as now the combinatorial factors are not easily reduced to the case of two strands of the same length. We present in figure 5.3.5 a plot of the function for $m_1 = 6$ and $m_2 = 12$. We observe again the asymptotes at the boundary values of α_1 and α_2. Let us recall once again that α_1 and α_2 are defined only in the open interval (0,1), as otherwise we would not have the strands necessary to have the process studied. Therefore, the polynomial is of order one in the range of interest, and so we confirm the behaviour described in the first line of equation (5.3.29). To finish this section let us study the case of the $\mathcal{O}_{(r)}^{-\dot{-}}$ operator.

$\mathcal{O}_{(r)}^{-\dot{-}}$ operator For the $\sum_{r=1}^{n}\mathcal{O}_{(r)}^{-\dot{-}}$ operator consider the state

$$\psi = \sum_{p=0}^{m}\left(A\,|{+}{+}\rangle_{\frac{N}{m}}\right)^{p}\left(B\,|00\rangle_{\frac{N}{m}}\right)^{m-p}. \tag{5.3.73}$$

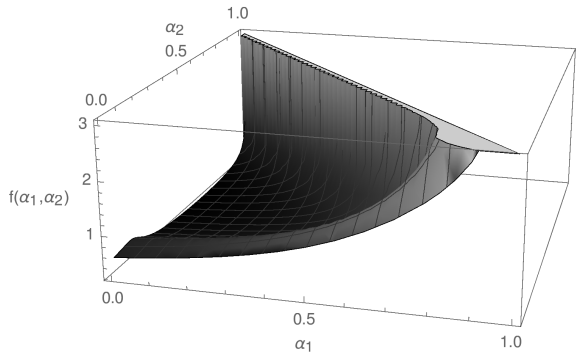

Figure 5.3.5: Behaviour of the coefficient $f(\alpha_1, \alpha_2)$ function for the $\langle \Sigma_2^{\dot{--}} \rangle$ in the long strand case. We can see that, as in the previous cases, we get asymptotes in the boundary values. In the plot, $m_1 = 6$ and $m_2 = 12$.

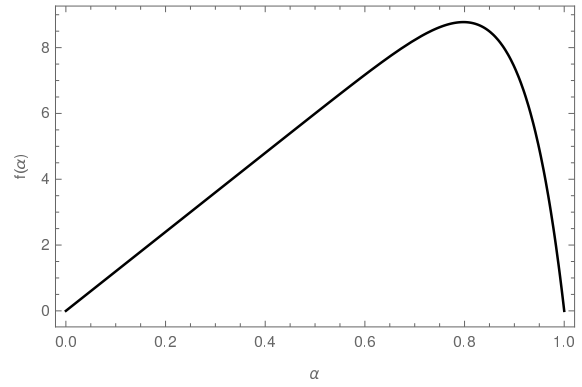

Figure 5.3.6: Behaviour of the function $f(\alpha)$ for the untwisted $\langle \mathcal{O}_{(r)}^{\dot{--}} \rangle$ one point function in the long strand case. As we can see we have a maximum of order one. Also, the function diverges for $\alpha = 1$ very rapidly, and so the divergence is not seen in this figure. In the plot $m = 12$.

Using the result (5.3.6) and section 5.3.1.3 we find that in this case the $f(\alpha)$ function is

$$f(\alpha) = \frac{\alpha \left(-(m+1) \left(\frac{1}{1-\alpha} \right)^m (1-\alpha)^m + \alpha m + 1 \right) - (\alpha - 1) m \alpha^m}{\alpha - 1}. \tag{5.3.74}$$

This function has an asymptote at $\alpha = 1$, but as always this is outside our range of interest. Otherwise it is finite, being zero for $\alpha = 0$ and with a finite maximum (of order m) close to one. We can see it in figure 5.3.6 for $m = 12$.

5.3.2 Three-charge states

Consider now a three-charge state,

$$\psi_{\{N^{(S)}_{\kappa,m_\kappa}\}} = \prod_{s=1}^{4}\prod_{\kappa}(|s\rangle_\kappa)^{N^{(s)}_\kappa}\prod_{\kappa,m_\kappa}\left(\frac{1}{m_\kappa!}(J^+_{-1})^{m_\kappa}|00\rangle_\kappa\right)^{N^{(00)}_{\kappa,m_\kappa}}. \tag{5.3.75}$$

Its norm is

$$|\psi(\{A^{(s)}_\kappa, B_{\kappa,m_\kappa}\})|^2 = \sum_{\{N^{(S)}_{\kappa,m_\kappa}\}}\mathcal{N}(\{N^{(S)}_{\kappa,m_\kappa}\})\left(\prod_{s,\kappa}|A^{(s)}_\kappa|^{2N^{(s)}_\kappa}\right)\left(\prod_{\kappa,m_\kappa}|B_{\kappa,m_\kappa}|^{2N^{(00)}_{\kappa,m_\kappa}}\right), \tag{5.3.76}$$

where

$$\mathcal{N}(\{N^{(S)}_{\kappa,m_\kappa}\}) = \left(\frac{N!}{\prod_{s,\kappa}N^{(s)}_\kappa!\kappa^{N^{(s)}_\kappa}}\right)\left(\frac{1}{\prod_{\kappa,m_\kappa}N^{(00)}_{\kappa,m_\kappa}!\kappa^{N^{(00)}_{\kappa,m_\kappa}}}\right)\prod_{\kappa,m_\kappa}\binom{\kappa}{m_\kappa}^{N^{(00)}_{\kappa,m_\kappa}}. \tag{5.3.77}$$

Notice that due to the insertions of the J^+_{-1} mode the N dependence of the norm is now more complicated. As in the two-charge case, we will first explain the approximation, and then we will go case by case giving the answers to the one point functions in this limit.

5.3.2.1 Method

The condition for the coefficients now reads [96]

$$\sum_{gs,\kappa}|A^{(gs)}_\kappa|^2 + \sum_{\kappa,m_\kappa}\binom{\kappa}{m_\kappa}|B_{\kappa,m_\kappa}|^2 = N, \tag{5.3.78}$$

and so, in addition to

$$|A^{(gs)}_i| = N\alpha^{(gs)}_i, \qquad \text{with} \qquad \alpha^{(gs)}_1 \in (0,1),\ \ \alpha^{(gs)}_2 \in \left(0, 1-\alpha^{(gs)}_1\right),\ \ ... \tag{5.3.79}$$

we need to set a parametrisation for the $|B_{\kappa,m_\kappa}|$ coefficients. This parametrisation is more subtle, as we need to consider things like

$$|B_{\kappa,m_\kappa}|^2 = \frac{N}{\binom{\kappa}{m_\kappa}}\beta_{\kappa,m_\kappa}, \tag{5.3.80}$$

with the β_{κ,m_κ} parameter running from zero to possibly a number bigger than one. Notice that, since we are in the long strand case, κ will be of order N, and m_κ can take any value between one and κ. We work this out explicitly for each case in the following sections.

So, if we absorb these extra factors in the β_{κ,m_κ}, plug all formulas in the norm of the

state and write the strands length as N/n_κ instead of κ we obtain

$$|\psi|^2 = N! \sum_{\{N^{(S)}_{\kappa,m_\kappa}\}} \frac{\prod_{\kappa,S} n_\kappa^{N^{(S)}_\kappa} \left(\alpha^{(S)}_\kappa\right)^{N^{(S)}_\kappa} \prod_{\kappa,m_\kappa} n_\kappa^{N^{(00)}_{n_\kappa,m_\kappa}} \beta^{N^{(00)}_{\kappa,m_\kappa}}_{n_\kappa,m_\kappa}}{\prod_{\kappa,S} N^{(S)}_{n_\kappa}! \prod_{\kappa,m_\kappa} N^{(00)}_{n_\kappa,m_\kappa}!} \prod_{\kappa,m_\kappa} \binom{\frac{N}{n_\kappa}}{m_\kappa}^{N^{(00)}_{\kappa,m_\kappa}}. \quad (5.3.81)$$

As we said above, we have N-dependence inside of the sum in this case. In some cases we will still be able to obtain an exact result, as we will be able to perform the sums. However, in other cases we will not be able to do so. Then, since the resulting polynomial will have now powers of N in the factors, what we will do is keep only the dominant term in the polynomial and compare the numerator and the denominator one. As shown in the previous cases, the denominator will always have a higher power of N than the numerator, and so the f function will be small. We start with a simple example to see explicitly how it works, and then we will give more general results for the rest of the operators.

5.3.2.2 Elementary example

We start with a simple example, just as in the previous section, and then we build up to more general ones. For this initial example we consider the untwisted $\mathcal{O}^{+\dot{-}}_{(r)}$ operator.

$\mathcal{O}^{+\dot{-}}_{(r)}$ operator Consider the state

$$\psi = \sum_{p=0}^{2} \left(A\,|{+}{+}\rangle_{\frac{N}{2}}\right)^p \left(BJ^+_{-1}\,|00\rangle_{\frac{N}{2}}\right)^{2-p} \quad (5.3.82)$$

which has norm

$$|\psi|^2 = \sum_{p=0}^{2} |A|^{2p}|B|^{2(2-p)}\mathcal{N}(p), \qquad \text{with} \qquad \mathcal{N}(p) = \frac{N!}{p!\left(\frac{N}{2}\right)^p(2-p)!}. \quad (5.3.83)$$

We want to find the one point function of $\sum_r \mathcal{O}^{+\dot{-}}_{(r)}$. This operator transforms a strand $|{+}{+}\rangle_{\frac{N}{2}}$ into a strand $J^+_{-1}\,|00\rangle_{\frac{N}{2}}$, and so we have

$$_{\frac{N}{2}}\langle 00|\, J^+_{-1} \sum_{r=1}^{\frac{N}{2}} \mathcal{O}^{+\dot{-}}_{(r)}\,|{+}{+}\rangle_{\frac{N}{2}} \sim_{\frac{N}{2}}\langle 00| \sum_{r=1}^{\frac{N}{2}} \mathcal{O}^{-\dot{-}}_{(r)}\,|{+}{+}\rangle_{\frac{N}{2}} = e^{i\frac{\sqrt{2}v}{R}}\,{}_{\frac{N}{2}}\langle 00|00\rangle_{\frac{N}{2}}\,. \quad (5.3.84)$$

The combinatorial factor α in this case is

$$\alpha = \frac{(3-p)!}{(2-p)!}\frac{2}{N}, \quad (5.3.85)$$

and thus we find

$$\langle \mathcal{O}^{+\dot{-}}_{(r)} \rangle_{\text{long}} = |\psi|^{-2} A\bar{B} \left[|A|^2 \frac{2}{N} e^{i\frac{\sqrt{2}v}{R}} |\psi'|^2 + |B|^2 \frac{4}{N} e^{i\frac{\sqrt{2}v}{R}} |\psi''|^2 \right], \tag{5.3.86}$$

where

$$\psi' = \left(\sum_r J^+_{-1(r)} |00\rangle_{\frac{N}{2}} \right) |{+}{+}\rangle_{\frac{N}{2}}, \qquad \psi'' = \left(\left(\sum_r J^+_{-1(r)} \right) |00\rangle_{\frac{N}{2}} \right)^2 \tag{5.3.87}$$

and so

$$|\psi'|^2 = \frac{N!}{\frac{N}{2}}, \qquad |\psi''|^2 = \frac{N!}{2}. \tag{5.3.88}$$

Plugging these expressions in yields

$$\langle \mathcal{O}^{+\dot{-}}_{(r)} \rangle_{\text{long}} = \langle \mathcal{O}^{+\dot{-}}_{(r)} \rangle_{\text{short}} \frac{\frac{4}{N}\left(\frac{|A|^2}{N} + \frac{|B|^2}{2} \right)}{\frac{|B|^4}{2} + \frac{2}{N}|A|^2|B|^2 + \frac{2}{N^2}|A|^4}, \tag{5.3.89}$$

where the short one point function is the one we computed before and is given by equation (5.2.36) for $n = 1$,

$$\langle \mathcal{O}^{+\dot{-}}_{(r)} \rangle_{\text{short}} = A\bar{B} e^{i\frac{\sqrt{2}v}{R}}. \tag{5.3.90}$$

Now, as mentioned above we use the relation

$$|A|^2 + \frac{N}{2}|B|^2 = N \tag{5.3.91}$$

and we set

$$|B|^2 = \alpha, \qquad \alpha \in (0, 2). \tag{5.3.92}$$

Then we obtain

$$\langle \mathcal{O}^{+\dot{-}} \rangle_{\text{long}} = \frac{2}{N} \langle \mathcal{O}^{+\dot{-}} \rangle_{\text{short}}. \tag{5.3.93}$$

Therefore, we see that in this initial case we obtain exactly the expected relation between both one point functions. Next we start calculating one point functions for generic cases.

5.3.2.3 Untwisted $\mathcal{O}^{-\dot{-}}_{(r)}$ operator

The aim of this section is to check that we recover the result from the two-charge case, by considering the same process as in the 1/4-BPS section but with a 1/8-BPS state now. Consider the state

$$\psi = \sum_{N^{(++)}=0}^{n} \sum_{N^{0(00)}=0}^{n-N^{(++)}} \left(A^{(++)} |{+}{+}\rangle_{\frac{N}{n}} \right)^{N^{(++)}} \left(B^{0(00)} |00\rangle_{\frac{N}{n}} \right)^{N^{0(00)}} \left(B^{1(00)} J^+_{-1} |00\rangle_{\frac{N}{n}} \right)^{N^{1(00)}} \tag{5.3.94}$$

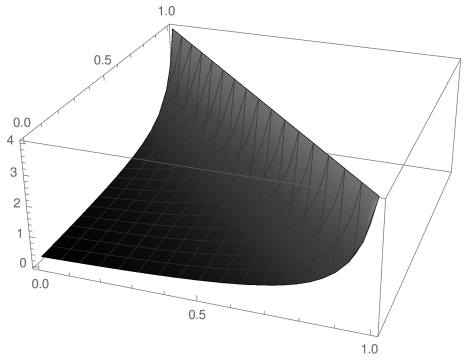

Figure 5.3.7: Graphical representation of the numerical coefficient for the $\mathcal{O}^{--\dot{-}}$ one point function in the long strand case. In the plot, $n = 4$.

We want to calculate the one point function in the long strand case for the $\mathcal{O}^{--\dot{-}}$ operator. The only on-trivial action of this operator on the state is when it performs the following transformation of strands,

$$\left(\sum_{r=1}^{N/n} \mathcal{O}^{--\dot{-}}_{(r)}\right) |{+}{+}\rangle_{\frac{N}{n}} \to |00\rangle_{\frac{N}{n}} \,. \tag{5.3.95}$$

The α coefficient in this case is

$$\alpha = N^{0(00)} + 1, \tag{5.3.96}$$

and after setting, as usual,

$$|A^{(++)}|^2 = \alpha N, \qquad |A^{0(00)}|^2 = \beta N, \qquad |A^{1(00)}|^2 = n(1-\alpha-\beta) \tag{5.3.97}$$

with

$$0 < \alpha < 1, \qquad 0 < \beta < 1 - \alpha \tag{5.3.98}$$

we obtain

$$\langle O^{--\dot{-}} \rangle_{\text{long}} = \frac{A^{(++)}\overline{A^{0(00)}}}{N} \cdot \frac{\sum_{N^{(++)}=0}^{n-1} \sum_{N^{0(00)}=1}^{n-N^{(++)}} N^{0(00)} \alpha^{N^{(++)}} \beta^{N^{0(00)}-1} (1-\alpha-\beta)^{N^{1(00)}} \frac{n^{N^{1(00)}-N^{(++)}-N^{0(00)}}}{N^{(++)}!N^{0(00)}!N^{1(00)}!}}{\sum_{N^{(++)}=0}^{n} \sum_{N^{0(00)}=0}^{n-N^{(++)}} \alpha^{N^{(++)}} \beta^{N^{0(00)}} (1-\alpha-\beta)^{N^{1(00)}} \frac{n^{N^{1(00)}-N^{(++)}-N^{0(00)}}}{N^{(++)}!N^{0(00)}!N^{1(00)}!}} \tag{5.3.99}$$

Mathematica can perform the sum ratio, giving

$$\langle O^{--\dot{-}} \rangle_{\text{long}} = \frac{A^{(++)}\overline{A^{0(00)}}}{N} \frac{n}{\alpha+\beta-n^2(\alpha+\beta-1)} \tag{5.3.100}$$

We present in figure 5.3.7 this result for the second factor plotted. We recover the expected $1/N$ behaviour except in the boundary values, as in the previous cases.

5.3.2.4 $\Sigma_2^{+\dot{-}}$ operator

This is the only twist operator one point function left to calculate in the long strand case, as we obtained results for the $\Sigma_n^{-\dot{-}}$ in the section 5.3.1.2. Also, let us recall from section 5.2.6 that for the twist n, 1/8-BPS one point function we need an extra commutator to obtain it, which we are not giving in this thesis. Thus, we calculate the twist two case, as we did in section 5.2.2 for the short strand case. Consider the state

$$\psi = \sum_{N^1=0}^{m} \sum_{N^0=0}^{m_2\left(1-\frac{N^1}{m}\right)} \left(A\,|{+}{+}\rangle_{\frac{N}{m_1}}\right)^{N^+} \left(B\,|00\rangle_{\frac{N}{m_2}}\right)^{N^0} \left(B^1 J_{-1}^{+}\,|00\rangle_{\frac{N}{m}}\right)^{N^1}, \tag{5.3.101}$$

where, as in the short strand case,

$$\frac{1}{m_1}+\frac{1}{m_2}=\frac{1}{m} \qquad \Longrightarrow \qquad m=\frac{m_1 m_2}{m_1+m_2} \tag{5.3.102}$$

and

$$\mathcal{N}=\frac{N!}{N^+!N^0!N^1!\left(\frac{N}{m_1}\right)^{N^+}\left(\frac{N}{m_2}\right)^{N^0}}. \tag{5.3.103}$$

Analogous to section 5.2.2, we have

$$\alpha=\frac{N^1+1}{2} \tag{5.3.104}$$

and

$$c_2=\frac{m_1+m_2}{2N}, \tag{5.3.105}$$

which lead to the result

$$\begin{aligned}\langle\Sigma_2^{+\dot{-}}\rangle_{\text{long}} &= N_{\Sigma_2}\frac{e^{i\frac{\sqrt{2}v}{R}}}{4}\frac{AB\bar{B}^1}{N}\cdot \\ &\cdot\frac{\sum_{N^1=1}^{m}\sum_{N^0=0}^{m_2\left(1-\frac{N^1}{m}\right)-1}(m_1+m_2)m^{N^1}\alpha^{N^+}\beta^{N^0}(1-\alpha-\beta)^{N^1}\frac{m_1^{N^+}m_2^{N^0}}{N^+!N^0!N^1!}}{\sum_{N^1=0}^{m}\sum_{N^0=0}^{m_2\left(1-\frac{N^1}{m}\right)}m^{N^1}\alpha^{N^+}\beta^{N^0}(1-\alpha-\beta)^{N^1}\frac{m_1^{N^+}m_2^{N^0}}{N^+!N^0!N^1!}}\end{aligned} \tag{5.3.106}$$

These sums cannot be obtained with Mathematica, and so we would need to approximate them. However, we do not need the exact result; the leading behaviour with N is enough. Since the sums only have factors of order one within them, that is, since they do not have any N's, their ratio will be a number much smaller than N, away from the boundaries of α and β. Therefore, we can approximate this one point function by

$$\langle\Sigma_2^{+\dot{-}}\rangle_{\text{long}} \approx N_{\Sigma_2}\frac{e^{i\frac{\sqrt{2}v}{R}}}{4}\frac{AB\bar{B}^1}{N}, \tag{5.3.107}$$

i.e. once again we learn that

$$\langle \Sigma_2^{+\dot{-}} \rangle_{\text{long}} \approx \frac{1}{N} \langle \Sigma_2^{+\dot{-}} \rangle_{\text{short}} \,. \tag{5.3.108}$$

5.3.2.5 Untwisted $\mathcal{O}_{(r)}^{+\dot{-}}$ operator in full generality

In this section we calculate the one point function of $\sum_{r=1}^{n} \mathcal{O}_{(r)}^{+\dot{-}}$ with the most general 1/8-BPS state. That is, we consider the state

$$\psi = \sum_{\{\mathcal{N}\}} \left[\left(A \left| ++ \right\rangle_{\frac{N}{\kappa}} \right)^{N^+} \left(\prod_{m_\kappa} B_{m_\kappa} \frac{\left(J_{-1}^+ \right)^{m_\kappa}}{m_\kappa!} \left| 00 \right\rangle_{\frac{N}{\kappa}} \right)^{N^0_{\kappa,m_\kappa}} \right]. \tag{5.3.109}$$

As we will see in a moment, the equations in this case cannot be written out in a closed form. However, we will still be able to give a result. We will work out the example $\kappa = 4$, and the general result follows easily from induction using the same process. So, let us consider $\kappa = 4$. The state ψ in this case reads

$$\begin{aligned} \psi = & \left(A \left| ++ \right\rangle_{\frac{N}{4}} \right)^4 + \sum_{p=0}^{3} \left(A \left| ++ \right\rangle_{\frac{N}{4}} \right)^p \otimes \\ & \otimes \left[\sum_{i_1=1}^{\frac{N}{4}} \ldots \sum_{i_{4-p}=i_{3-p}}^{\frac{N}{4}} \frac{B_{i_1} \cdot \ldots \cdot B_{i_{4-p}}}{i_1! \cdot \ldots \cdot i_{4-p}!} \left(J_{-1}^+ \right)^{i_1} \left| 00 \right\rangle_{\frac{N}{4}} \otimes \ldots \otimes \left(J_{-1}^+ \right)^{i_{4-p}} \left| 00 \right\rangle_{\frac{N}{4}} \right]. \end{aligned} \tag{5.3.110}$$

We have not found any easy way to write the norm of this state in a compact form that is understandable, so we write it all out explicitly. Once that is done, how terms are constructed in general will be clear from this example. That is why we leave all the factorials explicit in what follows. We have

$$\begin{aligned} \mathcal{N} = \frac{N!}{\left(\frac{N}{4}\right)^4} \Bigg\{ & \frac{1}{4!} + \frac{1}{3!} \sum_{i=1}^{\frac{N}{4}} \binom{\frac{N}{4}}{i} + \frac{1}{2!} \left(\frac{1}{2!} \sum_{i=1}^{\frac{N}{4}} \binom{\frac{N}{4}}{i}^2 + \sum_{i=1}^{\frac{N}{4}} \sum_{j=i+1}^{\frac{N}{4}} \binom{\frac{N}{4}}{i} \binom{\frac{N}{4}}{j} \right) + \\ & + \left(\frac{1}{3!} \sum_{i=1}^{\frac{N}{4}} \binom{\frac{N}{4}}{i}^3 + \frac{1}{2!} \sum_{i=1}^{\frac{N}{4}} \sum_{j=i+1}^{\frac{N}{4}} \binom{\frac{N}{4}}{i}^2 \binom{\frac{N}{4}}{j} + \right. \\ & \left. + \sum_{i=1}^{\frac{N}{4}} \sum_{j=i+1}^{\frac{N}{4}} \sum_{l=j+1}^{\frac{N}{4}} \binom{\frac{N}{4}}{i} \binom{\frac{N}{4}}{j} \binom{\frac{N}{4}}{l} \right) + \\ & + \left(\frac{1}{4!} \sum_{i=1}^{\frac{N}{4}} \binom{\frac{N}{4}}{i}^4 + \frac{1}{3!} \sum_{i=1}^{\frac{N}{4}} \sum_{j=i+1}^{\frac{N}{4}} \binom{\frac{N}{4}}{i}^3 \binom{\frac{N}{4}}{j} + \frac{1}{2!} \frac{1}{2!} \sum_{i=1}^{\frac{N}{4}} \sum_{j=i+1}^{\frac{N}{4}} \binom{\frac{N}{4}}{i}^2 \binom{\frac{N}{4}}{j}^2 + \right. \end{aligned}$$

$$+\frac{1}{2!}\sum_{i=1}^{\frac{N}{4}}\sum_{j=i+1}^{\frac{N}{4}}\sum_{l=j+1}^{\frac{N}{4}}\binom{\frac{N}{4}}{i}^2\binom{\frac{N}{4}}{j}\binom{\frac{N}{4}}{l}+$$
$$+\sum_{i=1}^{\frac{N}{4}}\sum_{j=i+1}^{\frac{N}{4}}\sum_{l=j+1}^{\frac{N}{4}}\sum_{t=l+1}^{\frac{N}{4}}\binom{\frac{N}{4}}{i}\binom{\frac{N}{4}}{j}\binom{\frac{N}{4}}{l}\binom{\frac{N}{4}}{t}\Bigg)\Bigg\}. \tag{5.3.111}$$

From this equation we can deduce how the terms look like for general κ. Looking at the state (5.3.110) it is clear that, in the three-charge strands terms, for each term with i_n sums we will have $p(n)$ terms, that is, the number of integer partitions of n terms. Each term will have as many sums as elements has every partition of n, and the binomial coefficient's powers correspond to the numbers in each partition (to its parts). Take the last parenthesis in (5.3.111) for instance. We have four sums in the state, and so we have $p(4) = 5$ terms in the norm. And the exponents of the binomials coefficients are given by the five possible partitions of four (see equation (2.1.14) or figure 6.4.4 for the partitions). Let us also recall that the coefficients in the state satisfy

$$|A|^2 + \sum_{i=1}^{\frac{N}{4}}\binom{\frac{N}{\kappa}}{m_\kappa}|B_{m_\kappa}|^2 = N. \tag{5.3.112}$$

In this case we have all the possibilities for the different number of insertions of the J^+_{-1} mode, and so we need to be more careful with the parametrisation of the equation above. Expanding the sum and dividing all the equation by N yields

$$1 = \frac{|A|^2 + |B_{\frac{N}{4}}|^2}{N} + |B_1|^2 + |B_{\frac{N}{4}-1}|^2 + N\left(|B_2|^2 + |B_{\frac{N}{4}-2}|^2\right) + O(N^2). \tag{5.3.113}$$

Recalling that we are in the large N limit, all coefficients except the first ones must be very small. Therefore, we can work with the parametrisation

$$|A|^2 = \alpha N, \qquad |B_i|^2 = \beta_{\frac{N}{4}} N, \qquad |B_1|^2 = \beta_1, \qquad |B_{\frac{N}{4}-1}|^2 = \beta_{\frac{N}{4}-1}, \tag{5.3.114}$$

and analogous for the rest coefficients. To simplify the expressions later, we will absorb all the powers of N of these parameters in the β_i. The running parameters labelled by the Greek letters taking values between zero and one, as usual. As in previous cases we use the commutator (5.2.31) to see that

$${}_{\frac{N}{4}}\langle 00|\, J^+_{-1}\sum_{r=1}^{\frac{N}{4}}\mathcal{O}^{+\dot{-}}_{(r)}\,|{+}{+}\rangle_{\frac{N}{4}} = {}_{\frac{N}{4}}\langle 00|00\rangle_{\frac{N}{4}}\, e^{i\frac{\sqrt{2}v}{R}}. \tag{5.3.115}$$

We are just missing the α coefficient to be able to get the answer for the one point function. Again, the expressions cannot be written easily in a compact way, so we go term by term to see the general result. Let α_i be the coefficient for the $p = i$ term, where p refers to the

sum index in equation (5.3.110). Clearly

$$\alpha_4 = \frac{4}{N}. \tag{5.3.116}$$

For the rest of the terms we will need to use the large N limit. We need to keep in mind that the operator $\mathcal{O}^{+\dot{-}}_{(r)}$ only generates states with one insertion of the J^+ mode. For $p = 3$ we have

$$3\frac{N!}{\left(\frac{N}{4}\right)^4}\frac{1}{3!}\sum_{i=1}^{\frac{N}{4}}\binom{\frac{N}{4}}{i} = \alpha_3\frac{1}{2}\frac{N!}{\left(\frac{N}{4}\right)^4}\left(\frac{N}{4}\sum_{i=2}^{\frac{N}{4}}\binom{\frac{N}{4}}{i} + \frac{1}{2}\left(\frac{N}{4}\right)^2\right). \tag{5.3.117}$$

Solving for α_3 we obtain

$$\frac{4}{N}\left(1 + \frac{\frac{N}{8}}{\sum_{i=1}^{\frac{N}{4}}\binom{\frac{N}{4}}{i} - \frac{N}{8}}\right) \approx \frac{4}{N}, \tag{5.3.118}$$

where in the last step we used the large N limit to approximate the second term in the parenthesis by zero. Similarly, for $p = 2$ we find

$$\alpha_2 = \frac{4}{N}\left(1 + \frac{\frac{2}{3}\left(\frac{N}{4}\right)^2 + \frac{1}{2}\frac{N}{4}\sum_{i=2}^{\frac{N}{4}}\binom{\frac{N}{4}}{i}}{\frac{1}{2!}\sum_{i=1}^{\frac{N}{4}}\binom{\frac{N}{4}}{i}^2 + \sum_{i=1}^{\frac{N}{4}}\sum_{j=i+1}^{\frac{N}{4}}\binom{\frac{N}{4}}{i}\binom{\frac{N}{4}}{j}}\right) \approx \frac{4}{N}, \tag{5.3.119}$$

and an analogous expression for $p = 1$. Therefore the value of α is the same for all terms,

$$\alpha \approx \frac{4}{N} \tag{5.3.120}$$

Since in the long strand limit κ (in equation (5.3.109)) is a small number, we thus learn that in general

$$\alpha \approx \frac{\kappa}{N}. \tag{5.3.121}$$

We are now ready to calculate the one point function. Again, the expressions are complicated, so we will be very explicit. As usual, we have

$$\langle \mathcal{O}^{+\dot{-}}_{(r)} \rangle = |\psi|^{-2} \langle \psi | \sum_{r=1}^{\frac{N}{4}} \mathcal{O}^{+\dot{-}}_{(r)} | \psi \rangle . \tag{5.3.122}$$

As we mentioned above, we need to keep in mind that the operator only generates strands with one insertion of the R-symmetry current, and so we need to be careful with the contractions. This also means that we do not have to worry about the factorials dividing when taking the modulus of the out state, as all factors that are not repeated in the bra and the ket and survive will be a one. Keeping all this in mind and using the substitutions

(5.3.114) we find

$$\begin{aligned}\langle \mathcal{O}^{+\dot{-}} \rangle \approx & |\psi|^{-2} A\bar{B}_1 e^{i\frac{\sqrt{2}v}{R}} \frac{4^5 N!}{N} \left\{ \frac{\alpha^3}{3!} + \alpha^2 \sum_{i=1}^{\frac{N}{4}} \beta_i \binom{\frac{N}{4}}{i} + \right. \\ & + \alpha \left[\frac{1}{2} \sum_{i=1}^{\frac{N}{4}} \beta_i^2 \binom{\frac{N}{4}}{i}^2 + \sum_{i=1}^{\frac{N}{4}} \sum_{j=i+1}^{\frac{N}{4}} \beta_i \beta_j \binom{\frac{N}{4}}{i} \binom{\frac{N}{4}}{j} \right] + \\ & + \frac{1}{3!} \sum_{i=1}^{\frac{N}{4}} \beta_i^3 \binom{\frac{N}{4}}{i}^3 + \frac{1}{2} \sum_{i=1}^{\frac{N}{4}} \sum_{j=i+1}^{\frac{N}{4}} \beta_i^2 \beta_j \binom{\frac{N}{4}}{i}^2 \binom{\frac{N}{4}}{j} + \\ & \left. + \sum_{i=1}^{\frac{N}{4}} \sum_{j=i+1}^{\frac{N}{4}} \sum_{k=j+1}^{\frac{N}{4}} \beta_i \beta_j \beta_k \binom{\frac{N}{4}}{i} \binom{\frac{N}{4}}{j} \binom{\frac{N}{4}}{k} \right\} =: |\psi|^{-2} A\bar{B}_1 e^{i\frac{\sqrt{2}v}{R}} \frac{4}{N} |\varphi|^2. \end{aligned} \tag{5.3.123}$$

If we now let $|\psi_\alpha|^2$ be the polynomial resulting from the norm of ψ after substituting with (5.3.114) without the common factors in front, we obtain

$$\langle \mathcal{O}^{+\dot{-}} \rangle \approx \frac{4}{N} A\bar{B}_1 e^{i\frac{\sqrt{2}v}{R}} \frac{|\varphi|^2}{|\psi|^2}. \tag{5.3.124}$$

And so, with the general observations done throughout this section we learn that, for general κ,

$$\left\langle \sum_{r=1}^{\frac{N}{\kappa}} \mathcal{O}^{+\dot{-}}_{(r)} \right\rangle \approx \frac{\kappa}{N} A\bar{B}_1 e^{i\frac{\sqrt{2}v}{R}} \frac{|\varphi|^2}{|\psi|^2}. \tag{5.3.125}$$

Comparing this result to its short strand case counterpart, equation (5.2.36) we see that, up to numbers of order one,

$$\frac{\langle \mathcal{O}^{+\dot{-}} \rangle_{\text{long}}}{\langle \mathcal{O}^{+\dot{-}} \rangle_{\text{short}}} \approx \frac{1}{N} f(N, \alpha, \beta_i), \tag{5.3.126}$$

where f is the polynomial described above. Notice that, maybe except for boundary values of the α, β_i variables, the polynomial f is a very small number, as the denominator has terms with higher powers of N than the numerator. Therefore, we see once again that the long strand one point function is parametrically smaller in N than the short strand one, *i.e.* at most

$$\langle \mathcal{O}^{+\dot{-}}_{(r)} \rangle_{\text{long}} \approx \frac{1}{N} \langle \mathcal{O}^{+\dot{-}}_{(r)} \rangle_{\text{short}}. \tag{5.3.127}$$

Let us finish this section with the calculation of the one point function for the modes of the R-symmetry current.

5.3.2.6 Untwisted $\left(J_{-1}^{+}\right)^{m}$ operator

We will now calculate the same one point function as in section 5.2.7. Just as in the short strand case we also calculate all $m-$point functions for $m \leq n$, as the calculation is analogous in all cases. Thus, consider the state

$$\psi = \sum_{p=0}^{n} \left(B \left|00\right\rangle_{\frac{N}{n}}\right)^{p} \left(B_m \frac{\left(J_{-1}^{+}\right)^{m}}{m!} \left|00\right\rangle_{\frac{N}{n}}\right)^{n-p}. \tag{5.3.128}$$

As before, we have

$$\mathcal{N}(p) = \frac{N!}{\left(\frac{N}{n}\right)^{n}} \frac{1}{p!(n-p)!} \binom{\frac{N}{n}}{m}^{n-p} \tag{5.3.129}$$

and

$$\alpha = n - p + 1. \tag{5.3.130}$$

Setting $|B|^2 = \alpha N$ as usual (where let us remind that this α is unrelated to the one above), and recalling that in this case we have

$$|B|^2 + \binom{\frac{N}{n}}{m} |B_m|^2 = N, \tag{5.3.131}$$

we see that we can sum exactly the expressions for the numerator and denominator. Notice that we can obtain the result for any m, even with the combinatorial factor of the equation above, as this factor will just increase the power of the corresponding factor in the norm of the state. The exact result for this one point function is thus

$$\left\langle \left(J_{-1}^{+}\right)^{m} \right\rangle = B\bar{B}_m \frac{n\binom{\frac{N}{n}}{m}^{3}}{\alpha N - (\alpha - 1)\binom{\frac{N}{n}}{m}^{2}} =: B\bar{B}_m f(\alpha). \tag{5.3.132}$$

As we can see in figure 5.3.8 $f(0) = n\binom{\frac{N}{n}}{m}$, and then it rapidly increases until we get to $\alpha = 1$, where $f(1) = \frac{n}{N}\binom{\frac{N}{n}}{m}^{3}$. Let us compare this result with the short strand case one, equation (5.2.64). Since the result for that case was independent of N, we see that in this case the long strand result is much bigger than the short strand one, for any value of the parameters.

5.4 Brief discussion of the results

Now that we have calculated some exemplary one point functions for short and long strands we can compare the results we obtained. We give a summary of the results and of the relations between them in chapter 7, but let us outline the main highlights here.

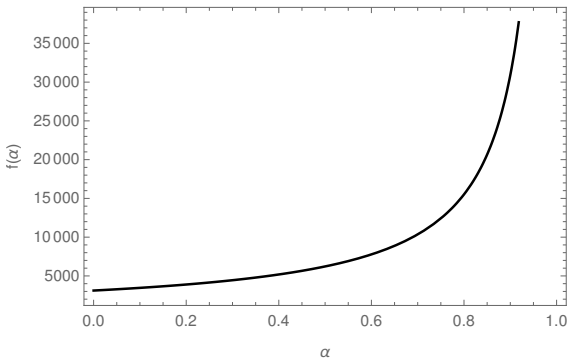

Figure 5.3.8: Behaviour of the function $f(\alpha)$ for the $\left(J^+_{-1}\right)^m$ one point function in the long strand case. There is no N suppression in this case. In the plot, $N = 100$, $n = 9$, $m = 4$. The function has the same behaviour for all the values of the parameters.

Let O be a chiral primary of the theory. The main result that we have obtained in this chapter is that

$$\langle O \rangle_{\text{long}} \sim \frac{\langle O \rangle_{\text{short}}}{N^r}, \tag{5.4.1}$$

where $r \geq 1$. This means that $\langle O \rangle_{\text{long}}$ is comparable to the supergravity corrections, that is, to higher derivative modes. Indeed, one could think of altering the states with which we calculate the one point functions to get bigger results, but then we are only rephrasing the issue. In that case we would need to act on the states with operators which are not in the supergravity theory. Therefore, the conclusion of this chapter is that one point functions of chiral primary operators in the long strand limit are suppressed by powers of N with respect to the short strand ones.

CHAPTER 6

Different ways of joining strands

In the previous chapters we have calculated correlation and one point functions for single trace chiral primary operators. In this chapter we take a slightly different direction, and study all the possible ways to join strands. To do so, we compare two values: the one point function $\langle \Sigma_n^{\dot{-}\dot{-}} \rangle$ and the one point function of multi-particle states $\langle (\Sigma_2^{\dot{-}\dot{-}})^{n-1} \rangle$. The first one translates in joining n strands (of any length) together at the same time, with one step. The second one consists in joining the n strands in $n-1$ steps, namely, joining them two by two. Both cases represented in figure 6.0.1.

As is obvious from the figure, in the first case, subfigure 6.0.1a, the number of ways in which the joining can be done is much smaller, as it only depends where within each strand the operator is inserted. However, in the other case, subfigure 6.0.1b, there are many ways to join, as the second application of the gluing operator could have joined the pair which was joined in the previous step to one of the two strands that was alone for instance. Hence, when joining the strands two by two the combinatorics are more complicated and will give a non-trivial contribution. We present work in this chapter which aims to compare both cases. Normalisations are the key point for this calculation, and they are related to integer partitions. The different countings are obtained in section 6.4.

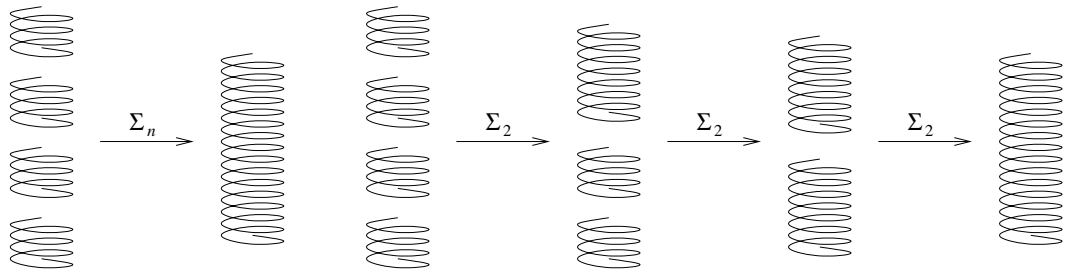

(a) All in one step (b) Two by two

Figure 6.0.1: Joining of strands using different operators. In (a) we join them using a single operator, Σ_n, which joins them all in one step. In (b) we join them two by two, in $n-1$ steps.

6.1 Layout

In section 6.2 we present the state with which we calculate all results. Section 6.3 is a reminder of the one point function result, which we presented in section 5.2.5. In section 6.4 we calculate the n-point function corresponding to the creation of a strand by joining strands two by two. Both results are compared in section 6.5. At the end of this chapter, in section 6.6, we also comment on all other possible ways of joining n strands.

6.2 Setting up

The procedure of this chapter is the same as in the previous one. The state that we start with in both cases is

$$\psi = \sum_{p=0}^{\frac{nN}{M}} \left(A \left| ++ \right\rangle_{\frac{M}{n}} \right)^p \left(B \left| ++ \right\rangle_M \right)^{\frac{N}{M}-\frac{p}{n}} . \tag{6.2.1}$$

The norm of this state is

$$|\psi|^2 = \sum_{p=0}^{\frac{nN}{M}} |A|^{2p} |B|^{\frac{N}{M}-\frac{p}{n}} \mathcal{N}(p), \tag{6.2.2}$$

where

$$\mathcal{N}(p) = \frac{N!}{p! \left(\frac{N}{M}-\frac{p}{n}\right)! \left(\frac{M}{n}\right)^p M^{\frac{N}{M}-\frac{p}{n}}}. \tag{6.2.3}$$

We will be able to give an exact answer for the relation between the one and the n-point functions, as both describe the same process at the end. Namely, all the calculations will be exactly the same, except for the α and c_n coefficients. Furthermore, the two results will only differ in factors proportional to n and M, and so all other contributions will cancel. We give more details and the results at the end of the chapter, after we have done all the

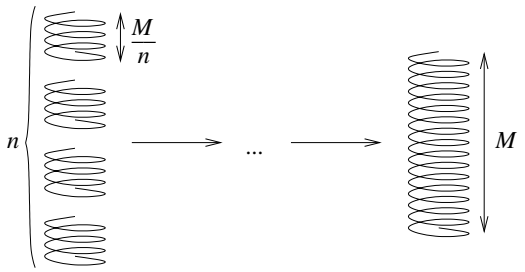

Figure 6.2.1: Initial and final states of the gluing process. The process starts with n strands of length M/n and finishes with all of them together, *i.e.* with a single strand of length M.

combinatorics. In what follow we assume $n \gg 1$ but not necessarily comparable to N. The final result will be valid for any $n \gg 1$.

In figure 6.2.1 we present a cartoon to visualise the state and the gluing process. Drawing only the strands involved in the gluing, we start with n strands of length M/n and end up with a single strand of length M. In both cases we need the Σ^{--} operator, so that the final state has the correct charges. In this chapter we write out the normalisations of the twist operators explicitly, as they play an important role. Let us now compute the α coefficient and the c coefficient for both cases, to be able to compare both results.

6.3 $\langle \Sigma_n^{--} \rangle$ coefficients

We have done this calculation in section 5.2.5; let us just rewrite the result here to have it at hand. The α coefficient is

$$\alpha = \frac{M}{n!}\left(\frac{N}{M} - \frac{p}{n} + 1\right), \tag{6.3.1}$$

and the c_n coefficient is

$$c_n = M^{1-n} n^{\frac{M}{2}+\frac{n}{2}-\frac{M}{n}} \left((n-1)^2 (n\bar{a})^{(n-2)} \Lambda^{-1}\right)^{\frac{1}{2}(n-1)\left(1-\frac{M}{n}\right)} \tag{6.3.2}$$

with

$$\Lambda = \left(1 + n(n-1)^{(n-1)} - n^{n-1}\right) \tag{6.3.3}$$

and

$$\bar{a}^{n-1} = n\left(1 - \frac{1}{n}\right)^{n-1} - 1. \tag{6.3.4}$$

Let us now calculate these factors for the $(n-1)$-point function, which will have more complicated combinatorics.

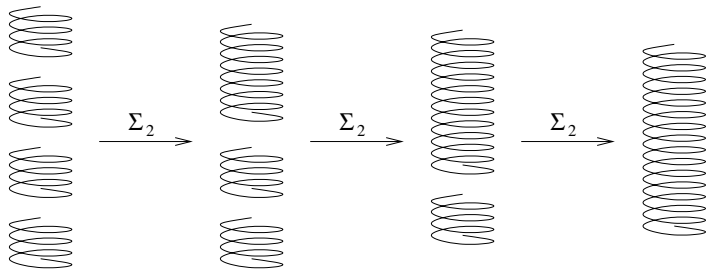

Figure 6.4.1: Joining the strands two by two. The order in which we do it here is the opposite from figure 6.0.1b. Here we keep gluing all the strands to one same strand, which keeps growing while the rest remain untouched.

6.4 Calculation of $\langle(\Sigma_2^{-\dot{-}})^{n-1}\rangle$

The initial and final states are, of course, the same ones as before, and thus we have

$$\left(\Sigma_2^{-\dot{-}}\right)^{n-1}\left[\left(|{+}{+}\rangle_{\frac{M}{n}}\right)^{p}(|{+}{+}\rangle_M)^{p_2}\right] = c_{n2b2}\alpha\left[\left(|{+}{+}\rangle_{\frac{M}{n}}\right)^{p-n}(|{+}{+}\rangle_M)^{p_2+1}\right]. \qquad (6.4.1)$$

We need the coefficients c_{n2b2} and α. However, looking at the picture 6.0.1b again we notice that this case is more subtle. In the picture we joined strands two by two, however we chose a particular ordering. That is, we joined all strands by pairs, to have $n/2$ strands of length $2M/n$, then we joined these in pairs again to have $n/4$ strands of length $4M/n$, then to have $n/8$ strands of length $8M/n$, and so on until the end, where we have only one strand of length M. Clearly, this is only one way of doing the gluing process. Instead, we could have joined all new strands to the same one, creating an increasingly long strand, and leaving the rest untouched. We depict this process in figure 6.4.1, again for $n = 4$.

The final result for the coefficients may depend on the way in which we join the strings. We calculate the two limit cases, which are the ones depicted in figures 6.0.1b and 6.4.1. In what follows we find which one gives the leading contribution, we check in how many ways the gluing can be done for general n and then we approximate the result for the $(n-1)$-point function, obtaining a lower bound and an estimate for the upper bound.

6.4.1 c_{n2b2} coefficient

We start the calculation by obtaining the c coefficient. First let us recall what the coefficient for two strands is. As we said in the previous chapters, it was first computed in [131], and in our case at hand is

$$c_2 = \frac{\frac{M}{n}+\frac{M}{n}}{2\frac{M}{n}\frac{M}{n}} = \frac{n}{M}. \qquad (6.4.2)$$

The c coefficient depends on the length of both strands that are being joined together, and so it might different for each case. Let us do first the case depicted in figure 6.4.1 which we denote by c_{2b2t}. In this case we simply need to apply that coefficient repeatedly, with one of the strands increasing in length one by one at each step. The product gives

$$c_{n2b2t} = \frac{\frac{M}{n}+\frac{M}{n}}{2\frac{M}{n}\frac{M}{n}} \cdot \frac{\frac{2M}{n}+\frac{M}{n}}{2\frac{2M}{n}\frac{M}{n}} \cdot \frac{\frac{3M}{n}+\frac{M}{n}}{2\frac{3M}{n}\frac{M}{n}} \cdot \ldots \cdot \frac{\frac{(n-1)M}{n}+\frac{M}{n}}{2\frac{(n-1)M}{n}\frac{M}{n}} = \frac{M}{2^{n-1}\left(\frac{M}{n}\right)^n}. \tag{6.4.3}$$

Let us now compute it for the other case, the one shown in figure 6.0.1b. In this case, we join all the strands in pairs, then we join all the pairs in pairs again, and so on until we reach the final state. Therefore, we have the coefficient c_2 $n/2$ times, that same coefficient for strands of double length $n/4$ times and so on. More concretely, we have

$$\begin{aligned} c_{n2b2p} &= \left(\frac{1}{\frac{M}{n}}\right)^{\frac{n}{2}} \cdot \left(\frac{1}{2\frac{M}{n}}\right)^{\frac{n}{4}} \cdot \left(\frac{1}{4\frac{M}{n}}\right)^{\frac{n}{8}} \cdot \left(\frac{1}{8\frac{M}{n}}\right)^{\frac{n}{16}} \cdot \ldots \cdot \frac{1}{\frac{n}{2}\frac{M}{n}} = \\ &= \prod_{j=1}^{\log_2 n} \left(\frac{1}{2^{j-1}\frac{M}{n}}\right)^{\frac{n}{2^j}}. \end{aligned} \tag{6.4.4}$$

We can easily calculate this product taking its logarithm and summing the resulting equation. After doing so we obtain

$$c_{n2b2} = n\left(\frac{n}{2M}\right)^{n-1}. \tag{6.4.5}$$

As we can see, this result is exactly equal to c_{n2b2t}, *i.e.* the c coefficient is the same for both joining processes. So, to simplify notation from now on let us define

$$c_{n2b2} := c_{n2b2p} (= c_{n2b2t}). \tag{6.4.6}$$

Since the c coefficients are the same all the difference in the result will come from the comparison of the number of terms; from the α coefficient. Let us calculate it.

6.4.2 Counting the number of terms

Counting the number of terms is the most involved part of the computation of this n-point function. We need to take into account all the possibilities for the application of each Σ_2 operator, and also the different ways in which we can join the strings. As before, we calculate the contribution for the two limit cases, figures 6.4.1 and 6.0.1b, and see which one is dominant. Then we calculate the total number of ways in which we can join the strands two by two in order to get the final strand of length M, and then we approximate the result. As is being hinted, all this also involves some integer partition theory.

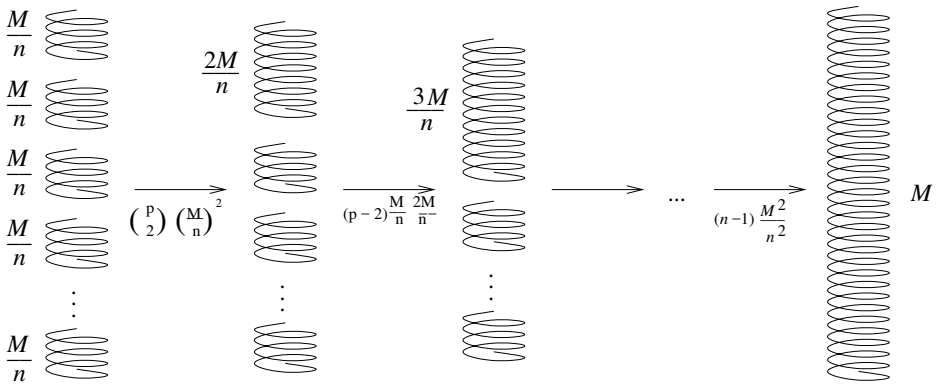

Figure 6.4.2: Joining strands accumulating them all in the top one. We include some of the combinatorial factors here. The gluing operator can be inserted, for each strand, at any position within it.

Let us first count in how many ways the Σ_2 operators can act in the case where we accumulate all strands in one, that is, in the case of figure 6.4.1. To make things more visual we include a picture again with some of the factors involved, figure 6.4.2. We start with p strands of length M/n. In the first step we join two of these, so we need to pick two of them, $\binom{p}{2}$. Then, each of the two strands has M/n insertion points for the operator. Thus, the combinatorial factor for the first step is

$$\binom{p}{2}\left(\frac{M}{n}\right)^2. \tag{6.4.7}$$

Similarly, for the second step we need to pick one of the $p-2$ strands of length M/n and join it to the $2M/n$ strand, giving

$$(p-2)\frac{M}{n}\frac{2M}{n}, \tag{6.4.8}$$

and so on. We notice that all factors after the first one will have $(M/n)^2$ and a product of the length of the long strand times how many single strands we have left. Therefore, the total number of ways in which we can do this kind of joining is

$$\binom{p}{2}\left(\frac{M}{n}\right)^2\prod_{i=2}^{n-1}\left(\frac{M}{n}\right)^2 i(p-i) = \frac{1}{2}\left(\frac{M}{n}\right)^{2n}(n-1)!\frac{p!}{(p-n)!}. \tag{6.4.9}$$

Notice that this result is valid for any n. We will now calculate the opposite case, the one shown in figure 6.0.1b. In this case we will need to assume n to be a power of 2, to simplify the expressions. As we will comment later in section 6.4.4, nothing qualitatively new happens when n is not a power of 2.

The counting is completely analogous to the one above, but the product will be harder to compute this time. Again, to make things visual we include a picture of the gluing

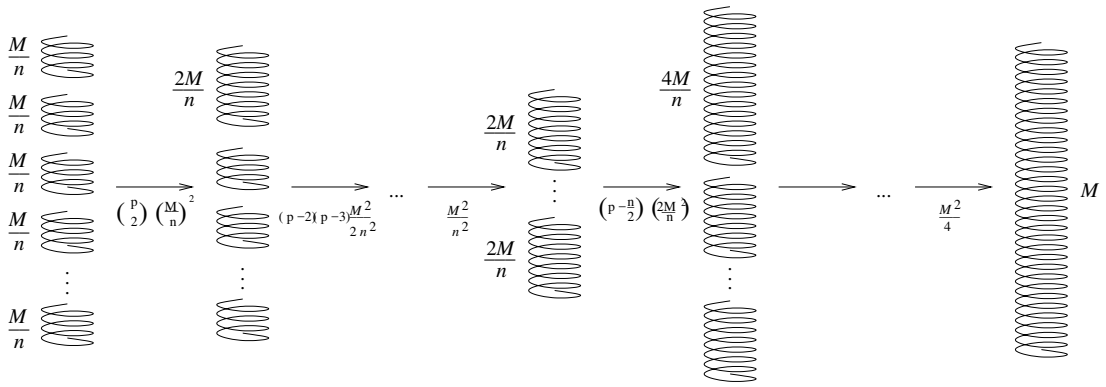

Figure 6.4.3: Joining strands creating pairs of equal size. We sketch the start of the procedure only. We include some of the combinatorial factors here. The gluing operator can be inserted, for each strand, at any position within it.

process with some numbers, figure 6.4.3. The first step is the same one as before. The second step this time will be to take two of the remaining $p-2$ strands of length M/n and join them in another pair of length $2M/n$. We can do this in

$$\binom{p-2}{2}\left(\frac{M}{n}\right)^2 \tag{6.4.10}$$

ways, as we can see in figure 6.4.3. Next, we repeat the process but now we will have two strands of length M/n less, as we joined two in the previous step. Repeating this process, we see that the factor that we obtain from creating $n/2$ strands of length $2M/n$ is

$$\left(\prod_{i=0}^{\frac{n}{2}-1}\binom{p-2i}{2}\left(\frac{M}{n}\right)^2\right) = \left(\frac{M}{n}\right)^n \frac{1}{2^{\frac{n}{2}}}\frac{p!}{(p-n)!}. \tag{6.4.11}$$

Now we need to repeat the same process, but we start with $n/2$ strands of length $2M/n$ and join them in pairs to create strands of length $4M/n$. We can look for all the coefficients again and multiply them, or just use the equation above and change it accordingly. In any case, the result for moving our state from $n/2$ $2M/n$ strands to $n/4$ $4M/n$ strands is

$$\left(\prod_{i=0}^{\frac{n}{4}-1}\binom{p-\frac{n}{2}-2i}{2}\left(\frac{2M}{n}\right)^2\right) = \left(\frac{2M}{n}\right)^{\frac{n}{2}} \frac{1}{2^{\frac{n}{4}}}\frac{(p-\frac{n}{2})!}{(p-n)!}. \tag{6.4.12}$$

We need to keep repeating this process until we have just two strands of length $M/2$, and then the final step is just to join them. We have also included this last coefficient in figure 6.4.3. Let us recall that we are assuming n to be a power of two, and so we end up using all the initial strands following this process. If we write all the contributions together we obtain

$$\left[\left(\frac{M}{n}\right)^n \frac{1}{2^{\frac{n}{2}}}\frac{p!}{(p-n)!}\right]\cdot\left[\left(\frac{2M}{n}\right)^{\frac{n}{2}} \frac{1}{2^{\frac{n}{4}}}\frac{(p-\frac{n}{2})!}{(p-n)!}\right].$$

$$\cdot \left[\left(\frac{4M}{n} \right)^{\frac{n}{4}} \frac{1}{2^{\frac{n}{8}}} \frac{(p-\frac{n}{2}-\frac{n}{4})!}{(p-n)!} \right] \cdot \ldots \cdot \left[\binom{p-n+2}{2} \left(\frac{(n-2)M}{n} \right)^2 \right] =$$

$$= \prod_{j=1}^{\log_2 n} \left[\left(\prod_{i=0}^{\frac{n}{2^j}-1} \binom{p-\sum_{k=1}^{j-1} \frac{n}{2^k} - 2i}{2} \right) \left(\frac{2^{j-1}M}{n} \right)^2 \right]. \tag{6.4.13}$$

The product in i is straightforward to compute, but the product in j is more involved. After doing the i multiplication, we separate the product above in three products, which we will calculate separately. They are

$$\left(\prod_{j=1}^{\log_2 n} 2^{(2j-3)\frac{n}{2^j}} \right) \cdot \left(\prod_{j=1}^{\log_2 n} \left(\frac{M}{n} \right)^{\frac{n}{2^{j-1}}} \right) \cdot \left(\prod_{j=1}^{\log_2 n} \frac{\left(p - \frac{n}{2^j}(2^j-2)\right)!}{(p-n)!} \right). \tag{6.4.14}$$

The first two factors are easy to obtain. The first one is

$$\left(\prod_{j=1}^{\log_2 n} 2^{(2j-3)\frac{n}{2^j}} \right) = 2^{\sum_{j=1}^{\log_2 n} \frac{nj}{2^{j-1}}} 2^{-\sum_{j=1}^{\log_2 n} \frac{3n}{2^j}} = \frac{2^{n-1}}{n^2}, \tag{6.4.15}$$

and the second one is

$$\left(\prod_{j=1}^{\log_2 n} \left(\frac{M}{n} \right)^{\frac{n}{2^{j-1}}} \right) = \left(\frac{M}{n} \right)^{2(n-1)}. \tag{6.4.16}$$

We need some more work to obtain the result for the third product. The product as it is cannot be calculated for generic p as far as we are aware, as there is no formula that gives its result. We will consider the case $p = n$, as that one can be summed. Notice that in this case the product reduces to the product of factorials of all the powers of 2 until n,

$$\left(\prod_{j=1}^{\log_2 n} \left(\frac{n}{2^{j-1}} \right)! \right). \tag{6.4.17}$$

As far as we are aware, there is no exact expression for this product either. However it grows very fast, and so Stirling's formula, which we gave in equation (5.2.2), will be a good approximation[1]. Let us rewrite, for convenience, the product above as

$$F(k) := \prod_{j=0}^{k-1} \left(2^{k-j}\right)!, \tag{6.4.18}$$

where we are using $n = 2^k$, for some $k \in \mathbb{N}$. Then,

$$\ln F(k) = \sum_{j=0}^{k-1} \ln \left[\left(2^{k-j}\right)! \right]. \tag{6.4.19}$$

[1] Using Stirling's approximation with the exact product (not setting $p = n$) also results in a sum which cannot be performed by any methods we are aware of.

Using Stirling's approximation, this can be rewritten for large n as

$$\ln F(k) \approx \sum_{j=0}^{k-1} \left(2^{k-j} \ln\left(2^{k-j}\right) - 2^{k-j}\right) = 2n \ln\left(\frac{n}{2}\right) + 2\ln 2 + 2 - 2n, \tag{6.4.20}$$

where in the second equality we computed the sums and substituted back to n. Then, the third factor gives

$$\prod_{j=1}^{\log_2 n} \left(\frac{n}{2^{j-1}}\right)! \approx n^{2n} 4^{1-n} e^{2-2n}. \tag{6.4.21}$$

We have now calculated the three factors that we needed in equation (6.4.14). Multiplying them, we see that the total number of ways in which we can do this kind of joining is, for large n and n being a power of 2,

$$\left(\frac{M^2}{2e^2}\right)^{n-1}. \tag{6.4.22}$$

We now need to compare both results, (6.4.9) with $p = n$ and (6.4.22). Clearly (6.4.22) is bigger, as we are in the large n limit. To be more precise, if we take the logarithm of both expressions and use Stirling's approximation for (6.4.9) we obtain

$$2n \ln M - n \ln n - \ln 2 - 2n + 1 + (n-1)\ln(n-1), \tag{6.4.23}$$

whereas taking the logarithm of (6.4.22) yields

$$2n \ln M - 2\ln M - (n-1)\ln\left(2e^2\right). \tag{6.4.24}$$

Since we are taking the large n limit, (6.4.22) is bigger.

This means that there are many more ways to join the strands by creating pairs of equal size than accumulating them all together in one big strand, which was to be expected. However, we are not finished with the counting. We just saw that the counting is bigger when we join them in pairs, and in the previous section we saw that the c coefficient is the same for both cases. However, these are the two limit cases. There are many ways in which we can join all the strands. For instance, we could create three pairs of length $2M/n$, and then join everything together in one big strand by accumulating them, just as we did above. That is, we can have a process which is a combination of both limit processes that we just calculated.

It is important to notice though that we calculated the two limit cases, and any other case will be a mixture of the two, and so will give a smaller result than (6.4.22) and bigger than (6.4.9). However, there are a lot of intermediate cases; there are a lot of ways in which the n strands can be joined. The number of ways may in fact change the scaling with n of the result, and so we need to calculate it.

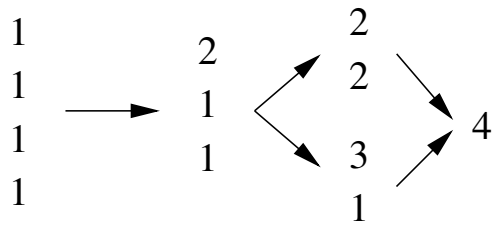

Figure 6.4.4: There are two different ways in which we can go from the partition 1,1,1,1 to the partition 4.

So, the problem at hand now is to find in how many ways we can join all the strands in one. As it seems natural at this point, this problem is also within the integer partitions theory. This counting is equivalent to finding in how many ways we can go from the partition of n 1, ..., 1 to the partition n by adding numbers in pairs. For example, for four we have only two ways, as we show in figure 6.4.4. Finding this for arbitrary n is again a very difficult problem in number theory. And again, as far as we are aware there is no exact formula for this counting. However, the scaling with n is known for the case of large n. Paul Erdős and collaborators found that, if $f(n)$ is the number we want to find and c_1 and c_2 are constants, then [144]

$$c_1^n n^{\frac{n}{2}} < f(n) < c_2^n n^{\frac{n}{2}}. \tag{6.4.25}$$

They suggest c_1 to be 0.75 and find c_2 to be $8\sqrt{2}$. For details on the proof we refer to that paper. We just want to mention that in the proof Stirling's formula is also used, and so our previous assumption of n being large is consistent. We do include a figure inspired by that paper to illustrate the problem better, and show that $f(n)$ grows very fast by studying the case $n = 7$; figure 6.4.5. For our case at hand we will ignore the constants, as we are only concerned about the scaling with n and the main contribution comes from the other factor. Therefore, we approximate it by saying that the number of ways in which we can join n strands two by two to get a single strand is $n^{\frac{n}{2}}$.

We now have all the coefficients that we need to compute the one point function, so let us put them all together.

6.4.3 Result

In the previous section we learned that the dominant way in which the strings are joined two by two is the one depicted in figure 6.4.3. However, we were able to calculate the α coefficient in that case, as we could not do the counting for generic p. Therefore, we will use the coefficients that we obtained for the other case. Since we know that is the smallest case, the result that we obtain is a lower bound. First let us find α, which corresponds

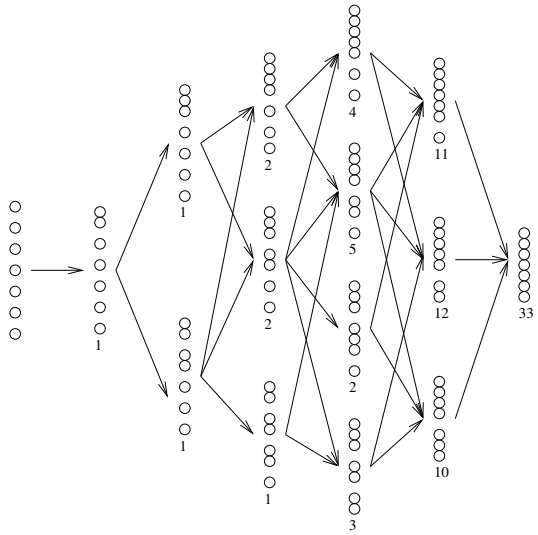

Figure 6.4.5: Number of ways of going from the partition 1,...,1 to 7. The numbers next to the partitions are the number of distinct paths from the original set. In this case we have $f(7) = 33$. Figure taken from [144].

to the matching of number of terms. We calculated the number of ways in which we can apply the $n-1$ Σ_2 operators in the case where we keep gluing the single length strands to the same one in (6.4.9). Therefore, we have

$$\frac{1}{2}\left(\frac{M}{n}\right)^{2n}(n-1)!\frac{p!}{(p-n)!}\mathcal{N}(p) = \alpha\mathcal{N}(p-n). \tag{6.4.26}$$

Solving for α we obtain

$$\alpha_{2b2t} = M\left(\frac{N}{M} - \frac{p}{n} + 1\right)\frac{1}{2}\left(\frac{M}{n}\right)^{n}(n-1)!. \tag{6.4.27}$$

Before we compare both results we give the result of this $(n-1)$-point function in the short strand case, so that we can already compare its result to the one obtained in section 6.3. It is

$$\left\langle\left(\Sigma_2^{\dot{--}}\right)^{n-1}\right\rangle_t = (N_{\Sigma_2})^{n-1}A^n\bar{B}c_{n_{2b2t}}\frac{1}{2}\left(\frac{M}{n}\right)^{n}(n-1)!, \tag{6.4.28}$$

where N_{Σ_2} is given in equation (2.1.62) and $c_{n_{2b2t}}$ is given in (6.4.3). Now, this is the one point function if the only gluing process we consider is the one depicted in figure 6.4.2. As we have seen, this process is the one that will give the smallest answer to the one point function. Even if it is the only one that we have calculated exactly, as we have argued we have $n^{n/2}$ ways of doing this process, and the α factors for all the other processes will be bigger. We can check this if we set $p = n$ in (6.4.9) and compare it to (6.4.22). If we want to obtain an answer for the full one point function we need to consider all joinings. Clearly, if we multiply the result (6.4.28) by the number of ways we can join, we will

obtain a lower bound for this $(n-1)$-point function. Hence, the answer is

$$\left\langle \left(\Sigma_2^{\dot{--}}\right)^{n-1} \right\rangle > A^n \bar{B} M (n-1)! \left(\frac{\sqrt{n}}{2}\right)^n \left(\frac{n}{N(N-1)}\right)^{\frac{n-1}{2}} . \tag{6.4.29}$$

6.4.4 n not being a power of two

We have now computed both n-point functions. As we saw in section 6.3, the result of the one point function of $\Sigma_n^{\dot{--}}$, equation (5.2.47) is valid for any n. However, as we have just seen, (6.4.29) is only valid when n is a power of two, because we join the strands in pairs. This does not mean that we can only calculate this $n-1$-point function in that case, though. If n is not a power of two we simply need to look for the biggest power of two smaller than n, do the process for that subset, and do the same for the smaller subset which is not a power of two. Clearly the result will be longer to write, but the calculation is exactly the same, and we will just end up with a product of results of the form (6.4.29). For tidiness we keep assuming that n is a power of two.

6.5 Comparison of results

We now have all the results we needed, so the last thing that we have to do is to compare the result of both calculations, to see which one is bigger. Let us recall again that (6.4.29) is a lower bound, and so the scaling of n of this one point function is higher than what we use in this section. Also, notice that to compare both results we do not need to use the answers we obtained in the short strand limit, nor we need to take the long strand limit or worry about the $f(\alpha)$ polynomial. The process described by both operators is the same, and so the calculations are exactly the same except for the α and c coefficients. Since these are independent of the sum index (except for a term in the α coefficient, which is the same in both cases), all factors which are different for both calculations come out of the sums, and thus the sums cancel. Therefore, to compare both answers we only need to divide the c and α factors and the normalisations of the twists. By doing so we obtain

$$\frac{\left\langle \left(\Sigma_2^{\dot{--}}\right)^{n-1} \right\rangle}{\left\langle \Sigma_n^{\dot{--}} \right\rangle} \gtrsim \frac{n!(n-1)! M^n n^{\frac{M}{n}} \left(\frac{2}{N(N-1)}\right)^{\frac{n-1}{2}}}{2^n n^{\frac{M}{2}+\frac{n}{2}} \left((n-1)^2 (n\bar{a})^{n-2} \Lambda^{-1}\right)^{\frac{1}{2}(n-1)\left(1-\frac{M}{n}\right)} \left(\frac{n}{N(N-1)\ldots(N-n+1)}\right)^{\frac{1}{2}}}, \tag{6.5.1}$$

where

$$\Lambda = \left(1 + n(n-1)^{(n-1)} - n^{n-1}\right) \tag{6.5.2}$$

and

$$\bar{a}^{n-1} = n\left(1 - \frac{1}{n}\right)^{n-1} - 1. \tag{6.5.3}$$

As we can see, depending on the values of M and n the fraction above will either go to zero or infinity in the large N limit. Namely, for large values of M it will go to infinity. To see this more clearly, let us simplify the result. Let us recall that we are assuming $n \gg 1$, however we can have the case $1 \ll n \ll N$. Let us assume this is the case. Then, the equation above simplifies to

$$\frac{\left\langle \left(\Sigma_2^{--}\right)^{n-1} \right\rangle}{\left\langle \Sigma_n^{--} \right\rangle} \gtrsim \frac{n!(n-1)!M^n n^{\frac{M}{n}}}{2^{\frac{n+1}{2}} n^{\frac{M}{2}+\frac{n}{2}+\frac{1}{2}} \left((n-1)^2(n\bar{a})^{n-2}\Lambda^{-1}\right)^{\frac{1}{2}(n-1)\left(1-\frac{M}{n}\right)}} N^{1-\frac{n}{2}}. \tag{6.5.4}$$

Let us now approximate for large n, just as we did at the end of chapter 4, and assume $M \approx N$. Then, we find

$$\frac{\left\langle \left(\Sigma_2^{--}\right)^{n-1} \right\rangle}{\left\langle \Sigma_n^{--} \right\rangle} \approx \frac{n!(n-1)!M^{1+\frac{n}{2}} n^{\frac{M}{2n}}}{2^{\frac{n+1}{2}} n^n}, \tag{6.5.5}$$

which leads to

$$\frac{\left\langle \left(\Sigma_2^{--}\right)^{n-1} \right\rangle}{\left\langle \Sigma_n^{--} \right\rangle} \to +\infty \qquad \text{for} \qquad M \approx N \to \infty. \tag{6.5.6}$$

So, if M is of order N then $\langle(\Sigma_2^{--})^{n-1}\rangle$ will be bigger. If M is orders of magnitude smaller than N then the one point function $\langle\Sigma_n^{--}\rangle$ has a bigger value. Thus, the joining of strands with multiple twist operators should also need to be considered, as the expectation values of both calculations can be of the same order of magnitude depending on the case.

As we have seen there are many contributions that play a role here, but the main difference comes from combinatorics. There are many ways in which all the Σ_2 operators can be inserted, and that gives a very big contribution, whereas for Σ_n the process is much more restricted, the number of ways in which the gluing can be done is much smaller, and so the coefficients also are. Let us recall that we have done the comparison with a lower bound of $\langle(\Sigma_2^{--})^{n-1}\rangle$. By looking at equations (6.4.14) and (6.4.22) we see that its upper bound will have higher powers of n and M. Therefore, the qualitative comparison done above holds in the same way for the upper bound as well.

There is an obvious extension to this result to obtain a stronger one, which we consider in the next section. Up until now we have been concerned about two ways of joining strands: all at the same time, or by pairs. However, there are many more ways to join strands. So far we have only used the Σ_2 twist and the Σ_n, but there are also twist operators Σ_i, for $2 \leq i \leq n$. Let us see how this is translated in terms of n-point functions.

6.6 All possible ways of joining the strands

As we just said, we have computed the n-point function when we join strands two by two, and when we join them all at the same time. However, we could have also joined them all three by three, if n was a power of three. Or with any combination of gluing operators, up to Σ_n. That is, for every n we have as many possibilities for joining them as possible combinations of twist operators are there that will join them all together. Rephrasing this in terms of integer partitions, there are as many ways of joining the n strands as there are partitions of n that do not contain 1 as a part. This is another hard problem in number theory related to integer partitions. The sequence that results from this counting is recorded in the On-Line Encyclopedia of Integer Sequences (OEIS). It is the sequence A002865 [145]. Again, there is no exact formula for this counting, but it grows exponentially fast with n. There is an approximate formula for this counting, which is

$$\frac{\pi e^{\sqrt{\frac{2n}{3}}\pi}}{12\sqrt{2}n^{\frac{3}{2}}}\left[1-\frac{3\frac{\sqrt{\frac{3}{2}}}{\pi}+\frac{13\pi}{24\sqrt{6}}}{\sqrt{n}}+\frac{\frac{217\pi^2}{6912}+\frac{9}{2\pi^2}+\frac{13}{8}}{n}\right]. \tag{6.6.1}$$

So, there are many ways to do the joining, and in the previous sections we have calculated the two limit cases. Let us recall that the final answer for the one point functions is highly dependant on the combinatorics of the joining of the strands, that is, in how many ways we can apply the gluing operators. Clearly joining the strands two by two is the case where we have the most combinations, and joining them all together in one step is the case where we have the least. We also need to take into account the normalisations of the twists, which will give different powers of N. Thus, just as it happened in the previous case, equation (6.5.1), in all the intermediate cases the corresponding one point function will have a value comparable to $\langle\Sigma_n\rangle$ depending on how big M (and n) are.

Calculating the n-point functions in the middle by the same methods we used would not be straightforward, as we would need to count all the possible ways of joining. For Σ_2 we used the result from Erdős' paper [144], but that counting has not been studied for any other integer as far as we are aware. To finish this chapter let us give an example to illustrate what the counting problem is.

Assume that n is a power of m, where m is a natural number bigger than two. Thus, let $n = m^k$, for some positive integer k. It is straightforward to see that if we want to join all the strands using only Σ_m we will need to do $(n-1)/(m-1)$ steps, that is, that the n-point function that we would want to calculate is $\langle(\Sigma_m)^{\frac{n-1}{m-1}}\rangle$. However, to calculate it we would need to know in how many ways we can join the n strands by joining m in each step. As we said above, this has only been studied for $m = 2$ so far, which is the calculation we did in the previous section. Just to get an idea, the number of possible

ways grows very fast for $m > 2$ as well, but slower than for two, as would be expected. For example, if $m = 3$, then we have one combination for $k = 1$, five combinations for $k = 2$ and 5,026,161 combinations for $k = 3$. Also, we would need to consider all combinations of twist operators that add up to n, which again results in problems within the theory of integer partitions that have not been solved, as far as we are aware.

These countings need to be studied carefully in all their limits, as they might point towards other relevant subclasses of microstates. The bounds given for the results might also help in the holographic calculations, as some of these multi-particle one point functions are also relevant in supergravity.

CHAPTER 7

Review of results and conclusions

In this section we collect all the main results obtained in this part of the thesis.

7.1 Correlation function for a twist n operator

The main result of chapter 4 is the correlation function (4.3.102), which is

$$\begin{aligned}&\langle \mathcal{O}_M^{R(0,0))} | \mathcal{O}_n^{(0,0)} | \prod_{i=1}^{n} \mathcal{O}_{m_i}^{R(0,0)} \rangle = \\ &= \frac{M^{\frac{1}{2}(M+2-n)}}{n} \prod_i |1-\bar{a}_i|^{\frac{1}{2}(m_i-1)(n-1)} \prod_j m_j^{-\frac{1}{2}(m_j+1)} \prod_{j\neq k} |\bar{a}_j - \bar{a}_k|^{\frac{1}{2}(1-m_k)},\end{aligned} \tag{7.1.1}$$

where

$$\bar{a}_i = \frac{1+\bar{a}e^{i\phi_i}}{1-\frac{m_i}{M}}, \qquad \bar{a} = \left(\frac{M}{m_1} \prod_{i=2}^{n} \left(1-\frac{m_i}{M}\right) - 1 \right)^{\frac{1}{n-1}} \tag{7.1.2}$$

and the phases are

$$(n-1) \in 2Z: \quad \phi_i = \frac{(i-1)\pi}{n-1}, \quad \phi_{i+1} = -\frac{(i-1)\pi}{n-1}, \quad i \in 2Z, \quad i \geq 2$$

$$n \in 2Z: \quad \phi_2 = 0, \quad \phi_i = \frac{(i-1)\pi}{n-1}, \quad \phi_{i+1} = -\frac{(i-1)\pi}{n-1}, \quad (i-1) \in 2Z, \quad i \geq 3. \tag{7.1.3}$$

For $n = 2, 3$ this expression greatly simplifies. Plugging $n = 2$ yields

$$\langle \mathcal{O}_M^{R(0,0))} | \mathcal{O}_2^{(0,0)}(w_0) | \mathcal{O}_{m_1}^{R(0,0)} \mathcal{O}_{m_2}^{R(0,0)} \rangle = \frac{M}{2m_1 m_2}, \tag{7.1.4}$$

and with $n = 3$ the result is

$$\langle \mathcal{O}_M^{R(0,0))} | \mathcal{O}_3^{(0,0)}(w_0) | \mathcal{O}_{m_1}^{R(0,0)} \mathcal{O}_{m_2}^{R(0,0)} \mathcal{O}_{m_3}^{R(0,0)} \rangle = \frac{M}{3m_1 m_2 m_3}. \tag{7.1.5}$$

The other explicit result we have given is for the case of equal m_i,

$$\begin{aligned} &\langle \mathcal{O}_M^{R(0,0))} | \mathcal{O}_n^{(0,0)} | \left(\mathcal{O}_{M/n}^{R(0,0)} \right)^n \rangle = \\ &\qquad M^{1-n} n^{\frac{M}{2}+\frac{n}{2}-\frac{M}{n}} \left((n-1)^2 (n\bar{a})^{(n-2)} \Lambda^{-1} \right)^{\frac{1}{2}(n-1)\left(1-\frac{M}{n}\right)} \end{aligned} \tag{7.1.6}$$

where

$$\Lambda = \left(1 + n(n-1)^{(n-1)} - n^{n-1} \right). \tag{7.1.7}$$

For large n this simplifies to

$$\langle \mathcal{O}_M^{R(0,0))} | \mathcal{O}_n^{(0,0)}(w_0) | \left(\mathcal{O}_{\frac{M}{n}}^{R(0,0)} \right)^n \rangle \approx \left(\frac{n}{M} \right)^n n^{-\frac{M}{2n}} e^{\frac{1}{2}(M-n)}. \tag{7.1.8}$$

7.2 One point functions

This is not meant to be a list of all one point functions, but a summary of the results of the exemplary cases solved in chapter 5. We start by listing the results in the short strand case.

7.2.1 Short strand one point functions

In the short strand case we have obtained the following results:

$$\begin{aligned} \langle \Sigma_2^{+\dot{-}} \rangle_{\text{short}} &= \frac{e^{i\frac{\sqrt{2}v}{R}}}{4} \frac{(n_l + p_l)}{n_l\, p_l} A_{n_l}^{(++)} B_{p_l}^{0(00)} \overline{B_{n_l+p_l}^{1(00)}} \left(\frac{2}{N(N-1)} \right)^{\frac{1}{2}}, \\ \left\langle \sum_{r=1}^{n} \mathcal{O}_{(r)}^{-\dot{-}} \right\rangle_{\text{short}} &= \frac{A\bar{B}}{n}, \\ \left\langle \sum_{r=1}^{n} \mathcal{O}_{(r)}^{+\dot{-}} \right\rangle_{\text{short}} &= \frac{1}{n} A \overline{B^1} e^{i\frac{\sqrt{2}v}{R}}, \end{aligned}$$

$$\begin{aligned}
\langle \Sigma_n^{--\dot{-}} \rangle_{\text{short}} &= |\Sigma_n^{--\dot{-}}|^{-1} c_n \frac{N - \frac{\bar{p}M}{n}}{n!} A^n A_2^{-1} = \\
&= A^n \bar{A}_2 \frac{c_n}{n!} \left(\frac{n}{N(N-1)\cdot ...\cdot (N-n+1)} \right)^{\frac{1}{2}}, \\
\left\langle \left(J_{-1}^{+} \right)^m \right\rangle_{\text{short}} &= B\bar{B}_m \frac{1}{n} \binom{n}{m}, \\
\left\langle \bigotimes_{r=1}^{n} \mathcal{O}_{(r)}^{--\dot{-}} \right\rangle &= A^n \bar{B}^n \frac{N!}{n!} \frac{(1-\alpha)^n}{(N-n)!}.
\end{aligned} \tag{7.2.1}$$

These results are equations (5.2.19), (5.2.27), (5.2.36), (5.2.47), (5.2.64) and (5.2.72) respectively. We have also given some combinatorics to calculate the $\langle \Sigma_n^{+-\dot{-}} \rangle$ one point function for 1/8-BPS states. However we have not given the final answer for that correlator, as to do that we need the commutator $[\Sigma_n^{+-\dot{-}}, \otimes_r J_{(r)}]$.

7.2.2 Long strand one point functions

In the two-charge case we have obtained general results for the $\Sigma_n^{--\dot{-}}$ and for the $\mathcal{O}_{(r)}^{--\dot{-}}$ operators. They are

$$\begin{aligned}
&\langle \Sigma_n^{--\dot{-}} \rangle_{\text{long}} = \\
&= \left(\prod_{i=1}^{n} A_i \right) \bar{A} N^{1-n} \left(\left(\frac{n}{Q} \right)^{\frac{N}{2}(n-1)} \left(\frac{1}{n} \right)^{\frac{N}{2}} \right)^{\frac{1}{m}} \left(\frac{n}{N(N-1)...(N-n+1)} \right)^{\frac{1}{2}} f(\alpha_1, ..., \alpha_n), \\
&\langle \mathcal{O}_{(r)}^{--\dot{-}} \rangle_{\text{long}} = A_1 \bar{A}_2 \frac{1}{N} f(\alpha),
\end{aligned} \tag{7.2.2}$$

which are equations (5.3.28) and (5.3.34). $f(\alpha_1, ..., \alpha_n)$ are polynomials independent of N, with the α_i parameters taking values in the $(0, 1)$ interval. The polynomials are of order one for all values of the α_i, and they diverge at the (excluded) boundary values. We have given explicit examples of the polynomials in section 5.3.1.4.

In the three-charge case we have obtained the following results,

$$\begin{aligned}
\langle \mathcal{O}_{(r)}^{+-\dot{-}} \rangle_{\text{long}} &= A\bar{B} e^{i\frac{\sqrt{2}v}{R}} \frac{2}{N} \qquad \text{(initial example)}, \\
\langle \mathcal{O}_{(r)}^{--\dot{-}} \rangle_{\text{long}} &= \frac{A^{(++)} \overline{A^{0(00)}}}{N} \frac{n}{\alpha + \beta - n^2(\alpha + \beta - 1)}, \\
\langle \Sigma_2^{+-\dot{-}} \rangle_{\text{long}} &\approx N_{\Sigma_2} \frac{e^{i\frac{\sqrt{2}v}{R}}}{4} \frac{AB\bar{B}^1}{N}, \\
\left\langle \sum_{r=1}^{\frac{N}{\kappa}} \mathcal{O}_{(r)}^{+-\dot{-}} \right\rangle_{\text{long}} &\approx \frac{\kappa}{N} A\bar{B}_1 e^{i\frac{\sqrt{2}v}{R}} \frac{|\varphi|^2}{|\psi|^2} \qquad \text{(see subsec. 5.3.2.5)},
\end{aligned}$$

$$\left\langle \left(J_{-1}^{+}\right)^{m} \right\rangle_{\text{long}} = B\bar{B}_m \frac{n\binom{N}{m}^3}{\alpha N - (\alpha-1)\binom{N}{m}^2}, \tag{7.2.3}$$

which are equations (5.3.89), (5.3.99), (5.3.107), (5.3.125) and (5.3.132).

7.2.3 Comparison between short and long strand results

Comparing the results we have seen that

$$\begin{aligned}
\langle \Sigma_2^{\dot{-}\dot{-}} \rangle_{\text{long}} &\sim \frac{1}{N} \langle \Sigma_2^{\dot{-}\dot{-}} \rangle_{\text{short}}, \\
\langle \Sigma_3^{\dot{-}\dot{-}} \rangle_{\text{long}} &\sim \frac{1}{N^2} \langle \Sigma_3^{\dot{-}\dot{-}} \rangle_{\text{short}}, \\
\langle \Sigma_n^{\dot{-}\dot{-}} \rangle_{\text{long}} &\sim N^{1-n} \left(\frac{1}{n}\right)^N \langle \Sigma_n^{\dot{-}\dot{-}} \rangle_{\text{short}}, \qquad n \geq 4, \quad \text{(same strand length)}, \\
\langle \mathcal{O}_{(r)}^{\dot{-}\dot{-}} \rangle_{\text{long}} &\sim \frac{1}{N} \langle \mathcal{O}_{(r)}^{\dot{-}\dot{-}} \rangle_{\text{short}}, \\
\langle \mathcal{O}_{(r)}^{+\dot{-}} \rangle_{\text{long}} &\sim \frac{1}{N} \langle \mathcal{O}_{(r)}^{+\dot{-}} \rangle_{\text{short}}, \\
\langle \Sigma_2^{+\dot{-}} \rangle_{\text{long}} &\sim \frac{1}{N} \langle \Sigma_2^{+\dot{-}} \rangle_{\text{short}}, \\
\langle (J_{-1}^{+})^m \rangle_{\text{long}} &\approx N \langle (J_{-1}^{+})^m \rangle_{\text{short}},
\end{aligned} \tag{7.2.4}$$

which are equations (5.3.29), (5.3.35), (5.3.127) and (5.3.108). As we can see, all the long strand ones are suppressed by at least $1/N$ with respect to the short ones, except for the R-symmetry current mode. As we said, this indicates that one point functions for long strand states are comparable to supergravity corrections.

7.3 Different ways of joining strands

In section 6.4 we have been concerned about the n-point function for the $\Sigma_2^{\dot{-}\dot{-}}$ twist operator. We have obtained a lower bound for it, equation (6.4.29), which is

$$\left\langle \left(\Sigma_2^{\dot{-}\dot{-}}\right)^{n-1} \right\rangle > A^n \bar{B} M (n-1)! \left(\frac{\sqrt{n}}{2}\right)^n \left(\frac{n}{N(N-1)}\right)^{\frac{n-1}{2}}. \tag{7.3.1}$$

We have also estimated the upper bound, counted all other n-point functions of products of twist operators and commented the result. In the last section we have found the exact

result, using the lower bound for $\langle(\Sigma_2^{--})^{n-1}\rangle$,

$$\frac{\left\langle\left(\Sigma_2^{--}\right)^{n-1}\right\rangle}{\left\langle\Sigma_n^{--}\right\rangle}\gtrsim\frac{n!(n-1)!M^n n^{\frac{M}{n}}\left(\frac{2}{N(N-1)}\right)^{\frac{n-1}{2}}}{2^n n^{\frac{M}{2}+\frac{n}{2}}\left((n-1)^2(n\bar{a})^{n-2}\Lambda^{-1}\right)^{\frac{1}{2}(n-1)\left(1-\frac{M}{n}\right)}\left(\frac{n}{N(N-1)...(N-n+1)}\right)^{\frac{1}{2}}},\tag{7.3.2}$$

and we have also seen that the number of combinations of twist operators that study the same process scales like

$$\frac{\pi e^{\sqrt{\frac{2n}{3}}\pi}}{12\sqrt{2}n^{\frac{3}{2}}}\left[1-\frac{3\frac{\sqrt{\frac{3}{2}}}{\pi}+\frac{13\pi}{24\sqrt{6}}}{\sqrt{n}}+\frac{\frac{217\pi^2}{6912}+\frac{9}{2\pi^2}+\frac{13}{8}}{n}\right],\tag{7.3.3}$$

and so we have a large number of n-point functions which, depending in the lengths of the strands we join, will have values comparable (or bigger) to $\langle\Sigma_n^{--}\rangle$.

7.4 Conclusions

The main result of chapter 4 is a general expression for the amplitude for joining n strings using a twist operator, equation (4.3.102). As discussed in section 4.2, this amplitude can be used to compute one point functions for supergravity operators in 2-charge and 3-charge black hole microstates, as shown in chapter 5. While the black hole microstate programme was the main motivation for the current work, correlation functions in the orbifold SCFT are interesting in a number of other contexts.

In the early days of AdS/CFT, the spectrum and cubic couplings for six-dimensional $\mathcal{N}=4b$ supergravity were calculated [146, 147]; these allowed the spectrum of chiral primary operators and three point functions of chiral primaries to be calculated. The correlation functions discussed here could be matched with higher point functions from the supergravity side, although this would require higher point supergravity interactions to be computed.

The holographic duality for $AdS_3\times S^3\times S^3\times S^1$ was for a long time mysterious, with conjectures for the corresponding SCFT with large $\mathcal{N}=4$ supersymmetry discussed in [148, 149]. There has recently been considerable progress on this subject, see [150–153], with the holographic duals being conjectured to be symmetric orbifolds of minimal models. The supergravity spectrum was computed in detail in [151], to match with the dual SCFT. Integrability was also used to study the spectrum in [154]. The techniques of chapter 4 would be relevant to computing correlation functions in the orbifold CFT to match the holographic correlation functions.

Chapters 5 and 6 further expand the precision holography calculations of the D1-D5 system, in particular by showing explicitly that one point functions in the long string are suppressed parametrically with N with respect to the short string ones. This relation was already discussed in the early works of Lunin and Mathur [116, 121], where they argued this suppression in the presence of long twists. These results and the techniques for the combinatorial factors would be relevant for the matching with the supergravity side, as well as for corroborating the expected behaviours of the different n-point functions. See chapter 11 for the outlook of this work.

Part III

Counting

CHAPTER 8

Introduction

As mentioned in the general introduction, section 1.5, Strominger and Vafa were the firsts to reproduce the entropy of a black hole by counting microstates in string theory [45]. That, combined with the advent of the holographic principle led to the study of black hole microstates and the most widely accepted explanation to date: the fuzzball proposal [155]. As seen in the previous parts, the most studied system is the D1-D5, where many microstates have been explicitly constructed. In particular we have studied the so-called superstrata solutions. We have used them in chapters 5 and 6, where we have performed precision holography calculations.

To reproduce the entropy of the black hole the microstates do not need to be characterised though, as mentioned earlier. They only need to be counted. Therefore, a natural question that comes to mind is: what fraction of the total number of microstates are superstrata solutions? The most direct way to work towards answering this question is to count them in the CFT: since there is a CFT description of the microstates, if one is able to count how many have the superstrata structure then the desired ratio would be found.

It is known that, in the D1-D5-P system, the total number of microstates is obtained by counting in how many ways we can add the momentum P to the strings [35, 69]. There is also ongoing effort to refine this calculation, and match the counting of black hole microstates to black hole entropy at sub-leading orders. This is achieved by using mock modular forms and supersymmetric indices, among other advanced mathematical

methods. See [156, 157] for reviews and [158] for recent results in black hole microstate counting in higher dimensions.

Our aim in this part is different, in the sense that we want to count directly and exactly a subclass of microstates. Therefore we will not be using supersymmetric indices nor any dualities. Our only tools will be some basic definitions and theorems on integer partitions. At the end of chapter 9 we also present a computer program written in C which performs the counting in a very efficient way, but has some limitations that we will discuss later.

CHAPTER 9

Direct counting of states

In this chapter we tackle a similar problem as in part II but from a different perspective. Using the CFT description we present preliminary results on the counting of how many microstates have been understood so far. To do so we translate this counting problem to a number theory problem within the theory of integer partitions.

9.1 Layout

The plan of this chapter is to recall the CFT structure of superstrata microstates and realise that counting them can be understood as a simple number theory problem. This is done in section 9.2 for integer modes of the R-symmetry current. In section 9.3 we present the C code which implements this counting and comment it. Last, we present some preliminary results on the counting for fractional modes in section 9.4.

9.2 Counting of CFT states: integer modes

The main goal in this section is to count what fraction of the total number of microstates are superstrata solutions with integer modes for the R-symmetry current. In other words,

we want to count how many terms does

$$\sum_{\{N^{(S)}_{\kappa,m_\kappa}\}} \left(\prod_{s,\kappa} (A^{(s)}_\kappa \left|s\right\rangle_\kappa)^{N^{(s)}_\kappa} \prod_{\kappa,m_\kappa} \left(\frac{B_{\kappa,m_\kappa}}{m_\kappa!} (J^+_{-1})^{m_\kappa} \left|00\right\rangle_\kappa \right)^{N^{(00)}_{\kappa,m_\kappa}} \right). \tag{9.2.1}$$

have. The Fourier coefficients and numerical factors are irrelevant for our counting, so we will be dropping them from now on. The constraints on the indices are essential for this counting however, so let us recall them here. The total winding for a physical states is N, and so the strands must satisfy

$$\sum_{S,\kappa} \left|S\right\rangle^{N^S_{\kappa,m_\kappa}}_\kappa = N. \tag{9.2.2}$$

Also, the power m_κ must be smaller or equal than κ, as otherwise the state vanishes. See chapter 5 for some explicit examples.

Counting how many states of the form (9.2.1) satisfy the constraints above is not straightforward. Thus we start by considering simpler states, and formulating and solving the counting for those cases. After that we will build up to the general case we just described.

9.2.1 Counting the simplest 1/4-BPS states

As a first approximation we will count the number of states under the assumption that we have only one kind of strand, say, $\left|++\right\rangle_n$. So, in the constraint (9.2.2) this translates to setting $S = ++$. Then, we can have terms like

$$\left|++\right\rangle_N, \qquad \left|++\right\rangle_{N-1} \left|++\right\rangle_1, \qquad \ldots \qquad , \qquad \prod_{i=1}^{N} \left|++\right\rangle_1 \tag{9.2.3}$$

and all other possible combinations of products of strands that add up to N. Clearly, finding the number of terms is equivalent to finding the number of ways the positive integer N can be written as a sum of positive integers. This is known as finding the partitions of N, which is a classic problem in number theory [159]. See section 2.1.1 for the definition of this problem.

The answer is given in terms of unrestricted partitions, which are counted by a number that is usually denoted $p(N)$ and is exactly what we are looking for. It can be computed using Euler's recursion formula [159], but we would like to find an exact, non-recursive answer. There is a closed expression for $p(N)$ [112], which may not be directly relevant

for us but is useful to keep in mind. It is

$$p(N) = \frac{1}{\pi\sqrt{2}} \sum_{k=1}^{\infty} \sqrt{k} A_k(N) \frac{\mathrm{d}}{\mathrm{d}N} \left(\frac{1}{\sqrt{N - \frac{1}{24}}} \sinh \left[\frac{\pi}{k} \sqrt{\frac{2}{3} \left(N - \frac{1}{24} \right)} \right] \right), \tag{9.2.4}$$

where

$$A_k(N) = \sum_{\substack{h \bmod k \\ (h,k)=1}} \omega_{h,k} e^{-2\pi i N h/k}, \tag{9.2.5}$$

with $\omega_{h,k}$ the following $24k$th root of unity,

$$\omega_{h,k} = e^{\pi i s(h,k)}, \tag{9.2.6}$$

and where $s(h,k)$ is the Dedekind sum

$$s(h,k) = \sum_{\mu=1}^{k-1} \left(\frac{\mu}{k} - \left[\frac{\mu}{k} \right] - \frac{1}{2} \right) \left(\frac{h\mu}{k} - \left[\frac{h\mu}{k} \right] - \frac{1}{2} \right). \tag{9.2.7}$$

This closed expression is not very manageable, however we are interested in the value for $N \to \infty$. The asymptotic expression for $p(N)$ when N is large is [159]

$$p(N) \sim \frac{e^{\pi\sqrt{\frac{2}{3}}\sqrt{N}}}{4N\sqrt{3}}, \qquad N \to \infty. \tag{9.2.8}$$

Notice that this already gives us an important result. This means that the number of states which consist only of products of $|{+}{+}\rangle_n$ strands, namely

$$\sum_{\substack{\sum_\kappa \kappa N_\kappa^{(++)} = N \\ 1 \le \kappa \le N}} \left(\prod_\kappa (A_\kappa^{(++)} |{+}{+}\rangle_\kappa)^{N_\kappa^{(++)}} \right), \tag{9.2.9}$$

is already

$$p(N) \sim \frac{e^{\pi\sqrt{\frac{2}{3}}\sqrt{N}}}{4N\sqrt{3}} \tag{9.2.10}$$

for $N \to \infty$. Thus this counting is already recovering the expected exponential growth for the total number $d(N)$ of microstates of the system, as expected. Let us recall that $d(N)$ at leading order is [35]

$$d(N) \approx e^{2\pi\sqrt{\frac{C}{6}N}}, \tag{9.2.11}$$

where $C = 12$ for $\mathbb{T}^4$ and $C = 24$ for K3. This counting with one colour is counting the ground states corresponding to only one cohomology. When taking all of them into account, equation (9.2.11) is recovered.

As we have just seen for this warm-up example there is an exact formula which gives the counting, equation (9.2.4). However this will not be the case for more complicated

countings. In the more complicated cases it will be very useful to write a generating function for the problem. Namely, a function which after we expand as a polynomial gives us $p(n)$ as the numerical factor for the n-th power term.

9.2.1.1 Generating function

The generating function for this problem is well known. However, let us give some intuition to see where this function comes from, as it will make the following sections more transparent. We want to find all possible ways to write a given integer N as a sum of positive integers. N itself is a way of writing it, and then we have to start considering all combinations of smaller numbers, until we have N 1's. As a start, consider the sum

$$q^0 + q + q^2 + q^3 + \dots \,. \tag{9.2.12}$$

Each term can be thought of as having as many 1's as the power of q. That is, q would represent 1, q^2 would represent 1 + 1 and so on. Consider the same for the 2's,

$$q^0 + q^2 + q^4 + q^6 + \dots \,, \tag{9.2.13}$$

where in this case q^2 would be 2, q^4 would be 2 + 2 and in general the n^{th} term would correspond to having n 2's (which is the term q^{2n}). Now consider the multiplication of these two sums,

$$(1 + q + q^2 + q^3 + \dots)(1 + q^2 + q^4 + q^6 + \dots). \tag{9.2.14}$$

After we multiply them we obtain the following sum,

$$\begin{aligned}(1 + q + q^2 + q^3 + \dots)(1 + q^2 + q^4 + q^6 + \dots) = 1 + q + 2q^2 + 2q^3 + \dots = \\ = 1 + a_1 q + a_2 q_2 + \dots\end{aligned} \tag{9.2.15}$$

If we think of each term before multiplying as the number of 1's or 2's, it is clear that the number a_n in the final sum is the number of ways of writing n as a sum of 1's and/or 2's. For instance, $a_3 = 2$ because we have 1 + 1 + 1 and 2 + 1 (2 + 1 and 1 + 2 are the same partition of 3). These two come from multiplying q^3 in the first parenthesis with 1 in the second parenthesis and q in the first parenthesis with q^2 in the second parenthesis.

Hence, we have just found the generating function for all partitions of N where the biggest number possible in any partition is 2. We will denote this restricted partition by $p_2(N)$. Notice also that the sum for each number, each parenthesis in equation (9.2.15), is a geometric series, which we know how to sum for $q < 1$. To be more precise, let $q \in \mathbb{R}$,

$|q| < 1$. Then

$$\sum_{n=0}^{\infty} q^n = \frac{1}{1-q^n}. \tag{9.2.16}$$

Clearly, if we consider $j \in \mathbb{N} \setminus \{0\}$ we then have

$$1 + \sum_{n=1}^{\infty} p_j(n) q^n = \prod_{n=1}^{j} \frac{1}{1-q^n} \tag{9.2.17}$$

which is the generating function for the integer partitions that we were looking for. Notice that

$$\lim_{j\to\infty} p_j(n) = p(n). \tag{9.2.18}$$

and, in particular, the equality above holds for all $j \geq n$ without the limit.

In the following sections we will be interested in other restrictions for the integer partitions. In particular, we will be interested in finding partitions of N in which the largest part has size j, and j is present in the partition. In other words, partitions where j is the biggest number that appears. We will denote them by $p(N, j)$. This turns out to be equal to the number partitions of N into j parts, as can be seen representing the partitions graphically. Notice also that

$$p(n) = \sum_{j=1}^{n} p(n, j), \tag{9.2.19}$$

and that all partitions counted by $p(N, j)$ are also counted by $p_j(N)$.

We will also be interested in the generating function for this restricted partition. From our discussion above, it is clear that a generating function for $p(N, j)$ is

$$\prod_{n=1}^{j} \frac{1}{1-q^n} - \prod_{n=1}^{j-1} \frac{1}{1-q^n}. \tag{9.2.20}$$

Another generating function for this restricted partition is

$$q^j \prod_{n=1}^{j} \frac{1}{1-q^n}. \tag{9.2.21}$$

Coming back to unrestricted partitions, we would like to obtain the asymptotic expression (9.2.8) from the generating function (9.2.17). This is achieved using Meinardus' theorem. We leave the discussion of this theorem for the next section, as its result is more general.

9.2.2 Counting 1/4-BPS states: adding colours

In the last section we did the counting using only $|{+}{+}\rangle_\kappa$ ground states. The objective is now to repeat this counting but in a more general way; we want to solve the same counting problem but using all five ground states. Hence we are now counting general 1/4-BPS states, which with out notation read

$$\sum_{\substack{\sum_{\kappa,S}\kappa N_\kappa^{(S)}=N \\ 1\leq\kappa\leq N}} \left(\prod_\kappa (A_\kappa^{(S)}\,|S\rangle_\kappa)^{N_\kappa^{(S)}}\right), \tag{9.2.22}$$

where now $S = {+}{+}, {+}{-}, {-}{+}, {-}{-}, 00$. As before, we keep the Fourier coefficients $A_\kappa^{(S)}$ for completeness, but they do not play any role in the counting. Just as in the previous case, we would like to formulate this problem in a more manageable way, that is, in terms of integer partitions. We are now counting the same as we were doing before, but we have more possibilities for each strand. Namely, for a single strand of length N we will have five possibilities, and many in the other cases as each strand can now have five different appearances. This is the same as having coloured strands of the same kind or, equivalently, as counting partitions of N but now using five colours to write each part in the partition. Then, we have to count again the number of ways of writing N as a sum of positive integers, and now we have to consider all possible colour combinations for each partition. For example, for $N = 3$ with three colours, blue, red and yellow, three different terms can be

$$1_{\text{blue}} + 1_{\text{blue}} + 1_{\text{blue}}, \qquad 1_{\text{blue}} + 1_{\text{blue}} + 1_{\text{red}}, \qquad 1_{\text{yellow}} + 1_{\text{yellow}} + 1_{\text{yellow}}. \tag{9.2.23}$$

In this case in total we have ten possibilities, which comes from the combinatorial number

$$\binom{\text{number of colours + number of parts - 1}}{\text{number of parts}}, \tag{9.2.24}$$

where number of parts corresponds to the number of parts (numbers) in the partition under consideration. We explain these combinatorics in section 9.3. In our case S represents 5 different strands, so that is equivalent to having 5 colours in this formulation. With our description of the generating function for one colour (for one ground state) in the previous section, it is now straightforward to obtain it for this case.

9.2.2.1 Generating function

Recalling our previous discussion on how to obtain the generating function for $p(N)$ it is clear that we only need to consider the same product many times. Therefore, the

generating function for $p^5(N)$, the number of integer partitions of N with five colours is

$$p^5(N) = \prod_{n=1}^{\infty} \frac{1}{(1-q^n)^5} \tag{9.2.25}$$

or, in general, to the power of $c \in \mathbb{N}$ when considering c colours.

As we mentioned earlier, the asymptotic expression for $p^5(N)$ is given by Meinardus' theorem ([112] chapter 6). As we will sketch the start of its proof as a guidance for future work in subsection 9.2.3.2, let us state the theorem with the corresponding definitions [112].

Consider the function

$$f(\tau) = \prod_{n=1}^{\infty} (1-q^n)^{-a_n} = 1 + \sum_{n=1}^{\infty} r(n) q^n, \tag{9.2.26}$$

where $q = e^{-\tau}$, Re $\tau > 0$ and $a_n \in \mathbb{R}^+ \cup \{0\}$. Consider also the Dirichlet series

$$D(s) = \sum_{n=1}^{\infty} \frac{a_n}{n^s}, \qquad (s = \sigma + it) \tag{9.2.27}$$

which is assumed to converge for $\sigma > \alpha \in \mathbb{R}^+$. So, $D(s)$ possesses an analytic continuation in the region $\sigma \geq -C_0$, with $0 < C_0 < 1$, and in this region $D(s)$ is analytic except for a pole of order 1 at $s = \alpha$ with residue A. Further assumptions are

$$D(s) = \mathcal{O}(|t|^{C_1}) \tag{9.2.28}$$

uniformly in $\sigma \geq -C_0$ as $|t| \to \infty$, where C_1 is a fixed positive real number, and also, if we set

$$g(\tau) = \sum_{n=1}^{\infty} a_n q^n, \qquad q = e^{-\tau}, \tag{9.2.29}$$

with $\tau = y + 2\pi i x$, $x, y \in \mathbb{R}$, then we also assume that for $|\arg \tau| > \pi/4$, $|x| \leq 1/2$,

$$\mathrm{Re}(g(\tau)) - g(y) \leq -C_2 y^{-\epsilon} \tag{9.2.30}$$

for sufficiently small y, where ϵ is an arbitrary fixed positive number and C_2 is a suitably chosen positive real number depending on ϵ. We are now ready to state Meinardus' theorem.

Theorem 9.2.1. *As* $n \to \infty$,

$$r(n) = C n^{\kappa} e^{n^{\frac{\alpha}{\alpha+1}}\left(1+\frac{1}{\alpha}\right)[A\Gamma(\alpha+1)\zeta(\alpha+1)]^{\frac{1}{\alpha+1}}} (1 + \mathcal{O}(n^{-\kappa_1})),$$

where $\zeta(s)$ is the Riemann zeta function, and

$$\begin{aligned} C &= e^{D'(0)}[2\pi(1+\alpha)]^{-\frac{1}{2}}[A\Gamma(\alpha+1)\zeta(\alpha+1)]^{\frac{1-2D(0)}{2+2\alpha}}, \\ \kappa &= \frac{D(0)-1-\frac{\alpha}{2}}{1+\alpha}, \\ \kappa_1 &= \frac{\alpha}{\alpha+1}\min\left(\frac{C_0}{\alpha}-\frac{\delta}{4},\frac{1}{2}-\delta\right), \end{aligned} \tag{9.2.31}$$

with δ an arbitrary real number.

Let us now get the asymptotic expansion for (9.2.25). We have $a_n = 5$ for all n. Then, the Dirichlet series is just five times the Riemann zeta function,

$$D(s) = 5\zeta(s). \tag{9.2.32}$$

Therefore, we have

$$D(0) = -\frac{5}{2}, \qquad D'(0) = -\frac{5}{2}\log(2\pi), \tag{9.2.33}$$

and also $\alpha = 1$ and $A = 5$. Using as well that

$$\zeta(2) = \frac{\pi^2}{6}, \tag{9.2.34}$$

and noticing that (9.2.28) and (9.2.30) are satisfied because

$$g(\tau) = \frac{5}{1-e^{-\tau}}, \tag{9.2.35}$$

then we find that the asymptotic formula for the partition function with 5 colours $p^5(n)$ is

$$\lim_{n\to\infty} p^5(n) = \sqrt{\frac{5}{3}}\frac{5}{96}\frac{1}{n^2}e^{\sqrt{\frac{10}{3}}\pi\sqrt{n}}. \tag{9.2.36}$$

Again we find an exponential of $\sqrt{n}$. Let us recall that the total number of microstates in the D1D5 system is, at leading order in $\mathbb{T}^4$, $e^{2\sqrt{2}\pi\sqrt{n}}$. For five colours the numerical factor in front of the exponential is

$$\sqrt{\frac{10}{3}} = 1.82574, \tag{9.2.37}$$

which is consistent with the total counting and with the fraction of ground states taken [35]. For $c \in \mathbb{Z}^+$ colours the asymptotic expression is, analogously,

$$p^c(n) \approx \frac{c^{\frac{1}{4}(1+c)}}{2\cdot 2^{\frac{1}{4}(1+3c)}3^{\frac{1}{4}(1+c)}}n^{-\frac{\alpha+c+2}{4}}e^{2\pi\sqrt{\frac{c}{6}}\sqrt{n}}. \tag{9.2.38}$$

We have now seen how the exact counting is obtained for two-charge microstates. Let us recall that the aim of this section is to count a subclass of three-charge microstates though, the superstrata, given in the CFT by equation (9.2.1). The next subsection

presents progress towards obtaining this counting.

9.2.3 Counting the simplest 1/8-BPS state: adding a special colour

Let us recall equation (9.2.1), which are the states that we now want to count,

$$\sum_{\{N^{(S)}_{\kappa,m_\kappa}\}} \left(\prod_{s,\kappa} (A^{(s)}_\kappa \left|s\right\rangle_\kappa)^{N^{(s)}_\kappa} \prod_{\kappa,m_\kappa} \left(\frac{B_{\kappa,m_\kappa}}{m_\kappa!} (J^+_{-1})^{m_\kappa} \left|00\right\rangle_\kappa \right)^{N^{(00)}_{\kappa,m_\kappa}} \right). \tag{9.2.39}$$

Again, the Fourier parameters $A^{(s)}_\kappa, B_{\kappa,m_\kappa}$ are irrelevant for our counting at hand. Notice that the three-charge strands have a more complicated structure, and when translated to the integer partition language they do not correspond to just adding another colour. These 1/8-BPS strands look like

$$\left(J^+_{-1}\right)^{m_\kappa} \left|00\right\rangle_\kappa , \tag{9.2.40}$$

where $m_\kappa \leq \kappa$. That is, for a given κ, m_κ is an integer that goes from 1 to κ. Certainly if we want to consider fixed momentum P, a fixed third charge then m_κ will not have this freedom[1]. However it is also useful to consider the case where m_κ can take any of its values, as it gives insightful information as we show below.

So, let us consider the case where $1 \leq m_\kappa \leq \kappa$. In this case the three-charge strands add many more terms to the counting than a colour does in the two-charge case. Namely, every time we have a strand of length κ that is 1/8-BPS, we need to consider κ times that state, because we will have the κ possible powers for the J^+_{-1} operator. In terms of the colours terminology, we can think about this as a special colour. Imagine a colour, say, purple, which every time that paints a number n it makes that partition count n times. Let us give an example to clarify what we just said. Let $N = 3$, and consider the partition $2_{\text{purple}} + 1_{\text{red}}$. It needs to be considered twice, as 2_{purple} can correspond to

$$J^+_{-1} \left|00\right\rangle_2 \qquad \text{or} \qquad \left(J^+_{-1}\right)^2 \left|00\right\rangle_2 . \tag{9.2.41}$$

Let us recall once more that, as we said above, counting in this way we are not fixing P, the momentum added to the black hole. This means that, in particular, this counting will give an upper bound for the total number of this kind of states. However there are other interesting results that can be obtained by studying this case. Keeping this in mind, let us find the generating function for the partitions with 5 colours plus the special one, $p^{*6}(N)$.

[1] In this case m_κ is fixed, but we need to consider products of the R-symmetry current which in total add up to the desired charge. We do not consider this case in this thesis.

9.2.3.1 Generating function

After our discussions on generating functions in previous subsections, obtaining the generating function for this case is easy[2]. If we want the generating function for the counting with five colours plus the special one, then the product has two different factors: one corresponding to the five normal colours, and another factor corresponding to the special. To obtain the factor for the special colour, we can write once again the power series in q. Then, we need to multiply each term by the number we are considering, as many times as it appears. For instance, for the 1s we do not have to add any extra factors. For the 2s we would have

$$1 + 2q^2 + 2^2q^4 + 2^3q^6 + ..., \tag{9.2.42}$$

and analogous for all other numbers. Thus, the generating function is

$$\begin{aligned} &\prod_{N=1}^{\infty} \frac{1}{(1-q^N)^5}(1 + Nq^N + N^2q^{2N} + N^3q^{3N} + ...) = \\ &= \prod_{N=1}^{\infty} \frac{1}{(1-q^N)^5}\frac{1}{(1-Nq^N)}. \end{aligned} \tag{9.2.43}$$

There is an important caveat here. The generating function that we have just written does not include the $S(N)$ symmetry, as can be first seen at $N = 4^3$. In order to take into account the $S(N)$ symmetry we should consider instead

$$\prod_{N=1}^{\infty} \left(\frac{1}{1-q^N}\right)^N. \tag{9.2.44}$$

While the results obtained with (9.2.43) are still an interesting initial case, it would be very interesting to study the generating function we have just written in detail, to see how the $S(N)$ symmetry affects the result. We leave that as future work.

The objective now is to obtain the asymptotic expression for $p^{*6}(n)$. In the previous cases we have used Meinardus' theorem, which gives us the large n behaviour. This theorem cannot be directly used though, as the generating function has a different form; the theorem does not apply with the new factor we have. We then have three ways to continue this problem. One option is to expand Meinardus' theorem and find the proof for the case we need. In the next section we present the start of the proof for Meinadurs' theorem and show where it stops working, leading the path to future work. Another option would be to obtain the asymptotic expression using modular forms, in the spirit of [156]. We do not pursue this approach in this thesis. Last, we can do numerics to obtain the result using brute force and computers. This is the approach we follow in section 9.3.

[2]We thank Professor George E. Andrews for this generation function and his explanations on the topic, via private communication.

[3]We thank Rodolfo Russo for pointing this out.

9.2.3.2 Asymptotics for the special colour

The aim of this section is to show the difficulties involved in extending Meinardus' theorem to the case with the special colour. This subsection follows from theorem 9.2.1 and the definitions above, and we will be using the same notation, definitions and statements without writing them again.

The proof of Meinardus' theorem uses the saddle point method, and to apply it we need to know how $f(\tau)$ behaves in the half-plane $\mathrm{Re}(\tau) > 0$, specially near $\tau = 0$. In order to figure this out, the first step in the proof is the following lemma.

Lemma 9.2.2. *Under the assumptions on $f(\tau), D(s)$ and $g(\tau)$ given above 9.2.1, with $\tau = y + 2\pi i x$,*

$$f(\tau) = \exp\left(A\Gamma(\alpha)\zeta(\alpha+1)\tau^{-\alpha} - D(0)\log\tau + D'(0) + \mathcal{O}(y^{C_0})\right) \tag{9.2.45}$$

uniformly in x as $y \to 0$, provided $|\arg\tau| \leq \pi/4$, $|x| \leq 1/2$. Also, there exists a positive ϵ_1 such that

$$f(y + 2\pi i x) = \mathcal{O}\left(\exp\left[A\Gamma(\alpha)\zeta(\alpha+1)y^{-\alpha} - C_3 y^{-\epsilon_1}\right]\right) \tag{9.2.46}$$

uniformly in x with $y^\beta \leq |x| \leq 1/2$, as $y \to 0$, where

$$\beta = 1 + \frac{\alpha}{2}\left(1 - \frac{\delta}{2}\right), \qquad \textit{with } \; 0 < \delta < \frac{2}{3}, \tag{9.2.47}$$

and C_3 a fixed real number.

The proof starts as follows. First we write

$$\log f(\tau) = -\sum_{\nu=1}^{\infty} a_\nu \log(1 - e^{-\nu\tau}) = \sum_{k=1}^{\infty}\frac{1}{k}\sum_{\nu=1}^{\infty} a_\nu e^{-\nu k\tau}. \tag{9.2.48}$$

Now, recall that $e^{-\tau}$ is the Mellin transform of $\Gamma(s)$, *i.e.*,

$$e^{-\tau} = \frac{1}{2\pi i}\int_{\sigma_0 - i\infty}^{\sigma_0 + i\infty} \tau^{-s}\Gamma(s)\mathrm{d}s \qquad (\text{for } \; \mathrm{Re}(\tau) > 0,\ \sigma_0 > 0). \tag{9.2.49}$$

If we apply it to the exponential we get

$$\begin{aligned}\log f(\tau) &= \frac{1}{2\pi i}\int_{1+\alpha-i\infty}^{1+\alpha+i\infty}\left(\sum_{k=1}^{\infty}\frac{1}{k}k^{-s}\right)\left(\sum_{\nu=1}^{\infty} a_\nu \nu^{-s}\right)\tau^{-s}\Gamma(s)\mathrm{d}s = \\ &= \frac{1}{2\pi i}\int_{1+\alpha-i\infty}^{1+\alpha+i\infty}\zeta(s+1)D(s)\tau^{-s}\Gamma(s)\mathrm{d}s,\end{aligned} \tag{9.2.50}$$

where the interchange of summation and integration is permissible due to the absolute convergence of the resulting integrated series. Then the proof follows by changing the line

of integration, taking into account the poles of the integral, and using known properties about the Riemann zeta function.

For our case at hand we have

$$f(\tau) = \prod_{N=1}^{\infty} (1-q^N)^{-a_N}(1-Nq^N)^{-1}, \tag{9.2.51}$$

from where

$$\log f(\tau) = \sum_{k=1}^{\infty}\sum_{\nu=1}^{\infty}(a_\nu + \nu^k)e^{-\nu k\tau}, \tag{9.2.52}$$

that is, we have one term that is the same as before and another term which is new. This new term is more complicated, as it has the indices of the two sums. After plugging the Mellin transform this leads to

$$\log f(\tau) = \frac{1}{2\pi i}\int_{1+\alpha-i\infty}^{1+\alpha+i\infty}\sum_{k=1}^{\infty}\sum_{\nu=1}^{\infty}\frac{1}{k}(a_\nu+\nu^k)\nu^{-s}\tau^{-s}k^{-s}\Gamma(s)\mathrm{d}s, \tag{9.2.53}$$

assuming we can still move the sums inside the integral. After we perform one sum we end up in one of the two following cases. If we sum first over ν we end up with

$$\sum_{k=1}^{\infty} k^{-s-1}\zeta(s-k). \tag{9.2.54}$$

If we sum first over k we end up with

$$\sum_{\nu=1}^{\infty}\nu^{-s}\mathrm{Ploylog}(1+s,\nu). \tag{9.2.55}$$

To have a similar proof as the one presented in [112] we need to either write the sum above in a known form, or to know its properties. There is no obvious easy form for these sums, and we have not studied their properties any further. Let us turn our attention now to a numerical study of the problem.

9.3 Numerical implementation

In this section we tackle the problem with a completely different method: we try to count the partitions numerically. We do this following two different strategies. First, since we have the generating functions for all the cases we can just expand them out up to very high order and study the coefficients. This is easily done with Mathematica [161].

A second way to do this counting numerically is by brute force. So, counting all partitions directly. In this section we present a program written in C which implements this

counting in a very efficient way. The downside of this software we created is computation time. For all these counting problems the computation time grows exponentially, and so we can only obtain relatively low numbers with them. However, it is a very useful tool to gain some insight on the problem and how the partitions are distributed in a first instance, and since it constructs all partitions it also gives us more information than the one that can be obtained from the partition function. Another advantage of this code is that it can be easily adapted to other countings. If we want to count another subclass of microstates for which we do not know the generating function, we can still just add the combinatorics to this code and gain some insight for the initial hundred numbers or so. Let us now describe how the program counts.

As we mentioned, computationally this is a very hard problem. So we need a good strategy in order to solve it in the most efficient way. Constructing and writing out all partitions is a possibility, but not the best one. A lot of memory is used to save them, as it also grows exponentially. Writing them in a disk is also not an option, for the same reason.

The best plan would be to find a closed formula for the counting, but that is a very hard problem in number theory. However, what we can do is obtain a formula which, even if it looks complicated, can be easily calculated by a computer. And this is what we present here, for all three cases of the previous section. We have obtained a constructive, non-recursive formula for $p(N)$, $p^n(N)$ and $p^{*n}(N)$, which is crucial for implementing this problem numerically. For the first case, where we want to count the partitions of N with only one colour, the formula is

$$p(N) = 1 + \sum_{A=2}^{N} \sum_{i_{A-0}=1}^{\lfloor \frac{N}{A} \rfloor} \sum_{i_{A-1}=0}^{\left\lfloor \frac{N-i_{A-0}(A-0)}{A-1} \right\rfloor} \cdots \sum_{i_2=0}^{\left\lfloor \frac{N-\sum_{j=0}^{A-3} i_{A-j}(A-j)}{2} \right\rfloor} 1, \tag{9.3.1}$$

where i_k, $2 \leq k \leq A$, $k \in \mathbb{N}$ is the number of k's in the sequence (parts of the sequence which are equal to k) and the number of 1's is what remains until N, *i.e.* $i_1 = N - \sum_{k=2}^{A} i_k k$. To give an idea of what the formula does, each sum in i_k corresponds to a number which forms that partition. We start considering the partition where (if allowed for that partition) there is a number two, then two number twos, and so on. After that we add one number three and consider all possibilities with the one's and the two's, then we do the same with two number three's and so on for all numbers, until we arrive to the partition N.

Notice that each sum over A is independent, and so this computation can be easily parallelised. In other words, we can run each sum in A (9.3.1) independently, which in particular means that we can obtain any $p_n(N)$ without having to compute all other

partitions. Note also that this formula does not only give $p(N)$, but it also tells us explicitly all sequences of numbers that sum N. This is essential when we want to paint the partitions with colours. Last, when running this program all different numbers and their multiplicity are saved in just two vectors, of length N, as we only need to keep track and update the summation indices. Therefore, the memory usage is very small, and allows us to compute fairly big numbers (much bigger than computation time allows).

Since computation time is a problem and doing some parallelisation is straightforward, we made use of the University's supercomputing facilities, IRIDIS 4. Thanks to it more results were obtained, but the problem is so computationally complex that obtaining the partitions for 250 gets close to the default computation time limit. In figure 9.3.1 we present some of the results for this case obtained with IRIDIS, which we explain later in subsection 9.3.1. Since results for bigger numbers cannot be obtained in this way, it is hard to reproduce the known asymptotic expression for $p(N)$, in anticipation for the special colour case, where we do not know it.

Using the data gathered from the supercomputer there are other approaches that we can take to try to recover the asymptotic expression. However, we expect them all to fail, as if we can find an easy way to estimate the value of $p(N+1)$ from the previous ones graphically, we would be solving in polynomial time a problem which takes exponential time to solve. Consider for instance a plot where in the x axis we have the partitions where the biggest part is x, and in the y axis the number of partitions that satisfy this. This is figure 9.3.1 for the case with one colour. Then, we can try to obtain a curve which reproduces the behaviour of some known $p(N)$, and try to obtain the curve for the next values of N. However, as far as we are aware this curve for $p(N)$ is not easily approximated by any simple function, and thus this option is a dead end. Instead, we can think of taking the logarithm on the values of the x axis. Then the resulting function looks very much like e^{-x^2}, but not exactly. Again, though, we hit a dead end, as the approximation is only good close to the numbers used as data, and quickly diverges for greater ones. And the errors cannot be controlled, so the graphic method is not an option.

Let us now consider the coloured cases. Equation (9.3.1) can easily be changed so that it counts with colours. As we said, the equation that the program calculates goes through all partitions, constructing them. In the case with one colour, there is only one partition with the same parts, and that is why the sum indices account for all partitions. In the coloured case though we may have many partitions with the same parts, as the parts can be painted with different colours. So we need to find a combinatorial factor which accounts for these extra partitions.

In order to find it, we group the sequences in subsets of equal numbers. Consider the

sequence

$$a_0a_0...a_0a_1...a_1...a_n...a_n, \tag{9.3.2}$$

which, if we consider the sum of all a_i's, gives N (so, (9.3.2) is a partition of N), and where the part a_i appears n_i times. Let

$$I := \{a_i \in \mathbb{Z}^+ : n_i > 1\} \tag{9.3.3}$$

be the set of all different numbers which appear more than once in the sequence, and

$$I_t := \{a_i \in \mathbb{Z}^+ : 0 \leq i \leq n\} \tag{9.3.4}$$

be the set of all different numbers in the sequence. Then, if we have c colours, the total number of terms that we have when we add colours to the partition of N (9.3.2) is

$$\left(\prod_{a_i \in I} \binom{c+n_i-1}{n_i}\right)\left(\prod_{a_i \in I_t \setminus I} c\right). \tag{9.3.5}$$

The first factor corresponds to the numbers which appear more than once in the partition. The number of possibilities is the number of combinations with repetition: we have c colours of the same number, and we count all possible ways of choosing n_i of them. Order does not matter and we can repeat colours. The second factor corresponds to parts which appear only once in the partition, and so we just have to multiply by the number of colours to count them all. Equation (9.3.5) can be rewritten as

$$\prod_{a_i \in I_t} \binom{c+n_i-1}{n_i}. \tag{9.3.6}$$

This is the number of different possible partitions with the same numbers but different colours. Therefore, if we want $p^c(N)$ we just need to plug this in equation (9.3.1) to obtain the formula we want,

$$1 + \sum_{A=2}^{N} \sum_{i_{A-0}=1}^{\lfloor \frac{N}{A} \rfloor} \sum_{i_{A-1}=0}^{\left\lfloor \frac{N-i_{A-0}(A-0)}{A-1} \right\rfloor} \cdots \sum_{i_2=0}^{\left\lfloor \frac{N-\sum_{j=0}^{A-3} i_{A-j}(A-j)}{2} \right\rfloor} \prod_{k=0}^{A-2} \binom{c+i_{A-k}-1}{i_{A-k}}. \tag{9.3.7}$$

Computation time is of course worse with the coloured case with respect to the non-coloured one, as at each step we now need to calculate a combinatorial number in addition to updating the limits. We present some results obtained with this code in the next subsection, 9.3.1.

Last, we need to deal with the special colour case. So, we have to find an expression analogous to equation (9.3.5), but for the special colour. To count the combinations with

the special colour, we first count all possible combinations of that partition without the numbers painted by the special colour, and then we add them back. Recalling that the appearance of the special colour means that we count that partition as many times as the product of numbers painted by that colour, we just need to consider one more colour and multiply by the corresponding numbers. So, we need to count all combinations that involve the special colour and know what that colour is painting in order to multiply for the correct amount.

Consider again the generic partition given in equation (9.3.2), to see how this works. We now have $c+1$ colours, where the extra one is the special one, purple. As an example, let us assume $n_0 > 1$, $n_1 > 2$, and consider the counting for the partition where the only parts painted in purple are the three numbers

$$a_{0_{\text{purple}}} a_{0_{\text{purple}}} a_{1_{\text{purple}}}. \tag{9.3.8}$$

When counting these partitions, we have a factor coming from all parts of the partition which are not a_0 nor a_1. In other words, we have a first factor which is the same as in the previous section and corresponds to the partition $a_2...a_2...a_n...a_n$. We also have a factor analogous to this one for all a_0's and a_1's which are not painted for the special colour. And then we need to to multiply by $a_0a_1a_1$, as this is what the special colour accounts for. Therefore, the counting for this example sequence is

$$a_0a_1a_1 \left(\prod_{\substack{a_i \in I \\ i \neq 0,1}} \binom{c+n_i-1}{n_i} \right) \left(\prod_{a_i \in I_t \setminus I} c \right) \binom{c+(n_0-1)-1}{n_0-1} \binom{c+(n_1-2)-1}{n_1-2}. \tag{9.3.9}$$

We need to do an analogous counting for all possible sequences where there is purple. Adding for all of them gives the contribution of the special colour. Notice that, as expected, in this case the number of partitions grows in a much faster way. To see this with a couple of numbers, consider for instance the following sequence for 32,

$$5 \quad 4 \quad 4 \quad 4 \quad 3 \quad 3 \quad 3 \quad 3 \quad 2 \quad 1. \tag{9.3.10}$$

With one colour, 32 has 8349 partitions. With 5 colours, this combination only already has 306250 terms. With 6 colours, one of them being purple, some of the first paintings give

$$\begin{aligned}
5_{\text{purple}} &\qquad 306250 \text{ terms} \\
4_{\text{purple}} &\qquad 525000 \text{ terms} \\
4_{\text{purple}}4_{\text{purple}} &\qquad 700000 \text{ terms} \\
4_{\text{purple}}4_{\text{purple}}4_{\text{purple}} &\qquad 560000 \text{ terms}
\end{aligned}$$

$$5_{\text{purple}}4_{\text{purple}}3_{\text{purple}} \qquad 787500 \text{ terms}, \tag{9.3.11}$$

and so on.

We can make the above counting for the special colour more systematically. Given a subset of equal numbers, for instance n_0, a_0, we can count the colours and the special colour by summing over all possibilities of painting with the special colour and multiplying by the corresponding number. That means, computing

$$\sum_{m=0}^{i_{A-k}} \binom{i_{A-k}-m+c-2}{i_{A-k}-m} (A-k)^m. \tag{9.3.12}$$

If we do this for every subset of equal numbers in a given partition, and multiply all the results we obtain the total counting that we want. Therefore, the formula to count all colours (including the special) for the partitions is

$$1+\sum_{A=2}^{N}\sum_{i_{A-0}=1}^{\lfloor \frac{N}{A} \rfloor}\sum_{i_{A-1}=0}^{\left\lfloor \frac{N-i_{A-0}(A-0)}{A-1} \right\rfloor} \cdots \sum_{i_2=0}^{\left\lfloor \frac{N-\sum_{j=0}^{A-3} i_{A-j}(A-j)}{2} \right\rfloor} \prod_{k=0}^{A-2}\sum_{m=0}^{i_{A-k}} \binom{i_{A-k}-m+c-2}{i_{A-k}-m}(A-k)^m. \tag{9.3.13}$$

This is the formula implemented in our program to count all partitions with c colours plus the special one. Now that we have presented the method, we turn to the analysis of the data.

9.3.1 Distribution of the number of states according to their length

As we mentioned earlier, graphical methods are not able to solve this problem. However there are some interesting insights that can be obtained from the data of our program and from the expansion of the generating function with Mathematica. As we have reviewed in parts I and II, for the three-charge black hole we expect most of the microstates to be in the long string sector. In terms of partitions, this translates in having the distribution of partitions peak at higher and higher numbers as we increase N. To be more precise, for each N we want to plot $p(N, j)$ for $1 \leq j \leq N$. Let us recall that $p(N, j)$ gives partitions of N in which the largest part has size j, and j is present in the partition. In figure 9.3.1 we present this plot for the case with one colour. Figure 9.3.2 has the plot for the case with five colours, and figure 9.3.3 presents it for the case of five colours plus the special one. Each coloured curve represents one number, N, as the legend shows. Then the curves give, for each value j in the x axis, the value of $p(N, j)$. As we can see for the monocromatic case, figure 9.3.1 the distributions are peaked at a relatively low number. Also, this peak in j moves to the right, to bigger numbers as we increase N, as we would

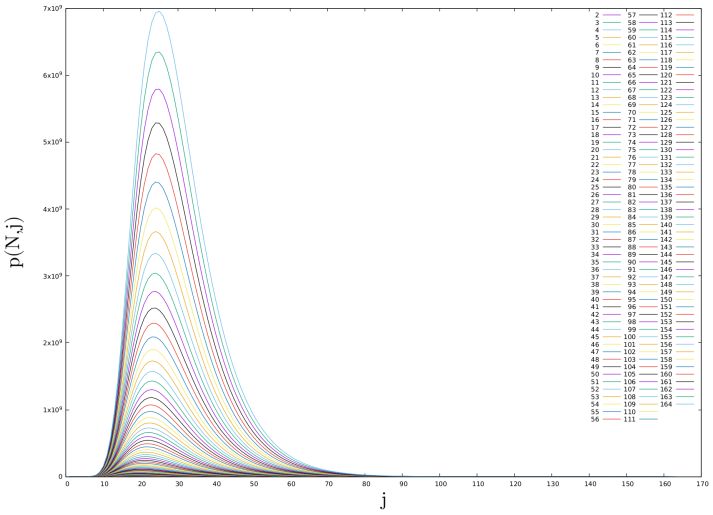

Figure 9.3.1: Curves N, $p(N, j)$ for the first 164 N's in the monocrom case, to see the peaks plotted in 9.3.4

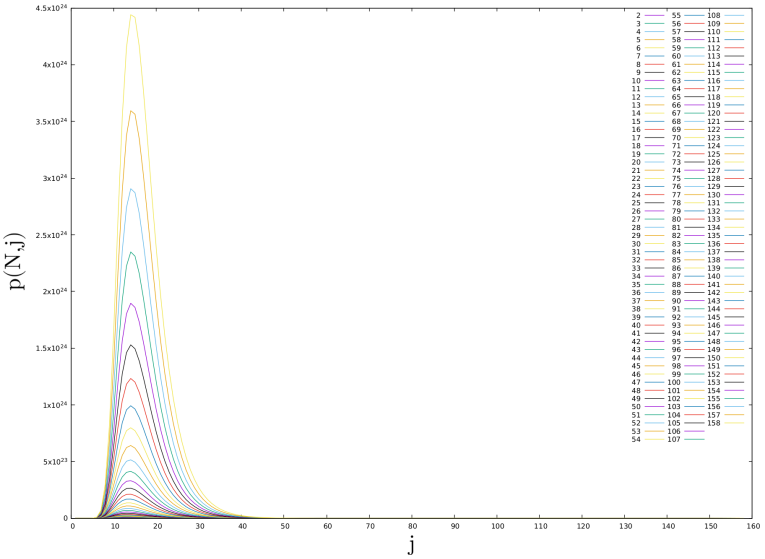

Figure 9.3.2: Curves N, $p(N, j)$ for the first 158 N's in the colour case, to see the peaks plotted in 9.3.5

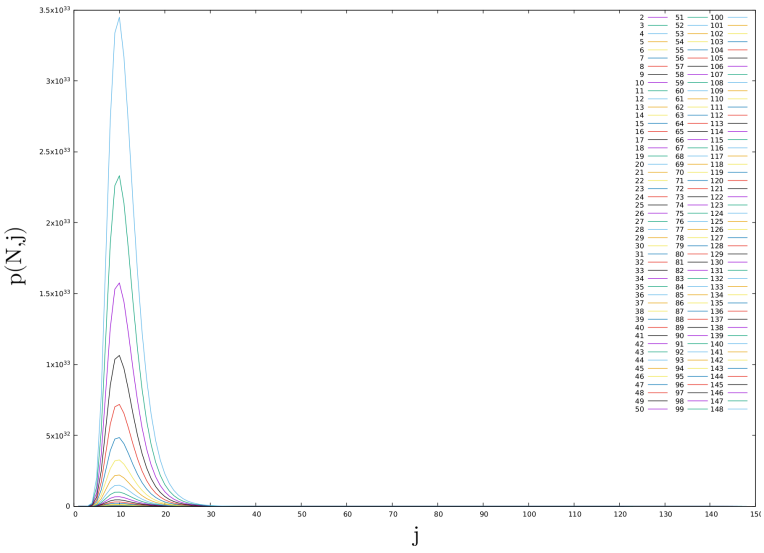

Figure 9.3.3: Curves N, $p(N, j)$ for the first 148 N's in the special case, to see the peaks plotted in 9.3.6

expect. The same happens for the case with five colours, figure 9.3.2, even though in this case the peak is narrower and starts at lower numbers. If we add more colours this change accentuates more, and for a large number of colours the peak stays at one.

The situation seems to be different for the case with the special colour, though, figure 9.3.3. In this case we are considering states with maximum charge j, and as we can see the peaks are even narrower and they seem to stop moving to the right. In order to see if this is true, we can obtain results for much higher numbers using Mathematica and the generating function, as we mentioned earlier.

So, consider now the plots where in the x axis we represent N, and in the y axis we represent the maximum of the previous curves, that is, $\max_j p(N, j)$. For example, if $N = 132$ has a y value of 9 it means that for the number 132, most of the partitions have 9 as the biggest number. The monocromatic case corresponds to figure 9.3.4. As we can see, the intuition we got from the curves seems to be right, as this plot is still clearly growing for $N = 5000$, and it does not seem to stabilise.

$$\max_{j\in\{1,\dots,N\}} p(N, j) \tag{9.3.14}$$

for each N. The same happens in the coloured case, figure 9.3.5. For $N = 5000$ it is growing as well, in a very similar way to the previous case. The opposite happens when we add the special colour, though. As we can see in figure 9.3.6, the maximum grows very quickly to eleven, and then it stabilises there. Notice that in this case we ran the code for many more numbers, up to $N = 10,000$. So, this plot seems to indicate that for the special colour, for the superstrata microstates of momentum at most j, the distribution

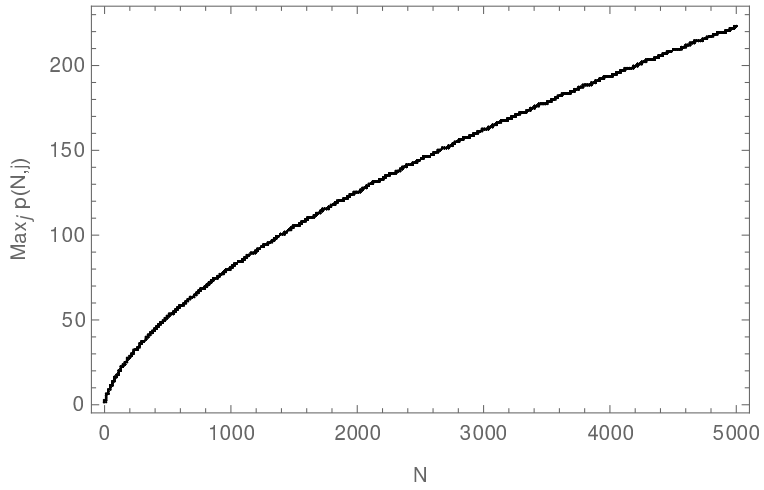

Figure 9.3.4: For each N we plot $\max_j p(N, j)$, that is, if $p(N, j)$ gives the number of partitions of N where the largest term is j, the plot shows for each N where most of the states are. For the case with just one colour, we see that as $N \to \infty$ the peak also goes to infinity.

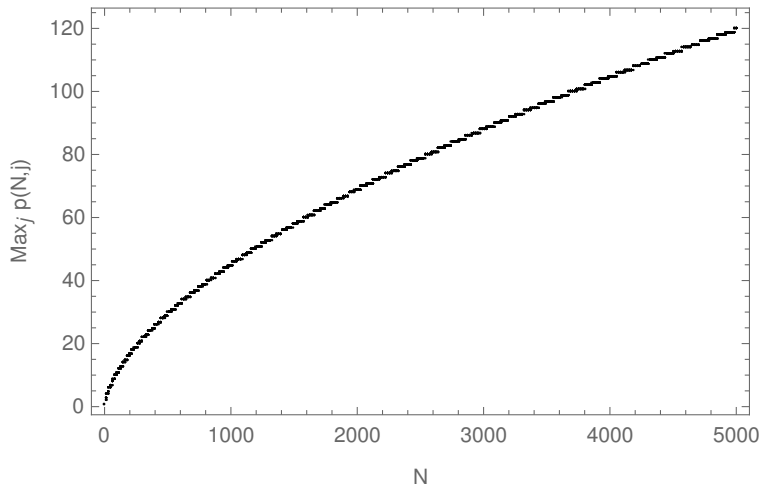

Figure 9.3.5: For each N we plot $\max_j p(N, j)$, that is, if $p(N, j)$ gives the number of partitions of N where the largest term is j, the plot shows for each N where most of the states are. For the case with five colours, we see that as $N \to \infty$ the peak also goes to infinity.

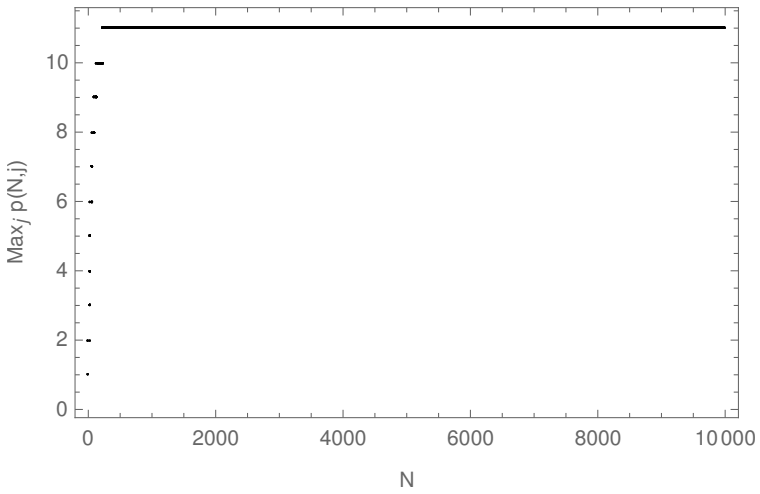

Figure 9.3.6: For each N we plot $\max_j p(N,j)$, that is, if $p(N,j)$ gives the number of partitions of N where the largest term is j, the plot shows for each N where most of the states are. For the case with five colours plus the special one, we see that as $N \to \infty$ the peak stabilises at 11.

of states seems to be highly peaked at a very low number, $j = 11$.

As we have mentioned earlier, these are preliminary results which should be supported by analytic statements, but they seem to indicate that the superstrata microstates of the form (9.4.3)are not mostly distributed in the large P charge sector, as would be expected. Thus, the next natural step is to count and do this same analysis for more general superstrata states, with fractional modes. We do that in the next section.

9.4 Counting of CFT states: fractional modes

As we have mentioned in the introduction 8, most of the 1/8-BPS states are expected to be represented by fractional modes of the R-symmetry current. In this section we try to do the counting for these states. As always, the first step is to understand how the counting works and look for the generating function.

9.4.1 Counting special classes of microstates

Let us start by counting special classes of superstrata microstates. As an example, consider the counting for the following states obtained from FSF (2.2.7) [89]

$$(|{+}{+}\rangle_k)^{n_1} \prod_{\hat{m},\hat{n},\hat{p}} \left((J^+_{-1/k})^{k\hat{p}} |00\rangle_{k^2\hat{p}}\right)^{n_{2,\hat{p}}} \left((J^+_{-1/k})^{k\hat{n}} |{+}{+}\rangle_{k(k\hat{n}+1)}\right)^{n_{3,\hat{n}}} \otimes$$

$$\otimes \left((J^+_{-1/k})^{k\hat{m}} |--\rangle_{k(k\hat{m}-1)} \right)^{n_{4,\hat{m}}} . \tag{9.4.1}$$

In this case an exact counting is not needed. After considering the constraints in the different parameters, the $N \to \infty$ behaviour of the total counting is polynomial, not exponential. Let us see this.

As mentioned in [89], to obtain three-charge solutions using FSF all strands need to have windings which have a common divisor greater than one. In the case above, this common divisor is k. Since the sum of the lengths of all strands must be N, k has to be a divisor of N, condition that we easily find from the previous one. The $\hat{m}$ and $\hat{n}$ can be written in terms of $\hat{p}$, and once this number is fixed the number of strands of each kind will also be determined. To show that this counting grows polynomially, we do it for the case where we have four different strands, for any k. If we have one, two or three the result will also be polynomial, and since the total number of microstates is exponential we do not need to worry about the exact number.

Therefore, assume we have four different strands, with k being the common factor. As we said, we have one degree of freedom, $\hat{p}$, which will give us four different numbers (the product of a length of a kind of strand times the number of insertions of that strand). Hence, this counting is equivalent to finding four natural numbers n_1, n_2, n_3 and n_4 which add up to N/k, where the order of the factors matters. To find how many integers satisfy this, we can think about it in the following way. Let $N/k = 6$. We have to find in how many ways we can separate six dots using three bars, understanding that two bars in the same place means that one of the four numbers is zero. Let us give a visual example; the solution $6 = 2 + 0 + 1 + 3$ would correspond to

$$2 + 0 + 1 + 3 \quad \longleftrightarrow \quad \cdot\cdot || \cdot | \cdot\cdot \tag{9.4.2}$$

Now, overcounting, we can do this in $(N/k - 1)^3$ ways. This is overcounting as the order in which we put the bars is counted by that, but it does not matter. Correcting this means subtracting a term with a lower power of N, and thus is irrelevant. Now, this counting is for fixed k. We have to repeat it for all positive integers k which are multiple of N. The number of divisors of N is given by $\sigma_0(N)$, the number-of-divisors function of N. This number is of order one for large integers, as we show in figure 9.4.1. Thus, adding for all divisors of N will still give a polynomial in N, and adding to that all possible combinations of strands will also be polynomial. The key point here is that all strands in the state come from the same FSF operation, and thus there is a common factor k which greatly restricts the number of possibilities. To finish this chapter we present work in progress for a more general counting of fractional modes.

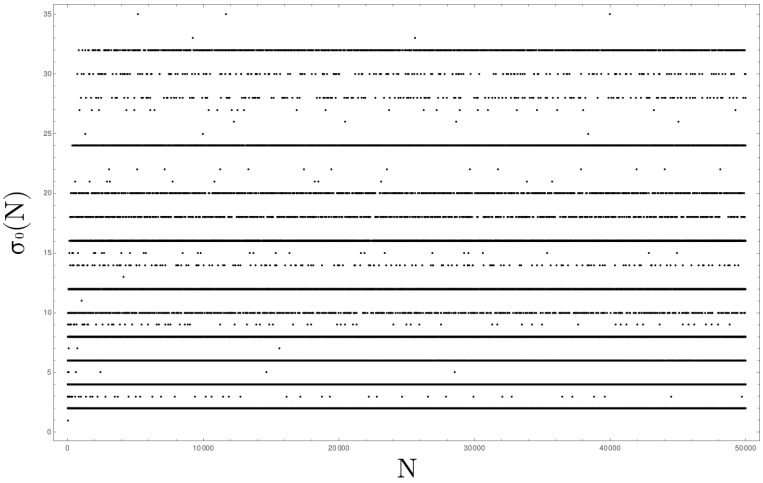

Figure 9.4.1: Number of divisors of N, up to 50,000. This number does not go above 35 for the first 50,000 integers.

9.4.2 Towards a more general counting of fractional modes

In this subsection we start investigating a more general case for counting fractional modes of the R-symmetry current. As we mentioned earlier, in this case it is expected that the microstate distribution should peak at short two-charge states, long three-charge ones. The state that we are concerned with now is

$$\sum_{\{N^{(S)}_{\kappa,m_\kappa}\}} \left(\prod_{s,\kappa} (A^{(s)}_\kappa \left|s\right\rangle_\kappa)^{N^{(s)}_\kappa} \prod_{\kappa,m_\kappa} \left(\frac{B_{\kappa,m_\kappa}}{m_\kappa!} (J^+_{-\frac{a}{b}})^{m_\kappa} \left|00\right\rangle_\kappa \right)^{N^{(00)}_{\kappa,m_\kappa}} \right). \tag{9.4.3}$$

Notice that we are taking both strands in the state to be of the same length. In this case we do consider N_P fixed, and count the partitions of P (of N_P) into fractions where the biggest denominator possible is N. As a first approximation we over count, to get a flavour of how this case works.

We want to find all rational numbers between 0 and N which denominator is at most N. We assume that all of them are acceptable fractions to get N_P momentum charge, as we assume that the exponent of this fractional mode is such that the product of the mode times the exponent can always be N_P. In other words, given a strand like

$$\left(J^+_{-\frac{a}{b}}\right)^c \left|00\right\rangle_N, \qquad a,b,c \in \mathbb{Z}^+ \tag{9.4.4}$$

we are setting $1 \leq b \leq N$, a to take all possible values such that a/b can be all rational numbers from $1/N$ to N_P, and we assume that there always exists a c such that the total momentum added is N_P. This is why we are over counting.

Let us give an example of what we are counting exactly. Let $N = 4$, $N_P = 3$. In this

case, we have 18 rational numbers, which are

$$\frac{1}{4},\ \frac{1}{3},\ \frac{1}{2},\ \frac{2}{3},\ \frac{3}{4},\ 1,\ \frac{5}{4},\ \frac{4}{3},\ \frac{3}{2},\ \frac{5}{3},\ \frac{7}{4},\ 2,\ \frac{9}{4},\ \frac{7}{3},\ \frac{5}{2},\ \frac{8}{3},\ \frac{11}{4},\ 3. \tag{9.4.5}$$

Finding all different rational numbers between $1/N$ and N_P means that we need to know how many integers are there relatively prime to n, with $1 \leq n \leq N \cdot N_P$, $n \in \mathbb{N}$. Euler's phi function $\varphi(n)$ ([159] chapter 2) counts all positive integers up to a given integer n that are relatively prime to n. Hence, the sum

$$\sum_{i=2}^{N} \varphi(i) \tag{9.4.6}$$

gives us all our rational numbers between two consecutive integers. If we include $\phi(1)$ in the sum we also get the integer number. Hence, if we want this integer to be at most N_P, we need to consider those fractions N_P times. Thus, the number of rational numbers between $1/N$ and N_P that we want is

$$N_P \sum_{i=1}^{N} \varphi(i). \tag{9.4.7}$$

Let us go back to the example (9.4.5) to see an example of the formula. We have

$$\varphi(1) = 1, \quad \varphi(1) = 1, \quad \varphi(1) = 2, \quad \varphi(1) = 2, \quad \sum_{i=1}^{N} \varphi(i) = 6. \tag{9.4.8}$$

As we said, this 6 is the number of our rational numbers between 0 and 1, 1 included. And we have this as many times as integer we need until we reach N_P, thus we multiply the sum by N_P, obtaining (9.4.7).

Now, (9.4.7) by itself is a very small number. However, we have to count this in combination with all other strands, and with any lengths. In other words, we want to count how many terms does

$$\sum_{\{N^{(S)}_{\kappa,m_\kappa}\}} \left(\prod_{s,\kappa} (A^{(s)}_{\kappa} \left|s\right\rangle_{\kappa})^{N^{(s)}_{\kappa}} \prod_{\kappa,m_\kappa} \left(\frac{B_{\kappa,m_\kappa}}{m_\kappa!} (J^{+}_{-\frac{a}{b}})^{m_\kappa} \left|00\right\rangle_{\kappa} \right)^{N^{(00)}_{\kappa,m_\kappa}} \right) \tag{9.4.9}$$

have, where $a, b \in \mathbb{Z}^+$, $b \leq \kappa$, $a/b \leq N_P$ and m_κ is such that $am_\kappa/b = N_P$. Therefore, we can think of the counting of this new state as having 5 colours plus a different special colour, which could be, say, cyan.

Following the argument of the previous generating function sections, we see that the

generating function in this case is

$$\prod_{N=1}^{\infty} \frac{1}{(1-q^N)^5} \frac{1}{\left(1 - N_P \left(\sum_{i=1}^{N} \varphi(i)\right) q^N\right)}. \tag{9.4.10}$$

It would be interesting to study in depth the asymptotics of this generating function. If we check the distribution of the number of states according to their length, in this case it seems to be peaked at an even shorter length than in subsection 9.3.1. The exact number at which it peaks depends on N_P. The higher N_P, the shorter the length of the strand where it peaks. For $N_P = 2$ it seems to stabilise at 7. For $N_P = 3$, at 3. For $N_P = 4, 5$, at 2. After that, at 1.

CHAPTER 10

Review of results and conclusions

10.1 Direct counting of states

The main results of chapter 9 are the generating functions which count the superstrata microstates, and the results that come out of their study. They are equation (9.2.43), which is

$$\prod_{N=1}^{\infty} \frac{1}{(1-q^N)^5} \frac{1}{(1-Nq^N)}, \tag{10.1.1}$$

and equation (9.4.10), which is

$$\prod_{N=1}^{\infty} \frac{1}{(1-q^N)^5} \frac{1}{\left(1-N_P\left(\sum_{i=1}^{N}\varphi(i)\right)q^N\right)}. \tag{10.1.2}$$

Associated with the first one we have the distribution in lengths of a subclass of superstrata geometries, the ones which read

$$\sum_{\{N^{(S)}_{\kappa,m_\kappa}\}} \left(\prod_{s,\kappa} (A^{(s)}_\kappa \left|s\right\rangle_\kappa)^{N^{(s)}_\kappa} \prod_{\kappa,m_\kappa} \left(\frac{B_{\kappa,m_\kappa}}{m_\kappa!} (J^+_{-1})^{m_\kappa} \left|00\right\rangle_\kappa \right)^{N^{(00)}_{\kappa,m_\kappa}} \right). \tag{10.1.3}$$

Another important result are the equations (9.3.1), (9.3.7) and (9.3.13), which allowed us to implement this counting in a very efficient C code. The last of these formulas, which

is the most general one out of the three, is

$$1+\sum_{A=2}^{N}\sum_{i_{A-0}=1}^{\lfloor\frac{N}{A}\rfloor}\sum_{i_{A-1}=0}^{\left\lfloor\frac{N-i_{A-0}(A-0)}{A-1}\right\rfloor}\cdots\sum_{i_2=0}^{\left\lfloor\frac{N-\sum_{j=0}^{A-3}i_{A-j}(A-j)}{2}\right\rfloor}\prod_{k=0}^{A-2}\sum_{m=0}^{i_{A-k}}\binom{i_{A-k}-m+c-2}{i_{A-k}-m}(A-k)^m. \tag{10.1.4}$$

10.2 Conclusions

There is ongoing work in the literature, in order to obtain sub-leading corrections to the exact counting of microstates [156, 157]. However, we have followed a different approach here, and started to count exactly certain classes of microstates which have been explicitly constructed. We have given preliminary work, which seems to indicate that the subclasses of microstates constructed so far are highly non-generic. As we mentioned in the introduction of this part, chapter 8, most of the states are expected to be in the long string sector, since one can distribute the momentum in more ways there. However, the superstrata geometries that we have considered seem to be peaked at a very short string length.

The superstrata states for which we have presented most of the work are one of the few ones so far which have been explicitly constructed in the CFT, and which one point functions have been showed to agree with the supergravity ones [88]. The fact that these states peak at short strings is consistent with the two-charge case, as for that case it has been shown that supergravity cannot account for the majority of the microstates of the corresponding black hole [35].

Part IV

Discussion

CHAPTER 11

Conclusions and future work

As we have seen, in this thesis we have presented work extending the precision holography calculations for the D1-D5 system, in the field theory side. As we have already discussed, in part II we have calculated correlation functions for twist n operators joining n twist operators of arbitrary twist, which was a necessary building block to develop the precision holography calculations further. We have used that result to calculate one point functions both in the long and short string sectors, and we have checked the expected suppression of the long one point functions with respect to the short ones. We have also presented bounds on one point functions of multi-particle twist operators, in order to compare the result with the associated one point function with higher twist. We have obtained a bound for their relation, which could be further used to study different ways of joining n strands of any twist. The expected behaviour [35] for them all is recovered, even though certain limits need to be taken carefully.

In part III we have shown results on the distribution of a subclass of superstrata states in the long and short string spectrum. Interestingly, most of the states seem to be peaked at the short string, whereas in general we would expect them to be peaked in the long string, as they are three-charge states. This result may be consistent with our expectation arising from the two-charge case. Due to large supersymmetry, many microstates have extrapolations to supergravity, *i.e.* one can write supergravity solutions. However, their curvature is comparable to corrections in the interior. Therefore, effectively supergravity solutions do not account for most of the microstates of that system.

11.1 Future work

There are many interesting directions in which the work presented in this thesis can be extended. In chapter 5 we have given some examples of calculations of one point functions, and the methods used can be easily extended to more cases. However, we have also mentioned cases where there is further work required in order to obtain results. For instance, in section 5.2.6 we were able to do some combinatorics, but we were not able to give the final result. That was because the commutator between $\Sigma_n^{+\dot{-}}$ and $\otimes_r J_{(r)}$ is not known. So, a natural extension to that section is to obtain that commutator, probably using the bosonisation formulas presented in section A.4, and then calculate more general classes of one point functions.

Other natural extensions of that chapter involve the holographic matching. More concretely, it would be interesting to calculate the same one point functions from the gravity side, in order to match the results. It would also be interesting to find the gravity duals of the multi-trace operators that we have considered.

It would also be interesting to refine the counting done in chapter 6 for the multi-particle one point function, in order to obtain exact results rather than bounds. Finding a formula to obtain the exact result for the multi-particle one point functions of any combination of twists would also be possible future work, especially if the same calculation is also done in the gravity side and the results matched. Also, since we saw that $c_{n2b2t} = c_{n2b2p}$ it would be interesting to see if the c_{n2b2} coefficient is always the same when joining strands in pairs, for all possible combinations. Last, the limit of equation (6.5.1) should be studied more carefully, in order to see what is that ratio in different limits.

Part III can be extended in many ways. First of all, in section 9.2.3.2 we have showed where the proof for Meinardus' theorem stops working for our case, but we have not gone beyond that. It would be very interesting to expand the proof in order to find the asymptotics for the special colour. In that way we would be able to compare the total number of states in the system with the growth of this class of superstrata, which would be very interesting. It would also be very interesting to expand the proof so that it also includes the case with the other special colour mentioned in section 9.4.2. In that case we are fixing the momentum, so the direct comparison of that growth with the total number of states would be very relevant.

In order to do all this there may be the need to work with modular forms. That would also connect better with the current literature and ongoing work on finding the subleading corrections to the total counting. With the results obtained with our computer program it would also be interesting to obtain bounds for the number of states of the cases counted.

This could be obtained graphically or from the generating function, taking appropriate combinations.

In the wider black hole microstates programme, one would like to know how typical microstates look like. Generic fuzzballs are expected to have a very stringy interior, and string theory in curved backgrounds is a topic which is still very poorly understood. The results of this thesis extend the understanding of some of the microstate solutions that have been obtained so far.

This thesis has focused on the D1-D5 system, but there is ongoing work to understand black hole microstates in other systems. In particular, there are current efforts in trying to understand features of typical non-extremal black hole microstates in the Sachdev-Ye-Kitaev (SYK) model [162, 163]. This may be thought of as a toy model, which insights could be extrapolated to other models. Since the microstate study in SYK is very different from the D1-D5 picture it would be good to explore the connections between them.

It is also crucial to investigate the possible detections of the microstates. As mentioned in the introduction, physics is no more than finding the best model which fits observation. Therefore, that connection should be made as soon as possible, and the black hole microstate story is at a point where this needs to be considered.

Since gravitational waves can now be detected and a field has started around them with a very promising future, it seems natural to ask whether the quantum structure of black holes would affect the emission of such waves. It has been recently argued that fuzzballs may cause late-time echoes in the gravitational waves emitted from black hole mergers [101, 164]. While the statistical significance of such studies is not clear [102, 165], this is an argument which deserves to be pushed further, especially with the increased sensitivity detectors that are planned for the future.

There are other approaches on the possible detection of signals on gravitational waves caused by fuzzballs. Recent work [67] suggests that, if one is able to calculate the multipole moments of the fuzzballs, then near future detectors should be able to detect the quantum structure.

APPENDIX A

$\mathcal{N} = 4$ algebra

In this appendix we give further notation and background on the CFT this thesis is based, and we also review the basic definitions to have all conventions together. Our notation for this appendix follows closely that of [104].

The symmetries of the system are the $SO(4)$ of the R-symmetry, corresponding to the isometry of the S^3, and another $SO(4)$, which corresponds to the rotations of the torus. We write these two $SO(4)$ symmetries as $SU(2) \times SU(2)$. Namely, we write the R-symmetry $SO(4)$ as $SU(2)_L \times SU(2)_R$, where the subindices L and R correspond to left and right. We use Greek letters α for the left $SU(2)_L$ indices and dotted Greek letters $\dot{\alpha}$ for the right $SU(2)_R$ ones. Similarly, we use capital Latin letters A and dotted capital Latin letters $\dot{A}$ to represent the two $SU(2)$ coming from the $SO(4)_I$ of the torus. We use a, b, c for any $SU(2)$ triplet, and i for $SO(4)$ vector indices.

For each copy of the CFT we have four bosons $X^i(z, \bar{z})$, which we usually denote by $[X]^{\dot{A}A}$, where

$$[X]^{\dot{A}A} = \frac{1}{\sqrt{2}} X^i \left(\sigma^i\right)^{\dot{A}A}. \tag{A.0.1}$$

We also have four doublets of fermions for each copy,

$$\psi^{\alpha\dot{A}}(z),\ \tilde{\psi}^{\dot{\alpha}\dot{A}}(\bar{z}). \tag{A.0.2}$$

There are two complex fermions (and the hermitean conjugates) in the left sector, and

the same in the right sector. We have thus four real degrees of freedom in each sector, because the hermitean conjugation of the fermions is

$$\left(\psi^{\alpha\dot{A}}\right)^{\dagger}(z) = -\epsilon_{\alpha\beta}\epsilon_{\dot{A}\dot{B}}\psi^{\beta\dot{B}}(z) = -\psi_{\alpha\dot{A}}(z). \tag{A.0.3}$$

The sign convention we use is

$$\epsilon_{12} = -\epsilon^{12} = 1. \tag{A.0.4}$$

Before we give the OPEs and commutators of the currents let us remind the notation for the sigma matrices. We use ladder operators, and so we choose the $\{+, -, 3\}$ base for the triplet of $SU(2)$. The Pauli matrices in this base read

$$\sigma^{+} = 2\begin{pmatrix} 0 & 1 \\ 0 & 0 \end{pmatrix}, \qquad \sigma^{-} = 2\begin{pmatrix} 0 & 0 \\ 1 & 0 \end{pmatrix}, \qquad \sigma^{3} = \begin{pmatrix} 1 & 0 \\ 0 & -1 \end{pmatrix}. \tag{A.0.5}$$

Also, as we have said the D1-D5 system has $\mathcal{N} = (4, 4)$ supersymmetry, so we have thirty-two supercharges, which we denote by $G^{\alpha A}_{(r)}$. Let us briefly discuss them.

A.1 Supercharges

As we just said, the system we study has thirty-two supercharges. From the left $SU(1, 1|2)$ supergroup generators we have eight supercharges, as each mode has four components (see table A.1.1 for the list). We have eight more which are the analogous ones in the right sector. All these add up to sixteen. The other sixteen come from applying the currents to a product of a left and right ground states (one for the state, four for applying one supersymmetry charge to the state, four from applying two, four from applying three, one acting with them all and the two remaining are obtained acting with the J).

Throughout this thesis we work with two and three-charge states, which are $\frac{1}{4}$ and $\frac{1}{8}$-BPS respectively. However this requires some clarification. Since we are working in the field theory dual to the AdS_3 factor in the near horizon of the black hole, we have the conformal enhancement [105]. And this means that our states will be, from this point of view, $\frac{1}{2}$-BPS and $\frac{1}{4}$-BPS, instead of $\frac{1}{4}$ and $\frac{1}{8}$. Therefore, the states that we have been calling $\frac{1}{4}$-BPS (following the notation of [89] and [88]) will be annihilated by half of the supercharges (by half of the G's). The $\frac{1}{8}$-BPS states will be annihilated by a quarter.

To not mix any notations and not cause confusions we will keep calling the states $\frac{1}{4}$-BPS and $\frac{1}{8}$-BPS, but the counting of supercharges will agree with the statements above. Also, since the $\frac{1}{8}$-BPS states are added by adding momentum on the left sector, the supercharges that will change how they act from the $\frac{1}{4}$ to the $\frac{1}{8}$-BPS states will be all in the left sector.

NS sector	R sector
$G^{+1}_{\frac{1}{2}}$	G^{+1}_{1}
$G^{+2}_{\frac{1}{2}}$	G^{+2}_{0}
$G^{+1}_{-\frac{1}{2}}$	G^{+1}_{0}
$G^{+2}_{-\frac{1}{2}}$	G^{+2}_{-1}
$G^{-1}_{\frac{1}{2}}$	G^{-1}_{0}
$G^{-2}_{\frac{1}{2}}$	G^{-2}_{1}
$G^{-1}_{-\frac{1}{2}}$	G^{-1}_{-1}
$G^{-2}_{-\frac{1}{2}}$	G^{-2}_{0}

Table A.1.1: Correspondence between the modes of the supercharges in the NS sector and in the R sector

To finish this section let us give the relation of the supercharges in the NS and R sectors. The correspondence of the modes of the supercharges in both sectors is obtained from the following expansion [166]

$$\begin{aligned} G^{+1}(z) &= \sum_{m\in\mathbb{Z}} G^{+1}_{m+\frac{\eta}{2}+\frac{1}{2}} z^{-m-\frac{\eta}{2}-2} \\ G^{+2}(z) &= \sum_{m\in\mathbb{Z}} G^{+2}_{m-\frac{\eta}{2}+\frac{1}{2}} z^{-m+\frac{\eta}{2}-2} \\ G^{-1}(z) &= \sum_{m\in\mathbb{Z}} G^{-1}_{m-\frac{\eta}{2}+\frac{1}{2}} z^{-m+\frac{\eta}{2}-2} \\ G^{-2}(z) &= \sum_{m\in\mathbb{Z}} G^{-2}_{m+\frac{\eta}{2}+\frac{1}{2}} z^{-m-\frac{\eta}{2}-2}. \end{aligned} \tag{A.1.1}$$

The NS sector corresponds to $\eta = 0$ and the R sector corresponds to $\eta = 1$. With this we can give now the correspondence in both sectors of the eight relevant modes of the supercharges. We present this relation in table A.1.1.

A.2 Currents and OPEs

We give the expressions for a single copy of the $\mathcal{N} = 4$ CFT (so, we only have left sector). Therefore, we have the R-symmetry current $J^a(z)$, the supercharges $G^{\alpha A}(z)$ and the stress-energy tensor $T(z)$. Their expressions in terms of free fields are

$$J^a(z) = \frac{1}{4}\epsilon_{\dot{A}\dot{B}}\psi^{\alpha\dot{A}}\epsilon_{\alpha\beta}(\sigma^{*a})^{\beta}{}_{\gamma}\psi^{\gamma\dot{B}},$$

$$
\begin{aligned}
G^{\alpha A}(z) &= \psi^{\alpha\dot{A}}\,[\partial X]^{\dot{B}A}\,\epsilon_{\dot{A}\dot{B}},\\
T(z) &= \frac{1}{2}\epsilon_{\dot{A}\dot{B}}\epsilon_{AB}\,[\partial X]^{\dot{A}A}\,[\partial X]^{\dot{B}B} + \frac{1}{2}\epsilon_{\alpha\beta}\epsilon_{\dot{A}\dot{B}}\psi^{\alpha\dot{A}}\partial\psi^{\beta\dot{B}}.
\end{aligned}
\tag{A.2.1}
$$

Before we proceed, let us give the relations between this notation and the one used in [103]. First, the relation between the fermions is

$$
\psi^{+\dot{1}} = \Psi^1, \qquad \psi^{-\dot{1}} = -\Psi^2, \qquad \psi^{+\dot{2}} = \Psi^{2\dagger}, \qquad \psi^{-\dot{2}} = \Psi^{1\dagger}.
\tag{A.2.2}
$$

Similarly, for the bosons we have

$$
[X]^{\dot{1}1} = X^1, \qquad [X]^{\dot{1}2} = -X^{2\dagger}, \qquad [X]^{\dot{2}1} = X^2, \qquad [X]^{\dot{2}2} = X^{1\dagger}.
\tag{A.2.3}
$$

With these we can find the relation between the supercharges in both notations,

$$
G^{11} = G^1, \qquad G^{21} = -G^2, \qquad G^{12} = \left(G^2\right)^\dagger, \qquad G^{22} = \left(G^1\right)^\dagger.
\tag{A.2.4}
$$

Now, we choose the normalisations of the fields such that

$$
\begin{aligned}
\langle\psi^{\alpha\dot{A}}(z)\psi^{\beta\dot{B}}(w)\rangle &= -\frac{\epsilon^{\alpha\beta}\epsilon^{\dot{A}\dot{B}}}{z-w},\\
\langle[X]^{\dot{A}A}\,(z)\,[X]^{\dot{B}B}\,(w)\rangle &= 2\epsilon^{\dot{A}\dot{B}}\epsilon^{AB}\log|z-w|.
\end{aligned}
\tag{A.2.5}
$$

The OPEs between the currents are

$$
\begin{aligned}
J^a(z)J^b(w) &\sim \frac{c}{12}\frac{\delta^{ab}}{(z-w)^2} + i\epsilon^{ab}{}_c\frac{J^c(w)}{z-w}\\
J^a(z)G^{\alpha A}(w) &\sim \frac{1}{2}(\sigma^{*a})^\alpha{}_\beta\frac{G^{\beta A}(w)}{z-w}\\
G^{\alpha A}(z)G^{\beta B}(w) &\sim -\frac{c}{3}\frac{\epsilon^{AB}\epsilon^{\alpha\beta}}{(z-w)^3} +\\
&\quad + \epsilon^{AB}\epsilon^{\beta\gamma}(\sigma^{*a})^\alpha{}_\gamma\left[2\frac{J^a(w)}{(z-w)^2} + \frac{\partial J^a(w)}{z-w}\right] - \epsilon^{AB}\epsilon^{\alpha\beta}\frac{T(w)}{z-w}\\
T(z)J^a(w) &\sim \frac{J^a(w)}{(z-w)^2} + \frac{\partial J^a(w)}{z-w}\\
T(z)G^{\alpha A}(w) &\sim \frac{3}{2}\frac{G^{\alpha A}(w)}{(z-w)^2} + \frac{\partial G^{\alpha A}(w)}{z-w}\\
T(z)T(w) &\sim \frac{c}{2}\frac{1}{(z-w)^4} + 2\frac{T(w)}{(z-w)^2} + \frac{\partial T(w)}{z-w}.
\end{aligned}
\tag{A.2.6}
$$

The OPEs of the currents with the free fields are

$$
\begin{aligned}
J^a(z)\psi^{\alpha\dot{A}}(w) &\sim \frac{1}{2}(\sigma^{*a})^\alpha{}_\beta\frac{\psi^{\beta\dot{A}}(w)}{z-w}\\
G^{\alpha A}(z)[\partial X(w)]^{\dot{B}B} &\sim \epsilon^{AB}\left(\frac{\psi^{\alpha\dot{B}}(w)}{(z-w)^2} + \frac{\partial\psi^{\alpha\dot{B}}(w)}{z-w}\right)
\end{aligned}
$$

$$
\begin{aligned}
G^{\alpha A}(z)\psi^{\beta\dot{A}}(w) &\sim \epsilon^{\alpha\beta}\frac{[\partial X(w)]^{\dot{A}A}}{z-w} \\
T(z)[\partial X(w)]^{\dot{A}A} &\sim \frac{[\partial X(w)]^{\dot{A}A}}{(z-w)^2} + \frac{[\partial^2 X(w)]^{\dot{A}A}}{z-w} \\
T(z)\psi^{\alpha\dot{A}}(w) &\sim \frac{1}{2}\frac{\psi^{\alpha\dot{A}}(w)}{(z-w)^2} + \frac{\partial\psi^{\alpha\dot{A}}(w)}{z-w}.
\end{aligned} \tag{A.2.7}
$$

Notice that the supercharges $G^{\alpha A}$ mix the Poincaré supercharges and the superconformal ones, as we can see from the OPEs above and which will be made explicit in the commutators below.

A.3 Commutators

Here we give the commutators between the modes of the currents, so first we recall the mode definition. Let $\mathcal{A}$ be an operator of dimension Δ. The modes of $\mathcal{A}$ are defined by

$$
\mathcal{A}_n = \oint \frac{\mathrm{d}z}{2\pi i}\mathcal{A}(z)z^{\Delta+n-1}, \qquad \mathcal{A}(z) = \sum_n \mathcal{A}_n z^{-(\Delta+n)}. \tag{A.3.1}
$$

Notice that the R-symmetry current J has weight 1 (this weight can be read from the OPE between the current and the stress-energy tensor – it is the coefficient of the $(z-w)^{-2}$ term), and so the modes match with the power of z. With the supercharges $G^{\alpha A}$ this will not be the case, as their weight is 3/2. Also, in the NS sector the supercharges will have half-integer modes, whereas in the R sector they will have integer modes, as we have just discussed in the previous section. The fractional modes are given by [116]

$$
\mathcal{A}_{\frac{n}{m}} = \oint \frac{\mathrm{d}z}{2\pi i}\sum_{r=1}^{m}\mathcal{A}_{(r)}(z)e^{2\pi i\frac{n}{m}(r-1)}z^{\Delta+\frac{n}{m}-1}. \tag{A.3.2}
$$

The mode algebra is

$$
\begin{aligned}
\left[J^a_m, J^b_n\right] &= \frac{c}{12}m\delta^{ab}\delta_{m+n,0} + i\epsilon^{ab}{}_c J^c_{m+n} \\
\left[J^a_m, G^{\alpha A}_n\right] &= \frac{1}{2}(\sigma^{*a})^{\alpha}{}_{\beta}G^{\beta A}_{m+n} \\
\left\{G^{\alpha A}_m, G^{\beta B}_n\right\} &= -\frac{c}{6}(m^2-\frac{1}{4})\epsilon^{AB}\epsilon^{\alpha\beta}\delta_{m+n,0} + \\
&\quad + (m-n)\epsilon^{AB}\epsilon^{\beta\gamma}(\sigma^{*a})^{\alpha}{}_{\gamma}J^a_{m+n} - \epsilon^{AB}\epsilon^{\alpha\beta}L_{m+n} \\
[L_m, J^a_n] &= -nJ^a_{m+n} \\
\left[L_m, G^{\alpha A}_n\right] &= (\frac{m}{2}-n)G^{\alpha A}_{m+n} \\
[L_m, L_n] &= c\frac{m^3-m}{12}\delta_{m+n,0} + (m-n)L_{m+n}.
\end{aligned} \tag{A.3.3}
$$

Now, let α_n be the modes of the ∂X modes. Then the commutation between the current modes and the fields modes are

$$\begin{aligned}
\left[\alpha_m^{\dot{A}A}, \alpha_n^{\dot{B}B}\right] &= m\epsilon^{\dot{A}\dot{B}}\epsilon^{AB}\delta_{n+m,0} \\
\left\{\psi_m^{\alpha\dot{A}}, \psi_n^{\beta\dot{B}}\right\} &= -\epsilon^{\alpha\beta}\epsilon^{\dot{A}\dot{B}}\delta_{m+n,0} \\
\left[J_m^a, \psi_n^{\alpha\dot{A}}\right] &= \frac{1}{2}(\sigma^{*a})^{\alpha}{}_{\beta}\psi_{m+n}^{\beta\dot{A}} \\
\left[G_m^{\alpha A}, \alpha_n^{\dot{B}B}\right] &= -n\epsilon^{AB}\psi_{m+n}^{\alpha\dot{B}} \\
\left\{G_m^{\alpha A}, \psi_n^{\beta\dot{A}}\right\} &= \epsilon^{\alpha\beta}\alpha_{m+n}^{\dot{A}A} \\
\left[L_m, \alpha_n^{\dot{A}A}\right] &= -n\alpha_{m+n}^{\dot{A}A} \\
\left[L_m, \psi_n^{\alpha\dot{A}}\right] &= -(\frac{m}{2}+n)\psi_{m+n}^{\alpha\dot{A}}.
\end{aligned} \tag{A.3.4}$$

Also, let us recall here that the global part of the $\mathcal{N}=4$ superconformal algebra forms the supergroup $SU(1,1|2)$. This group is generated by $\{J_0^a, G^{\alpha A}_{\pm\frac{1}{2}}, L_0, L_{\pm 1}\}$.

A.3.1 Commutators with fractional modes

The commutator with fractional modes is obtained in the exact same way as the one above, with the exception that we only have non-trivial commutation in the copies where our operator is different from the identity. Namely, consider the commutator

$$\left[\left(J^a_{-\frac{1}{k}}\right)^{\alpha\beta}, O^{\beta\dot{\alpha}}\right]. \tag{A.3.5}$$

As we see in (A.3.2), now we only sum over some of the copies of the four-torus. Let us show all steps explicitly;

$$\begin{aligned}
\left[\left(J^a_{-\frac{1}{k}}\right)^{\alpha\beta}, O^{\beta\dot{\alpha}}\right] &= \left[\oint \frac{\mathrm{d}z}{2\pi i}\sum_{r=1}^{k}\left(J^a_{(r)}\right)^{\alpha\beta} e^{-\frac{2\pi i(r-1)}{k}} z^{-\frac{1}{k}}, O^{\beta\dot{\alpha}}\right] = \\
&= \sum_{r=1}^{k}\left[\oint \frac{\mathrm{d}z}{2\pi i}\left(J^a_{(r)}\right)^{\alpha\beta} e^{-\frac{2\pi i(r-1)}{k}} z^{-\frac{1}{k}}, O^{\beta\dot{\alpha}}\right] = \\
&= \sum_{r=1}^{k}\oint \frac{\mathrm{d}z}{2\pi i} e^{-\frac{2\pi i(r-1)}{k}} z^{-\frac{1}{k}}\frac{1}{2}\frac{\left(\sigma^a_{(r)}\right)^{\alpha\beta} O^{\beta\dot{\alpha}}}{z-w}.
\end{aligned} \tag{A.3.6}$$

We do not need to worry about the negative power of z (just as before we had $z \in \mathbb{Z}$), because we are computing the commutator with the OPE, and thus we have a limit when the two operators approach (i.e., we have $z \to w$ and so the only poles come from the negative powers of $(z-w)$). Therefore, the result is completely analogous to the integer

case,

$$\sum_{r=1}^{k}\oint\frac{\mathrm{d}z}{2\pi i}e^{-\frac{2\pi i(r-1)}{k}}z^{-\frac{1}{k}}\frac{1}{2}\frac{\left(\sigma^a_{(r)}\right)^{\alpha\beta}O^{\beta\dot{\alpha}}}{z-w}=$$
$$=\frac{1}{2}\sum_{r=1}^{k}e^{-\frac{2\pi i(r-1)}{k}}e^{-i\frac{1}{k}\frac{v\sqrt{2}}{R}}\left(\sigma^a_{(r)}\right)^{\alpha\beta}O^{\beta\dot{\alpha}}. \tag{A.3.7}$$

Thus, we see that the commutators are analogous, just changing the integer value n by a fraction and, more importantly, summing only over some of the copies of the four-torus.

A.4 Bosonisation

As we have mentioned in section 2.1.2, in order to write the expression of the twist operator in terms of free fields we need to bosonise the fermions. Bosonisation is an exact equivalence between a theory of fermionic fields and a theory of bosonic fields, which is particular of two-dimensional theories. This equivalence can easily be seen by comparing the OPE expansions of fermions and exponentials of bosons.

Bosonisation in the D1-D5 system has been widely used [88, 103, 129]. However, the bosonisation formulas for the fermions have to be written carefully, so that the bosonised fields still commute between them, as fermions do. In order to accomplish this cocycles need to be introduced; namely, extra exponential factors which ensure that all commutation and anticommutation properties are conserved. However, in the literature these factors are not always included, as they are not always essential for all calculations. Following [129] we give the bosonisation formulas for our system with cocycles. We bosonise the fermions in the basis which diagonalises the action of the twists, that is, the fermions we defined in equation (2.1.26). Let

$$\begin{aligned}\psi_\rho^{+\dot{1}}&=e^{i\pi c_\rho}e^{-iH^1_\rho}, &\qquad \psi_\rho^{+\dot{2}}&=e^{i\pi c_\rho}e^{iH^2_\rho},\\ \psi_\rho^{-\dot{2}}&=-e^{iH^1_\rho}e^{-i\pi c_\rho}, &\qquad \psi_\rho^{-\dot{1}}&=e^{-iH^2_\rho}e^{-i\pi c_\rho},\end{aligned} \tag{A.4.1}$$

where

$$c_\rho=\frac{1}{2}\left(p^1_\rho+p^2_\rho+\tilde{p}^1_\rho-\tilde{p}^2_\rho\right), \tag{A.4.2}$$

with p^i_ρ being the momentum of the scalar field H^i_ρ, $i=1,2$. For the antiholomorphic side we consider analogous relations,

$$\begin{aligned}\tilde{\psi}_\rho^{\dot{+}\dot{1}}&=e^{i\pi\tilde{c}_\rho}e^{-i\tilde{H}^1_\rho}, &\qquad \tilde{\psi}_\rho^{\dot{+}\dot{2}}&=e^{i\pi\tilde{c}_\rho}e^{i\tilde{H}^2_\rho},\\ \tilde{\psi}_\rho^{\dot{-}\dot{2}}&=-e^{i\tilde{H}^1_\rho}e^{-i\pi\tilde{c}_\rho}, &\qquad \tilde{\psi}_\rho^{\dot{-}\dot{1}}&=e^{-i\tilde{H}^2_\rho}e^{-i\pi\tilde{c}_\rho},\end{aligned} \tag{A.4.3}$$

with

$$\tilde{c}_\rho = \frac{1}{2}\left(p^2_\rho - p^1_\rho - \tilde{p}^2_\rho - \tilde{p}^1_\rho\right). \tag{A.4.4}$$

The commutation relations between them are

$$\left[H^i_\rho, p^j_{\rho'}\right] = i\delta_{ij}\delta_{\rho\rho'}, \qquad \left[\tilde{H}^i_\rho, \tilde{p}^j_{\rho'}\right] = i\delta_{ij}\delta_{\rho\rho'}. \tag{A.4.5}$$

All the others commute. Using the bosonised fermions we can now write an expression for the twist operator in terms of free fields. We have, for instance,

$$\Sigma_k^{\dot{-}\dot{-}} = \prod_{\rho=1}^{k-1}\left(\sigma^X_\rho \tilde{\sigma}^X_\rho e^{i\pi\frac{\rho}{k}c_\rho} e^{-i\frac{\rho}{k}H^1_\rho} e^{-i\frac{\rho}{k}H^2_\rho} e^{-i\pi\frac{\rho}{k}c_\rho} e^{i\pi\frac{\rho}{k}\tilde{c}_\rho} e^{-i\frac{\rho}{k}\tilde{H}^1_\rho} e^{-i\frac{\rho}{k}\tilde{H}^2_\rho} e^{-i\pi\frac{\rho}{k}\tilde{c}_\rho}\right). \tag{A.4.6}$$

Bibliography

[1] J. Garcia i Tormo and M. Taylor, *Correlation functions in the D1-D5 orbifold CFT*, *Journal of High Energy Physics* **2018** (Jun, 2018) 12.

[2] J. Garcia, Tormo and M. Taylor, *One point functions for black hole microstates*, 1904.10200.

[3] Particle Data Group collaboration, M. Tanabashi et al., *Review of Particle Physics*, *Phys. Rev. D* **98** (2018) 030001.

[4] A. Einstein, *The Foundation of the General Theory of Relativity*, *Annalen Phys.* **49** (1916) 769–822.

[5] J. Polchinski, *String Theory: Volume 1, An Introduction to the Bosonic String*. Cambridge Monographs on Mathematical Physics. Cambridge University Press, 1998.

[6] J. Polchinski, *String Theory: Volume 2, Superstring Theory and Beyond*. Cambridge Monographs on Mathematical Physics. Cambridge University Press, 1998.

[7] Virgo, LIGO Scientific collaboration, B. P. Abbott et al., *Observation of Gravitational Waves from a Binary Black Hole Merger*, *Phys. Rev. Lett.* **116** (2016) 061102, [1602.03837].

[8] Virgo, LIGO Scientific collaboration, B. Abbott et al., *GW151226:*

Observation of Gravitational Waves from a 22-Solar-Mass Binary Black Hole Coalescence, *Phys. Rev. Lett.* **116** (2016) 241103, [1606.04855].

[9] LIGO Scientific and Virgo Collaboration collaboration, B. P. Abbott, R. Abbott, T. D. Abbott, F. Acernese, K. Ackley, C. Adams et al., *GW170104: Observation of a 50-Solar-Mass Binary Black Hole Coalescence at Redshift 0.2*, *Phys. Rev. Lett.* **118** (Jun, 2017) 221101.

[10] LIGO Scientific Collaboration and Virgo Collaboration collaboration, B. P. Abbott, R. Abbott, T. D. Abbott, F. Acernese, K. Ackley, C. Adams et al., *GW170814: A Three-Detector Observation of Gravitational Waves from a Binary Black Hole Coalescence*, *Phys. Rev. Lett.* **119** (Oct, 2017) 141101.

[11] Virgo, LIGO Scientific collaboration, B. P. Abbott et al., *GW170608: Observation of a 19-solar-mass Binary Black Hole Coalescence*, *Astrophys. J.* **851** (2017) L35, [1711.05578].

[12] Virgo, LIGO Scientific collaboration, B. Abbott et al., *GW170817: Observation of Gravitational Waves from a Binary Neutron Star Inspiral*, *Phys. Rev. Lett.* **119** (2017) 161101, [1710.05832].

[13] P. Amaro-Seoane, H. Audley, S. Babak, J. Baker, E. Barausse, P. Bender et al., *Laser Interferometer Space Antenna*, *ArXiv e-prints* (Feb., 2017) , [1702.00786].

[14] L. Barack et al., *Black holes, gravitational waves and fundamental physics: a roadmap*, 1806.05195.

[15] K. Schwarzschild, *Über das Gravitationsfeld eines Massenpunktes nach der Einsteinschen Theorie*, *Sitzungsberichte der Königlich Preußischen Akademie der Wissenschaften (Berlin), 1916, Seite 189-196* (1916) .

[16] S. Hawking and G. Ellis, *The Large Scale Structure of Space-Time*. Cambridge Monographs on Mathem. Cambridge University Press, 1973.

[17] R. Penrose, *Singularities of spacetime.* in *Theoretical principles in astrophysics and relativity* (W. R. N.R. Liebowitz and P.O.Vandervoort, eds.), pp. 217-243. Chicago University Press, 1978.

[18] S. W. Hawking, *Particle Creation by Black Holes*, *Commun. Math. Phys.* **43** (1975) 199–220.

[19] R. Wald, *General Relativity*. University of Chicago Press, 2010.

[20] J. D. Bekenstein, *Black holes and entropy*, *Phys. Rev.* **D7** (1973) 2333–2346.

[21] S. W. Hawking, *Breakdown of Predictability in Gravitational Collapse*, *Phys. Rev.* **D14** (1976) 2460–2473.

[22] W. G. Unruh and R. M. Wald, *Information Loss*, *Rept. Prog. Phys.* **80** (2017) 092002, [1703.02140].

[23] S. D. Mathur, *What Exactly is the Information Paradox?*, *Lect. Notes Phys.* **769** (2009) 3–48, [0803.2030].

[24] S. D. Mathur, *The Information paradox: A Pedagogical introduction*, *Class. Quant. Grav.* **26** (2009) 224001, [0909.1038].

[25] S. D. Mathur, *What the information paradox is not*, 1108.0302.

[26] S. D. Mathur, *The information paradox: conflicts and resolutions*, *Pramana* **79** (2012) 1059–1073, [1201.2079].

[27] D. N. Page, *Information in black hole radiation*, *Phys. Rev. Lett.* **71** (1993) 3743–3746, [hep-th/9306083].

[28] S. D. Mathur and D. Turton, *Comments on black holes I: The possibility of complementarity*, *JHEP* **01** (2014) 034, [1208.2005].

[29] A. Almheiri, D. Marolf, J. Polchinski and J. Sully, *Black Holes: Complementarity or Firewalls?*, *JHEP* **02** (2013) 062, [1207.3123].

[30] A. Almheiri, D. Marolf, J. Polchinski, D. Stanford and J. Sully, *An Apologia for Firewalls*, *JHEP* **09** (2013) 018, [1304.6483].

[31] D. Marolf and J. Polchinski, *Gauge/Gravity Duality and the Black Hole Interior*, *Phys. Rev. Lett.* **111** (2013) 171301, [1307.4706].

[32] S. D. Mathur and D. Turton, *The flaw in the firewall argument*, *Nucl. Phys.* **B884** (2014) 566–611, [1306.5488].

[33] D. Freedman and A. Van Proeyen, *Supergravity*. Cambridge University Press, 2012.

[34] K. Skenderis, *Black holes and branes in string theory*, *Lect. Notes Phys.* **541** (2000) 325–364, [hep-th/9901050].

[35] K. Skenderis and M. Taylor, *The fuzzball proposal for black holes*, *Phys. Rept.* **467** (2008) 117–171, [0804.0552].

[36] G. 't Hooft, *Dimensional reduction in quantum gravity*, in *Salamfest 1993:0284-296*, pp. 0284–296, 1993. gr-qc/9310026.

[37] L. Susskind, *The World as a hologram*, *J. Math. Phys.* **36** (1995) 6377–6396, [hep-th/9409089].

[38] L. Susskind and E. Witten, *The Holographic bound in anti-de Sitter space*, hep-th/9805114.

[39] J. M. Maldacena, *The Large N limit of superconformal field theories and supergravity*, *Int. J. Theor. Phys.* **38** (1999) 1113–1133, [hep-th/9711200].

[40] S. S. Gubser, I. R. Klebanov and A. M. Polyakov, *Gauge theory correlators from noncritical string theory*, *Phys. Lett.* **B428** (1998) 105–114, [hep-th/9802109].

[41] E. Witten, *Anti-de Sitter space and holography*, *Adv. Theor. Math. Phys.* **2** (1998) 253–291, [hep-th/9802150].

[42] O. Aharony, S. S. Gubser, J. M. Maldacena, H. Ooguri and Y. Oz, *Large N field theories, string theory and gravity*, *Phys. Rept.* **323** (2000) 183–386, [hep-th/9905111].

[43] P. H. Ginsparg, *APPLIED CONFORMAL FIELD THEORY*, in *Les Houches Summer School in Theoretical Physics: Fields, Strings, Critical Phenomena Les Houches, France, June 28-August 5, 1988*, pp. 1–168, 1988. hep-th/9108028.

[44] M. S. Virasoro, *Subsidiary conditions and ghosts in dual resonance models*, *Phys. Rev.* **D1** (1970) 2933–2936.

[45] A. Strominger and C. Vafa, *Microscopic origin of the Bekenstein-Hawking entropy*, *Phys. Lett.* **B379** (1996) 99–104, [hep-th/9601029].

[46] J. L. Cardy, *Operator Content of Two-Dimensional Conformally Invariant Theories*, *Nucl. Phys.* **B270** (1986) 186–204.

[47] W. Israel, *Event Horizons in Static Vacuum Space-Times*, *Phys. Rev.* **164** (Dec, 1967) 1776–1779.

[48] W. Israel, *Event horizons in static electrovac space-times*, *Communications in*

Mathematical Physics **8** (Sep, 1968) 245–260.

[49] B. Carter, *Axisymmetric Black Hole Has Only Two Degrees of Freedom*, *Phys. Rev. Lett.* **26** (Feb, 1971) 331–333.

[50] J. D. Bekenstein, *Black hole hair: 25 - years after*, in *Physics. Proceedings, 2nd International A.D. Sakharov Conference, Moscow, Russia, May 20-24, 1996*, pp. 216–219, 1996. gr-qc/9605059.

[51] P. T. Chrusciel, *'No hair' theorems: Folklore, conjectures, results*, *Contemp. Math.* **170** (1994) 23–49, [gr-qc/9402032].

[52] O. Lunin and S. D. Mathur, *AdS / CFT duality and the black hole information paradox*, *Nucl. Phys.* **B623** (2002) 342–394, [hep-th/0109154].

[53] O. Lunin and S. D. Mathur, *Metric of the multiply wound rotating string*, *Nucl. Phys.* **B610** (2001) 49–76, [hep-th/0105136].

[54] O. Lunin and S. D. Mathur, *Statistical interpretation of Bekenstein entropy for systems with a stretched horizon*, *Phys. Rev. Lett.* **88** (2002) 211303, [hep-th/0202072].

[55] S. D. Mathur, *A Proposal to resolve the black hole information paradox*, *Int. J. Mod. Phys.* **D11** (2002) 1537–1540, [hep-th/0205192].

[56] O. Lunin, S. D. Mathur and A. Saxena, *What is the gravity dual of a chiral primary?*, *Nucl. Phys.* **B655** (2003) 185–217, [hep-th/0211292].

[57] J. de Boer, S. El-Showk, I. Messamah and D. Van den Bleeken, *A Bound on the entropy of supergravity?*, *JHEP* **02** (2010) 062, [0906.0011].

[58] S. D. Mathur, *Resolving the black hole causality paradox*, *Gen. Rel. Grav.* **51** (2019) 24, [1703.03042].

[59] V. Jejjala, O. Madden, S. F. Ross and G. Titchener, *Non-supersymmetric smooth geometries and D1-D5-P bound states*, *Phys. Rev.* **D71** (2005) 124030, [hep-th/0504181].

[60] V. Cardoso, O. J. C. Dias, J. L. Hovdebo and R. C. Myers, *Instability of non-supersymmetric smooth geometries*, *Phys. Rev.* **D73** (2006) 064031, [hep-th/0512277].

[61] B. D. Chowdhury and S. D. Mathur, *Radiation from the non-extremal fuzzball*, *Class. Quant. Grav.* **25** (2008) 135005, [0711.4817].

[62] B. D. Chowdhury and S. D. Mathur, *Pair creation in non-extremal fuzzball geometries*, *Class. Quant. Grav.* **25** (2008) 225021, [0806.2309].

[63] S. D. Mathur, *Tunneling into fuzzball states*, *Gen. Rel. Grav.* **42** (2010) 113–118, [0805.3716].

[64] S. D. Mathur, *How fast can a black hole release its information?*, *Int. J. Mod. Phys.* **D18** (2009) 2215–2219, [0905.4483].

[65] B. Guo, S. Hampton and S. D. Mathur, *Can we observe fuzzballs or firewalls?*, *JHEP* **07** (2018) 162, [1711.01617].

[66] T. Hertog and J. Hartle, *Observational Implications of Fuzzball Formation*, 1704.02123.

[67] G. Raposo, P. Pani and R. Emparan, *Exotic compact objects with soft hair*, 1812.07615.

[68] I. Bena and N. P. Warner, *Black holes, black rings and their microstates*, *Lect. Notes Phys.* **755** (2008) 1–92, [hep-th/0701216].

[69] S. D. Mathur, *The Quantum structure of black holes*, *Class. Quant. Grav.* **23** (2006) R115, [hep-th/0510180].

[70] M. Shigemori, *Exotic branes and black hole microstates*, *Int. J. Mod. Phys. Conf. Ser.* **21** (2013) 77–91.

[71] O. Lunin, J. M. Maldacena and L. Maoz, *Gravity solutions for the D1-D5 system with angular momentum*, hep-th/0212210.

[72] M. Taylor, *General 2 charge geometries*, *JHEP* **03** (2006) 009, [hep-th/0507223].

[73] I. Kanitscheider, K. Skenderis and M. Taylor, *Fuzzballs with internal excitations*, *JHEP* **06** (2007) 056, [0704.0690].

[74] K. Skenderis and M. Taylor, *Fuzzball solutions and D1-D5 microstates*, *Phys. Rev. Lett.* **98** (2007) 071601, [hep-th/0609154].

[75] I. Kanitscheider, K. Skenderis and M. Taylor, *Holographic anatomy of fuzzballs*,

JHEP **04** (2007) 023, [hep-th/0611171].

[76] S. D. Mathur, A. Saxena and Y. K. Srivastava, *Constructing 'hair' for the three charge hole*, *Nucl. Phys.* **B680** (2004) 415–449, [hep-th/0311092].

[77] I. Bena and P. Kraus, *Microscopic description of black rings in AdS / CFT*, *JHEP* **12** (2004) 070, [hep-th/0408186].

[78] S. Giusto, S. D. Mathur and A. Saxena, *3-charge geometries and their CFT duals*, *Nucl. Phys.* **B710** (2005) 425–463, [hep-th/0406103].

[79] O. Lunin, *Adding momentum to D-1 - D-5 system*, *JHEP* **04** (2004) 054, [hep-th/0404006].

[80] V. Balasubramanian, P. Kraus and M. Shigemori, *Massless black holes and black rings as effective geometries of the D1-D5 system*, *Class. Quant. Grav.* **22** (2005) 4803–4838, [hep-th/0508110].

[81] P. Berglund, E. G. Gimon and T. S. Levi, *Supergravity microstates for BPS black holes and black rings*, *JHEP* **06** (2006) 007, [hep-th/0505167].

[82] S. Giusto and R. Russo, *Adding new hair to the 3-charge black ring*, *Class. Quant. Grav.* **29** (2012) 085006, [1201.2585].

[83] S. Giusto and R. Russo, *Perturbative superstrata*, *Nucl. Phys.* **B869** (2013) 164–188, [1211.1957].

[84] S. Giusto, O. Lunin, S. D. Mathur and D. Turton, *D1-D5-P microstates at the cap*, *JHEP* **02** (2013) 050, [1211.0306].

[85] S. Giusto and R. Russo, *Superdescendants of the D1D5 CFT and their dual 3-charge geometries*, *JHEP* **03** (2014) 007, [1311.5536].

[86] I. Bena, S. Giusto, R. Russo, M. Shigemori and N. P. Warner, *Habemus Superstratum! A constructive proof of the existence of superstrata*, *JHEP* **05** (2015) 110, [1503.01463].

[87] B. Chakrabarty, D. Turton and A. Virmani, *Holographic description of non-supersymmetric orbifolded D1-D5-P solutions*, *JHEP* **11** (2015) 063, [1508.01231].

[88] S. Giusto, E. Moscato and R. Russo, *AdS_3 holography for 1/4 and 1/8 BPS*

geometries, *JHEP* **11** (2015) 004, [1507.00945].

[89] I. Bena, E. Martinec, D. Turton and N. P. Warner, *Momentum Fractionation on Superstrata*, *JHEP* **05** (2016) 064, [1601.05805].

[90] I. Bena, S. Giusto, E. J. Martinec, R. Russo, M. Shigemori, D. Turton et al., *Smooth horizonless geometries deep inside the black-hole regime*, *Phys. Rev. Lett.* **117** (2016) 201601, [1607.03908].

[91] I. Bena, E. Martinec, D. Turton and N. P. Warner, *M-theory Superstrata and the MSW String*, 1703.10171.

[92] E. J. Martinec and S. Massai, *String Theory of Supertubes*, *JHEP* **07** (2018) 163, [1705.10844].

[93] A. Bombini and S. Giusto, *Non-extremal superdescendants of the D1D5 CFT*, *JHEP* **10** (2017) 023, [1706.09761].

[94] I. Bena, D. Turton, R. Walker and N. P. Warner, *Integrability and Black-Hole Microstate Geometries*, *JHEP* **11** (2017) 021, [1709.01107].

[95] I. Bena, P. Heidmann and P. F. Ramirez, *A systematic construction of microstate geometries with low angular momentum*, *JHEP* **10** (2017) 217, [1709.02812].

[96] I. Bena, S. Giusto, E. J. Martinec, R. Russo, M. Shigemori, D. Turton et al., *Asymptotically-flat supergravity solutions deep inside the black-hole regime*, *JHEP* **02** (2018) 014, [1711.10474].

[97] G. Bossard, S. Katmadas and D. Turton, *Two Kissing Bolts*, *JHEP* **02** (2018) 008, [1711.04784].

[98] S. Giusto, R. Russo and C. Wen, *Holographic correlators in AdS_3*, *JHEP* **03** (2019) 096, [1812.06479].

[99] N. Ceplak, R. Russo and M. Shigemori, *Supercharging Superstrata*, *JHEP* **03** (2019) 095, [1812.08761].

[100] P. Heidmann and N. P. Warner, *Superstratum Symbiosis*, 1903.07631.

[101] J. Abedi, H. Dykaar and N. Afshordi, *Echoes from the Abyss: Tentative evidence for Planck-scale structure at black hole horizons*, *Phys. Rev.* **D96** (2017) 082004, [1612.00266].

[102] J. Westerweck, A. Nielsen, O. Fischer-Birnholtz, M. Cabero, C. Capano, T. Dent et al., *Low significance of evidence for black hole echoes in gravitational wave data*, *Phys. Rev.* **D97** (2018) 124037, [1712.09966].

[103] J. R. David, G. Mandal and S. R. Wadia, *Microscopic formulation of black holes in string theory*, *Phys. Rept.* **369** (2002) 549–686, [hep-th/0203048].

[104] S. G. Avery, *Using the D1D5 CFT to Understand Black Holes*. PhD thesis, Ohio State U., 2010. 1012.0072.

[105] H. J. Boonstra, B. Peeters and K. Skenderis, *Duality and asymptotic geometries*, *Phys. Lett.* **B411** (1997) 59–67, [hep-th/9706192].

[106] A. Pakman and A. Sever, *Exact N=4 correlators of AdS(3)/CFT(2)*, *Phys. Lett.* **B652** (2007) 60–62, [0704.3040].

[107] A. Dabholkar and A. Pakman, *Exact chiral ring of AdS(3) / CFT(2)*, *Adv. Theor. Math. Phys.* **13** (2009) 409–462, [hep-th/0703022].

[108] M. R. Gaberdiel and I. Kirsch, *Worldsheet correlators in AdS(3)/CFT(2)*, *JHEP* **04** (2007) 050, [hep-th/0703001].

[109] M. Taylor, *Matching of correlators in AdS(3) / CFT(2)*, *JHEP* **06** (2008) 010, [0709.1838].

[110] A. Jevicki, M. Mihailescu and S. Ramgoolam, *Gravity from CFT on S**N(X): Symmetries and interactions*, *Nucl. Phys.* **B577** (2000) 47–72, [hep-th/9907144].

[111] J. M. Maldacena and L. Susskind, *D-branes and fat black holes*, *Nucl. Phys.* **B475** (1996) 679–690, [hep-th/9604042].

[112] G. Andrews, *The Theory of Partitions*. No. v. 2 in Computers & Typesetting. Addison-Wesley Publishing Company, Advanced Book Program, 1976.

[113] A. Galliani, S. Giusto, E. Moscato and R. Russo, *Correlators at large c without information loss*, *JHEP* **09** (2016) 065, [1606.01119].

[114] A. Galliani, S. Giusto and R. Russo, *Holographic 4-point correlators with heavy states*, *JHEP* **10** (2017) 040, [1705.09250].

[115] A. Bombini, A. Galliani, S. Giusto, E. Moscato and R. Russo, *Unitary 4-point correlators from classical geometries*, *Eur. Phys. J.* **C78** (2018) 8, [1710.06820].

[116] O. Lunin and S. D. Mathur, *Three point functions for M(N) / S(N) orbifolds with N=4 supersymmetry*, *Commun. Math. Phys.* **227** (2002) 385–419, [hep-th/0103169].

[117] A. Schwimmer and N. Seiberg, *Comments on the N = 2,3,4 superconformal algebras in two dimensions*, *Physics Letters B* **184** (1987) 191 – 196.

[118] R. Blumenhagen and E. Plauschinn, *Introduction to Conformal Field Theory: With Applications to String Theory*. Lecture Notes in Physics. Springer Berlin Heidelberg, 2009.

[119] E. J. Martinec and W. McElgin, *String theory on AdS orbifolds*, *JHEP* **04** (2002) 029, [hep-th/0106171].

[120] E. J. Martinec and W. McElgin, *Exciting AdS orbifolds*, *JHEP* **10** (2002) 050, [hep-th/0206175].

[121] O. Lunin and S. D. Mathur, *Correlation functions for M**N / S(N) orbifolds*, *Commun. Math. Phys.* **219** (2001) 399–442, [hep-th/0006196].

[122] K. Skenderis and M. Taylor, *Kaluza-Klein holography*, *JHEP* **05** (2006) 057, [hep-th/0603016].

[123] K. Skenderis and M. Taylor, *Holographic Coulomb branch vevs*, *JHEP* **08** (2006) 001, [hep-th/0604169].

[124] S. G. Avery and B. D. Chowdhury, *Emission from the D1D5 CFT: Higher Twists*, *JHEP* **01** (2010) 087, [0907.1663].

[125] S. G. Avery, B. D. Chowdhury and S. D. Mathur, *Deforming the D1D5 CFT away from the orbifold point*, *JHEP* **06** (2010) 031, [1002.3132].

[126] S. G. Avery and B. D. Chowdhury, *Intertwining Relations for the Deformed D1D5 CFT*, *JHEP* **05** (2011) 025, [1007.2202].

[127] S. G. Avery, B. D. Chowdhury and S. D. Mathur, *Excitations in the deformed D1D5 CFT*, *JHEP* **06** (2010) 032, [1003.2746].

[128] B. A. Burrington, A. W. Peet and I. G. Zadeh, *Twist-nontwist correlators in M^N/S_N orbifold CFTs*, *Phys. Rev.* **D87** (2013) 106008, [1211.6689].

[129] B. A. Burrington, A. W. Peet and I. G. Zadeh, *Operator mixing for string states in*

the D1-D5 CFT near the orbifold point, *Phys. Rev.* **D87** (2013) 106001, [1211.6699].

[130] B. A. Burrington, S. D. Mathur, A. W. Peet and I. G. Zadeh, *Analyzing the squeezed state generated by a twist deformation*, *Phys. Rev.* **D91** (2015) 124072, [1410.5790].

[131] Z. Carson, S. Hampton, S. D. Mathur and D. Turton, *Effect of the deformation operator in the D1D5 CFT*, *JHEP* **01** (2015) 071, [1410.4543].

[132] Z. Carson, S. Hampton, S. D. Mathur and D. Turton, *Effect of the twist operator in the D1D5 CFT*, *JHEP* **08** (2014) 064, [1405.0259].

[133] B. A. Burrington, A. W. Peet and I. G. Zadeh, *Bosonization, cocycles, and the D1-D5 CFT on the covering surface*, *Phys. Rev.* **D93** (2016) 026004, [1509.00022].

[134] Z. Carson, S. Hampton and S. D. Mathur, *Second order effect of twist deformations in the D1D5 CFT*, *JHEP* **04** (2016) 115, [1511.04046].

[135] Z. Carson, S. Hampton and S. D. Mathur, *Full action of two deformation operators in the D1D5 CFT*, *JHEP* **11** (2017) 096, [1612.03886].

[136] Z. Carson, S. Hampton and S. D. Mathur, *One-Loop Transition Amplitudes in the D1D5 CFT*, *JHEP* **01** (2017) 006, [1606.06212].

[137] B. A. Burrington, I. T. Jardine and A. W. Peet, *Operator mixing in deformed D1D5 CFT and the OPE on the cover*, *JHEP* **06** (2017) 149, [1703.04744].

[138] Z. Carson, I. T. Jardine and A. W. Peet, *Component twist method for higher twists in D1-D5 CFT*, *Phys. Rev.* **D96** (2017) 026006, [1704.03401].

[139] B. A. Burrington, I. T. Jardine and A. W. Peet, *The OPE of bare twist operators in bosonic S_N orbifold CFTs at large N*, *JHEP* **08** (2018) 202, [1804.01562].

[140] S. Hampton, S. D. Mathur and I. G. Zadeh, *Lifting of D1-D5-P states*, *JHEP* **01** (2019) 075, [1804.10097].

[141] A. Pakman, L. Rastelli and S. S. Razamat, *Diagrams for Symmetric Product Orbifolds*, *JHEP* **10** (2009) 034, [0905.3448].

[142] A. Pakman, L. Rastelli and S. S. Razamat, *Extremal Correlators and Hurwitz Numbers in Symmetric Product Orbifolds*, *Phys. Rev.* **D80** (2009) 086009,

[0905.3451].

[143] A. Pakman, L. Rastelli and S. S. Razamat, *A Spin Chain for the Symmetric Product CFT(2)*, *JHEP* **05** (2010) 099, [0912.0959].

[144] P. Erdős, R. K. Guy and J. Moon, *On refining partitions*, *Journal of the London Mathematical Society* **2** (1975) 565–570.

[145] *The On-Line Encyclopedia of Integer Sequences.* Published electronically at https://oeis.org, Sequence A002865.

[146] S. Deger, A. Kaya, E. Sezgin and P. Sundell, *Spectrum of D = 6, N=4b supergravity on AdS in three-dimensions x S**3*, *Nucl. Phys.* **B536** (1998) 110–140, [hep-th/9804166].

[147] G. Arutyunov, A. Pankiewicz and S. Theisen, *Cubic couplings in D = 6 N=4b supergravity on AdS(3) x S**3*, *Phys. Rev.* **D63** (2001) 044024, [hep-th/0007061].

[148] J. de Boer, A. Pasquinucci and K. Skenderis, *AdS / CFT dualities involving large 2-D N=4 superconformal symmetry*, *Adv. Theor. Math. Phys.* **3** (1999) 577–614, [hep-th/9904073].

[149] S. Gukov, E. Martinec, G. W. Moore and A. Strominger, *The Search for a holographic dual to AdS(3) x S**3 x S**3 x S**1*, *Adv. Theor. Math. Phys.* **9** (2005) 435–525, [hep-th/0403090].

[150] M. R. Gaberdiel and M. Kelm, *The symmetric orbifold of $\mathcal{N} = 2$ minimal models*, *JHEP* **07** (2016) 113, [1604.03964].

[151] L. Eberhardt, M. R. Gaberdiel, R. Gopakumar and W. Li, *BPS spectrum on $AdS_3 \times S^3 \times S^3 \times S^1$*, *JHEP* **03** (2017) 124, [1701.03552].

[152] L. Eberhardt, M. R. Gaberdiel and W. Li, *A holographic dual for string theory on $AdS_3 \times S^3 \times S^3 \times S^1$*, *JHEP* **08** (2017) 111, [1707.02705].

[153] M. R. Gaberdiel, R. Gopakumar and C. Hull, *Stringy AdS_3 from the worldsheet*, *JHEP* **07** (2017) 090, [1704.08665].

[154] M. Baggio, O. Ohlsson Sax, A. Sfondrini, B. Stefański and A. Torrielli, *Protected string spectrum in AdS_3/CFT_2 from worldsheet integrability*, *JHEP* **04** (2017) 091, [1701.03501].

[155] S. D. Mathur, *The Fuzzball proposal for black holes: An Elementary review*, *Fortsch. Phys.* **53** (2005) 793–827, [hep-th/0502050].

[156] A. Dabholkar, S. Murthy and D. Zagier, *Quantum Black Holes, Wall Crossing, and Mock Modular Forms*, 1208.4074.

[157] I. Mandal and A. Sen, *Black Hole Microstate Counting and its Macroscopic Counterpart*, *Nucl. Phys. Proc. Suppl.* **216** (2011) 147–168, [1008.3801].

[158] M. Fluder, S. M. Hosseini and C. F. Uhlemann, *Black hole microstate counting in Type IIB from 5d SCFTs*, 1902.05074.

[159] T. Apostol, *Introduction to Analytic Number Theory*. Undergraduate Texts in Mathematics. Springer New York, 1998.

[160] M. Green, M. Green, J. Schwarz and E. Witten, *Superstring Theory: Volume 1, Introduction*. Cambridge Monographs on Mathematical Physics. Cambridge University Press, 1988.

[161] W. R. Inc., "Mathematica, Version 10.4.1.0."

[162] I. Kourkoulou and J. Maldacena, *Pure states in the SYK model and nearly-AdS_2 gravity*, 1707.02325.

[163] J. De Boer, R. Van Breukelen, S. F. Lokhande, K. Papadodimas and E. Verlinde, *Probing typical black hole microstates*, 1901.08527.

[164] N. Oshita and N. Afshordi, *Probing microstructure of black hole spacetimes with gravitational wave echoes*, *Phys. Rev.* **D99** (2019) 044002, [1807.10287].

[165] A. B. Nielsen, C. D. Capano, O. Birnholtz and J. Westerweck, *Parameter estimation for black hole echo signals and their statistical significance*, 1811.04904.

[166] N. Gaddam, A. Gnecchi, S. Vandoren and O. Varela, *Rholography, Black Holes and Scherk-Schwarz*, *JHEP* **06** (2015) 058, [1412.7325].